



Cycloalkenyl macromonomers from new multifunctional inimers : a platform for graft, bottle-brush and mikto-arm star copolymers

Duc Anh Nguyen

► To cite this version:

Duc Anh Nguyen. Cycloalkenyl macromonomers from new multifunctional inimers : a platform for graft, bottle-brush and mikto-arm star copolymers. Polymers. Le Mans Université, 2016. English. NNT : 2016LEMA1001 . tel-01316553

HAL Id: tel-01316553

<https://theses.hal.science/tel-01316553>

Submitted on 17 May 2016

HAL is a multi-disciplinary open access archive for the deposit and dissemination of scientific research documents, whether they are published or not. The documents may come from teaching and research institutions in France or abroad, or from public or private research centers.

L'archive ouverte pluridisciplinaire **HAL**, est destinée au dépôt et à la diffusion de documents scientifiques de niveau recherche, publiés ou non, émanant des établissements d'enseignement et de recherche français ou étrangers, des laboratoires publics ou privés.

Thèse de Doctorat

Duc Anh NGUYEN

*Mémoire présenté en vue de l'obtention du
grade de Docteur de l'Université du Maine
sous le label de L'Université Nantes Angers Le Mans*

École doctorale : 3MPL

Discipline : Chimie des Matériaux, CNU 33

Spécialité : Chimie et Physicochimie des Polymères

Unité de recherche : IMMM, UMR n°6283, CNRS

Soutenue le 7 Janvier 2016

Thèse N :

Cycloalkenyl macromonomers from new multifunctional inimers: A platform for graft, bottle-brush and mikto-arm star copolymers

JURY

Rapporteurs: **Sophie GUILLAUME**, Director of Research CNRS, Université de Rennes 1
Jean-Luc SIX, Professor, Université de Lorraine

Examineurs: **Daniel GRANDE**, Director of Research CNRS, Université Paris-Est Créteil

Directeur de Thèse: **Laurent FONTAINE**, Professor, Université du Maine

Co-directeur de Thèse: **Véronique MONTEBAULT**, Professor, Université du Maine

Co-encadrant de Thèse: **Sagrario PASCUAL**, Maître de Conférence - HDR, Université du Maine

Luận văn này xin được gửi tới...

Bố mẹ

Thầy cô

Anh chị

Hà

Bạn bè và những người tôi yêu mến

Acknowledgements

This work was performed in the Méthodologie et Synthèse des Polymères (MSP) Laboratory, Institut des Molécules et Matériaux du Mans (IMMM) – UMR 6283 CNRS in Université du Maine, Le Mans, France. I would like to express my sincere gratitude to my supervisor, Professor Laurent Fontaine to support me to be in the MSP laboratory, to entrust me this thesis, for his leading in the work, his advices, enthusiasm and availability.

I would like to express my great thanks to Vietnam government, Vietnam Ministry of Education and Training, VIED and 911 Program for the financial support, to University of Sciences and Technology of Hanoi (USTH) for their support for the time I was in France.

I would like to express my sincere gratitude to my co-supervisor, Professor Véronique Montembault for her advices and availability in my works, for her kindness and support me in 3 years I was in France, for her mobilization and smile sometimes I was deep in the lack of motivation, and for all her help from the first date to the last date I was in laboratory. I can not find the word which can adequate my sincere gratitude to her. I thank her for everything.

I would like to give many grateful thanks to my co-supervisor, Dr Sagrario Pascual for her advices, enthusiasm, kindness and availability, for the experiences she shared not only in science but also many thing, her patience to explain me about SEC, DLS analyses and carefully correction of my thesis manuscript.

I am in honor to get the acceptance of Dr. Sophie Guillaume and Professor Jean-Luc Six as reporters of my thesis. I would like to express my sincere gratitude for their advices and evaluation.

I also would like to express my sincere gratitude to Dr. Daniel Grande for his agreement to be the president of my thesis defense committee, for his advices, evaluation and recognition to our work.

I express my gratitude to Dr. Sandie Piogé for her kindness, and availability, for her help and experiences, her patience and meticulousness to help me complete my manuscript. I also associate

Acknowledgements

my thanks to Dr. Flavien Leroux not only for his help in my experiments and experiences from his works but also his kindness and friendliness in the laboratory.

Many thanks to Mr. Alexandre Benard for his analyses in SEC-MALLS and his kindness in laboratory. I also associate many thanks to Mrs. Emmanuelle Mebold for her patience to analyze my “freaky” samples in MALDI-ToF mass and SEC-DMF analyses.

I also thank to Mrs. Mireille Barthe for her SEC-THF, Mrs. Amélie Durand and Mr. Corentin Jacquemmoz for NMR and Mrs. Patricia Gangnery for HRMS mass analyses.

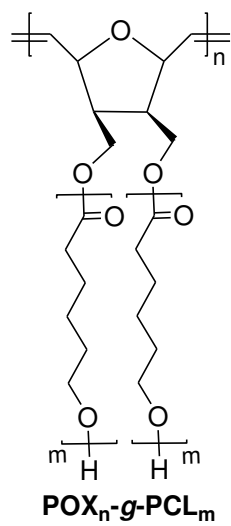
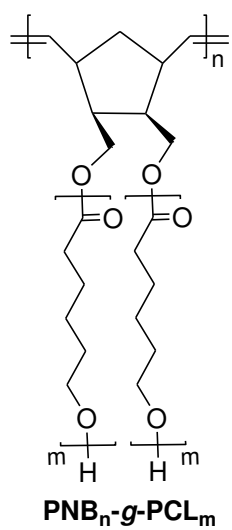
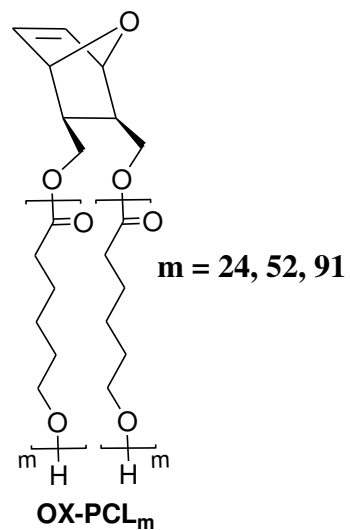
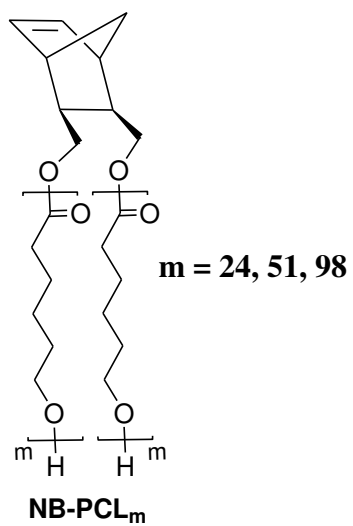
I would like to give many thanks to Mrs. Anita Loiseau, Mrs. Aline Lambert, Mr. Clément Briere for their goodness and availability in MSP laboratory.

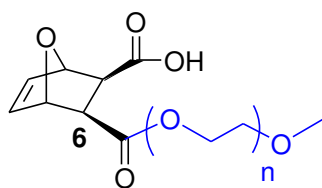
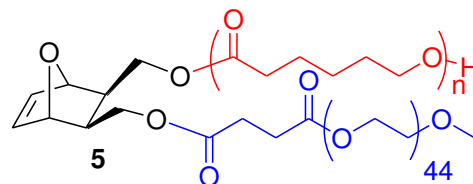
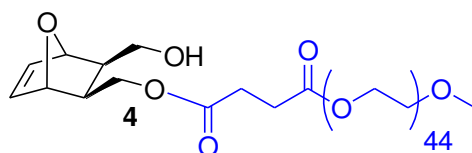
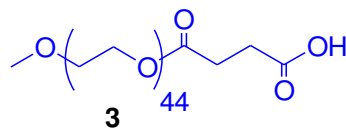
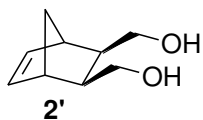
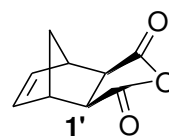
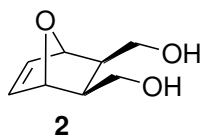
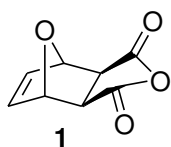
I would like to express my thanks to Dr. Nguyen Thi Thanh Thuy, Dr. Ho The Hien not only for their help, experiences in my works, but also for everything they share and advise for a new coming Vietnamese to live in France.

I thank to my colleagues in MSP laboratory, Marie, Joachim, Mael, Maud, Antoine, Corentin, Nguyet, Thai, Koy, Suwat, Nhung, Emilie, Ying-rak, Khrishna for their availability, goodness and sympathy.

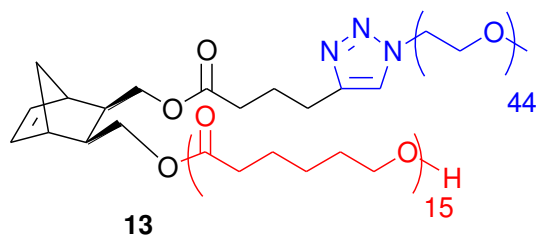
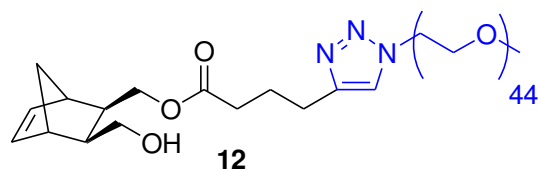
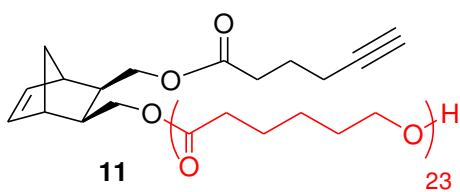
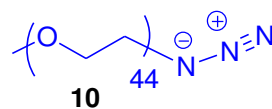
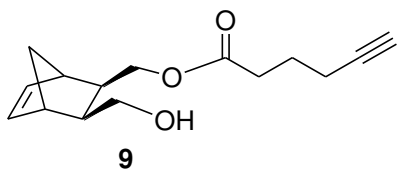
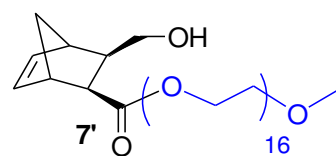
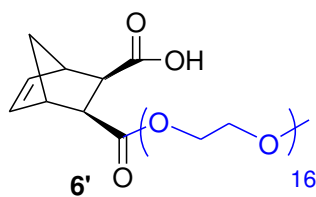
Many thanks to my friends, Nhi, Huy, Bach, Hien, Hung and the other Vietnamese in Le Mans for their spiritual support and unforgettable memories. Thank to Stephane, Jane, Bertrand and LMB who gave me great moments in Le Mans.

Finally, I would like to give a great thanks to my family, my parent and my younger sister who always stay beside me, support and encourage me in everything. And Ha, thank you very much for your patience to be with me, your shared motivation mobilized me to overcome all the difficult moments to reach this point.

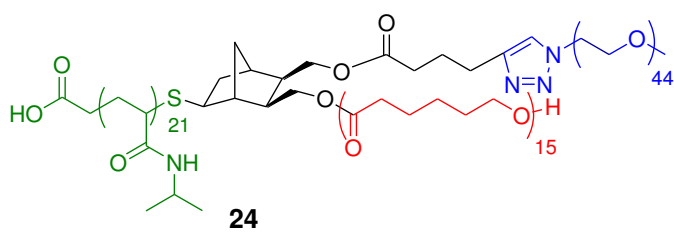
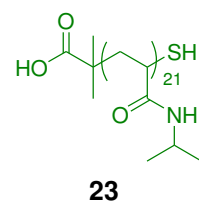
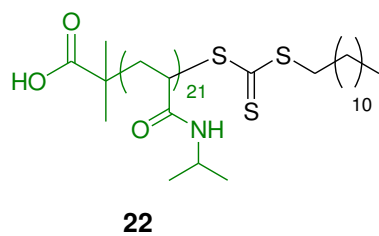
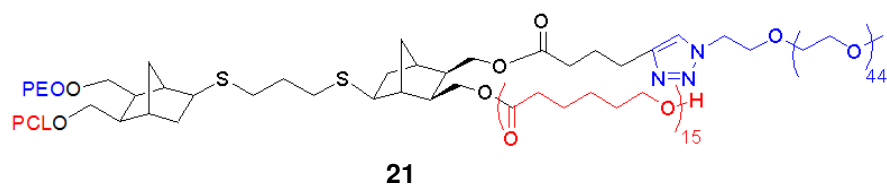
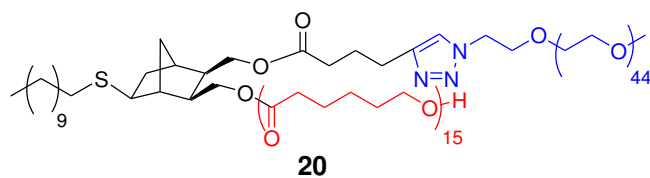
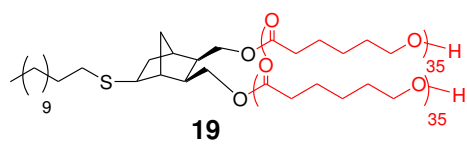
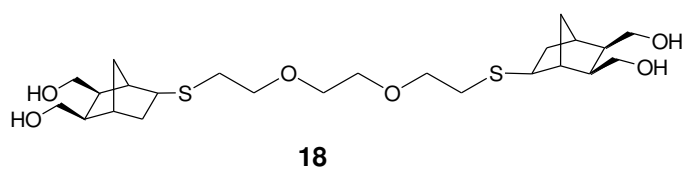
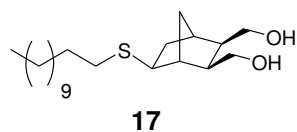
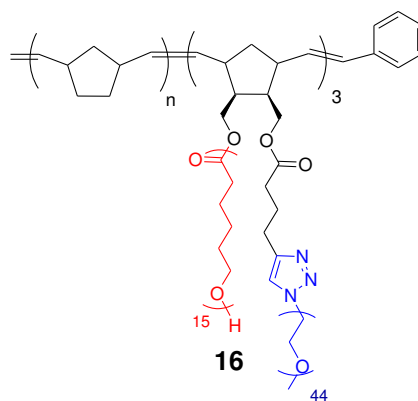
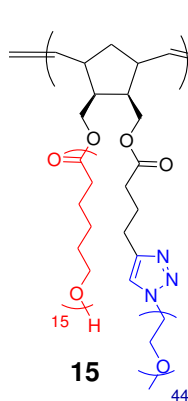
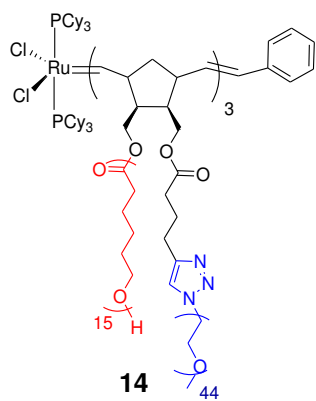




6a: n = 16
6b: n = 44



13a: n = 10
13b: n = 15
13c: n = 25
13d: n = 36



LIST OF ABBREVIATIONS

AIBN	Azobisisobutyronitrile
CL	ϵ -Caprolactone
CMC	Critical micellar concentration
Conv.	Conversion
D_M	Dispersity
DCC	<i>N,N'</i> -Dicyclohexylcarbodiimide
DCM	Dichloromethane
DCTB	2-[(2 <i>E</i>)-3-(4- <i>tert</i> -butylphenyl)-2-methylprop-2-enylidene]malononitrile
DDMAT	S-Dodecyl-S'-(α,α' -dimethyl- α'' -acetic acid)trithiocarbonate
DLS	Dynamic light scattering
DMAP	4-(<i>N,N</i> -Dimethylamino)pyridine
DMF	<i>N,N</i> -Dimethylformamide
DMPA	2,2-Dimethoxy-2-phenylacetophenone
DMPP	Dimethylphenylphosphine
DP _n	Number-average degree of polymerization
DP _{n,NMR}	Number-average degree of polymerization calculated from NMR
DP _{n,theo}	Theoretical number-average degree of polymerization
EO	Ethylene oxide
FT-IR	Fourier Transformed InfraRed spectroscopy
G1	Grubbs' first generation catalyst
G2	Grubbs' second generation catalyst
G3	Grubbs' third generation (bromopyridine as ligands) catalyst
G3'	Grubbs' third generation (pyridine as ligands) catalyst
HRMS	High Resolution Mass Spectrometry
m/z	Mass-to-charge ratio
MALDI-ToF	Matrix-Assisted Laser Desorption-Ionization-Time of Flight
M _n	Number-average molar mass
M _{n,SEC}	Number-average molar mass in SEC analysis

List of abbreviations

$M_{n,NMR}$	Number-average molar mass in NMR analysis
mPEG	Poly(ethylene glycol) monomethyl ether
NaTFA	Sodium trifluoroacetate
NB	Norbornene
NB $\text{PEO}_{44}\text{PCL}_x$	Norbornenyl-functionalized PEO- <i>b</i> -PCL macromonomer containing 44 units of EO and x units of CL
NIPAM	<i>N</i> -isopropylacrylamide
NMR	Nuclear Magnetic Resonance
PCL	Poly(ϵ -caprolactone)
PDi	Polydispersity
PDMS	Polydimethylsiloxane
PE	Polyethylene
PEO	Poly(ethylene oxide) monomethyl ether
PEO- <i>b</i> -PCL	Poly(ethylene oxide)- <i>block</i> -poly(ϵ -caprolactone)
PEO- N_3	Azido-terminated poly(ethylene oxide)
PMDETA	<i>N,N,N',N',N''</i> -Pentamethyldiethylenetriamine
PNIPAM	Poly(<i>N</i> -isopropylacrylamide)
PNIPAM-SH	Thiol-functionalized PNIPAM
PS	Polystyrene
r. t.	Room temperature
RAFT	Reversible Addition-Fragmentation chain Transfer
RI	Refractive Index
ROMP	Ring-Opening Metathesis Polymerization
ROP	Ring-Opening Polymerization
SEC	Size Exclusion Chromatography
SEC MALLS	SEC multi-angle laser light scattering
TBD	1,5,7-triazabicyclo[4.4.0]dec-5-ene
TEA	Triethylamine
TGA	Thermogravimetric analysis
THF	Tetrahydrofuran
UV	Ultra-violet

Table of contents

General introduction	1
-----------------------------------	----------

Chapter 1. Bibliography study

Introduction	7
I. Ring-opening metathesis polymerization	9
<i>I.1. Introduction.....</i>	<i>9</i>
<i>I.2. ROMP mechanism.....</i>	<i>10</i>
<i>I.3. ROMP: a living polymerization</i>	<i>12</i>
<i>I.4. From multi-components to well-defined single-component initiators</i>	<i>13</i>
II. The polymerization of lactones via ROP	18
<i>II.1. Introduction</i>	<i>18</i>
<i>II.2. ROP with organometallic catalysts</i>	<i>18</i>
<i>II.3. ROP with organocatalysts</i>	<i>22</i>
<i>II.4. Conclusion</i>	<i>29</i>
III. Synthesis of graft copolymers from ROMP-able macromonomers including PEO and/or PCL.....	31
<i>III.1. Synthesis of graft copolymers from PEO-based ROMP-able macromonomers</i>	<i>32</i>
<i>III.1.1. PEO-based ROMP-able macromonomers obtained by anionic polymerization.....</i>	<i>32</i>
<i>III.1.2. PEO-based ROMP-able macromonomer obtained by chemical modification.....</i>	<i>38</i>
<i>III.1.3. PEO-based ROMP-able macromonomers synthesized by 'click' chemistry</i>	<i>46</i>
<i>III.2. Synthesis of graft copolymers from PCL-based macromonomers via metathesis polymerization.....</i>	<i>49</i>
Conclusion	59
References.....	61

Chapter 2. Synthesis and characterization of high grafting density bottle-brush poly(oxa)norbornene-g-poly(ϵ -caprolactone)

Introduction	69
Experimental	69
Results and discussion	71
Conclusions.....	75
Notes and references.....	76
Supporting Information	77

Chapter 3. Synthesis and self-assembling properties of amphiphilic (oxa)norbornenyl-functionalized PEO-b-PCL copolymers

Introduction	91
I. Synthesis of oxanorbornenyl-functionalized PEO-PCL copolymers from <i>exo</i> oxanorbornene dimethanol	93
I.1. Synthesis of <i>exo</i> 7-oxabicyclo[2.2.1]hept-5-ene-2,3-dimethanol	94
I.2. Synthesis of <i>exo</i> oxanorbornene-terminated PEO	95
I.3. Synthesis of oxanorbornenyl-functionalized PEO-b-PCL copolymers	100
II. Synthesis of (oxa)norbornenyl-functionalized PEO copolymers from (oxa)norbornene anhydrides	102
II.1. Esterification between oxanorbornene anhydride and PEO	103
II.2. Esterification between norbornene anhydride and PEO	107
II.3. Reduction of carboxylic acid-functionalized norbornene-terminated PEO.....	109
III. Synthesis of norbornenyl-functionalized PEO-b-PCL copolymers by combination of “click chemistry” and ROP	111
III.1. Synthesis of hydroxyl- and alkynyl-functionalized norbornene	112
III.2.1. Synthesis of alkynyl-functionalized norbornenyl-terminated PCL	113
III.2.2. Synthesis of norbornenyl-functionalized PEO-b-PCL copolymers.....	115
III.3. Synthesis of norbornenyl-functionalized PEO-b-PCL copolymers by ‘click’ reaction followed by ROP of CL	117
III.3.1. Synthesis of hydroxyl-functionalized norbornenyl-terminated PEO.	117
III.3.2. Synthesis of norbornenyl-functionalized PEO-b-PCL	119
IV. Self-assembling properties of amphiphilic norbornenyl PEO-b-PCL copolymers.....	122
IV.1. Critical micellar concentration (CMC) of copolymers in water	123

IV.2. Determination of hydrodynamic diameter of micelles via dynamic light scattering (DLS).....	126
Conclusions.....	129
References.....	131
Experimental section	134

Chapter 4. Norbornenyl-functionalized PEO-b-PCL block copolymers as a platform to target comb-like, umbrella-like graft and (mikto-arm) star copolymers

Introduction	145
I. Synthesis of a ROMP macroinitiator and umbrella-like copolymer using ROMP macroinitiator	147
I.1. Synthesis of ROMP macroinitiator from norbornenyl-functionalized PEO-b-PCL copolymer and Grubbs I.....	147
I.2. Synthesis of umbrella-like copolymers using ROMP macroinitiator	149
II. Synthesis of graft copolymers from ROMP of norbornenyl-functionalized PEO-b-PCL macromonomer	152
III. Synthesis of (mikto-arm) star copolymers by thiol-ene reactions of norbornenyl-functionalized PEO-b-PCL copolymer	158
III.1. Thiol-ene reaction using norbornene dimethanol	160
III.2. Thiol-ene reaction using norbornenyl-functionalized bispoly(ϵ -caprolactone) copolymer.....	162
III.3. Thiol-ene reaction using norbornenyl-functionalized PEO-b-PCL copolymer.....	165
III.4. Synthesis of (PCL, PEO, PNIPAM) mikto-arm star copolymers from norbornenyl functionalized PEO-b-PCL copolymer	168
Conclusion	172
References.....	174
Experimental section	177
 General conclusion.....	 189

General introduction

The design and the elaboration of well-defined polymer architectures has become an important goal in macromolecular science.¹ Thanks to the development of controlled/living polymerization methods, a large range of polymers with different topologies such as block, gradient, star, hyperbranched, dendritic, cyclic, and graft has been successfully synthesized. Aided by recent advances in polymer chemistry, including controlled/living polymerization methods such as ring-opening polymerization (ROP), atom transfer radical polymerization (ATRP), reversible addition/fragmentation chain transfer (RAFT), nitroxide mediated polymerization (NMP), ring-opening metathesis polymerization (ROMP), and ‘click’ chemistry, growing attention has been paid to the synthesis of well-defined copolymers. Those new synthetic techniques enable to attain an unprecedented high degree of control over the macromolecular structure with desired functional groups, chemical compositions, lengths of side chains and of backbone, and grafting densities.^{2,3}

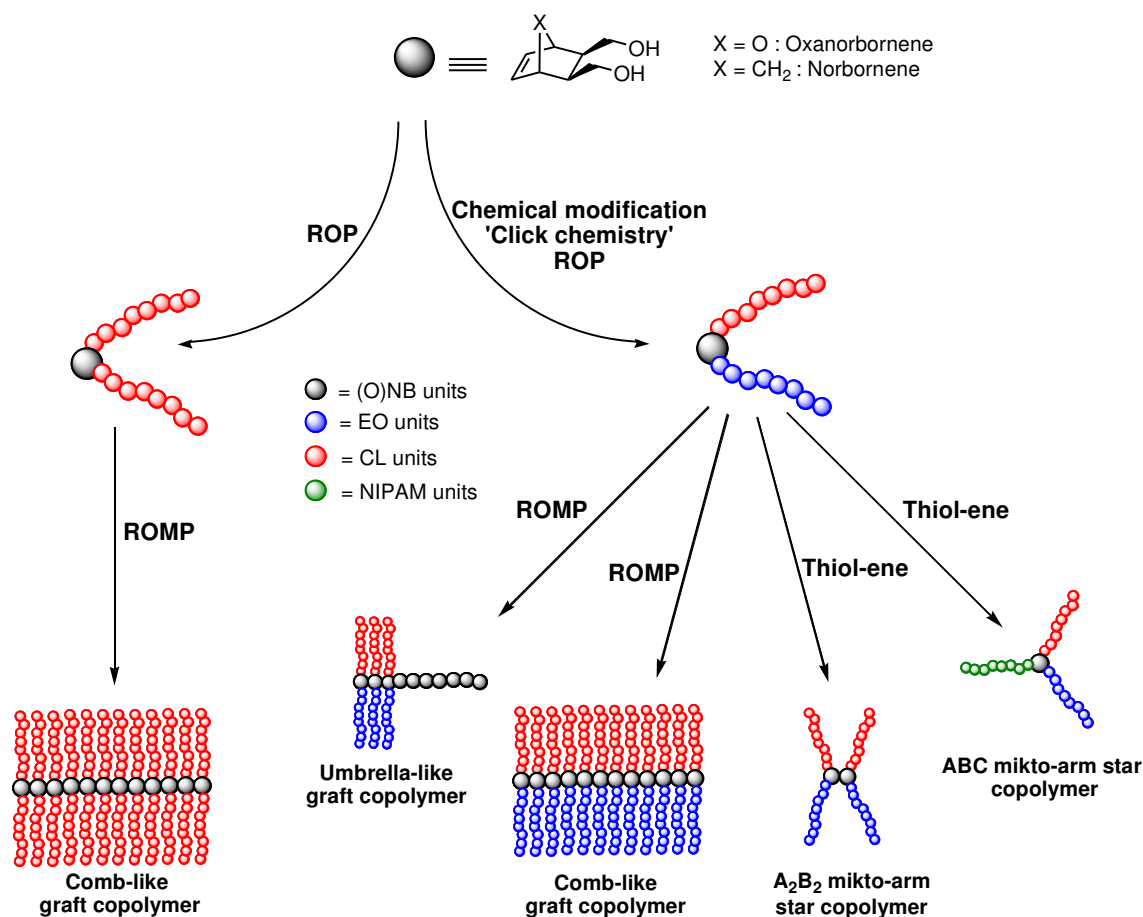
ROMP is nowadays an especially efficient tool to prepare well-defined graft copolymers through the ‘grafting-through’ or macromonomer route when combined with other control/living polymerization processes.⁴⁻⁷ Thanks to the development of well-defined ROMP initiators synthesis, an exponential increase of studies involving ROMP has been reported for the synthesis of controlled macromolecular architectures.⁸ Among the various ROMP-able cycloolefin-containing functional monomers, norbornene (NB), oxanorbornene (ONB), and their derivatives are the most common functionalized groups involved in macromonomers synthesis in order to obtain graft copolymers.⁹⁻¹³

In addition, the various choices of side chain polymers have given rise to the use of graft copolymers in different applications. Among them, poly(ethylene oxide) (PEO) and poly(ϵ -caprolactone) (PCL) are usable candidates to elaborate nanostructures to be used in various applications, especially as biomaterials.² PEO is a hydrophilic, non-toxic, biocompatible polymer, which has found numerous applications in the fields of biomaterials and biotechnologies.¹⁴⁻¹⁶ PCL is a very useful polymer that brings important specific properties such as hydrophobicity¹⁷, biocompatibility,¹⁸ controlled (bio)degradation,¹⁹ and that is easy to synthesize *via* ROP of ϵ -caprolactone (CL).²⁰

Many studies related to the synthesis of graft copolymers containing PEO side chains using the combination of ROMP and either anionic polymerization or chemical modification (post-polymerization functionalization) have been reported.^{9,21-24} Especially, PEO segments are usually combined with an hydrophobic component forming amphiphilic graft copolymers.^{25,26} The combination of ROP of CL in order to obtain PCL-based macromonomers followed by ROMP, enables the synthesis of controlled degradable graft copolymers.^{27,28} Up to now, only one report has been devoted to the synthesis of a graft copolymer containing simultaneously PEO and PCL grafts.²⁹ The random copolymers prepared from polyethylene-, PCL-, PEO-, and polystyrene-based NB were successfully synthesized by ROMP copolymerization with quantitative macromonomers conversions.

Besides, polymers containing a (cyclo)olefin functionality show high reactivity toward the thiol-ene hydrothiolation reaction. A few studies have reported the high reactivity of NB and derivatives towards thiols.³⁰⁻³² The thiol-ene reaction applied to NB-functionalized polymers opens the way to various macromolecular topologies such as multiblock, star, and network copolymers. While a few works have described the reactivity of NB-functionalized PEO toward the thiol-ene reaction³³⁻³⁶ no study has been published about the reactivity of either NB-functionalized PCL or NB-functionalized PEO/PCL copolymers toward thiol-ene reactions.

In this context, this work aims at synthesizing, characterizing, and investigating the reactivity in ROMP and in thiol-ene reaction of a series of new (oxa)norbornenyl-functionalized macromonomers incorporating PEO and/or PCL chains, starting from *exo*-(oxa)norbornene dimethanol as the initial material (Scheme 1).



Scheme 1. Synthetic pathways to macromolecular topologies starting from (oxa)norbornenyl-functionalized copolymers.

This Ph.D manuscript is organized in four chapters:

The first chapter is a survey of the literature devoted to ROMP and ROP techniques, the synthesis and characterization of macromonomers containing ROMP-able functionality, PEO and/or PCL chains and their ROMP to obtain graft copolymers.

The second chapter describes the synthesis of hydrophobic (oxa)norbornenyl-functionalized bisPCL macromonomers by ROP and the investigation of their ROMP using ruthenium-based catalysts to obtain high density poly(oxa)norbornene-*g*-PCL copolymers.

The third chapter describes the synthesis of amphiphilic (oxa)norbornenyl-functionalized PEO-*b*-PCL copolymers using a combination of chemical modification, click chemistry, and ROP. The characterization of the self-assembling properties of those copolymers is also described.

The last chapter describes the synthesis of various macromolecular topologies, including graft and bottle-brush copolymers *via* ROMP and (mikto-arm) star copolymers *via* the thiol-ene reaction using the previous norbornenyl-functionalized PEO-*b*-PCL copolymers as a platform.

-
- ¹ K. A. Davis, K. Matyjaszewski, *Adv. Polym. Sci* **2002**, 159
- ² C. Feng, Y. Li, D. Yang, J. Hu, X. Zhang, X. Huang, *Chem. Soc. Rev.* **2011**, 40, 1282–1295
- ³ N. Hadjichristidis, S. Pispas, M. Pitsikalis, H. Iatrou, D. J. Lohse, *Graft copolymers, Encyclopedia of Polymer Science and Technology*, 3rd Ed., John Wiley & Sons Inc., Hoboken, New-York, **2004**
- ⁴ W. J. Feast, V. C. Gibson, A. F. Johnson, E. Khosravi, M. A. Mohsin, *J. Mol. Catal. A: Chem.* **1997**, 115-137
- ⁵ Y. Tsukahara, S. Namba, J. Iwasa, Y. Nakano, K. Kaeriyama, M. Takahashi, *Macromolecules* **2001**, 34, 2624-2629
- ⁶ J. B. Matson, G. H. Grubbs, *J. Am. Chem. Soc.* **2008**, 130, 6731-6733
- ⁷ G. Morandi, V. Montembault, S. Pascual, S. Legoupy, L. Fontaine, *Macromolecules* **2006**, 39, 2732-2735
- ⁸ R. H. Grubbs, E. Khosravi, *Handbook of Metathesis*, 2nd Ed., vol.3. Wiley-VCH, Weinheim, **2015**
- ⁹ V. Héroguez, S. Breunig, Y. Gnanou, M. Fontanille, *Macromolecules* **1996**, 29, 4459-4464
- ¹⁰ L. Pichavant, C. Bourget, M. C. Durrieu, V. Héroguez, *Macromolecules* **2011**, 44, 7879-7887
- ¹¹ J. Zou, G. Jafr, E. Themistou, Y. Yap, Z. A. P. Wintrob, P. Alexandridis, A. C. Ceacareanu, C. Cheng, *Chem. Commun.* **2011**, 47, 4493-4495
- ¹² K. Breitenkamp, J. Simeone, E. Jin, T. Emrick, *Macromolecules* **2002**, 35, 9249-9252
- ¹³ J. A. Johnson, Y. Y. Lu, , A. O. Burts, Y. Xia, A. C. Durrell, D. A. Tirrell, R. H. Grubbs, *Macromolecules* **2010**, 43, 10326-10335
- ¹⁴ A. Iyer, K. Mody, B. Jha, *Enzyme and Microbial Technology*, **2006**, 38, 220-222
- ¹⁵ G. M. T. Calazans, R. C. Lima, F. P. De França, C. E. Lopes, *Int. J. Biol. Macromol.*, **2000**, 27, 245-247
- ¹⁶ M. M. Amiji, *Biomaterials*, **1995**, 16, 593-599
- ¹⁷ M. Labet, W. Thielemans, *Chem. Soc. Rev.*, **2009**, 38, 3484-3504

- ¹⁸ V. R. Sinha, K. Bansal, R. Kaushik, R. Kumria and A. Trehan, *Int. J. Pharm.*, **2004**, 278, 1-23
- ¹⁹ R. Chandra and R. Rustgi, *Prog. Polym. Sci.*, **1998**, 23, 1273-1335
- ²⁰ C. X. F. Lam, S. H. Teoh and D. W. Hutmacher, *Polym. Int.*, **2007**, 56, 718-728
- ²¹ S. Breunig, V. Héroguez, Y. Gnanou, M. Fontanille, *Macromol. Symp.* **1995**, 95, 151-166
- ²² J. Zou, G. Jafr, E. Themistou, Y. Yap, Z. A. P. Wintrob, P. Alexandridis, A. C. Ceacareanu, C. Cheng, *Chem. Commun.* **2011**, 47, 4493-4495
- ²³ S. F. Alfred, Z. M. Al-Bardi, A. E. Madkour, K. Lienkamp, G. N. Tew, , *J. Polym. Sci., Part A: Polym. Chem.* **2008**, 46, 2640-2648
- ²⁴ D. Le, V. Montembault, J. C. Soutif, M. Rutnakornpituk, L. Fontaine, *Macromolecules* **2010**, 43, 5611-5617
- ²⁵ D. Neugebauer, *Polym. Int.* **2007**, 56, 1469-1498
- ²⁶ Y. Li, J. Zou, B. P. Das, M. Tsianou, C. Cheng, *Macromolecules* **2012**, 45, 4623-4629
- ²⁷ Q. Fu, J. M. Ren, G. G. Qiao, *Polym. Chem.* **2012**, 3, 343-351
- ²⁸ D. Yang, W. Huang, J. Yu, J. Jiang, L. Zhang, M. Xie, *Polymer* **2010**, 51, 5100-5106
- ²⁹ H. Zhang, Z. Zhang, Y. Gnanou, N. Hadjichristidis, *Macromolecules* **2015**, 48, 3556-3562
- ³⁰ C. E. Hoyle, T. Y. Lee, T. Roper, *J. Polym. Sci. Part A: Polym. Chem.* **2004**, 42, 5301-5338
- ³¹ P. Theato, H.-A. Klok, *Functional Polymers by Post-Polymerization Modification*, Wiley-VCH, Weinheim, **2012**
- ³² A. B. Lowe, *Polym. Chem.* **2014**, 5, 4820-4870
- ³³ C. N. Walker, J. M. Sarapas, V. Kung, A. L. Hall, G. N. Tew, *ACS Macrolett.* **2014**, 3, 453-457
- ³⁴ M. M. Stamenović, P. Espeel, W. V. Camp, P. E. Du Prez, *Macromolecules* **2011**, 44, 5619-5630
- ³⁵ Q. Fu, J. Liu, W. Shi, *Prog. Org. Coat.* **2008**, 63, 100-109
- ³⁶ C. C. Lin, C. S. Ki, H. Shih, *J. App. Polym. Sci.* **2015**, DOI: 10.1002/App.41563

Chapter 1

Bibliography study

Introduction

Graft copolymers belong to a class of segmented copolymers and generally consist of a linear backbone of one composition and branches of a different composition randomly or regularly distributed throughout the backbone (Figure I). Graft copolymers offer the unique possibility of tailoring materials properties through their numerous structural variables that can be modified such as nature of the polymer backbone and composition and density of the grafts.¹ Through changes of these segments, properties such as morphology, order-disorder transitions and phase behavior can be modified.²

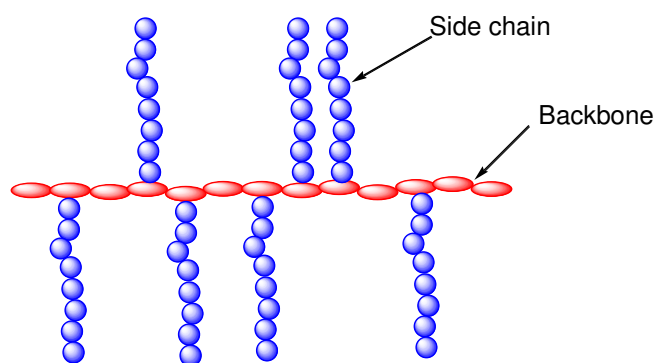
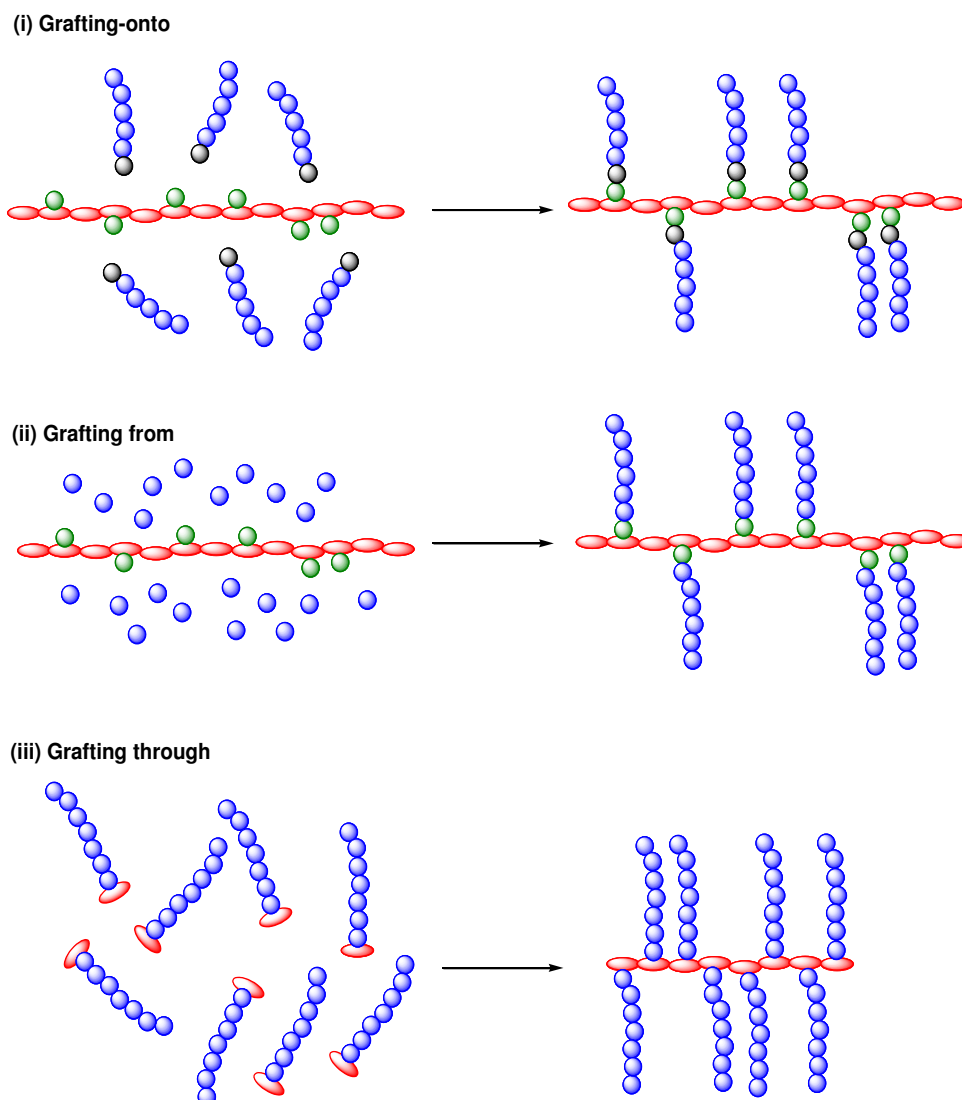


Figure I. Graft copolymers

Well-defined graft copolymers can be synthesized according to three general pathways: (i) the “grafting onto” method, in which side chains are preformed and then attached to the main chain polymer backbone; (ii) the “grafting from” method, in which the side chains are formed from active sites on the main chain backbone, these sites are able to initiate the polymerization leading to the synthesis of a graft copolymer; (iii) the “grafting through” method or macromonomer method, in which the macromonomers, oligomeric or polymeric chains bearing a polymerizable end-group, are polymerized to give the graft copolymer (Scheme I).³ The most commonly used method is the “grafting through” or macromonomer method which allows the control of grafts, backbone length, and grafting density.

**Scheme I.** Syntheses of graft copolymers

Ring-Opening Metathesis Polymerization (ROMP) has been established as the most common metathesis polymerization technique and become a powerful tool for the synthesis of well-defined graft copolymers according to the macromonomer route since the development of well-defined initiators.⁴ ROMP is an efficient synthetic method to polymerize unsaturated constrained rings such as norbornene, oxanorbornene, cyclobutene, and cyclooctene using metal alkylidene initiators. The discovery of well-defined molybdenum-based and ruthenium-based initiators has allowed polymerization without side reactions such as chain transfer and termination, giving rise to graft copolymers with narrow dispersity and precise control of functionality.⁵ Moreover, the large number of initiator systems based on transition metals can tolerate a wide range of

functionalities and the polymerization may be operated under mild conditions, such as room temperature and short reaction time.

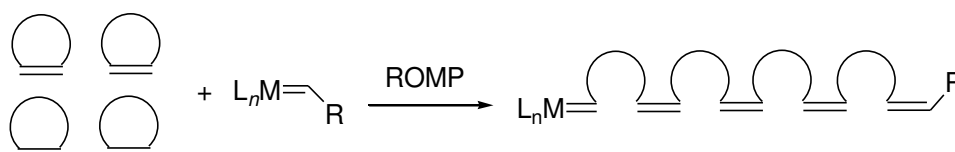
The “grafting through” method requires the previous synthesis of macromonomers, which are polymer chains containing a polymerizable end-group. The synthesis of macromonomers can be accomplished by almost any available polymerization techniques. In this chapter, we thus introduce the studies of ROMP, ring-opening polymerization (ROP) and almost precise synthesis of macromonomers containing a ROMP-able group bearing of poly(ethylene oxide) (PEO) chains or poly(ϵ -caprolactone) (PCL) chains and their ROMP to generate well-defined graft copolymers according to the macromonomer route.

I. Ring-opening metathesis polymerization

I.1. Introduction

Polymer chemistry has exploded within the twentieth century thanks to the development of many new polymerization methods. Although a relatively new polymerization process, ROMP has emerged as a powerful and applicable method for the synthesis of polymers which have complex architectures and useful functions.⁶⁻⁸


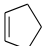
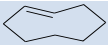




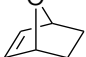
ROMP reaction, first studied in 1960s, has a mechanism based on olefin metathesis (from the Greek “meta” as changing and “thesis” as place). The mechanism of ROMP involves the reformation of double bonds simultaneously with the opening of unsaturated cyclic monomers. Thus, the number of double bonds is retained and the resulting polymers are constituted of repeating units containing carbon-carbon double bonds (Scheme I.1). The advances in ROMP can be attributed to tremendous efforts made by a large number of researches focusing on the development of well-defined transition metal alkylidene complexes as catalysts giving access to a wide range of polymers with well-defined structures and functions.⁹⁻¹¹



Scheme I.1. The formation of macromolecules *via* ROMP

The common cyclic olefin monomers used in ROMP include cyclobutene (CB), cyclopentene (CP), cyclooctene, norbornene (NB) and oxanorbornene (ONB) (Table I.1). Those unsaturated cyclic monomers possess a considerable strain energy¹² (> 5 kcal/mol) that is released during polymerization to provide enough driving force to overcome the unfavorable entropy change or free enthalpies for polymerization $\Delta G^0 < 0$.¹³ Like most of olefin metathesis reactions, ROMP is generally reversible but it is equilibrium-controlled. The equilibrium ring-chain distribution of resulting polymers of ROMP can be predicted by considering the thermodynamics *via* combined computational and theoretical methods from the free energy changes of reaction.^{2, 14}

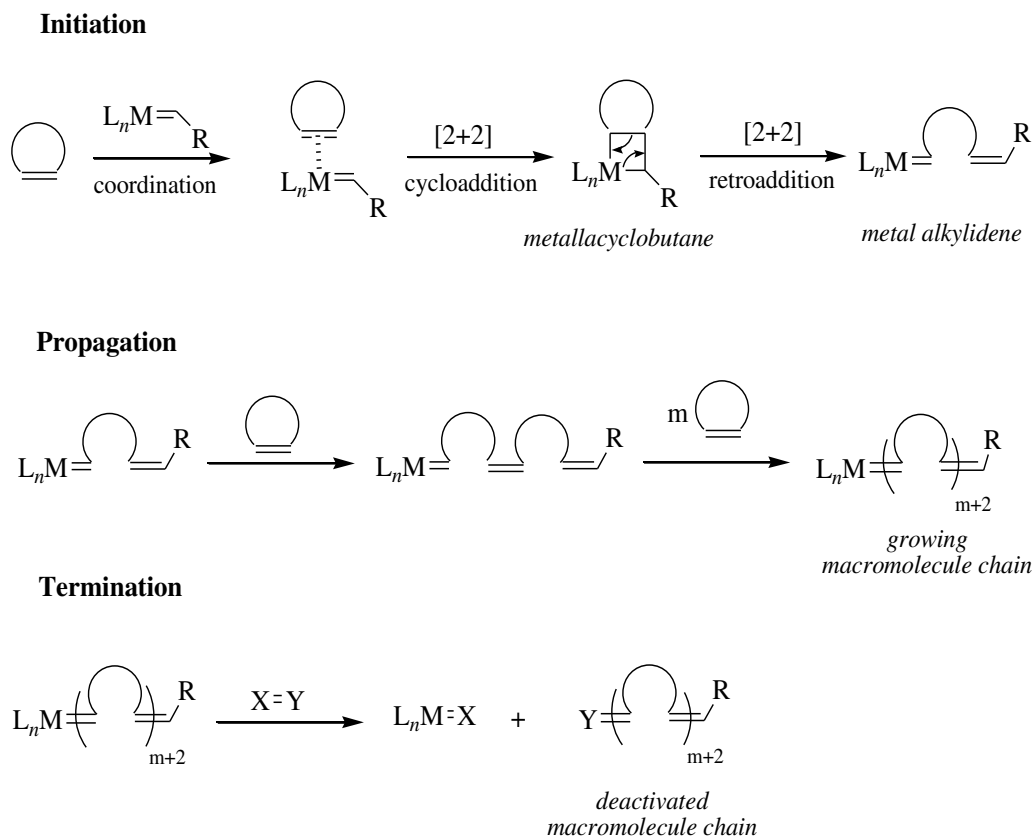
Table I.1. Structure and ΔG^0 for bulk polymerization of ROMP-able monomers¹³⁻¹⁵

Monomer	Structure	ΔG^0 (kJ/mol)
Cyclobutene		-105 ¹³
Cyclopentene		-6.3 ¹⁵
Cyclooctene (<i>trans</i>)		-20 ¹⁴
Cyclooctene (<i>cis</i>)		-19 ¹⁴
Cyclooctadi-1,5-ene (<i>trans</i>)		-24 ¹⁴
Cyclooctadi-1,5-ene (<i>cis</i>)		-19 ¹⁴
Norbornene		-47 ¹³
Oxanorbornene		Not known

I.2. ROMP mechanism

The first mechanism of olefin metathesis reaction was proposed by Herisson and Chauvin in 1971.¹⁶ The first step of ROMP mechanism involves coordination of a cyclic olefin to a transition metal alkylidene complex. Subsequent [2+2] cycloaddition affords a four-membered metallacyclobutane intermediate which forms the beginning of a growing polymer chain. This intermediate undergoes a retroaddition to afford a new metal alkylidene. Then the double bond from a new cyclic olefin monomer reacts with

the metal alkylidene in the same way during the propagation step until the polymerization stops. The termination of polymerization process is performed through the addition of a reagent which causes the deactivation of the transition metal alkylidene and removes it from the end of polymer chain. This reagent may also install a functional end-group onto the generated polymer (Scheme I.2).

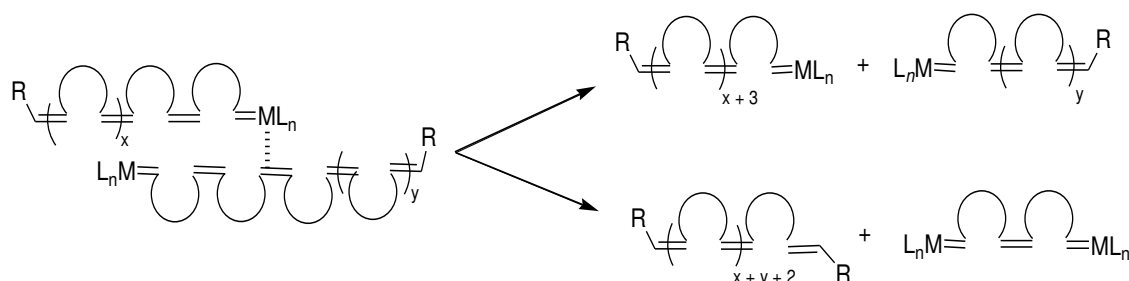


Scheme I.2. Mechanism of ROMP

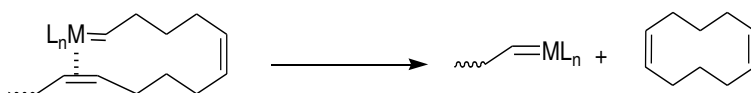
Secondary metathesis reactions can affect the ROMP process. The transition metal alkylidene complex can re-coordinate either onto an adjacent polymer alkene (intermolecular process or cross metathesis) or onto the growing polymer chain itself (intramolecular process, “backbiting” or ring-closing metathesis reaction) to produce macrocyclic oligomers (Scheme I.3). In an intermolecular chain-transfer reaction, the active metal alkylidene-terminated group on one polymer chain can react with any double bond along the backbone of an adjacent polymer chain. This transfer keeps the total number of polymer chains unalterable but the molar mass of individual polymers will increase or decrease accordingly. In an intramolecular reaction, the active metal alkylidene-terminated group reacts with any olefin group of itself to release a cyclic

oligomer and a polymer chain of reduced molar mass. Thus, chain-transfer reactions (intermolecular and/or intramolecular) effectively broaden the molar mass distribution (or dispersity) of the polymer system. It is necessary to minimize the chain-transfer reactions to generate well-defined polymer structures and controlled polymerization.^{6,7}

Intermolecular chain transfer



Intramolecular chain transfer (back-biting)



Scheme I.3. The secondary metathesis reactions in ROMP

1.3. ROMP: a living polymerization

The ‘living polymerization’ was defined as a ‘no chain transfer or termination’ process¹⁷, and affords polymers that have narrow molar mass distributions. In case of considered ‘living and controlled’ ROMP, the polymerization needs to exhibit following parameters: (i) a faster rate of the initiation step compared to the rate of propagation step, resulting in a high value of k_i/k_p (wherein k_i and k_p represent the initiation and propagation rate constants, respectively), (ii) a linear relationship between the degree of polymerization DP_n and the total monomer conversion and (iii) a narrow distribution of molar masses of obtained polymers or low dispersity values ($D_M < 1.5$).¹⁸ In case of ‘living and controlled’ polymerization, the synthesis of well-defined macromolecules with low dispersity and predictable molar masses are controlled by the initial monomer concentration to the initial initiator concentration ratio ($[M]_0/[I]_0$). In addition, it can give rise to well-defined block, graft and other architectural types of copolymers, or end-functionalized copolymers.¹⁹

In order to attain afore mentioned parameters, it is necessary to use very specific initiators (catalysts).^{*} They should include the following characteristics: (i) the conversion to growing polymer chain has to be fast and quantitative, (ii) the mediated polymer chain has to grow without any appreciable amount of chain transfer or premature termination, and (iii) the growing chain reacts with terminating agents to generate selective end-functionalization. Furthermore, initiators have to display a good solubility with common solvents and a high stability toward moisture, air and functional groups.⁷

1.4. From multi-components to well-defined single-component initiators

Early initiating systems were heterogeneous mixtures, sensitive toward air and moisture, and difficult to characterize. Those structurally “poorly-defined” initiator systems consisted in a mixture of metallic salts and alkylated compound or transition metallic salts such as: $\text{WCl}_6/\text{SnBu}_4$ ²⁰, $\text{W}(\text{CO})_6/\text{EtAlCl}_2$, $\text{WOCl}_4/\text{EtAlCl}_2$, $\text{MoO}_3/\text{SiO}_2$ ²¹⁻²³, $\text{MoCl}_5/\text{Et}_3\text{Al}$ ^{24,25}, $\text{Re}_2\text{O}_7/\text{Al}_2\text{Cl}_3$ ²⁶ ...

Those initiator systems rely on the “in situ” generation of the active metal-carbene species in the presence of strong Lewis acids and harsh conditions that make them incompatible with functional groups. ROMP which is initiated by such catalyst systems presents a slow initiation step leading the propagation step is also hard to control as a consequence of the instability of active species, leading to chain transfer reactions and to polymers with ill-defined structures.²⁷

The field of ROMP has found a growing interest in the last forty years due to the development of well-defined discrete carbene initiators with an improved tolerance toward functional groups and the ability to promote living polymerizations.

The development of stable metal-carbene and metal-alkylidene species (Figure I.1) instead of “in situ” metal-carbene species has allowed to overcome these disadvantages.¹¹ The first research using well-defined initiators for ROMP has been

^{*} The initiator in ROMP is named catalyst, although it is not a real catalyst that can be recovered after the reaction.

reported by Katz in 1976.^{28,29} They used the initiators **I1** and **I2** (Figure I.2) based on tungsten (W-based) for the ROMP of CB, COD and NB. Polymers with controlled number-average molar mass (M_n) have been reported for the first time but relatively high dispersity values ($D_M > 1.85$) have been obtained, because of incomplete initiation step and chain transfer reactions.

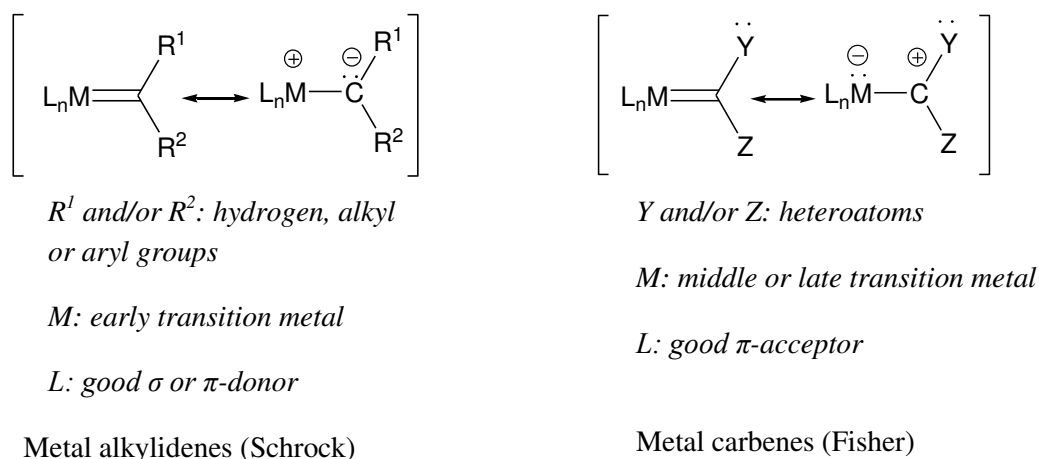


Figure I.1. Metal carbene and metal alkylidene species

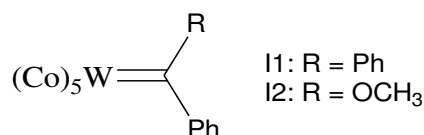


Figure I.2. First well-defined initiators based on tungsten **I1** and **I2**

Various metal-carbene complexes based on titanium (Ti-based) and tantalum (Ta-based) have been also used as initiators for ROMP. Gilliom *et al.* synthesized first well-defined catalysts based on titanium named bis(cyclopentadienyl)titanacyclobutane **I3** and **I4** (Figure I.3).^{30,31} ROMP of NB using **I3** or **I4** as catalyst generated a polynorbornene (PNB) with low dispersity values ($D_M < 1.1$) and M_n , determined by size exclusion chromatography (SEC) with a refractive index (RI) detection, which increased linearly with the monomer conversion. Cannizzo and Grubbs reported the synthesis of block copolymers from NB, dicyclopentadiene (DCP) with low dispersity values ($D_M = 1.08 - 1.14$) for diblock PNB-*b*-PCDP and triblock PCDP-*b*-PNB-*b*-PCDP copolymers with DP_n up to 50 for each segment using the initiator **I5** (Figure I.3) based

on titanacyclobutane.³² The Ta-based initiator **I6** (Figure I.3) has been used to perform a controlled polymerization of NB.³³ The Ti and Ta complexes are highly Lewis acidic as a result of extremely high oxidation states. These complexes react rapidly with heteroatom-containing functional groups leading to a limitation in their use in ROMP.

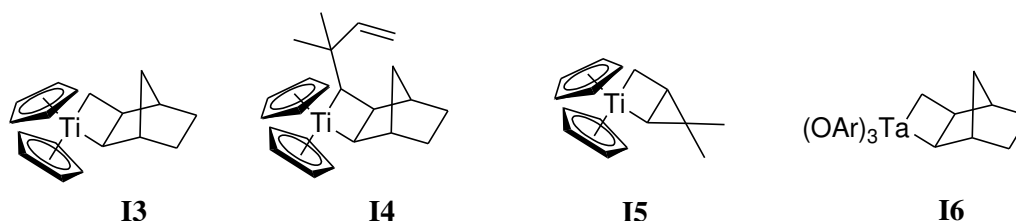


Figure I.3. Metal-cyclobutane complexes initiators based on titanium and tantalum for ROMP

The metal-alkylidene catalysts based on tungsten complexes (W-based) have also been used to initiate ROMP. Initiator **I7** (Figure I.4) allowed the well-controlled polymerization of NB with predictable M_n increasing with the ratio of initial monomer concentration to initial initiator concentration and low dispersity values ($D_M < 1.07$).³⁴ The W-based catalyst **I8** (Figure I.4) showed a reactivity in ROMP of derivative mono- and diester substituted NB derivatives at low temperature that depended on position and orientation of ester substituent.³⁵ The initiator **I9** (Figure I.4) has resulted in high stereoselectivity of the generated poly(1-methylnorbornene) explained on the basis of the favored configuration of the tungstacyclobutane intermediate with the two bulkiest alkyl substituents in 1,3-diequatorial positions.³⁶

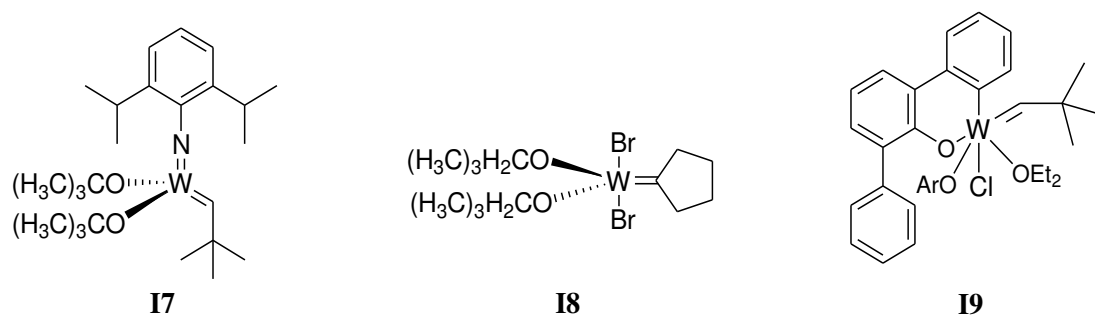


Figure I.4. Well-defined tungsten-based initiators for ROMP

Schrock's team and some other groups introduced the well-defined molybdenum alkylidene complexes (Mo-based) as initiators for ROMP. Although structurally similar to tungsten alkylidene complexes, these initiators exhibited a significant advance as they are efficient for a broader range of functionalized monomers containing ester, amide, ether, halogen, cyano groups... Thus, the initiators Schrock 1, 2 and 3 (Figure I.5) have been used in various polymerizations of NB, ONB, CB, or CP functionalized derivatives. Mo-based catalysts showed a greater tolerance toward oxygen, moisture and other impurities, and also were found to be more stable toward decomposition and side reactions.³⁷⁻⁴⁰ In addition, Mo-based catalysts also gave the capability to provide stereoregular polymers as reported by Bazan *et al.*⁴¹ and Feast *et al.*⁴² Polymers obtained from the living ROMP of 2,3-bis(trifluoromethyl)bicyclo[2.2.1]hepta-2,5-diene catalyzed by Schrock 1 were highly tactic with a > 98 % *trans* olefin group along the polymer backbone, but the same ROMP with Schrock 3 as catalyst led to a polymer with a > 98 % *cis* olefin content.^{41, 42}

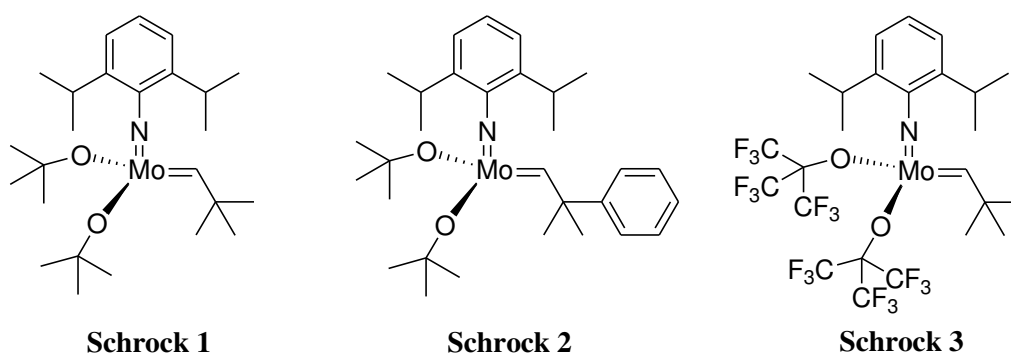


Figure I.5. Well-defined molybdenum-based initiators for ROMP

Early reports on the use of ruthenium alkylidene complex systems (Ru-based) in ROMP were published from the 1960s using the ill-defined $\text{RuCl}_3(\text{H}_2\text{O})_n$ ^{43,23} which facilitated the polymerization of various norbornene derivatives in protic media.⁴⁴ Nevertheless, the development of new well-defined Ru-based catalysts originates from the end of the 1980s.⁴⁵ Ru-based catalysts show a remarkable tolerance toward oxygen, water and functional groups.⁴⁶ Thus, the Ru-based system initiators have been used to polymerize a wide range of monomers and become the most used catalysts in ROMP today. The Grubbs' first generation catalyst (Grubbs 1) (Figure I.6) which has been

easily synthesized *via* an addition of the terminal olefin followed by a phosphine exchange from $(\text{PPh}_3)_3\text{RuCl}_2$ ⁴⁷ has been used for the synthesis of a wide range of functionalized polymers.⁴⁸⁻⁵⁰ The substitution of one of the tricyclohexylphosphine ligands with the bulky *N*-heterocyclic carbene (NHC) ligand (1,3-dimesityl-4,5-dihydroimidazol-2-ylidene - H_2IMes) produces ruthenium complex Grubbs' second generation catalyst (Grubbs 2) (Figure I.6), which displays improved catalytic activity, maintaining the high functional group tolerance and thermal stability.⁵¹ Nevertheless, Grubbs 2 catalyst, as well as the Hoveyda-Grubbs 2 (Figure I.6), provided polymers with uncontrolled molar masses and high dispersity in most cases. These catalysts exhibited a slow rate of initiation step and led to competing secondary chain transfer reactions. Grubbs' third generation initiators (Grubbs 3 and 3') (Figure I.7), that have weaker coordinating pyridine ligands according to the phosphine ligand of Grubbs 2, have enabled rapid ROMP initiation while maintaining high activity. Choi *et al.*⁵² reported the ROMP of various NB and ONB derivatives using Grubbs 3 as catalyst. The resulting polymers, obtained at $-20\text{ }^\circ\text{C}$, have high DP_n (up to 400) with very low dispersity values ($\text{D}_M < 1.10$). The PNB obtained at higher temperature have higher dispersity value ($\text{D}_M = 1.65$ at room temperature) showing the influence of chain transfer reactions in ROMP on temperature.⁵²

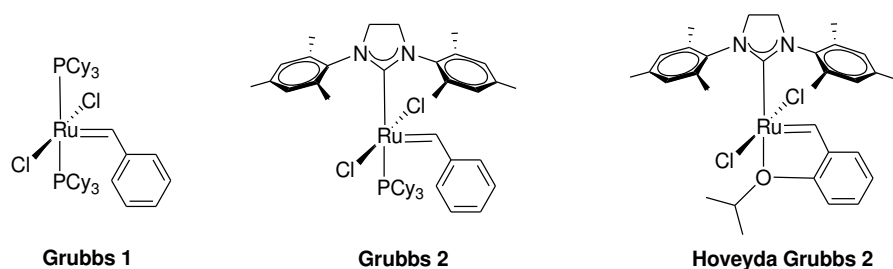


Figure I.6. Well-defined ruthenium-based Grubbs' first and second generations initiators for ROMP.

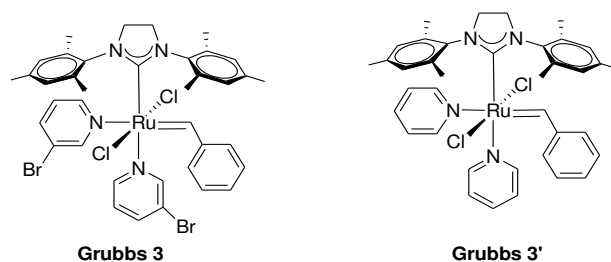
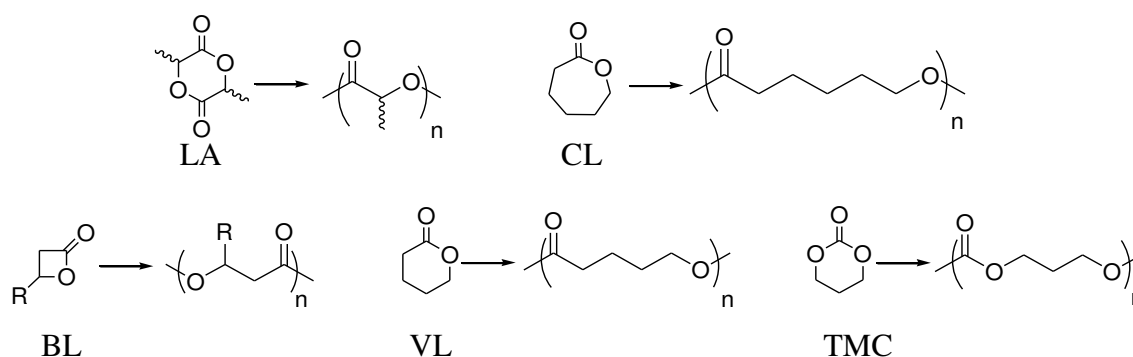


Figure I.7. Well-defined ruthenium-based Grubbs' third generation initiators for ROMP.

II. The polymerization of lactones via ROP

II.1. Introduction

Ring-Opening Polymerization (ROP) has been used since the beginning of the 1900s in order to polymerize cyclic monomers containing heteroatoms in the ring.⁵³ In particular, ROP has been proved as a useful synthetic route to introduce interesting polymers with controllable properties, for preparing biodegradable polyesters such as polylactones or polylactides from cyclic esters.⁵⁴ The ROP of cyclic esters was investigated in the 1930s as firstly reported by Carothers.^{55,56} Cyclic ester monomers including 1,3-trimethylene carbonate (TMC), lactic acid (LA), δ -valerolactone (VL), β -butyrolactone (BL), and ϵ -caprolactone (CL) (Scheme I.4)^{57,58,59,60} have demonstrated their reactivity in ROP.



Scheme I.4. Cyclic ester monomers and their corresponding polymers

ROP is carried out in the presence of catalysts and initiators. The mechanism of polymerization depends on the initiator type. The three major reaction mechanisms are cationic, anionic and coordination-insertion. However, high molar mass polymers have only been obtained by using anionic or coordination-insertion ROP.⁵⁷

II.2. ROP with organometallic catalysts

Since the first study of Klein *et al.*⁶¹ in the 1950s related to the metal-based catalytic systems for ROP of lactide, numerous researches have been carried out to enlighten the mechanism of coordination-insertion polymerization. A broad range of

initiators containing a metal center and ligands have been studied⁶² (Figure I.8) and allowed the preparation of well-defined polyesters.

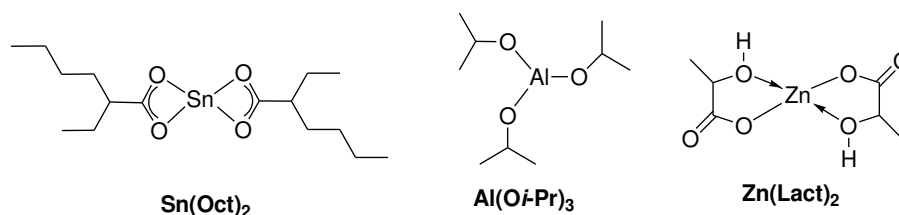
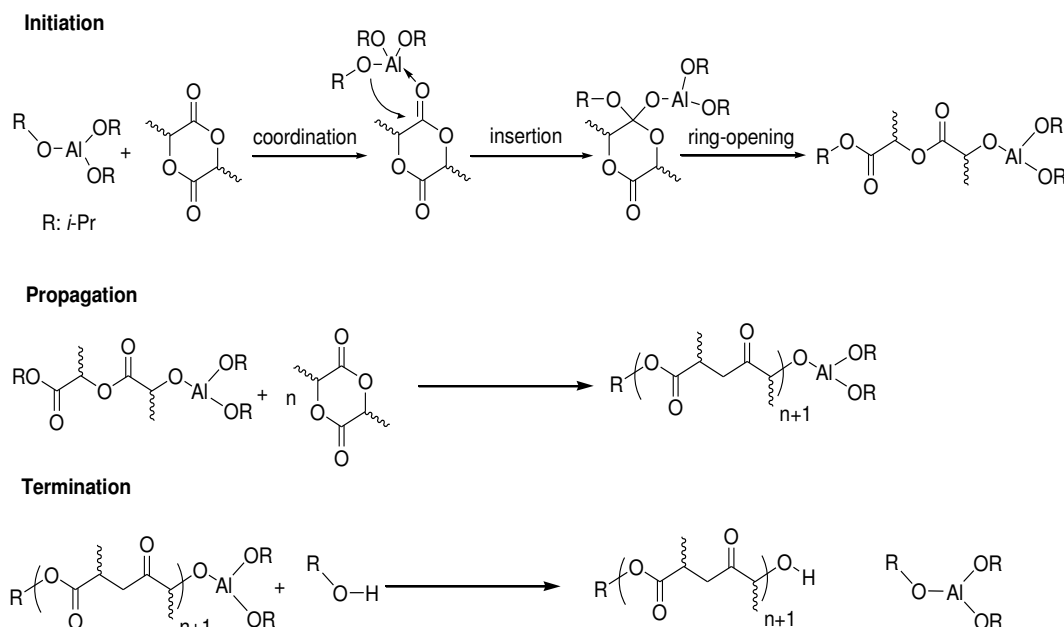


Figure I.8. Metal-based catalysts for ROP

The first three-steps coordination-insertion mechanism for the ROP of cyclic esters was reported by Dittrich *et al.* in 1971.⁶³ Teyssie⁶⁴ and Kricheldorf⁶⁵ independently provided experimental proofs of the mechanism of the ROP of lactide with aluminium isopropoxide ($\text{Al}(\text{O}i\text{-Pr})_3$) as the catalyst/initiator system (Scheme I.5). The first step consists in the coordination of a monomer to the Lewis-acidic metal center followed by the insertion of the alkoxy group onto the carbonyl carbon *via* nucleophilic addition. The lactone ring then typically opens *via* acyl-oxygen cleavage. The deactivation of metal-alkoxide bond occurs with the addition of a reagent to form a hydroxyl end group.



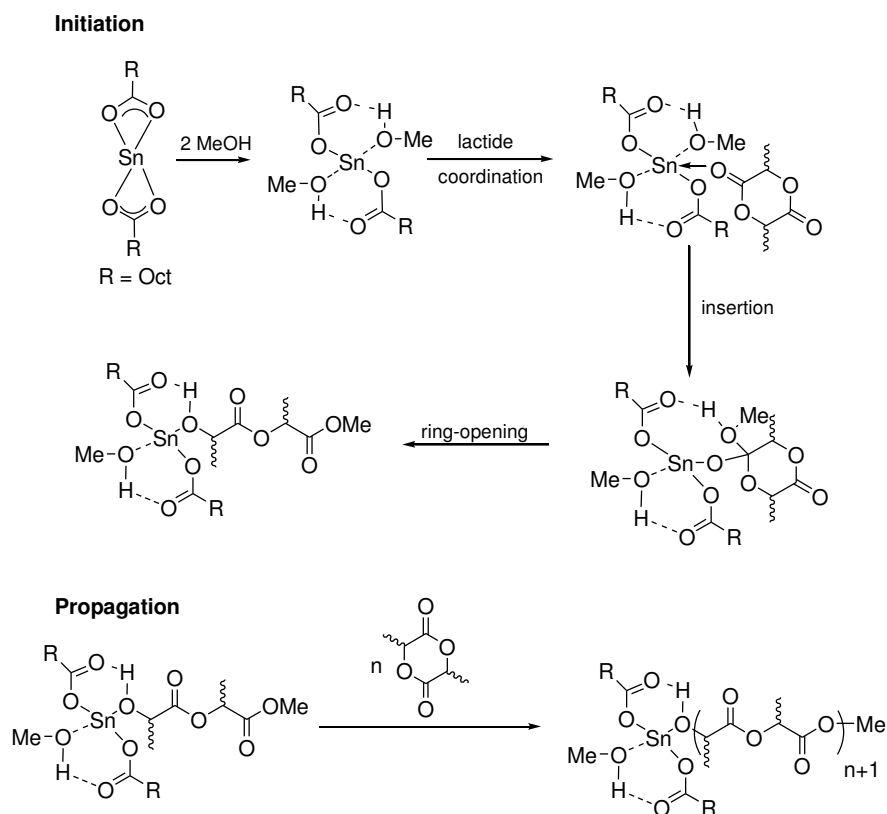
Scheme I.5. Coordination-insertion mechanism of polymerization of lactide with $\text{Al}(\text{O}i\text{-Pr})_3$ as the catalyst/initiator system⁵⁹

Teyssie and co-workers⁶⁶⁻⁶⁸ also reported the first successful use of $\text{Al}(\text{O}i\text{-Pr})_3$ as a catalyst/initiator system for ROP of CL. $\text{Al}(\text{O}i\text{-Pr})_3$ initiated ROP of CL according to a

coordination-insertion mechanism similar to LA. The polymerization of CL is generally carried out in solution (toluene, THF).⁶⁷ The resulting polymers formed a quantitative monomer conversion and showed narrow molar masses distribution at low temperature ($\bar{M}_n = 1.10$, yield of 100 % using a $[\text{CL}]_0/[\text{Al}]_0$ molar ratio equal to 482:1 at 0 °C).⁶⁸ The effect involved by the presence of a dissociating agent such as isopropanol to the ROP of CL was also reported.⁶⁸

Among the organometallic catalyst systems, catalysts based on tin (Sn-based) have become the most widely used complex as catalyst/initiator for ROP. Tin (II) bis(2-ethylhexanoate) ($\text{Sn}(\text{Oct})_2$) is well-known as a very effective and versatile catalyst for ROP of lactides and lactones. It is soluble in common organic solvents and lactone monomers, easy to handle and commercially available.⁵⁹ $\text{Sn}(\text{Oct})_2$ has a high catalytic reactivity: typical reaction times in bulk at 140 - 180 °C range from minutes to a few hours and allows the preparation of high molar mass polymers.⁵⁹ ROP with $\text{Sn}(\text{Oct})_2$ was found to be fast and well-controlled in the presence of highly active reagent such as an alcohol.^{69,70} Although the mechanism of ROP using $\text{Sn}(\text{Oct})_2$ is rather complicated, coordination-insertion mechanism is commonly accepted (Scheme I.6).⁷¹⁻⁷³ The first step includes the coordination of an alcohol or H_2O to $\text{Sn}(\text{Oct})_2$ followed by the coordination of lactones to the alkoxy-coordinated tin-center (Scheme I.6). It is also accepted that the ROP with $\text{Sn}(\text{Oct})_2$ can be initiated with active-hydrogen impurities in monomers. Finally, besides their involvement in polymerization initiation, protic reagents may also participated to reversible chain transfer reactions with the growing chain, making it essential to optimize carefully of the initial molar ratio of protic reagents and $\text{Sn}(\text{Oct})_2$.⁷²

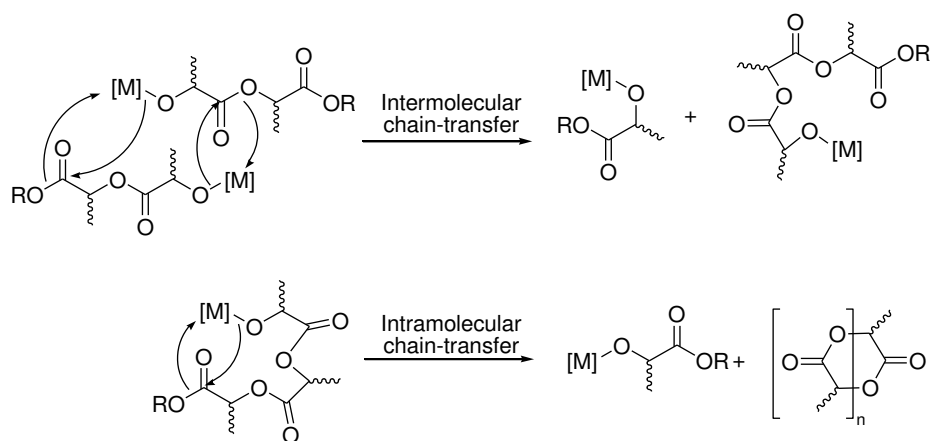
In comparison to ROP of cyclic esters using Sn-based and Al-based catalysts, the mechanism of ROP using zinc-based (Zn-based) catalysts has been much less studied. The combination of zinc lactate $\text{Zn}(\text{Lact})_2$ and a primary alcohol was demonstrated to increase the ROP reactivity of LA compared to Al-based catalysts and allows a well-controlled polymerization in a similar way as with Sn-based catalysts.⁷⁴



Scheme I.6. Initiation and propagation steps of the ROP using $\text{Sn}(\text{Oct})_2$

The molar mass control in organometallic-initiated coordination-insertion polymerization depends on the k_i/k_p ratio⁵⁹ (wherein k_i and k_p represent the initiation and propagation rate constants, respectively) but also on the presence of chain-transfer reactions when the ROP is carried out at high temperature and/or long reaction time.⁵⁷ These side reactions can occur both intermolecularly (between active metal alkoxide end-group and ester group of an adjacent polyester chain) and intramolecularly (between active metal alkoxide end-group and an ester group of the polyester chain and cyclic oligomers themselves)⁷⁵ (Scheme I.7) and lead to an increase in dispersity values of polyesters, sometimes making the molar masses of the resulting polymers irreproducible.⁵⁹ The extent of the undesirable chain-transfer reactions was found to strongly depend on the organometallic catalyst.⁷⁵ Transesterifications occur from the very first step of ROP of LA using $\text{Sn}(\text{Oct})_2$ but only at high monomer conversion with $\text{Al}(\text{Oi-Pr})_3$.

The use of $\text{Sn}(\text{Oct})_2$ as catalyst to obtain PCL-PLA block copolymers was reported by In't Veld *et al.*⁷⁶ in 1997. The bulky ROP of CL catalyzed by $\text{Sn}(\text{Oct})_2$ in the presence of ethanol as initiator is quantitative using a $[\text{CL}]_0/[\text{Sn}(\text{Oct})_2]_0$ molar ratio of 1000:1 at 110 °C. The PCL-*b*-PLA copolymers have been successfully prepared by successive addition of CL and LA as CL was polymerized first. When the synthesis of PLA-*b*-PCL copolymer was targeted by successive addition of LA followed by the addition of CL, a random PCL-PLA copolymer was obtained.



Scheme I.7. Chain-transfer reaction in ROP using an organometallic catalyst

Numerous studies reported that $\text{Sn}(\text{Oct})_2$ and other metal-based catalysts have not been completely removed by a purification method involving dissolution and precipitation.^{77,78} Although US Food and Drug Administration has approved $\text{Sn}(\text{Oct})_2$ as a food additive, the associated toxicity of most tin compounds is a disadvantage for its uses in biotechnology. Thus, while extraordinary advances have been made in organometallic catalysts in ROP,^{57,58} the metal-free organocatalysts are attracting growing interest as more economically and environmentally friendly alternatives for the ROP of polyesters.⁵⁹

II.3. ROP with organocatalysts

Organic-based catalysts in ROP have become a powerful alternative to metal-based catalysts. Many organocatalysts are simple, commercially available molecules that are typically easily purified and have long shelf lives thanks to their insensitivity to water and oxygen. Furthermore, organocatalysts are well suited to a wide range of reaction

conditions, solvents, and monomers. Finally, they are typically very easy to remove from the resulting polymers.⁷⁹

The first study of the use of an organocatalyst in ROP was reported by Nederberg *et al.*^{80,81} They used 4-(*N,N*-dimethylamino)pyridine (DMAP) (Figure I.9) as the catalyst for ROP of LA. Following the use of DMAP as a ROP catalyst, the field of organocatalysts for ROP has rapidly expanded and a wide range of nucleophilic bases was investigated for their activity in ROP. One of the most successful and widely studied catalyst belongs to the family of NHCs (Figure I.9).^{82,83} NHCs have been applied to a wide range of monomers including lactones^{84,85} and cyclic carbonates⁸⁶ and display extremely high reactivity during ROP of LA as 88 % of monomer was converted after 25 seconds at ambient temperature for a LA-to-initiator initial molar ratio ($[LA]_0/[I]_0$) of 200:1.⁸⁷ However, NHCs are sensitive toward air and are deactivated in the presence of water leading to long term storage problems.⁷⁹ While several methods related to the *in situ* generation of NHCs were reported,⁸⁸⁻⁹⁰ organic ‘super bases’ such as guanidine derivatives including 1,5,7-triazabicyclo[4.4.0]dec-5-ene (TBD) (Figure I.9), 1,8-diazobicyclo[5.4.0]-undec-7-ene (DBU) (Figure I.10), phosphine bases (Figure I.9) as well as organic acids (Figure I.10) allow to make ROP more accessible because of their high reactivity.⁷⁹

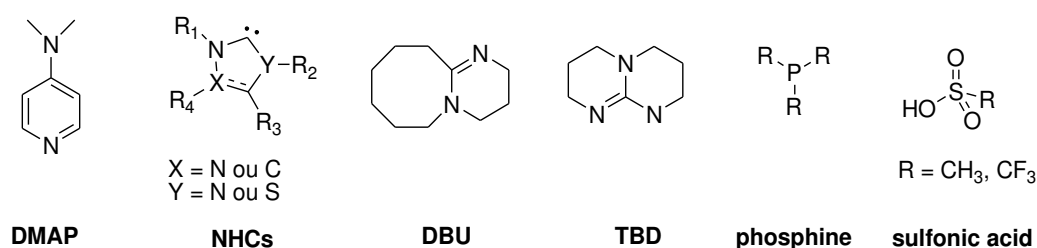
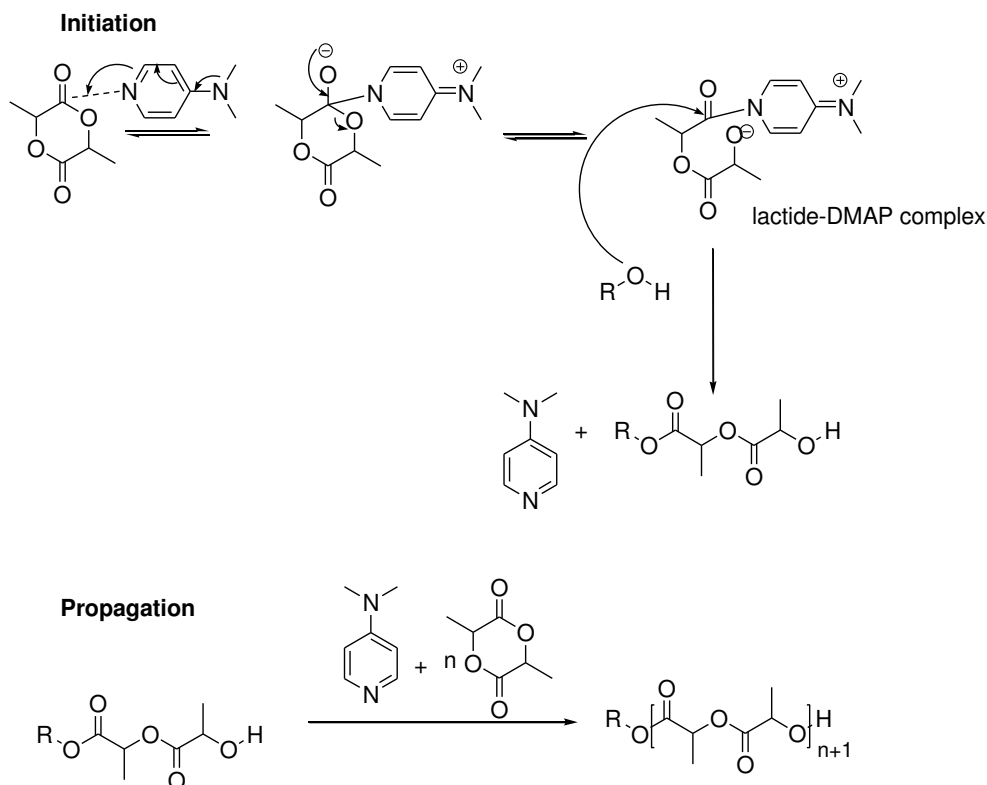


Figure I.9. Organocatalysts for ROP

The ROP of LA using DMAP as a catalyst was carried out in the presence of a primary or secondary alcohol used as the initiator. The resulting poly(lactic acid) (PLA) have DP_n up to 120 with a D_M of 1.14. A modest conversion of LA was observed with a DMAP-to-initiator initial molar ratio $[DMAP]_0/[I]_0$ of 0.1:1 after a long reaction time ($DP_{n,NMR} = 5$ after 96 h with an initial molar ratio $[LA]_0/[DMAP]_0/[I]_0 = 30:0.1:1$). The increase of DMAP-to-initiator molar ratio from 0.1:1 up to 2:1 led to the quantitative conversion with shortening reaction time ($DP_{n,NMR} = 29$ after 5 minutes of reaction with

an initial ratio $[LA]_0/[DMAP]_0/[I]_0 = 30:2:1$).^{80,81} Compared to metal complexes, long reaction times do not induce the broadening of molar masses distribution, indicating that the undesirable chain-transfer reactions are less effective. Bulk polymerization of LA using benzyl alcohol as the initiator also gave low \bar{D}_M values in 15-20 minutes depending on the targeted molar mass. The living character of polymerization was demonstrated by the linear correlation of molar mass *versus* monomer conversion in addition to experimental M_n closed to the predicted M_n based on monomer to initiator ratios and to narrow molar masses distributions.

Polymerization using DMAP as the catalyst was proposed to occur through monomer-activated mechanism (Scheme I.8) as an alcohol-activated mechanism cannot be ruled out. The mechanism involves a nucleophilic attack by DMAP on the lactide monomer to generate a lactide-DMAP complex. The protic initiator R-OH would react with this complex to form the hydroxyl-terminated ring-opened monomer with simultaneous liberation of the nucleophilic catalyst. Polymerization proceeds by reaction of the ω -hydroxyl-terminated group on growing polymer chain with a new lactide-DMAP complex. The use of DMAP as an organocatalyst has been extended to the ROP of CL using polysaccharide chitosan as the initiator in the presence of water as the swelling agent.⁹¹ Attempts by Jaipuri *et al.*⁹² to polymerize BL using DMAP as a catalyst resulted in only oligomers with $DP_n < 8$. VL and CL were polymerized in bulk using DMAP/DMAP-trifluoromethane sulfonic acid (TfOH) (Figure I.10) catalytic system: resulting PVL and PCL were obtained with high monomer conversions in the presence of *p*-phenylbenzylalcohol used as an initiator with a long time reaction.⁹³



Scheme I.8. Initiation and propagation steps of the ROP of LA using DMAP as the catalyst

The ROP using phosphorus-based and sulfur-based derivatives as catalysts was also studied (Figure I.10). Phosphorus-derived bases have shown a similar reactivity in ROP in comparison to the pyridine-based catalysts. In the presence of a benzyl alcohol initiator, phosphazene was found to be an effective ROP catalyst, generating narrow dispersed PLA ($D_M = 1.11-1.40$) with predictable molar masses ($DP_n = 30-100$).⁹⁴

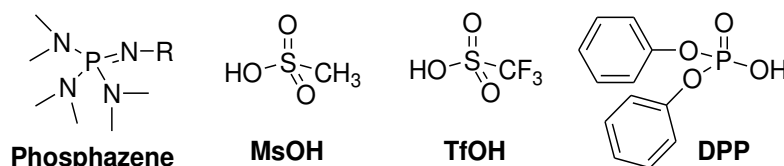
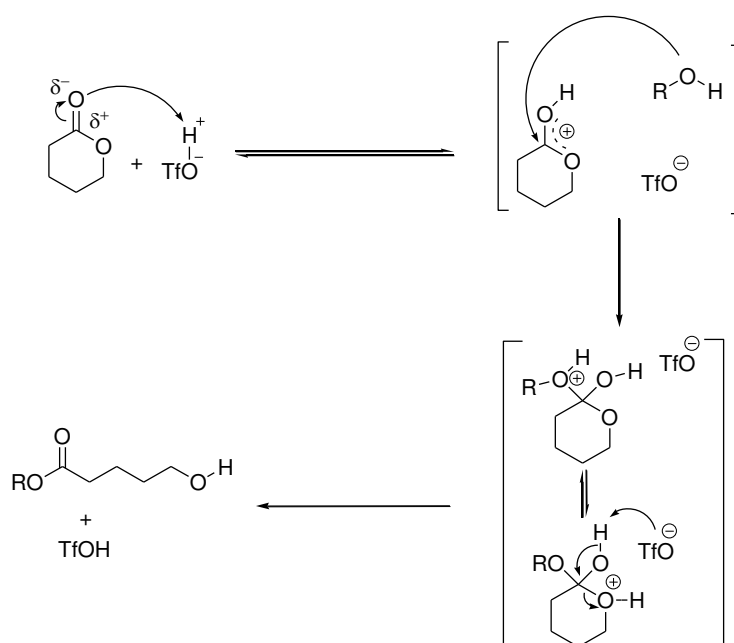


Figure I.10. Phosphorus-based and sulfur-based catalysts for ROP

In opposition with phosphorus-derived bases, the sulfur- and phosphorus-based acids catalysts showed a better reactivity in ROP of lactones such as VL and CL

compared to diester cyclic monomer (LA). TfOH and methyl sulfonic acid (MsOH) showed to be efficient catalysts for ROP of CL.^{95,96} Use of diphenylphosphate (DPP) in ROP of VL and CL generates well-controlled polymers with high monomer conversions.^{97,98} ROP using acids as catalysts can be described according to a monomer-activated cationic mechanism (Scheme I.9).^{99,100} Initiation of ROP occurs with the protonation of cyclic monomers followed by a nucleophilic attack from hydroxyl group of initiator followed by an elimination to open the cyclic ring. The propagation occurs in the same way with the nucleophilic attack from hydroxyl group of growing polymer chain onto the protonized monomer. The reaction stops since the presence of bases to neutralize the acid functionality.



Scheme I.9. Initiation step of the acid-catalyzed ROP of CL

In 2001, the carbene 1,3-bis(2,4,6-trimethylphenyl)imidazol-2-ylidene (IMes) (Figure I.11) was shown to catalyze the ROP of LA in the presence of an alcohol initiator in seconds at ambient temperature with a catalyst-to-monomer molar ratio of 0.5:100. The resulting PLAs were generated with well-defined molar masses and narrow dispersity values ($D_M < 1.16$).⁸⁷ A wide range of NHCs (Figure I.9) has shown to be efficient for ROP and the activity and selectivity behaviors toward polymerization

depend on the nature of carbenes and monomers.^{59,101} Recent studies indicate that the ROP of lactones such as BL, VL and CL using IMes as catalyst for ROP of lactones required longer polymerization times and generally resulted in broader molar mass distributions compared to LA.^{58,85} The less sterically demanding carbene 1,3-bis(dimethyl)imidazol-2-ylidene (IMe) (Figure I.11) polymerized CL, VL and BL with a good efficiency at ambient temperature to give polyesters with low dispersity values ($\bar{D}_M = 1.16 - 1.32$).^{85, 102}

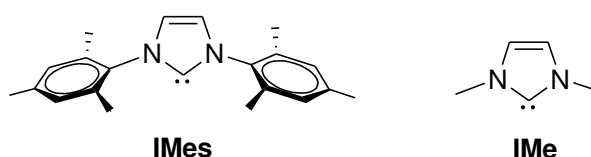


Figure I.11. NHCs catalysts for ROP

Bifunctional thiourea/amine¹⁰³ catalysts (Figure I.12) are of particular interest as their activity depends on the presence of both an electrophile-activation thiourea and a nucleophile-activating amine, making them suitable for dual activation of an electrophilic lactone and nucleophilic alcohol in ROP.

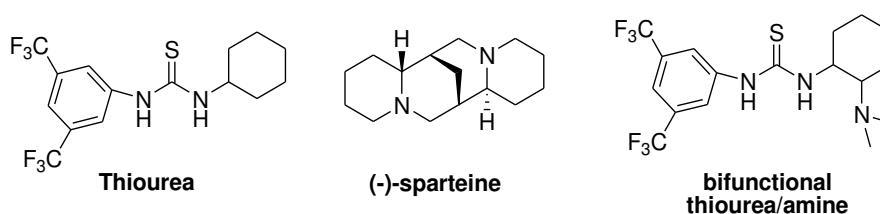


Figure I.12. Thiourea/amine catalysts for ROP

The thiourea/amine catalytic systems allowed the polymerization of LA with quantitative monomer conversions without any side reactions. Use of (-)-sparteine (Figure I.12) as the catalyst of ROP has also been found to provide an ideal balance

between reactivity and selectivity.¹⁰⁴ However, the use of thiourea/amine catalytic system leads to a slower ROP in comparison to the use of carbene as catalyst.¹⁰² Furthermore, such catalysts were found to be ineffective for polymerization of other cyclic esters such as VL or CL in comparison to LA.

The ‘super bases’ guanidine catalytic systems¹⁰³ (Figure I.12) have shown a stronger reactivity compared to (-)-sparteine. They give rise to polylactones at ambient temperature without any cocatalyst. Screening studies showed that DBU, TBD and *N*-methyl TBD (MTBD) (Figure I.13) are highly active catalysts for ROP in solution of LA using non-polar solvents.¹⁰⁵ The use of DBU or MTBD as catalyst in ROP of LA showed very high activity with a monomer conversion over than 98 % when initial $[LA]_0/[I]_0$ molar ratio is equal to 500:1. Side reactions only occurred with prolonged reaction time.¹⁰⁶ Cyclic esters such as VL and CL can be polymerized by TBD alone. ROP of these monomers using DBU and MTBD as catalysts can only occur in the presence of thiourea used as a cocatalyst.¹⁰⁵ In these conditions, the polymerization reached high monomer conversions (> 78 %) with initial $[lactones]_0/[I]_0$ molar ratios up to 200:1.

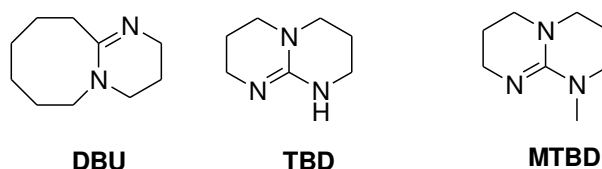
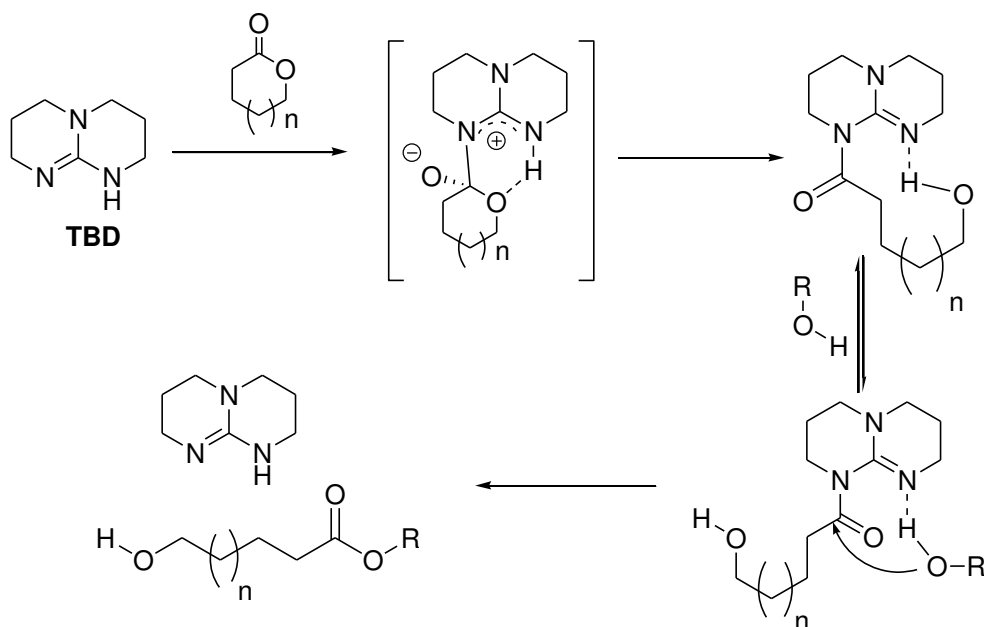


Figure I.13. Guanidine catalysts for ROP

TBD is well-known as the most active ROP catalyst in guanidine catalytic family. ROP of LA using TBD as the catalyst reached 95 % of monomer conversion after 1 minute of reaction at ambient temperature within a low catalyst to monomer molar ratio 1:1000 (1:200 for MTBD and 1:100 for DBU).¹⁰⁶ TBD also showed high reactivity in ROP of cyclic monomers which have low ring-strain energies such as CL, ω -pentadecalactone (PDL),¹⁰⁷ VL derivatives,¹⁰⁸ and δ -decalactone.¹⁰⁹ However, the high catalytic reactivity of TBD leads to secondary transesterification, broadening of molar masses distribution with reaction time.¹⁰⁵ Pratt *et al.*¹⁰⁵ suggested a monomer-activated

mechanism for the ROP using TBD, involving an acylation of TBD by the lactone, followed by displacement of the acylated TBD to the chain-end alcohol (Scheme I.10). The propagation of ROP using TBD occurs in the same way but is initiated by hydroxyl functionality of growing polymer chain. ROP stops in the presence of acid functionality to deactivate TBD. Isolation and characterization of ring-opened intermediate resulting from the reaction of TBD with BL provides support for this proposed mechanism.¹⁰⁴



Scheme I.10. Initiation step of the ROP of lactones using TBD as catalyst

II.4. Conclusion

The broad range of both initiators and catalysts for ROP offer different advantages and possibilities (Table I.2). Transition metal-based catalysts can be used for ROP of a wide range of cyclic ester monomers to produce high molar mass polyesters, but the sometimes or often difficult elimination of metal compound from products lead to the use of organocatalysts as an effective alternative. Organocatalysts complement transition metal catalysts because of their high reactivity at ambient temperature. In

addition, the easy elimination of organocatalysts allows the resulting polymers to be used in biological and microelectronic applications.

Table I.2. Organocatalytic ROP in comparison to transition metal-based catalytic ROP

Organocatalytic ROP	Transition metal-based catalytic ROP
<ul style="list-style-type: none">• High availability of the catalysts• No residual metal contaminant in resulting polymer• Easy elimination of catalyst• Reactions can take place at ambient temperature• Achievement of high molar mass polymers from active monomers• ROP of a wide range of monomers• Stereocontrolled ROP is possible	<ul style="list-style-type: none">• Low availability of the catalysts• Residual metal contaminants in resulting polymers• Difficult elimination of catalyst• Requirement of high temperature in almost cases• Achievement of high molar mass polymers• ROP of a wide range of monomers• Stereocontrolled ROP is difficult to achieve

III.Synthesis of graft copolymers from ROMP-able macromonomers including PEO and/or PCL

The “grafting through” method or macromonomer method which allows the control of grafts, backbone length, and grafting density is well-known as the most efficient pathway to synthesize graft copolymers through living or controlled/living polymerization techniques. Thanks to the development of well-defined catalysts, ROMP of macromonomers with a ROMP-able polymerizable end-group has become a well-established methodology for the synthesis of structurally precise polymers.

In particular, ROMP of poly(ethylene oxide) (PEO) macromonomers has been widely studied. PEO is a neutral, hydrophilic, highly mobile, synthetic polymer and non-toxic, which has found numerous applications in fields such as biomaterials and biotechnologies.¹¹⁰ Because of the unique properties of PEO, a wide range of complex structures of graft copolymers with PEO side chains has been designed in various ways, and hydrophilic PEO segments are usually combined with any hydrophobic component forming amphiphilic graft copolymers.¹¹¹

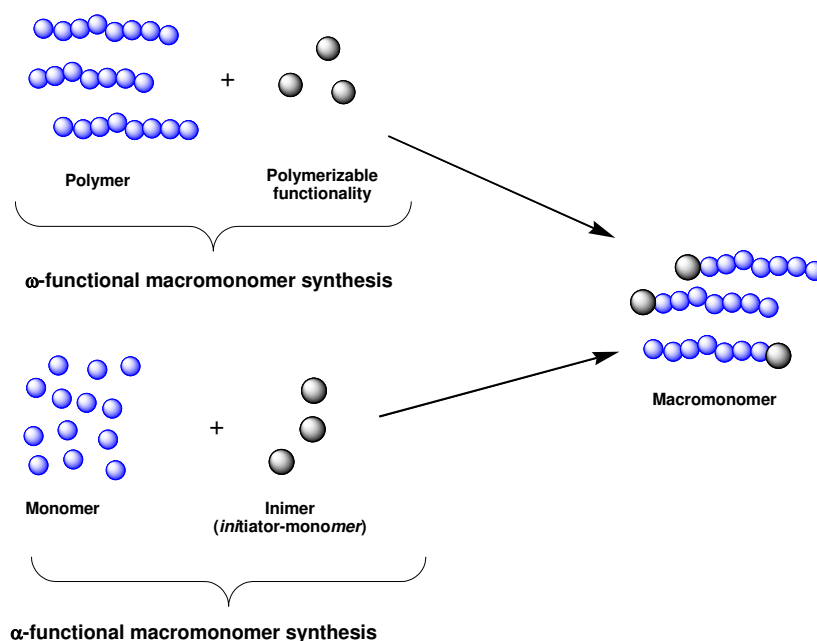
Combination of ROMP and ROP allows for the synthesis of graft copolymers based on polyesters, which degrade in a controlled fashion, with a broad range of properties. In the same way as for PEO macromonomers, a wide range of ROMP of poly(ϵ -caprolactone) (PCL) macromonomers has been studied. PCL is a non-toxic, hydrophobic aliphatic, semi-cristalline polymer, miscible with other polymers and biodegradable. PCL has been used in different fields of application such as biomaterials, microelectronic, adhesives and packaging since its properties can be controlled and made inexpensively.¹¹²

In this part, we thus introduce almost all examples for the precise synthesis of macromonomers containing PEO or PCL terminated by ROMP-able moieties by polymerization techniques such as anionic polymerization, chemical modification, ‘click’ chemistry and ring-opening polymerization (ROP). The synthesis of graft copolymer *via* ROMP of these macromonomers according to the “grafting through” method will also be described.

III.1. Synthesis of graft copolymers from PEO-based ROMP-able macromonomers

The ROMP-able PEO macromonomers can be obtained by two methods:

- The α -functionalized macromonomer synthesis, in which PEO is prepared *via* anionic polymerization from an initiator containing ROMP-able group.
- The ω -functionalized macromonomer synthesis, in which synthesized PEO by anionic polymerization is ω -functionalized with a ROMP-able group.



Scheme I.11. General methods of macromonomer synthesis

III.1.1. PEO-based ROMP-able macromonomers obtained by anionic polymerization

Héroguez *et al.* have been the first to report the synthesis of norbornenyl-terminated PEO¹¹³ macromonomers **M1** (Figure I.14) by anionic polymerization.

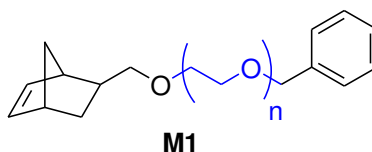
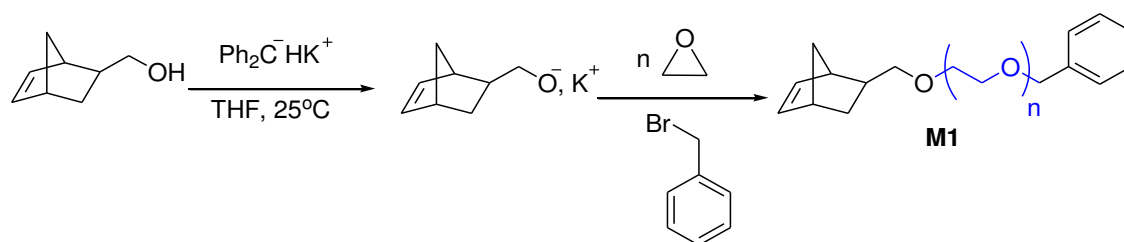


Figure I.14. Norbornenyl-terminated PEO macromonomers synthesized by Héroguez *et al.*¹¹³

The norbornenyl-terminated PEO macromonomers **M1** were prepared from anionic polymerization of ethylene oxide (EO) initiated by hydroxymethyl-5-bicyclo[2.2.1]heptene (NBCH₂OH) using diphenylmethyllpotassium (Ph₂CHK) as a deprotonating agent (Scheme I.12). Resulting **M1** were obtained with number-average molar mass, measured by size exclusion chromatography (SEC) with PEO standard calibration ($M_{n,SEC}$), ranging from 1500 to 4700 g/mol and low D_M (1.05-1.07). $DP_{n,NMR}$ calculated from ¹H NMR spectroscopy confirmed the polymerization of EO with a quantitative conversion.

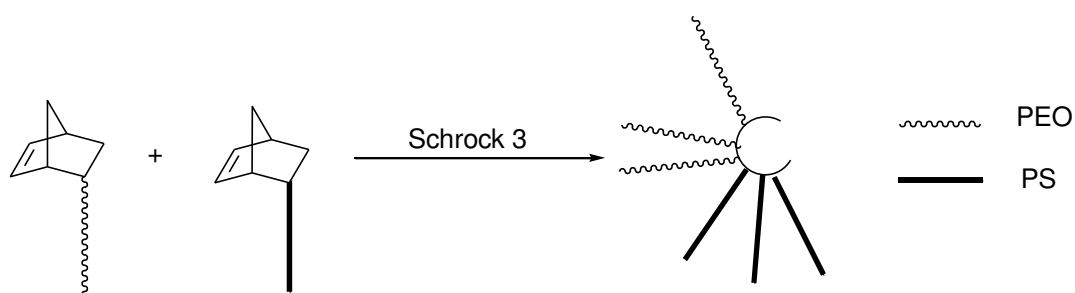


Scheme I.12. Synthesis of norbornenyl-terminated PEO **M1** *via* anionic polymerization of EO¹¹³

ROMP of **M1** ($M_{n,SEC}$ = 1500 and 2800 g/mol) using Schrock 3 catalyst (Figure I.5) as the initiator in toluene at ambient temperature allows to achieve a complete macromonomer conversion with DP_n = 5-25 and relatively narrow molar masses distribution (D_M < 1.3). In case of macromonomers of higher M_n (4700 g/mol), the polymerization yield always reached a plateau value of 30 %. With macromonomers of higher M_n (11000 g/mol), no polymerization occurred. In all cases, number average molar masses obtained from laser light scattering ($M_{n,LLS}$) of graft copolymers were much higher than the targeted values because the metal carbenes were prone to interact with the oxygen atoms of the PEO macromonomer, resulting in a decrease of the proportion of initiator available for coordination with the olefinic unsaturation of the macromonomer. Use of 1,2-diethoxyethane as the solvent for the ROMP of **M1** with a M_n = 4700 g/mol has allowed to increase the yield to 90 %. This solvent, which is a stronger base than the repeating units of PEOs, helps to prevent the coordination of the

metal vacant sites of the initiator by the oxygen atoms of PEO and allows the polymerization to proceed almost to completion.¹¹³

M1 ($M_n = 2800$ g/mol) was also copolymerized with norbornenyl-terminated PS via ROMP using Schrock 3 as the initiator to obtain an amphiphilic copolymer (Scheme I.13). The ROMP was first carried out sequentially in toluene, used as the solvent, with the introduction of PS macromonomer first according to its higher reactivity,^{114, 108} **M1** was added after 15 minutes of reaction. Three different molar ratios of **M1** to PS macromonomer were tested and the amount of Schrock 3 initiator was adjusted to obtain copolymers with DP_n ranging from 5 to 20. A statistical copolymerization between two macromonomers was also realized using Schrock 3 as the catalyst in toluene under similar conditions as sequential reaction. The SEC results of copolymers showed quantitative macromonomers conversion for all **M1** to PS macromonomer molar ratios, the values of M_n were in range of $3.3 \times 10^4 - 6.4 \times 10^4$ g/mol and show good agreement with the targeted values. Resulting copolymers have low D_M values ranging from 1.10 to 1.26.¹¹⁴



Scheme I.13. Copolymerization of norbornenyl-terminated PEO and norbornenyl-terminated PS macromonomers reported by Héroguez *et al.*¹¹⁴

Héroguez *et al.* investigated the synthesis of a series of norbornenyl-functionalized PEO macromonomers including **M3** and **M4** (Figure I.15).¹¹⁵ Norbornenyl-terminated PEO macromonomer **M2** was first synthesized according to the same method as already used for the synthesis of **M1** with a $M_{n,SEC}$ of 3750 g/mol and a low D_M (1.09). Norbornenyl-terminated carboxylic acid-functionalized PEO macromonomer **M3** and norbornenyl-terminated gentamicin sulfate-functionalized PEO macromonomer **M4** were then obtained by nucleophilic substitution from the hydroxyl end-group functionality of the norbornenyl-terminated PEO macromonomer.

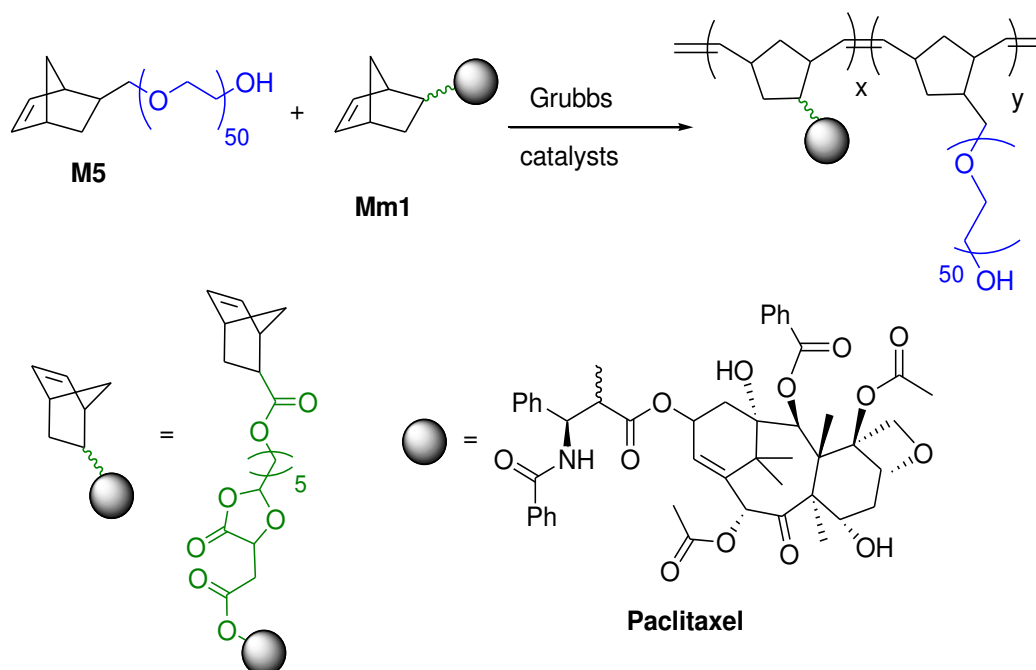


Figure 1.15. Norbornenyl-terminated PEO containing functional-end groups synthesized by Héroquez *et al.*¹¹⁵

Carboxylic acid group was chosen because it could permit the anchoring on biomaterial surface and the local delivery of the drug on the site of infection. The triamino-functionalized gentamicin sulfate, a wide-spectrum antibiotic usually used to prevent infections in orthopedic surgery, was chosen as it could easily link on modified macromonomers through a pH-sensitive imine bond. High functionalization yields of 75 and 99 % were obtained with both macromonomers **M3** and **M4**, respectively. Statistical copolymerization of **M3**, **M4** and NB was conducted in the presence of Grubbs 1 catalyst with a **M3/M4/NB/initiator** initial molar ratio of 4:4:160:1. The use of a dichloromethane (DCM)/ethanol mixture (35:65 in volume) for ROMP allowed high monomer and macromonomers conversions (≥ 92 %). The polynorbornene, insoluble in the medium, precipitates to form nanoparticles with hydrophobic core and hydrophilic PEO shell. Because of its hydrophilic properties, gentamicin sulfate is essentially located on the particle shells. Nanoparticles had z-average diameters of about 350 nm in DCM/ethanol mixture with a narrow molar masses distribution ($\text{PDI} \sim 0.3$). Gentamicin sulfate-functionalized nanoparticle system has proven its ability to be used as a pH-controlled drug delivery system.

Zou *et al.* presented the synthesis of *exo*-norbornenyl PEO macromonomer **M5**¹¹⁶ (Scheme I.14) by the same anionic polymerization method as reported by Héroquez's group.¹¹³ **M5** was obtained with a number-average molar mass measured by ^1H NMR spectrometry ($M_{n,\text{NMR}}$) of 2400 g/mol and a D_M of 1.10. The statistical

copolymerizations of **M5** and paclitaxel-functionalized norbornene monomer **Mm1** were carried out using Grubbs 1 or 3 as the initiators in DCM at ambient temperature with **M5**/initiator ratios of 25:1 and 100:1. Equimolar amounts of **M5** and **Mm1** were used to maintain significant grafting density and drug loading. When short backbones were targeted (**M5**/initiator initial molar ratio of 25:1), both Grubbs 3 and 1 catalysts were efficient initiators for ROMP and resulted in graft copolymers with low dispersities (1.04 and 1.11) within 15 min and 3 h, respectively. However, in case of longer backbone (**M5**/initiator initial molar ratio of 100:1), the ROMP initiated by Grubbs 1 catalyst became sluggish and resulted in a graft copolymer with a broad distribution of 1.34 after 19 h of reaction. In contrast, ROMP initiated by Grubbs 3 catalyst was completed within 1.5 h and produced a graft copolymer with a low \bar{D}_M of 1.09. Each graft copolymer contains high amount of paclitaxel, up to 24 wt %, as attested by ^1H NMR analysis. Under neutral conditions, *i.e.* pH = 7.0, the release of paclitaxel on graft copolymer was relatively slow but was much enhanced at pH of 5.5 as over 90 % of the paclitaxel moieties were released within 6 h due to highly efficient cleavage of the acid-sensitive cycloacetal linkages.



Scheme I.14. Norbornenyl-terminated PEO macromonomer and its copolymerization reported by Zou *et al.*¹¹⁶

Emrick's group has reported the example of synthesis and ROMP of a PEO macromonomer obtained by anionic polymerization with a different "ROMP-able" entity. Cyclooctenyl-terminated PEO macromonomers **M6** (Figure I.16) were obtained with \bar{D}_M of 1.1 and $M_{n,SEC}$, using PS standards calibration, of 1200 and 2300 g/mol.^{117,118} Amphiphilic graft copolymers were prepared by copolymerization of different molar ratios of cyclooctene/**M6** (92:8 - 80:20) with a macromonomer/initiator initial molar ratio of 250:1 using Grubbs 2 as the initiator and 1-hexene as the chain transfer agent in DCM at room temperature. The $M_{n,SEC}$ from 1.58×10^4 to 4.28×10^4 g/mol and \bar{D}_M of 1.9-2.1 were obtained. The copolymers showed comonomers incorporation into the graft copolymer in agreement with the feed ratios. The macromonomer **M6** (weight-average molar mass (M_w) = 4400 g/mol) was also copolymerized with cyclooctene and phenylazide-functionalized cyclooctene (**Mm2**, Figure I.16) for membrane coating applications. The graft copolymer was prepared using Grubbs 3 catalyst from a **Mm2**/**M6**/cyclooctene/G3 initial molar ratio of 40:40:110:1 and had a $M_{n,SEC}$ of 3.5×10^4 g/mol and a \bar{D}_M of 1.7. The phenylazide-functionalized graft copolymers have been used as an antifouling coating for poly(vinylidene fluoride) ultrafiltration membranes.¹¹⁸

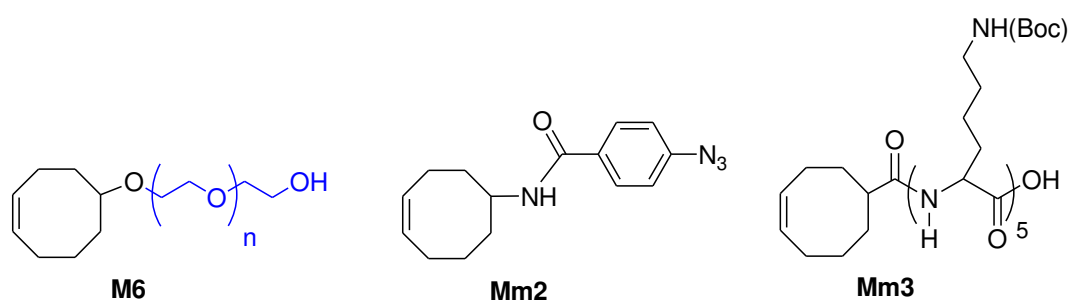


Figure I.16. Cyclooctenyl-terminated PEO macromonomers and cyclooctenyl-functionalized monomers synthesized by Emrick and co-workers.^{117,118}

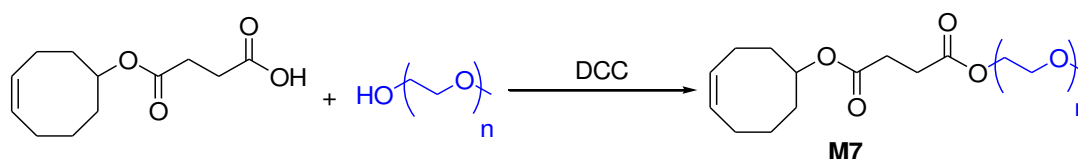
The ROMP copolymerization of a mixture including a **Mm3** (Figure I.16) to **M6** ($M_{n,SEC}$ = 1200 g/mol) initial molar ratio of 1:1 was performed, using Grubbs 3 in a **M6**/initiator molar ratio of 50:1 in a DCM/methanol (MeOH) mixture (50:50 in

volume), used as the solvent at ambient temperature. The *tert*-butyloxycarboxylic protected (Boc-protected) pentyllysine-functionalized PEO graft copolymer was characterized by SEC in tetrahydrofuran (THF) to give a $M_{n,SEC}$ of 36000 g/mol and a D_M of 1.7. The combination of light scattering in solution at both high and low ionic strengths and SEC results showed that the copolymer chains likely formed aggregated structures composed of an average of three chains in water. The copolymers were used for deoxyribonucleic acid (DNA) complexation and transfection.¹¹⁷

III.1.2. PEO-based ROMP-able macromonomer obtained by chemical modification

Numerous works of synthesis of graft copolymers by ROMP of macromonomers obtained by chemical modification of commercial PEO monomethyl ether have been reported.

Emrick's group presented the synthesis of cyclooctenyl macromonomers **M7** obtained by esterification between a carboxylic acid-functionalized cyclooct-5-enyl ester and two commercial PEO monomethyl ether of molar masses of 750 and 1000 g/mol (Scheme I.15) in the presence of dicyclohexylcarbodiimide (DCC).¹¹⁹



Scheme I.15. Cyclooctenyl-terminated PEO macromonomer synthesized via esterification reported by Breitenkamp *et al.*¹¹⁹

Macromonomers were then copolymerized with cyclooctene in the presence of Grubbs 1 or Grubbs 2 initiators in DCM at ambient temperature using a (macro)monomers/initiator initial molar ratio ranging from 100:1 to 500:1, macromonomer to cyclooctene initial molar ratios in the range of 1:1 to 1:9. By using Grubbs 1, (macro)monomers conversions ranging from 60 to 70 % were obtained with a decrease of $M_{n,SEC}$ from 3.3×10^5 g/mol to 1.8×10^5 g/mol upon decreasing the macromonomer-to-cyclooctene initial molar ratio from 1:1 to 1:9. Grubbs 2 showed a high efficiency for ROMP with complete (macro)monomer conversions. A decrease of

(macro)monomer-to-initiator initial molar ratios of 500:1 to 100:1 led to a decrease of molar masses. The graft copolymers were obtained with $M_{n,SEC}$ between 1.4×10^5 and 5.4×10^5 g/mol and with D_M ranging from 1.21 to 2.20.

Alfred *et al.* have described the synthesis of (oxa)norbornene-functionalized PEO macromonomers (Figure I.17) by esterification reactions of commercial PEO monomethyl ether 1100 and 2000 g/mol with (oxa)norbornene derivatives.¹²⁰

The authors presented the first ROMP homopolymerization of PEO macromonomers. Norbornenyl-terminated PEO macromonomers **M8** and **M9** with respectively one and two chains of PEO were obtained from PEO monomethyl ether. One oxanorbornenyl PEO macromonomer **M10** was also synthesized and contains two PEO chains of $M_n = 1100$ g/mol. The SEC and NMR characterizations of macromonomers **M9** and **M10** showed a few percent residual PEO which was removed after polymerization of macromonomers by precipitation from diethyl ether.

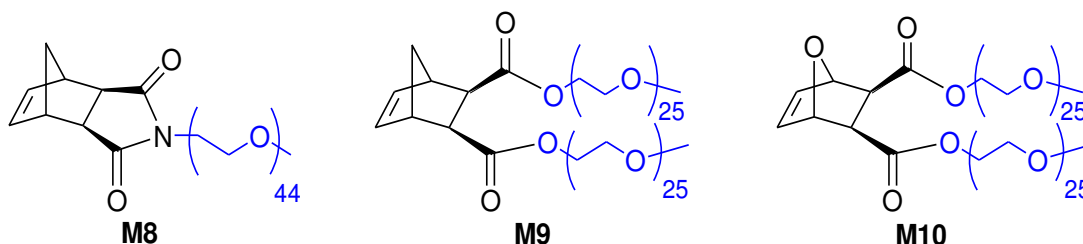


Figure I.17. Norbornenyl-terminated macromonomers bearing one or two PEO chains reported by Alfred *et al.*¹²⁰

They first investigated the polymerization of macromonomer **M8** using Grubbs 3 as the initiator in THF at room temperature, and have obtained a graft copolymer with $M_{n,SEC}$, using PS standards calibration, of 1.5×10^4 g/mol with a macromonomer-to-initiator initial molar ratio of 18:1. However, the D_M of resulting graft copolymer was high (1.6) and the molar masses distribution was multimodal. The ROMP of macromonomers **M9** and **M10** in the same conditions with macromonomer-to-initiator initial ratio of 27:1 and 8:1 for **M9** and **M10**, respectively, gave a nearly quantitative

conversion after 20 min. The dispersity values were low (1.04-1.17). The facile ability of **M9** and **M10** to polymerize with much lower D_M values compared to **M8** suggests that the imide functionality in **M8** plays a central role as reported by Breitenkamp *et al.*¹²¹ and Biagini *et al.*¹²² The characterization of graft copolymer from **M10** by static light scattering (SLS) shows that it was aggregated in water, with a M_w found by SLS (8.99×10^4 g/mol) larger by nearly three times than the expected value (2.4×10^4 g/mol).

Sankaran *et al.* have reported the synthesis by chemical modification of three classes of ROMP (macro)monomers: luminescent and electrochemiluminescent transition-metal-containing monomer (**Mm4**), biologically compatible macromonomer (**M11**) and bioconjugable monomer (**Mm5**) for drug delivery and tissue engineering applications (Figure I.18).¹²³

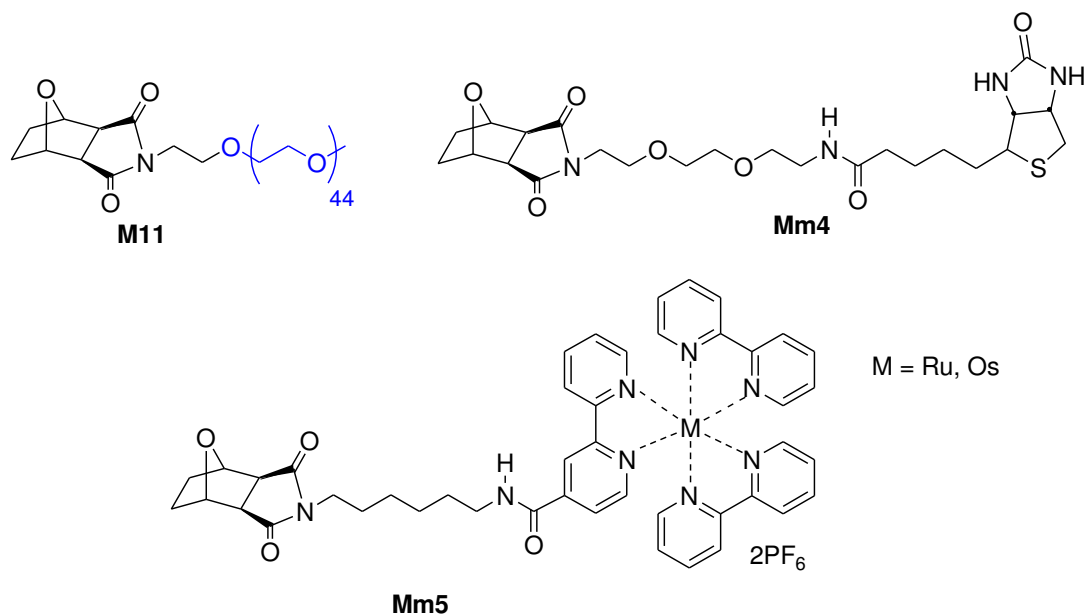


Figure I.18 Oxanorbornenyl-terminated PEO macromonomer and oxanorbornenyl-functionalized monomers synthesized by Sankaran *et al.*¹²³

Macromonomer **M11** was synthesized by Mitsunobu coupling of *exo*-7-oxabicyclo[2.2.1]-hept-5-ene-2,3-dicarboximide and PEO monomethyl ether ($DP_n = 44$). The copolymerization was used to efficiently combine the macromonomer **M12**

(Figure I.19) and two monomers to generate amphiphilic di- and triblock copolymers. The sequential copolymerization of **Mm4**, **M11** and **Mm5** was carried out using Grubbs 3 as the initiator and **Mm4/M11/Mm5/initiator** initial molar ratios between 10:2:0:1 and 20:5:3:1 in DCM at room temperature. Most copolymerizations were complete in less than 20 min. Metal-containing polymers could only be characterized by spectroscopic methods because of their interaction with the SEC stationary phase. The ^1H NMR analysis shows a quantitative incorporation of the (macro)monomers. Finally, the self-assembly of these copolymers in aqueous media formed star micelles with diameters between 4.2 and 43 nm and multiple luminescent metal units in their core, surrounding by biocompatible units to protect this core, and bioconjugable or bioconjugation units in their corona. These micellar aggregates were stable in the buffer aqueous conditions required for biological detection and exhibited potential applications for sensitive biological detection, but also for drug delivery and tissue engineering.

Grubbs's team reported the macromonomers synthesis from PEO monomethyl ether and norbornene derivatives.¹²⁴⁻¹²⁶ Macromonomer **M12** (Figure I.19) was synthesized from aminohydroxyl PEO and *exo* norbornene anhydride. PEO 600 g/mol ($\text{DP}_n = 12$) was found to provide the desired solubility while retaining high reactivity during ROMP. Mesylate leaving groups were added, based on their high stability and solubility, to the end of the PEO chain for later displacement by radioactive fluoride.

The sequential copolymerization of (macro)monomers **M12** and **Mm6** was carried out using Grubbs 3' catalyst with **M12/initiator** initial molar ratios ranging from 150:1 to 1200:1 and a **M12/Mm6** ratio of 3:1. All copolymerizations were completed in 30 min and the grafted-block copolymers were obtained with low D_M (1.01-1.18) for short backbone copolymers and a high D_M (1.73) for a longer backbone copolymer due to the deactivation of initiator during polymerization with $M_{n,\text{SEC}}$ up to 1.22×10^6 g/mol. The measurement of size of copolymer showed nanoparticle diameters ranging from 12.7 to 39.7 nm by atomic force microscopy (AFM) and of 47.4 – 142.5 by DLS. Grafted-block copolymers were then dispersed in water to form micelles. The cross-linking reaction of cinnamoyl groups was accomplished by irradiation of the micelles with UV light in degassed water at room temperature. Fluoride-18 was transported in hydrated

nanoparticles and the fluoride-18-functionalized nanoparticles were used as an *in vivo* molecular imaging agent.¹²⁴

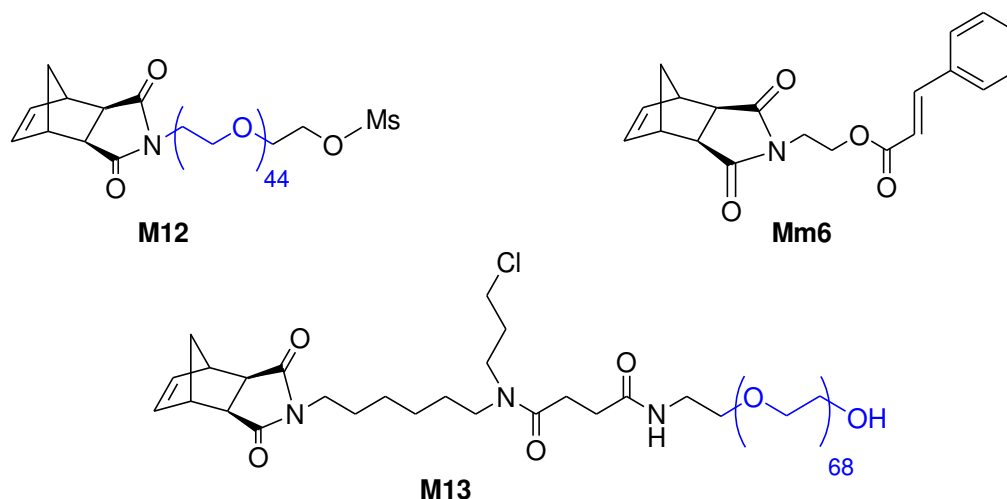


Figure I.19. Norbornene-terminated PEO macromonomers and norbornenyl-functionalized monomer synthesized by Grubbs's team¹²⁴⁻¹²⁶

For the macromonomer **M13** (Figure I.19), Grubbs and co-workers reported a two-step process (ROMP and chloride-azide exchange) to rapidly generate a series of azide-functional brush copolymers with variable DP_n ranging from 10 to 400. **M13** containing a PEO of molar mass of 3000 g/mol was synthesized in five steps from *exo-N*-(6-hydroxylhexyl)-5-norbornene-2,3-dicarboximide. Graft copolymers were prepared by ROMP of **M13** using Grubbs 3' as initiator in DCM at room temperature, quenching the polymerization by addition of ethyl vinyl ether, solvent exchange, and finally treatment with sodium azide for further attachment of a drug-alkyne derivative. The polymer characterization data demonstrated that ROMP of **M13** was well-controlled up to the highest DP_n targeted (400) with $M_{n,SEC}$ up to 1.96×10^6 g/mol and low D_M (1.04-1.27) with monomodal molar masses distributions and high macromonomer conversions (95 %). Chloride-azide exchange reaction occurred with equal efficiency for each copolymer. All copolymers have high solubility (> 100 mg/mL) in water. Aqueous DLS measurements confirm that their nanoscopic dimensions increased with the DP_n of PEO and were tunable over a broad range (radii from 3 to 25 nm) as relevant sizes for drug delivery applications. Then, the doxorubicin drug (DOX) (Figure I.20) was attached to

the polymers *via* copper catalyzed azide-alkyne cycloaddition (CuAAC) reaction and very high conversions (> 97 %) were reached. The photorelease of DOX from these materials was also studied for potential application as drug delivery.¹²⁶

Macromonomer **M14** (Figure I.20) was first synthesized by a two-steps process starting from **M13**: (i) chloride-azide exchange and (ii) azide-alkyne reaction between its azide functionality and alkyne functionality on alkynyl-terminated drug. Various series of macromonomers were synthesized, which contain a hydrophilic PEO chain, a hydrophobic drug functionality such as DOX or camptothecin (CT), which can be released under UV photolysis, for drug delivery applications.¹²⁵

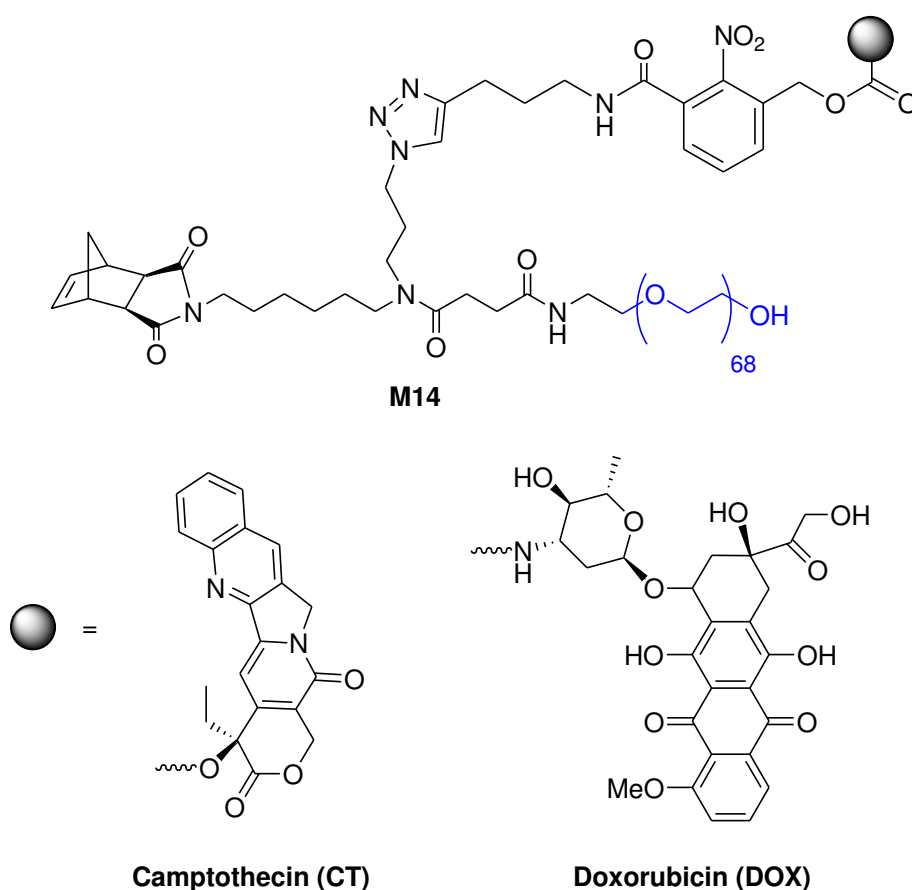


Figure I.20. Macromonomers **M14** loaded CT or DOX synthesized by Grubbs and co-workers.¹²⁵

M14 allowed to synthesize bivalent-brush polymers containing anticancer drugs with $M_{n,SEC}$ ranging from 3.3×10^4 to 4.99×10^5 g/mol and D_M values ranging from 1.04

to 1.38 by highly controlled ROMPs in the presence of Grubbs 3' in DCM at ambient temperature. The “grafting through” ROMP approach ensured that the weight percentage of drug loaded onto the brush copolymers was the same as the weight percentage of drug on the macromonomer and is independent of DP_n and conversion. Thus, copolymers carry 8.5 % CT and 12.6 % DOX, respectively. These values could be increased by shortening the length of the PEO or designing a macromonomer linked to more than one drug molecule.¹²⁵

Shi *et al.* presented the macromonomer **M15** (Figure I.21) synthesis from PEO monomethyl ether 1000 g/mol and isocyanate-functionalized cyclooctene.¹²⁷ The Fourier-transform infrared (FTIR) spectrum showed that the isocyanate group has completely reacted. The number-average molar mass measured by matrix assisted laser desorption/ionization-time of flight (MALDI-ToF) mass spectrometry ($M_{n,MALDI}$) and D_M of macromonomer **M15** are 1085 g/mol and 1.02, respectively.

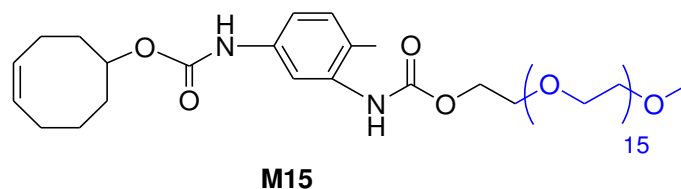


Figure I.21. Cyclooctenyl-terminated PEO macromonomer synthesized by Shi *et al.*¹²⁷

Copolymerization of **M15** and cyclooctene were performed in the presence of Grubbs 2 in DCM at room temperature with a (macro)monomers/initiator initial molar ratio of 250:1 and **M15** molar percentage in the mixture of **M15** and cyclooctene from 5 to 20 %. Four copolymers were obtained with $M_{n,SEC}$ ranging from 1.15×10^5 to 2.69×10^5 g/mol and with D_M values of 1.64 - 2.54. The surface properties of polycyclooctene-g-PEO films were evaluated through water contact angle and X-ray photoelectron spectroscopy (XPS). Water contact angle decreased from 87.7° to 65.8° along with increasing hydrophilicity by the increased content of PEO. The copolymers involved

[illegible]

The amphiphilic graft copolymers were synthesized *via* ROMP of **M16** using Grubbs 3 in DCM at room temperature with [**M16**]/initiator initial molar ratios ranging from 50:1 to 250:1. High macromonomer conversions were obtained in most cases. These conversions decreased along with the increase of molar mass of **M16**, as well as

[**M16**]/initiator initial molar ratio. Well-defined structures of copolymers were verified by the narrow and monomodal molar masses distribution ($\mathcal{D}_M = 1.11 - 1.23$). The differential scanning calorimetry (DSC) analyses showed the lower crystallinities and melting point (T_m) values of copolymers compared to their macromonomer precursors. The self-assembly behavior of the amphiphilic graft copolymers and macromonomers was measured in water *via* DLS. **M16** macromonomers have hydrodynamic diameter (D_h) values in a range of 68 to 164 nm increasing along with the decrease of hydrophobic block PLA, which indicated the formation of intermolecular aggregates in water. In the same conditions, copolymers obtained from **M16** macromonomers have much lower hydrodynamic diameters with D_h ranging from 15.2 to 20.9 nm. These amphiphilic graft copolymers with nanoscopic molecular sizes can lead to the formation of miniemulsions with unusually high stability and may be used to stabilize the interfaces of a variety of biphasic systems.

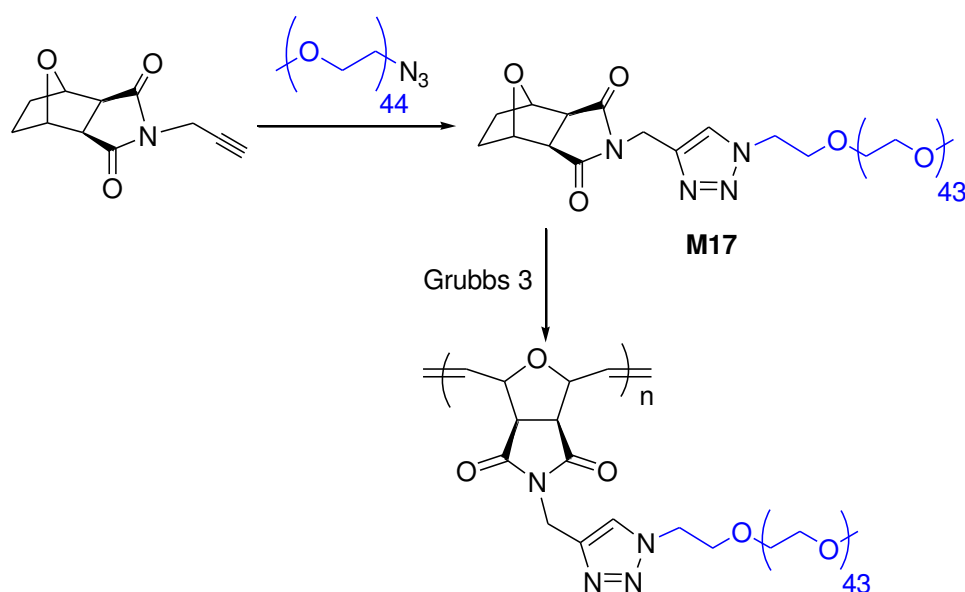
III.1.3. PEO-based ROMP-able macromonomers synthesized by ‘click’ chemistry

The development of ‘click’ chemistry such as Huisgen 1,3-dipolar cycloaddition gives rise to the synthesis of various well-defined macromonomers starting from commercially available polymers such as PEO. Use of CuAAC ‘click’ reaction in functionalization of ROMP-able macromonomers exhibited a high efficiency as described in several studies.

Le *et al.* presented the synthesis of several PEO macromonomers by CuAAC “click” reaction. Three macromonomers **M17**¹²⁹ (Scheme I.17) were prepared quantitatively from azide-functionalized PEO monomethyl ether of M_n of 500, 2000 and 5000 g/mol and alkyne-functionalized oxanorbornene in the presence of copper (I) bromide (CuBr) used as catalyst and *N, N, N', N', N''*-pentamethyldiethylenetriamine (PMDETA) used as ligand in DMF at ambient temperature. Pure *exo* oxanorbornene diastereoisomers were chosen as “ROMP-able” group because of their higher reactivity in ROMP than their *endo* counterparts.

The Grubbs 3 was used as initiator for the ROMP of the macromonomers. The macromonomer of M_n 500 g/mol ($n = 11$) was easily polymerized to nearly quantitative

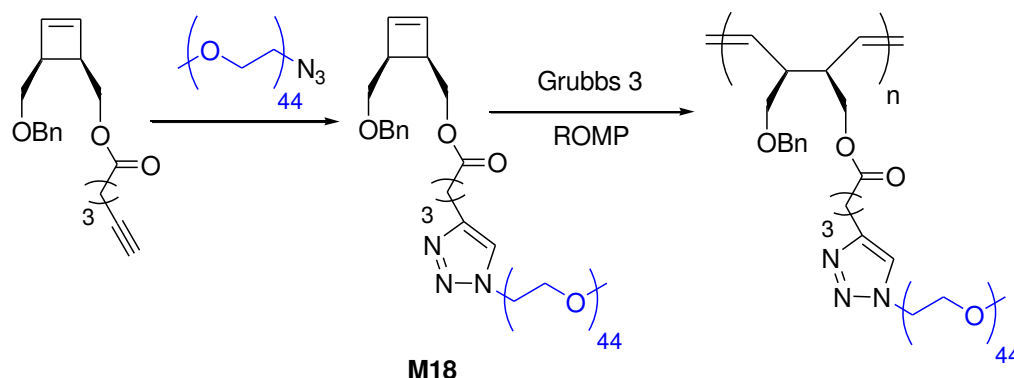
yield in DCM at ambient temperature in 1-4 h up to a macromonomer/initiator initial molar ratio of 100:1. The copolymers were obtained with $M_{n,SEC}$ ranging between 9900 and 29300 g/mol and with low D_M of 1.06-1.17. However, macromonomers of M_n 2000 and 5000 g/mol were only able to form copolymers with relatively short backbone length with a macromonomer/initiator initial molar ratio of 10/1 with low D_M (1.07 and 1.06, respectively). ROMP with higher macromonomer/initiator initial molar ratios (50:1 and 100:1) was also realized but the macromonomer conversions did not overcome 60 %. The 1H NMR results showed the increase of the *trans* in comparison to the *cis* configuration in polyoxanorbornene backbone along with the increase of PEO chain lengths.



Scheme I.17. Synthesis of oxanorbornenyl-terminated PEO macromonomers and their ROMP reported by Le *et al.*¹²⁹

Le *et al.* also presented macromonomer **M18**¹³⁰ (Scheme I.18), which was prepared *via* CuAAC ‘click’ reaction of alkyne-terminated cyclobutene and azide-terminated PEO monomethyl ether of M_n of 2000 g/mol in quantitative yield. The amphiphilic properties of **M18** were studied *via* measurement of critical micellar concentration (CMC) by using steady state fluorescence spectroscopy with pyrene as a probe. The

CMC value of **M18** was estimated to be 3 mg/mL. The self-organization of **M18** in water is expected to make it a good candidate for ROMP in aqueous dispersed media.

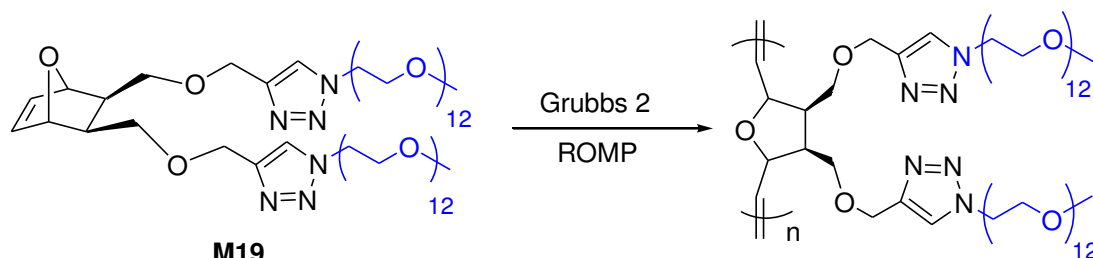


Scheme I.18. Synthesis of cyclobutenyl-terminated PEO macromonomers *via* ‘click’ chemistry and their ROMP reported by Le *et al.*¹³⁰

The ROMP of **M18** was carried out in the presence of Grubbs 2 in toluene at 70 °C or Grubbs 3 as the initiators in DCM at room temperature. Use of Grubbs 3 catalyst for ROMP of **M18** in DCM resulted in a macromonomer conversion of 75 % for an initial **M18**/initiator molar ratio of 10:1. Moreover, the SEC analysis showed bimodal traces indicating the partial conversion of **M18** using Grubbs 3 as the initiator in DCM. In contrast, quantitative macromonomer conversions were obtained in ROMP of **M18** using Grubbs 2 as the initiator in toluene for initial **M18**-to-initiator molar ratios up to 30, resulting in copolymers with $M_{n,SEC}$ in a range of 19.8×10^3 to 38.0×10^3 g/mol and narrow molar masses distributions ($\mathcal{D}_M = 1.07 - 1.11$).

ROMP of **M18** in miniemulsion dispersed media was studied with Grubbs 3 as the catalyst. The miniemulsion system was prepared by mixing under stirring the organic phase containing **M18**, Grubbs 3, and hexadecane and the water phase containing the surfactant, followed by an ultrasonication process. The final particle droplets hydrodynamic diameter (320 nm) did not vary from initial value (300 nm) indicating no destabilization during the polymerization. **M18** conversion reached to 50 % after 24 h and only 56 % after 38 h of reaction. ROMP of cyclobutenyl-terminated PEO macromonomer **M18** using Grubbs 3 as the initiator showed ill-defined graft copolymers as well as partial conversion either in solution or in miniemulsion.

Recently, Khosravi and co-workers reported the synthesis of oxanorbornenyl-functionalized PEO macromonomer **M19** (Scheme I.19) using a quantitative CuAAC reaction between azide-terminated PEO monomethyl ether of $M_n = 550$ g/mol and dialkyne-functionalized oxanorbornene.¹³¹



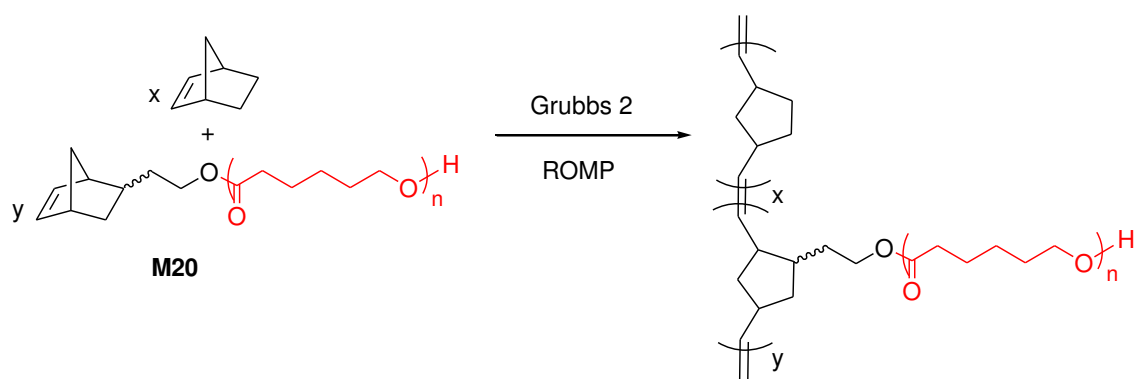
Scheme I.19. Oxanorbornenyl-functionalized PEO macromonomer and its ROMP reported by Khosravi and co-workers¹³¹

ROMP of **M19** was realized using Grubbs 2 as the initiator in chloroform (CHCl_3) at ambient temperature. The reaction was monitored by ^1H NMR using **M19** to initiator initial molar ratio of 10/1. The macromonomer conversion reached 3 % after 30 minutes and increased to 76 % for 24 h of reaction. Prolonged time of reaction did not allow increasing macromonomer conversion.

III.2. Synthesis of graft copolymers from PCL-based macromonomers via metathesis polymerization

Mecerreyes *et al.* published the first synthesis of norbornenyl-terminated PCL macromonomers **M20** (Scheme I.20) by ROP of CL using 2-diethylaluminumoxymethyl-5-norbornene as the initiator in toluene at room temperature.¹³² The ROP was stopped by adding a HCl solution to deactivate the initiator and has generated hydroxyl-end group on PCL chain. Resulting macromonomers had low D_M (< 1.20) for $[\text{CL}]_0/[\text{NB}]_0$ molar ratio ranging from 20 to 85, D_M became high (2.05) when the time required for the

complete monomer conversion is prolonged to 24 h. $M_{n,SEC}$ of the macromonomers ranged from 2100 to 9600 g/mol and were in good agreement with the calculated values.



Scheme I.20. Norbornenyl-terminated PCLs and their copolymerization with norbornene reported by Mecerreyes *et al.*¹³²

The macromonomers were then copolymerized with NB or NB acetate in the presence of Grubbs 2 used as initiator in chlorobenzene at ambient temperature and a NB/initiator initial molar ratio of 57:1. CL molar fraction in the comonomer feed ranges from 0.3 to 0.6. The copolymerization of **M20** and NB gave graft copolymers with yields of 60-70 % after 4 to 5 minutes of reaction, and $M_{n,SEC}$ ranging from 8.2×10^4 to 1.99×10^5 g/mol and D_M of 1.5 - 2.40. The graft copolymers composition was controlled by the NB/**M20** feed molar ratio as evidenced by ^1H NMR by comparing relative intensities of NB backbone and of CL grafts signals. The copolymerization of **M20** and NB acetate, which is less reactive than NB, is controlled and can be prevented from side transesterification. The resulting copolymers have been prepared in higher yields (70 – 90 %) and lower D_M (1.25 – 1.45) compared to the copolymerization using NB. The homopolymerization of **M20** was also realized with **M20**/Grubbs 2 initial molar ratios of 3:1 - 12:1. The graft copolymers were obtained with $M_{n,SEC}$ ranging from 2.4×10^4 to 8.8×10^4 g/mol and narrow molar masses distributions ($D_M = 1.10$ -1.15). The films obtained from these graft copolymers cast from CHCl_3 are clear and transparent in contrast to hazy films of mixture of macromonomer and PNB. This observation indicated that phase separation in the graft copolymers leads to microdomains which were smaller than in the corresponding homopolymer blends. DSC analyses confirmed these microphase separation behaviors as the observation of two glass transition

temperatures (T_g). Thermogravimetric analysis (TGA) of the graft copolymer showed two degradable steps: the first one corresponding to the degradation of PCL component at a higher degradable temperature compared to the one of PCL homopolymer, whereas PNB backbone was degraded in second step at a lower temperature compared to homopolynorbornene.

Xie *et al.* reported the synthesis of norbornenyl-functionalized PCL macromonomers **M21** (Figure I.22) from a heterotrifunctional inimer.¹³³ Their ROMP followed by atom transfer radical polymerization (ATRP) for the preparation of a brush copolymer containing a PNB backbone together with one hydrophobic PCL graft and one hydrophilic poly(2-(*N,N*-dimethylamino)ethyl methacrylate) (PDMAEMA) graft.

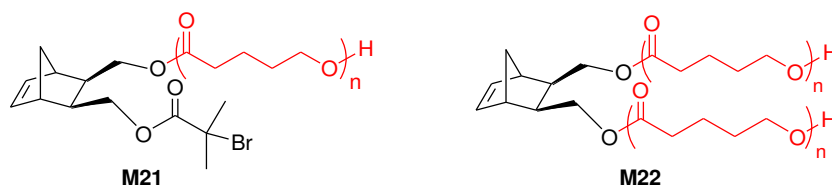
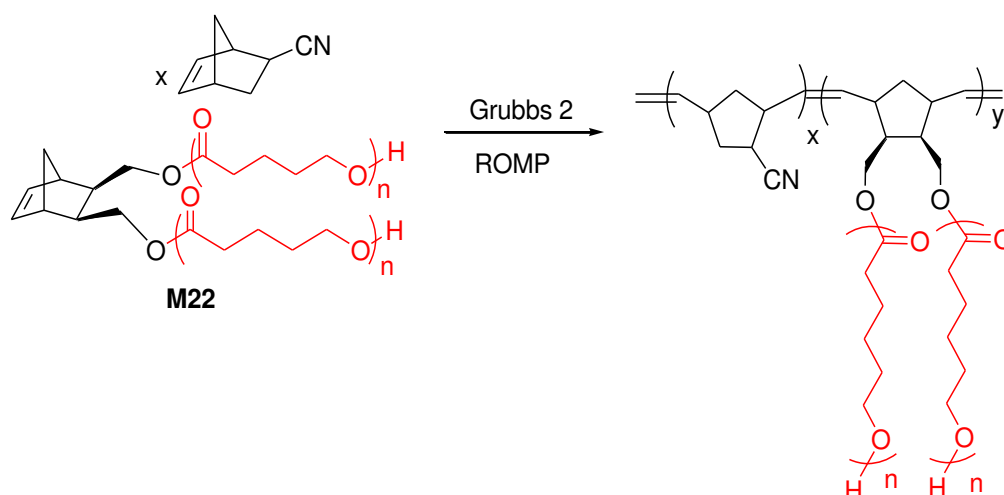


Figure I.22. Norbornenyl-functionalized PCL macromonomers synthesized by Xie *et al.*¹³³

M21 was prepared *via* ROP of CL from the hydroxyl functionality of 2-hydroxy-methyl-3-(2-bromoisobutyryloxymethyl)-5-norbornene used as the initiator with CL/inimer initial molar ratios of 10:1 and 25:1 using $\text{Sn}(\text{Oct})_2$ as the catalyst with a inimer/catalyst molar ratio of 100:1. Two macromonomers with different chain lengths were obtained with low D_M (1.1) and $M_{n,\text{SEC}}$ of 940 and 4300 g/mol. Both macromonomers were contaminated by residual unreacted CL. ROMP of the macromonomer ($M_{n,\text{SEC}} = 4300$ g/mol) was realized using Grubbs 2 in toluene at 60 °C with **M21**/initiator initial molar ratios of 5/1, 20/1 and 50/1. A resulting copolymer of targeted PNB backbone length of 5 with $M_{n,\text{SEC}} = 2.4 \times 10^4$ g/mol and low D_M of 1.2 was obtained after 4 h. The monomodal SEC profile attested a complete conversion. For higher **M21**/initiator molar ratios, trimodal SEC profiles were obtained resulting from unreacted macromonomer and the copolymer with a bimodal distribution. The shorter copolymer was then employed as macroinitiator for the ATRP of 2-(*N,N*-

dimethylamino)ethyl methacrylate (DMAEMA) to achieve a brush copolymer containing hydrophobic PCL grafts and hydrophilic PDMAEMA grafts. With progress of the reaction, the viscosity of the mixture increased. Adjusting the reaction time allowed to control the length of PDMAEMA segments. The monomodal SEC trace of resulting copolymer clearly showed the shift from macroinitiator trace and the variation of molar masses distribution ($\bar{D}_M = 1.6 - 1.8$) in comparison to macroinitiator ($\bar{D}_M = 1.1$). ^1H NMR analyses indicated that the initiation of ATRP did not occur quantitatively.

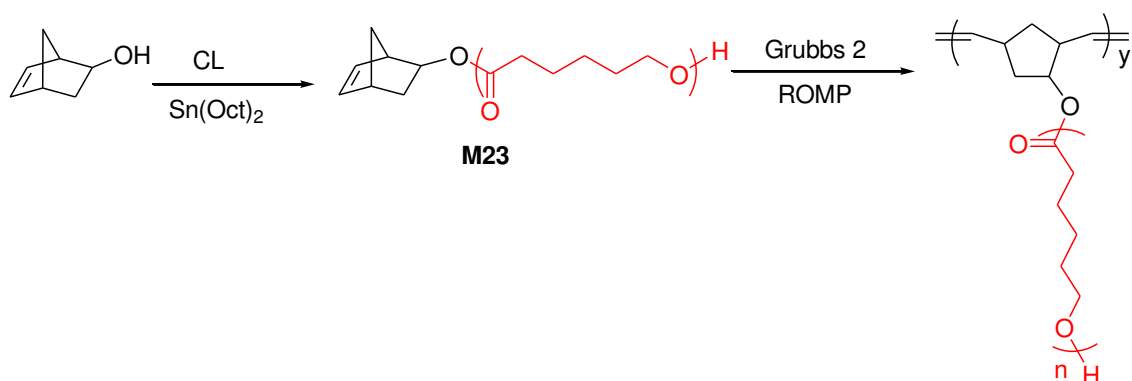
Xie's group also reported the synthesis of norbornenyl-functionalized PCL macromonomer **M22** (Figure I.22) *via* ROP of CL initiated by the dihydroxyl functionality of *exo,exo*-bicyclo[2.2.1]hept-5-ene-2,3-dimethanol using $\text{Sn}(\text{Oct})_2$ as the catalyst.¹³⁴ Two macromonomers **M22** with different lengths were prepared with $[\text{CL}]_0/[\text{OH}]_0/[\text{Sn}(\text{Oct})_2]_0$ initial molar ratios of 4800:80:1 and 1500:25:1 in toluene at 110 °C during 48 h. CL conversion reached 80 % for the lower molar ratio of catalyst, together with a $M_{n,\text{SEC}}$ of 5000 g/mol, a monomodal SEC trace and a narrow molar masses distribution ($\bar{D}_M = 1.2$). The increase of catalyst to initiator molar ratio led to an increase of CL conversion (86 %) and to an increase of molar mass ($M_{n,\text{SEC}} = 9400$ g/mol) together with a higher \bar{D}_M (1.4). **M22** was copolymerized with 5-cyano bicyclo[2.2.1]hept-2-ene (NB-CN) (Scheme I.21) to generate a copolymer in order to improve the brittle and poor processible properties of PNB. The incorporation of functional cyano groups in copolymer could enhance the strength of the materials since cyano group with strong polarity makes polymer chains more liable to aggregate.



Scheme I.21. Copolymerization of norbornenyl-functionalized PCL macromonomer **M22** reported by Yang *et al.*¹³⁴

The copolymerization of **M22** and NB-CN was realized using Grubbs 2 as the initiator in CHCl_3 at 70 °C with different $[\text{M22}]_0/[\text{NB-CN}]_0$ initial molar ratios of 1:20 and 1:40 and a **M22**/initiator initial molar ratio of 25:1. The copolymers were prepared in 50 % yield, with $M_{n,\text{SEC}}$ ranging from 72×10^3 to 151×10^3 g/mol and relatively high D_M (1.55 – 1.78) indicating that the ROMPs using Grubbs 2 are not well controlled. The thermal stability and crystallinity were also measured by TGA and DSC analyses. The mechanical properties of materials showed the highest tensile modulus, tensile strength and yield strength values for the copolymer with the longer PCL chain. Its lower value of elongation at break showed a good agreement with DSC result as the copolymer has higher crystallinity in comparison to the others. The results showed that the copolymer with the longer PCL graft length possessed a promising shape memory effect.

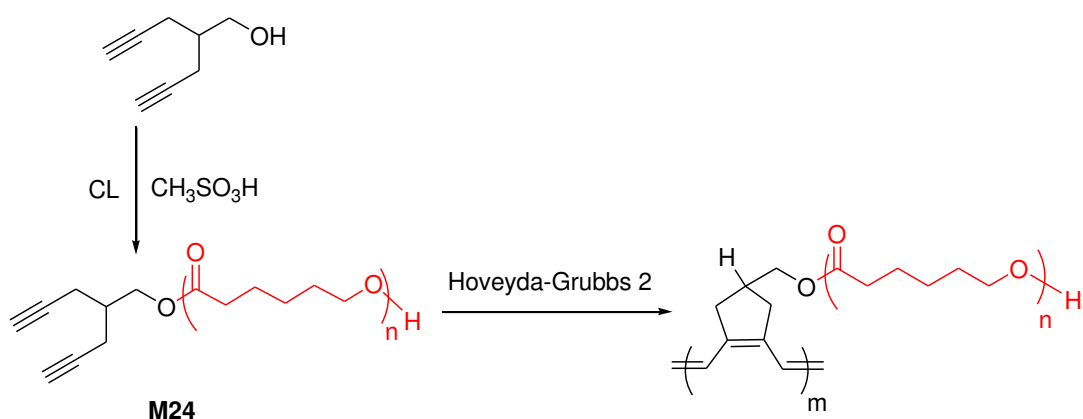
Fu *et al.* have also reported the synthesis of norbornenyl-terminated PCL macromonomers **M23** (Scheme I.22) by ROP of CL using 5-norbornene-2-ol as the initiator and $\text{Sn}(\text{Oct})_2$ as the catalyst.¹³⁵ The ROP was carried out in toluene at 110 °C for 24 h.



Scheme I.22. Synthesis of norbornenyl-terminated PCL macromonomers and their ROMP reported by Fu *et al.*¹³⁵

Five macromonomers were obtained with relative low \bar{D}_M (1.15 – 1.24) and $M_{n,SEC}$ between 2000 and 9500 g/mol. Quantitative ROMP of these macromonomers were carried out using Grubbs 3' in THF at room temperature and a macromonomer/initiator initial molar ratio of 200:1 to form high molar masses ($M_{n,SEC} = 4.18 \times 10^5$ - 2.99×10^6 g/mol) graft copolymers with narrow molar masses distribution ($\bar{D}_M = 1.24$ -1.34). The inclusion complexation of the prepared PNB-*g*-PCL bottle-brush copolymers with cyclodextrins afforded novel bottle-brush polypseudorotaxanes with a length of 350 ± 50 nm and a width of 50 ± 10 nm. The formation of bottle-brush polypseudorotaxanes was confirmed by NMR, X-ray diffraction analysis and DLS measurements. DSC and TGA analyses showed that the bottle-brush polypseudorotaxanes have higher thermal stability compared to their PCL bottle-brush precursors. Transmission electron microscopy (TEM) reveals that the resulting copolymers possess a unique elongated cylindrical morphology.

Kang *et al.* reported the first synthesis of brush copolymers *via* cyclopolymerization of macromonomers according to the 'grafting through' method.¹³⁶ The macromonomer **M24** (Scheme I.23) was prepared by ROP of CL initiated by a hydroxyl functionality on (3-methanol)-hepta-1,6-diyne using $\text{CH}_3\text{SO}_3\text{H}$ as the catalyst in DCM at 30 °C. **M24** was obtained with a $\text{DP}_{n,NMR}$ of 26, a $M_{n,NMR}$ of 3.09×10^3 g/mol and a narrow molar masses distribution ($\bar{D}_M = 1.20$).



Scheme I.23. Synthesis of dialkynyl-functionalized PCL macromonomers and their cyclopolymerization reported by Kang *et al.*¹³⁶

The cyclopolymerization of **M24** was realized using Hoveyda-Grubbs 2 (Figure I.7) as initiator with a **M24**/initiator initial molar ratio of 100/1 in THF at 50 °C and a quantitative macromonomer conversion was achieved within 1 h. The brush copolymer was obtained with a $M_{n,\text{SEC}}$ of 209.10^3 g/mol and a D_M of 1.63. The DSC analysis showed a small difference of T_m (58.5 °C and 53 °C) and enthalpy of fusion (114.4 J/g and 74.7 J/g) for **M24** and copolymer, respectively.

Leroux *et al.* reported the synthesis and ROMP of cyclobutenyl-functionalized PCL macromonomers **M25** and **M26** (Figure I.23).¹³⁷ **M25** and **M26** bearing one or two PCL arms, respectively, were prepared *via* ROP of CL selecting the organocatalyst TBD in the presence of *cis*-4-benzoxymethyl-3-hydroxymethylcyclobutene or *cis*-3,4-bis(hydroxymethyl)cyclobutene used as initiators. The ROP was carried out in toluene or THF at ambient temperature with CL/initiator feed molar ratios ranging from 18:1 to 96:1 with moderate-to-high monomer conversions. Well-defined macromonomers with the increase of PCL chain length along with the increase of CL/initiator initial molar ratios were obtained. Resulting macromonomers have narrow molar masses distributions ($D_M = 1.08 - 1.22$) and $M_{n,\text{SEC}}$ ranging from 3.9×10^3 to 13.7×10^3 g/mol.

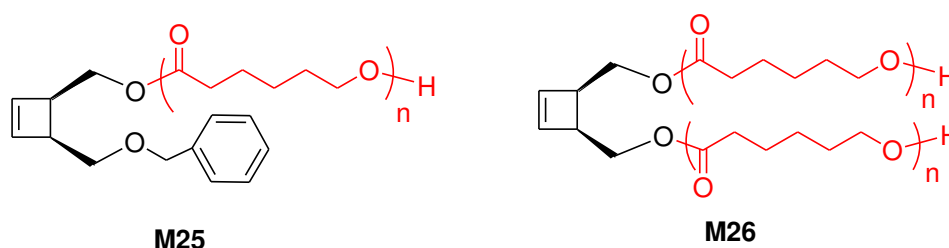


Figure I.23. Cyclobutenyl-functionalized PCL macromonomers synthesized by Leroux *et al.*¹³⁷

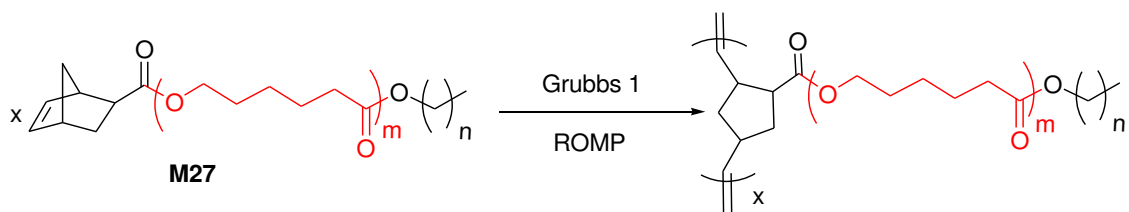
The ROMP of **M25** using Grubbs 2 as the initiator was realized in toluene or dichloroethane at 70 °C with **M25**/initiator initial molar ratios of 10:1, 50:1 and 100:1, and a concentration of macromonomer in solution of 0.01 or 0.04 mol/L. The obtained copolymers have low \bar{D}_M values (1.08-1.19) with $M_{n,SEC}$ ranging from 30.25×10^3 to 97.4×10^3 g/mol. The ROMP of **M25** was achieved quantitatively with a macromonomer of short PCL length ($DP_n = 16$) and short targeted backbone (**M25**/initiator molar ratio of 10/1). Decrease of macromonomer conversions were observed while increasing either PCL chain length or targeted backbone length. In a similar way, ROMPs of macromonomer bearing two PCL arms **M26** selecting Grubbs 2 as the initiator were carried out in toluene or dichloroethane at 70 °C. Resulting copolymers were achieved with \bar{D}_M values ranging from 1.05 to 1.30 and $M_{n,SEC}$ in a range of 22.95×10^3 and 17.22×10^4 g/mol.

Recently, Hadjichristidis' group reported the synthesis of graft copolymers bearing different grafts including polyethylene (PE), polystyrene (PS), PEO and PCL using copolymerization of norbornenyl-terminated macromonomers.¹³⁸ The norbornenyl-terminated macromonomers were synthesized by esterification of 5-norbornene-2-carboxylic acid with hydroxyl-terminated precursors. All macromonomers were obtained with low dispersity values ($\bar{D}_M = 1.05 - 1.14$) and high functionalities as exhibited by SEC and 1H NMR results.



using Grubbs 1 reported by Hadjichristidis and co-workers¹³⁸

of 1.12×10^5 and 5.08×10^5 g/mol for the **M27**/initiator initial molar ratios of 43:1 and 197:1, respectively.



Schem I.25. ROMP of **M27** reported by Hadjichristidis' team¹³⁸

Conclusion

The developments of the synthesis of well-defined transition metal-based initiator systems for ROMP and new organocatalyst systems in ROP of cyclic ester allow to synthesize a wide range of controlled structural copolymers. The ROMP using metal alkylidene complexes as the initiators resulted in various topologies of graft copolymers such as umbrella-like, comb-like and star-like...

ROMP is fast, functional group tolerant, reliable, flexible, and versatile, and allows for the synthesis of a broad different polymer architectures. However, precise control of the microstructure of the polymers is still a challenge.^{6,8} Well-defined ruthenium-based initiators have become the most commonly employed initiator in ROMP studies.⁶ Since 1995, a large number of researches related to the combination of ROMP and controlled/living polymerizations related to the synthesis of copolymers containing PEO and PCL *via* the ‘macromonomer route’ have been published. The ‘macromonomer route’ requires the synthesis of macromonomers containing ROMP-able functionality and PEO or PCL chain. Norbornene is usually used as the “ROMP-able” group because of its high reactivity in ROMP, but others have also been reported such as oxanorbornene, cyclobutene and cyclooctene. ROMP-able macromonomers containing PEO chain have been synthesized in the literature by anionic polymerization of EO initiated by ROMP-able functionality (α -functionalized macromonomer synthesis) or by chemical modification of synthesized PEO with ROMP-able functionality (ω -functionalized macromonomer synthesis). On the other hand, ROMP-able macromonomers containing PCL chain have been obtained by ROP of CL using organometallic catalysts or using organocatalyst.

Since the first use of DMAP as an organocatalyst for the ROP of LA in 2001, a wide range of studies focused on the use of organocatalysts in ROP of cyclic esters indicating that organocatalysis is an efficient substitute for transition metal-based catalysis. The use of organocatalysts allows to polymerize various cyclic esters under ambient conditions and to easily eliminate catalysts from the mixture of the resulting polymers.

In this work, we have investigated the synthesis of well-defined copolymers possessing a (oxa)norbornene functionality, a hydrophilic PEO chain and/or a

hydrophobic PCL chain by the combination of “click” chemistry and ROP. The self-assembling properties of the synthesized amphiphilic copolymers were then examined. We then evaluated the reactivity of norbornene functionality in either ROMP or thiol-ene reactions in order to obtain various architectures copolymers.

References

- ¹ N. Hadjichristidis, S. Pispas, M. Pitsikalis, H. Iatrou, D. J. Lohse, *Graft copolymers, cyclopedia of Polymer Science and Technology*, 3rd Ed., John Wiley & Sons Inc., Hoboken, New-York, **2004**
- ² C. Pugh, A. L. Kiste, *Prog. Polym. Sci.* **1997**, 22, 601-691
- ³ N. Hadjichristidis, M. Pitsikalis, H. Iatrou, *Adv. Polym. Sci* **2005**, 189, 1-124
- ⁴ M. A. Dunbar, S. L. Balof, A. N. Roberts, E. J. Valente, H. J. Schanz, *Organometallic* **2011**, 30, 199-203
- ⁵ R. H. Grubbs (Ed.), *Handbook of Metathesis*, vol. 1&3, Wiley-VHC, Weinheim, **2003**
- ⁶ R. H. Grubbs, E. Khosravi, *Handbook of Metathesis*, 2nd Ed., vol.3. Wiley-VCH, Weinheim, **2015**
- ⁷ C. W. Bielawski, R. H. Grubbs, *Prog. Polym. Sci* **2007**, 32, 1-29
- ⁸ O. Nuyken, S. Schneider, U. Frenzel, *Olefin Metathesis - Encyclopedia of Polymer Science and Technology*, Wiley-VCH, **2014**, 8, 149-206
- ⁹ Y. Chauvin, *Angew. Chem. Int. Ed.* **2006**, 45, 3740-3747
- ¹⁰ R. H. Grubbs, *Angew. Chem. Int. Ed.* **2006**, 45, 3760-3765
- ¹¹ R. R. Schrock, *Angew. Chem. Int. Ed.* **2006**, 45, 3748-3760
- ¹² P. v. R. Schleyer, J. E. William, K. R. Blanchard, *J. Am. Chem. Soc.* **1970**, 92, 2377-2386
- ¹³ B. Lebedev, N. Srnirnova, *Macromol. Chem. Phys.* **1994**, 195, 35-63
- ¹⁴ Z.-R. Chen, J. P. Claverie, R. H. Grubbs, J. A. Kornfield, *Macromolecules* **1995**, 28, 2147-2154
- ¹⁵ K. J. Ivin, T. Saegusa, *Ring opening polymerization*, vol. 1, Elsevier, **1984**
- ¹⁶ J. L. Herisson, Y. Chauvin, *Makromol. Chem.* **1971**, 141, 161-176
- ¹⁷ M. Szwarc, *Nature* **1956**, 178, 1168 -1169
- ¹⁸ K. Matyjaszewski, *Macromolecules* **1993**, 26, 1787-1788
- ¹⁹ O. W. Webster, *Science* **1991**, 251, 887-893
- ²⁰ G. Pampus, G. Lehnert, *Makromol. Chem.* **1974**, 175, 2605-2616
- ²¹ A. Greco, F. Pirolini, G. Dall'Asta, *J. Organomet. Chem.* **1973**, 60, 115-124
- ²² J. R. Kress, , M. J. M. Russell, M. G. Wesolek, J. A. Osborn, *J. Chem. Soc., Chem. Commun.* **1980**, 431-432
- ²³ Y. Wada, C. Nakaoka, A. Morikawa, *Chem. Lett.* **1988**, 25-26

-
- ²⁴ G. Natta, G. Motroni, *Angew. Makromol. Chem.*, **1971**, 51, 16-17
- ²⁵ G. Natta, G. Dall'Asta, G. Mazzanti, *Angew. Chem. Int. Ed.* **1964**, 3, 723-729
- ²⁶ K. Saito, T. Yamaguchi, K. Tanabe, T. Ogura, M. Yagi, *Bull. Chem. Soc. Jpn.* **1979**, 52, 3192-3197
- ²⁷ T. M. Trnka, R. H. Grubbs, *Acc. Chem. Res.* **2001**, 34, 18-29
- ²⁸ T. J. Katz, S. J. Lee, N. Acton, *Tetrahedron Lett.* **1976**, 17, 4247-4250
- ²⁹ T. J. Katz, N. Acton, *Tetrahedron Lett.* **1976**, 17, 4251-4254
- ³⁰ L. R. Gilliom, R. H. Grubbs, *Organometallics* **1986**, 5, 721-724
- ³¹ L. R. Gilliom, R. H. Grubbs, *J. Am. Chem. Soc.* **1986**, 108, 733-742
- ³² L. F. Cannizzo, R. H. Grubbs, *Macromolecules* **1988**, 21, 1961-1967
- ³³ K. C. Wallace, R. Schrock, *Macromolecules* **1987**, 20, 448-450
- ³⁴ R. R. Schrock, J. Feldman, L. F. Cannizzo, R. H. Grubbs, *Macromolecules* **1987**, 20, 1169-1172
- ³⁵ K. J. Ivin, J. Kress, J. A. Osborn, *Makromol. Chem.* **1992**, 193, 1695-1707
- ³⁶ J. L. Couturier, C. Paillet, M. Leconte, J. M. Basset, K. Weiss, *Angew. Chem. Int. Ed.* **1992**, 31, 628-631
- ³⁷ M. G. Perrot, B. M. Novak, *Macromolecules* **1995**, 28, 3492-3494
- ³⁸ S. T. Trzaska, L. B. W. Lee, R. A. Register, *Macromolecules* **2000**, 33, 9215-9221
- ³⁹ G. C. Bazan, R. R. Schrock, *Macromolecules* **1991**, 24, 817-823
- ⁴⁰ G. C. Bazan, J. H. Oskam, H. N. Cho, L. Y. Park, R. R. Schrock, *J. Am. Chem. Soc.* **1991**, 113, 6899-6907
- ⁴¹ G. C. Bazan, E. Khosravi, R. R. Schrock, W. J. Feast, V. C. Gibson, *Polym. Commun.* **1989**, 30, 258-260
- ⁴² W. J. Feast, V. C. Gibson, E. L. Marshall, *J. Chem. Soc. Chem. Commun.* **1992**, 1, 1157-1158
- ⁴³ G. Dall'Asta, G. Mazzanti, G. Natta, L. Porri, *Makromol. Chem.* **1962**, 56, 224-227
- ⁴⁴ L. Porri, R. Rossi, P. Diversi, A. Lucherini, *Makromol. Chem.* **1974**, 175, 3097-3114
- ⁴⁵ B. M. Novak, R. H. Grubbs, *J. Am. Chem. Soc.* **1988**, 110, 7542-7543
- ⁴⁶ G. C. Vougioukalakis, R. H. Grubbs, *Chem. Rev.* **2010**, 110, 1746-1787
- ⁴⁷ P. Schwab, M. B. France, J. W. Ziller, R. H. Grubbs, *Angew. Chem. Int. Ed.* **1995**, 34, 2039-2041
- ⁴⁸ D. M. Lynn, S. Kanaoka, R. H. Grubbs, *J. Am. Chem. Soc.* **1996**, 118, 784-790
-

- ⁴⁹ B. R. Maughon, R. H. Grubbs, *Macromolecules* **1997**, *30*, 3459-3469
- ⁵⁰ B. R. Maughon, M. Weck, B. Mohr, R. H. Grubbs, *Macromolecules* **1997**, *30*, 257-265
- ⁵¹ C. W. Bielawski, R. H. Grubbs, *Angew. Chem. Int. Ed.* **2000**, *39*, 2903-2906
- ⁵² T. L. Choi, R. H. Grubbs, *Angew. Chem. Int. Ed.* **2003**, *42*, 1743-1746
- ⁵³ A. Duda, A. Kowalski, *Handbook of ring-opening polymerization*, Chapter 1, Wiley-VCH, **2009**
- ⁵⁴ O. Nuyken, S. D. Pask, *Polymers (MPDI)* **2013**, *5*, 361-403
- ⁵⁵ W. H. Carothers, G. L. Dorough, F. J. van Natta, *J. Am. Chem. Soc.* **1932**, *54*, 761-772
- ⁵⁶ F. J. van Natta, J. W. Hill, W. H. Carothers, *J. Am. Chem. Soc.* **1934**, *56*, 455-457
- ⁵⁷ A. C. Albertsson, I. K. Varma, *Biomacromolecules* **2003**, *4*, 1466-1486
- ⁵⁸ N. E. Kamber, W. Jeong, R. M. Waymouth, R. C. Pratt, B. G. G. Lohmeijer, J. L. Hedrick, *Chem. Rev.* **2007**, *107*, 5813-5840
- ⁵⁹ O. Dechy-Cabaret, B. Martin-Vaca, D. Bourissou, *Chem. Rev.* **2004**, *104*, 6147-6176
- ⁶⁰ Y. Sarazin, J. F. Carpentier, *Chem. Rev.* **2015**, *115*, 3564-3614
- ⁶¹ J. Klein, H. H. Klein, *Makromol. Chem.* **1959**, *30*, 23-38
- ⁶² B. O'Keefe, M. A. Hillmyer, W. B. Tolman, *J. Chem. Soc. Dalton Trans.* **2001**, 2215-2224
- ⁶³ W. Dittrich, R. C. Schulz, *Angew. Makromol. Chem.* **1971**, *15*, 109-126
- ⁶⁴ P. Dubois, C. Jacob, R. Jérôme, P. Teyssié, *Macromolecules* **1991**, *24*, 2266-2270
- ⁶⁵ H. R. Kricheldorf, M. Berl, N. Scharnagl, *Macromolecules* **1988**, *21*, 286-293
- ⁶⁶ A. Lofgren, A. C. Albertsson, P. Dubois, R. Jerome, P. Teyssie, *Macromolecules* **1994**, *27*, 5566-5562
- ⁶⁷ N. Ropson, P. Dubois, R. Jerome, P. Teyssie, *Macromolecules* **1995**, *28*, 7589-7598
- ⁶⁸ C. Jacobs, P. Dubois, R. Jerome, P. Teyssie, *Macromolecules* **1991**, *24*, 3027-3034
- ⁶⁹ A. J. Niejenhuis, D. W. Grijpma, A. J. Pennings, *Macromolecules* **1992**, *25*, 6419-6426
- ⁷⁰ A. Duda, S. Penczek, A. Kowalski, J. Libiszowski, *Macromol. Symp.* **2000**, *153*, 41-53

- ⁷¹ H. R. Kricheldorf, I. Kreiser-Saunders, A. Stricker, *Macromolecules* **2000**, *33*, 702-709
- ⁷² A. Kowalski, A. Duda, S. Penczek, *Macromolecules* **2000**, *33*, 7359-7370
- ⁷³ M. Ryner, K. Stridsberg, A. C. Albertsson, H. von Schenk, M. Svensson, *Macromolecules* **2001**, *34*, 3877-3881
- ⁷⁴ H. R. Kricheldorf, I. Kreiser-Saunders, D. O. Damrau, *Macromol. Symp.* **2000**, *159*, 247-258
- ⁷⁵ J. Baran, A. Duda, A. Kowalski, R. Szymansky, S. Penczek, *Macromol. Symp.* **1997**, *123*, 93-101
- ⁷⁶ P. J. A. In't Veld, E. M. Velner, P. V. De Witte, J. Hamhuis, P.J. Dijkstra, J. Feijen, *J. Polym. Sci. Part A: Polym. Chem.* **1997**, *35*, 219-226
- ⁷⁷ G. Schwach, J. Coudane, R. Engel, M. Vert, *Polym. Bull.* **1996**, *37*, 771-776
- ⁷⁸ G. Schwach, J. Coudane, R. Engel, M. Vert, *Biomaterials* **2002**, *23*, 993-1002
- ⁷⁹ A. P. Dove, *ACS Macro. Lett.* **2012**, *1*, 1409-1412
- ⁸⁰ F. Nederberg, E. F. Connor, M. Moeller, T. Glauser, J. L. Hedrick, *Angew. Chem. Int. Ed.* **2001**, *40*, 2712-2715
- ⁸¹ F. Nederberg, E. F. Connor, M. Moeller, T. Glauser, J. L. Hedrick, *Chem. Commun.* **2001**, 2066-2067
- ⁸² E. F. Connor, G. W. Nyce, M. Myers, A. Mock, J. L. Hedrick, *J. Am. Chem. Soc.* **2002**, *124*, 914-915
- ⁸³ A. P. Dove, R. C. Pratt, B. G. G. Lohmeijer, D. A. Culkin, E. C. Hagberg, G. W. Nyce, R. M. Waymouth, J. L. Hedrick, *Polymer* **2006**, *47*, 4018-4025
- ⁸⁴ O. Coulembier, L. Mespouille, J. L. Hedrick, R. M. Waymouth, P. Dubois, *Macromolecules* **2006**, *39*, 4001-4008
- ⁸⁵ G. W. Nyce, T. Glauser, E. F. Connor, A. Mock, R. M. Waymouth, J. L. Hedrick, *J. Am. Chem. Soc.* **2003**, *125*, 3046-3056
- ⁸⁶ F. Nederberg, B. G. G. Lohmeijer, F. Leibfarth, R. C. Pratt, J. Choi, A. P. Dove, R. M. Waymouth, J. L. Hedrick, *Biomacromolecules* **2007**, *8*, 153-160
- ⁸⁷ D. A. Culkin, S. Csihony, W. Jeong, A. C. Sentman, G. W. Nyce, A. P. Dove, R. C. Pratt, J. L. Hedrick, R. M. Waymouth, *Polym. Prepr.* **2005**, *46*, 710-711

- ⁸⁸ O. Coulembier, A. R. Dove, , R. C. Pratt, A. C. Sentman, D. A. Culkin, L. Mespouille, P. Dubois, R. M. Waymouth, J. L. Hedrick, *Angew. Chem. Int. Ed.* **2005**, *44*, 4964-4968
- ⁸⁹ G. W. Nyce, S. Csihony, R. M. Waymouth, J. L. Hedrick, *Chem. Eur. J.* **2004**, *10*, 4073-4079
- ⁹⁰ M. Fevre, J. Pinaud, A. Leteneur, Y. Gnanou, J. Vignolle, D. Taton, K. Miqueu, J. M. Sotiropoulos, *J. Am. Chem. Soc.* **2012**, *134*, 6776-6784
- ⁹¹ H. Feng, C. M. Dong, *J. Polym. Sci. Part A: Polym. Chem.* **2006**, *44*, 5353-5361
- ⁹² F. A. Jaipuri, B. D. Bower, N. L. Pohl, *Tetrahedron: Asymmetry* **2003**, *14*, 3249-3252
- ⁹³ J. Kadota, D. Pavlovic, H. Hirano, A. Okada, Y. Agari, B. Bibal, A. Deffieux F. Peruch, *RSC Adv.* **2014**, *4*, 14725–14732
- ⁹⁴ M. Myers, E. F. Connor, T. Glauser A. Mock, G. W. Nyce, J. L. Hedrick, *J. Polym. Sci., Part A: Polym. Chem.* **2002**, *40*, 848-851
- ⁹⁵ D. Delcroix, B. Martin-Vaca, D. Bourissou, C. Navarro, *Macromolecules* **2010**, *43*, 8828-8835
- ⁹⁶ S. Gazeau-Bureau, D. Delcroix, B. Martin-Vaca, D. Bourissou, C. Navarro, S. Magnet, *Macromolecules* **2008**, *41*, 3782-3784
- ⁹⁷ K. Makiguchi, T. Satoh, T. Kakuchi, *Macromolecules* **2011**, *44*, 1999-2005
- ⁹⁸ D. Delcroix, A. Couffin, N. Susperregui, C. Navarro, L. Maron, B. Martin-Vaca, D. Bourissou, *Polym. Chem.* **2011**, *2*, 2249-2256
- ⁹⁹ H. R. Kricheldorf, R. Dunsing, A. Serra, *Macromolecules* **1987**, *20*, 2050-2057
- ¹⁰⁰ S. Penczek, *J. Polym. Sci, Part A: Polym. Chem.* **2000**, *38*, 1919-1933
- ¹⁰¹ M. Fèvre, J. Vignolle, Y. Gnanou, D. Taton, *Polymer Science: A Comprehensive Reference* **2012**, *4*, 67-115
- ¹⁰² N. E. Kamber, M. K. Kiesewetter, J. L. Hedrick, R. M. Waymouth, *Polym. Prepr.* **2006**, *47*, 570-571
- ¹⁰³ A. P. Dove, R. C. Pratt, B. G. G. Lohmeijer, R. M. Waymouth, J. L. Hedrick, *J. Am. Chem. Soc.* **2005**, *127*, 13798-13799
- ¹⁰⁴ R. C. Pratt, B. G. G. Lohmeijer, D. A. Long, P. N. P. Lundberg, A. P. Dove, H. B. Li, C. G. Wade, R. M. Waymouth, J. L. Hedrick, *Macromolecules* **2006**, *39*, 7863-7871

- ¹⁰⁵ R. C. Pratt, B. G. G. Lohmeijer, D. A. Long, R. M. Waymouth, J. L. Hedrick, *J. Am. Chem. Soc.* **2006**, *128*, 4556-4557
- ¹⁰⁶ B. G. G. Lohmeijer, R. C. Pratt, F. Leibfarth, J. W. Logan, D. A. Long, A. P. Dove, F. Nederberg, J. Choi, C. Wade, R. M. Waymouth, J. L. Hedrick, *Macromolecules* **2006**, *39*, 8574-8583
- ¹⁰⁷ M. Bouyahyi, M. P. F. Pepels, A. Heise, R. Duchateau, *Macromolecules* **2012**, *45*, 3356-3366
- ¹⁰⁸ H. Kim, J. V. Olsson, J. L. Hedrick, R. M. Waymouth, *ACS Macro. Lett.* **2012**, *1*, 845-847
- ¹⁰⁹ M. T. Martello, A. Burns, M. Hillmeyer, *ACS Macro. Lett.* **2012**, *1*, 131-135
- ¹¹⁰ J. M. Harris, *Poly(Ethylene Glycol) Chemistry: Biotechnical and Biomedical Applications*, Plenum Press, New York, **1992**
- ¹¹¹ D. Neugebauer, *Polym. Int.* **2007**, *56*, 1469-1498
- ¹¹² M. Labet, W. Thielemans, *Chem. Soc. Rev.* **2009**, *38*, 3484-3504
- ¹¹³ V. Héroguez, S. Breunig, Y. Gnanou, M. Fontanille, *Macromolecules* **1996**, *29*, 4459-4464
- ¹¹⁴ S. Breunig, V. Héroguez, Y. Gnanou, M. Fontanille, *Macromol. Symp.* **1995**, *95*, 151-166
- ¹¹⁵ L. Pichavant, C. Bourget, M. C. Durrieu, V. Héroguez, *Macromolecules* **2011**, *44*, 7879-7887
- ¹¹⁶ J. Zou, G. Jafr, E. Themistou, Y. Yap, Z. A. P. Wintrob, P. Alexandridis, A. C. Ceacareanu, C. Cheng, *Chem. Commun.* **2011**, *47*, 4493-4495
- ¹¹⁷ R. B. Breitenkamp, Z. Ou, K. Breitenkamp, M. Muthukumar, T. Emrick, *Macromolecules* **2007**, *40*, 7617-7624
- ¹¹⁸ R. Revanur, B. McCloskey, K. Breitenkamp, B. D. Freeman, T. Emrick, *Macromolecules* **2007**, *40*, 3624-3630
- ¹¹⁹ K. Breitenkamp, J. Simeone, E. Jin, T. Emrick, *Macromolecules* **2002**, *35*, 9249-9252
- ¹²⁰ S. F. Alfred, Z. M. Al-Bardi, A. E. Madkour, K. Lienkamp, G. N. Tew, , *J. Polym. Sci., Part A: Polym. Chem.* **2008**, *46*, 2640-2648
- ¹²¹ K. Breitenkamp, T. Emrick, *J. Polym. Sci., Part A: Polym. Chem.* **2005**, *43*, 5715-5721

- ¹²² S. C. G. Biagini, A. L. Parry, *J. Polym. Sci., Part A: Polym. Chem.* **2007**, *45*, 3178-3190
- ¹²³ N. B. Sankaran, A. Z. Rys, R. Nassif, M. K. Nayak, K. Metera, B. Chen, H. S. Bazzi, H. F. Sleiman, *Macromolecules* **2010**, *43*, 5530-5537
- ¹²⁴ J. B. Matson, G. H. Grubbs, *J. Am. Chem. Soc.* **2008**, *130*, 6731-6733
- ¹²⁵ J. A. Johnson, Y. Y. Lu, , A. O. Burts, Y. Xia, A. C. Durrell, D. A. Tirrell, R. H. Grubbs, *Macromolecules* **2010**, *43*, 10326-10335
- ¹²⁶ J. A. Johnson, Y. Y. Lu, A. O. Burts, J. H. Lim, M. G. Finn, J. T. Koberstein, N. J. Turro, D. A. Tirrell, R. H. Grubbs, *J. Am. Chem. Soc.* **2011**, *133*, 559-566
- ¹²⁷ H. Shi, D. Shi, Z. Yao, S. Luan, J. Jin, J. Zhao, H. Yang, P. Stagnaro, J. Yin, *Polym. Chem.* **2011**, *2*, 679-684
- ¹²⁸ Y. Li, J. Zou, B. P. Das, M. Tsianou, C. Cheng, *Macromolecules* **2012**, *45*, 4623-4629
- ¹²⁹ D. Le, V. Montembault, J. C. Soutif, M. Rutnakornpituk, L. Fontaine, *Macromolecules* **2010**, *43*, 5611-5617
- ¹³⁰ D. Le, V. Montembault, S. Pascual, D. Collette, V. Héroguez, L. Fontaine, *Polym. Chem.* **2013**, *4*, 2168-2173
- ¹³¹ A. M. Eissa, E. Khosravi, *Macromol. Chem. Phys.* **2015**, *216*, 964-976
- ¹³² M. Mecerreyes, D. Dahan, P. Lecomte, A. Demonceau, A. F. Noels, J. Jerome, *J. Polym. Sci., Part A: Polym. Chem.* **1999**, *37*, 2447-2455
- ¹³³ M. Xie, J. Dang, H. Han, W. Wang, J. Liu, X. He, Y. Zhang, *Macromolecules* **2008**, *41*, 9004-9010
- ¹³⁴ D. Yang, W. Huang, J. Yu, J. Jiang, L. Zhang, M. Xie, *Polymer* **2010**, *51*, 5100-5106
- ¹³⁵ Q. Fu, J. M. Ren, G. G. Qiao, *Polym. Chem.* **2012**, *3*, 343-351
- ¹³⁶ E. H. Kang, I. H. Lee, T. L. Choi, *ACS Macro. Lett.* **2012**, *1*, 1098-1102
- ¹³⁷ F. Leroux, V. Montembault, S. Pascual, W. Guerin, S. M. Guillaume, L. Fontaine, *Polym. Chem.* **2014**, *5*, 3476-3486
- ¹³⁸ H. Zhang, Z. Zhang, Y. Gnanou, N. Hadjichristidis, *Macromolecules* **2015**, *48*, 3556-3562

Chapter 2

**Synthesis and characterization of high grafting density
bottle-brush poly(oxa)norbornene-g-poly(ϵ -caprolactone)**

Synthesis and characterization of high grafting density bottle-brush poly(oxa)norbornene-g-poly(ϵ -caprolactone)

Duc Anh N'Guyen,^a Flavien Leroux,^a Véronique Montembault,^a Sagrario Pascual^a and Laurent Fontaine^{*a}

Received (in XXX, XXX) Xth XXXXXXXXXX 20XX, Accepted Xth XXXXXXXXXX 20XX

DOI: 10.1039/b000000x

Poly(ϵ -caprolactone)-based (oxa)norbornene macromonomers with two poly(ϵ -caprolactone) (PCL) chains on the polymerizable entity were synthesized through organocatalyst mediated ring-opening polymerization (ROP) in high yields, with excellent control over molecular weights (from 2 800 to 11 000 g/mol) and dispersities ($D_M < 1.26$). Ring-opening metathesis polymerization (ROMP) of these macromonomers was carried out using the very active, fast-initiating Grubbs' second generation catalyst and the fast-initiating, fast-propagating Grubbs' third generation catalyst. High grafting density poly(oxa)norbornene-g-PCLs were obtained with a backbone length between 10 and 100 repeating units and grafts length between 10 and 48 while retaining a narrow distribution of molecular weights, leading to comb or brush copolymers according to the lengths of backbone and graft chains. Thermal analyses show a higher stability of the bottle-brush poly(oxa)norbornene-g-PCLs compared to their PCL-based (oxa)norbornene macromonomers together with a weaker crystallinity resulting from steric hindrance.

Introduction

Graft copolymers are regularly branched macromolecules consisting of a backbone and side chains. They have attracted considerable attention in recent years as a result of their unique properties through selection of the polymer backbone and the graft chains.¹⁻³ The 'grafting through' strategy is being looked into as a privileged way to get access to regular multibranch polymer that are highly compact. Upon polymerization of macromonomers, polymers of extremely high branch density and uniform branch length can, indeed, be obtained.⁴⁻⁶ Nevertheless, the 'grafting through' strategy is likely to encounter steric hindrance during the polymerization of high molecular weight or sterically-bulky macromonomers.⁷⁻⁹ Ring-opening metathesis polymerization (ROMP) using a ruthenium-based catalyst has been reported as an efficient approach to synthesize high density brush polymers.¹⁰⁻¹³ Due to its high functional group tolerance, synthesis of macromolecular brushes can be carried out using various types of norbornenyl end-functionalized macromonomers through the 'grafting through' approach.¹⁴⁻¹⁶ Despite numerous works reporting the ROMP of macromonomers with (oxa)norbornenyl functionality obtained by various ionic and radical processes,^{11,14-16,17-24} ROMP of (oxa)norbornenyl-functionalized macromonomers with two side polymer chains directly connected on the polymerizable entity has been much less investigated: only polynorbornene-g-polystyrene²⁵, poly(oxa)norbornene-g-poly(ethylene oxide)²⁶ and polyoxanorbornene-g-poly(lactide)²⁷ have been successfully synthesized with a backbone length up to 27 for a number-average degree of polymerization (DP_n) of the macromonomer of 50.

In this paper the synthesis of well-defined graft copolymers by ROMP of (oxa)norbornene-functionalized macromonomers with two poly(ϵ -caprolactone) (PCL) side chains on the polymerizable entity is reported. Aliphatic polyesters such as PCL are interesting potential candidates as side chains for graft copolymers providing original features such as polarity, functionality and (bio)degradability.²⁸⁻³⁰ Organocatalyzed ring-opening polymerization (ROP) of ϵ -caprolactone was carried out from dihydroxyl derivative of (oxa)norbornene as the initiator.

Organocatalyzed ROP³¹⁻³⁵ has the distinct advantage over stannous octoate-catalyzed ROP to require lower reaction temperatures that are more compatible with the oxanorbornene moiety thermal stability.¹⁵ The resulting PCL-based (oxa)norbornene macromonomers with two PCL chains of variable length were subjected to ROMP using Grubbs' second and third generation catalysts. Influence of the nature of the length of PCL chains, polymerizable entity and Grubbs' catalyst was studied. Finally, the thermal properties of the bottle-brush poly(oxa)norbornene-g-PCL were characterized and compared to the PCL macromonomer precursors.

70 Experimental

General Characterization

Nuclear Magnetic Resonance (NMR) spectra were recorded on a Bruker Avance 400 spectrometer for ¹H NMR (400 MHz) and ¹³C NMR (100 MHz). Chemical shifts are reported in ppm relative to the deuterated solvent resonances. Number-average degrees of polymerization (DP_n) were determined by ¹H NMR analysis, based on the comparison of the integrations of the norbornene alkene protons at $\delta = 6.17$ ppm (2H, labeled (a) in Figure 2A) or the oxanorbornene alkene protons at $\delta = 6.39$ ppm (2H, labeled (a) in Figure S5A in ESI†) against the methylene group of PCL at 2.30 ppm (labeled (e) in Figures 2A and S5A in ESI†) (Table 1, Figure 2A and S3-S7 in ESI†). ϵ -Caprolactone (CL) conversions were determined from ¹H NMR spectra of the crude PCL sample, from the integration (Int) ratio $Int_{PCL}/[Int_{PCL} + Int_{CL}]$, using the $-CH_2OC(O)$ methylene triplet ($\delta_{PCL} = 4.00-4.14$ ppm, $\delta_{CL} = 4.19$ ppm). Number-average molecular weight (M_n) and dispersity ($D_M = M_w/M_n$) values were measured by Size Exclusion Chromatography (SEC) using tetrahydrofuran (THF) as an eluent, and carried out using a system equipped with a SpectraSYSTEM AS 1000 autosampler, with a Guard column (Polymer Laboratories, PL gel 5 μ m Guard column, 50 x 7.5 mm) followed by two columns (Polymer Laboratories, 2 PL gel 5 μ m MIXED-D columns, 2 x 300 x 7.5) and with a SpectraSYSTEM RI-150 detector. The instrument operated at a flow rate of 1.0 mL.min⁻¹ at 35 °C and was calibrated with narrow linear polystyrene (PS) standards with molecular weight ranging from 580 g.mol⁻¹ to 483 000 g.mol⁻¹. All elution curves were calibrated with polystyrene standards. $M_{n,SEC}$ values of PCLs were

calculated using the average correcting factors previously reported (PCL: $\overline{M}_{n,SEC} = \overline{M}_{n,SEC} \text{ raw data} \times 0.56^{36,37}$), thus taking into account the difference in hydrodynamic radius of PCL versus polystyrene. Matrix-Assisted Laser Desorption and Ionization Time Of Flight (MALDI-TOF) mass spectrometry analysis was performed on a Bruker Biflex III MALDI-TOF instrument equipped with a nitrogen laser operating at 337 nm, a 2 GHz sampling rate digitizer, pulsed ion extraction source and reflectron. The laser pulse width is 3 ns and maximum power is 200 mJ. Spectra were recorded in the linear mode with an acceleration voltage of 19 kV and a delay of 200 ns. 100 single shot acquisitions were summed to give the spectra and the data were analyzed using Bruker XTOF software. Samples were prepared by dissolving the matrix (*trans*-2-[3-(4-*tert*-butylphenyl)-2-methyl-2-propenylidene]malononitrile, DCTB) in the solvent (dichloromethane, DCM, 30 mg.mL⁻¹) and mixing with the polymer (2 mg.mL⁻¹) in the ratio 1:50 (v/v). An aliquot of this solution (1 mL) was spotted directly onto a thin layer of sodium trifluoroacetate in acetone (concentration 19 mg.mL⁻¹) that had been deposited to act as a cationizing agent. Differential Scanning Calorimetry (DSC) data were acquired using a TA Instruments Q100 connected to a computer in aluminum pans under nitrogen. The samples were heated from 20 °C to 100 °C, held at 100 °C for 20 min to erase any history effects, and then cooled to -65 °C, kept at -65 °C for 5 min, and heated again to 240 °C at a heating rate of 10 °C.min⁻¹. Crystallization temperatures (*T*_c) were obtained from the cooling scan, while melting transition temperatures (*T*_m) were obtained from the second heating scan to avoid the influence of thermal history. Thermogravimetric analyses (TGA) were performed at a heating rate of 10 °C.min⁻¹ from 40 °C up to 800 °C under a nitrogen flow of 90 mL.min⁻¹ on a TA Instruments Q500 apparatus.

Materials

All chemicals were purchased from Aldrich unless otherwise noted. Acetic acid (98.0%, Merck), dichloromethane (DCM, HPLC grade, Fisher Chemical), diethyl ether (technical grade), ethyl vinyl ether (99%, Acros), Grubbs' second generation catalyst (**G2**), bicyclo[2.2.1]hept-5-ene-2 *exo*, 3-*exo* dimethanol (**NB**, 97%), tetrahydrofuran (THF, > 99.8%) and 1,5,7-triazabicyclo[4.4.0]dec-5-ene (TBD, 98%) were used as received. ϵ -Caprolactone (CL, 99%, Acros) and toluene (99.9%) were distilled from CaH₂. DCM and THF were dried over dry solvent stations GT S100. 7-Oxabicyclo[2.2.1]hept-5-ene-2 *exo*, 3-*exo* dimethanol³⁸ (**OX**) and Grubbs' third generation catalyst³⁹ 1,3-bis(2,4,6-trimethylphenyl)-2-imidazolidinylidene)dichloro(phenyl methylene)bis(pyridine)ruthenium (**G3'**) were synthesized according to literature procedures.

General procedure for the preparation of PCL-based (oxa)norbornene macromonomers via ROP

A dry 10 mL Schlenk flask equipped with a stirring bar, a rubber septum, CL, TBD, inimer, and degassed anhydrous THF or toluene were introduced into a glovebox. The desired quantities of inimer (**NB** or **OX**) and TBD were added into the Schlenk flask and dissolved in degassed anhydrous THF or toluene (4.4 mL). The Schlenk flask was capped with a rubber septum and when an homogeneous solution was obtained, it was removed from the glovebox and immersed in an oil bath preset at 25 °C. CL (1 g, 8.76 mmol) was added to the Schlenk flask *via* a syringe (initial reaction time, *t* = 0) and the polymerization allowed to proceed. The reaction mixture was stirred over the appropriate time. The polymerization was quenched by the addition of acetic

acid solution in toluene (0.2 mL, 16.5 mmol/L). The resulting mixture was then concentrated to dryness under vacuum and the conversion determined by ¹H NMR analysis of the residue in CDCl₃. Finally, the crude polymer was dissolved in DCM (2 mL) and purified upon precipitation into cold diethyl ether (10 mL), filtered and dried overnight under reduced pressure (typical isolated yield 90-95%). The recovered polymer was then analyzed by NMR and SEC and MALDI-TOF mass spectrometry.

PCL-based oxanorbornene macromonomers. White powder. [CL]₀/[**OX**]₀/[TBD]₀ = 20/1/0.34 (Table 1, run 1); conversion > 99%; *DP*_{n,NMR} = 24; *M*_{n,SEC} = 2 900 g.mol⁻¹; *D*_M = 1.23. ¹H NMR (400 MHz, CDCl₃), δ (ppm): 6.39 (s, 2H, CH=CH), 4.80 (s, 2H, =CH-CH-O), 4.20 (m, 4H, CH-CH₂-O-C(O)), 4.06 (t, *J* = 6.8 Hz, 46H, CH₂-O-C(O) of the PCL repeating unit), 3.65 (t, *J* = 5.6 Hz, 4H, CH₂-OH), 2.30 (t, *J* = 7.6 Hz, 46H, O-C(O)-CH₂ of the PCL repeating unit), 2.00 (m, 2H, =CH-CH-CH), 1.75-1.55 (m, 92H, C(O)-CH₂-CH₂-CH₂-CH₂ of the PCL repeating unit), 1.45-1.35 (m, 46H, C(O)-(CH₂)₂-CH₂ of the PCL repeating unit) (Figure S5 in ESI[†]). ¹³C NMR (100 MHz, CDCl₃), δ (ppm): 173.00 (s, C=O), 135.48 (s, CH=CH), 80.37 (s, =CH-CH-O), 63.96 (s, CH₂-O-C(O) of the PCL repeating unit), 63.37 (s, CH-CH₂-OC(O)), 62.20 (s, -CH₂OH), 39.34 (s, =CH-CH-CH), 34.06 (s, O-C(O)-CH₂ of the PCL repeating unit), 32.35 (s, -CH₂-CH₂-OH), 28.20 (s, C(O)-CH₂-CH₂-CH₂-CH₂ of the PCL repeating unit), 25.27 (s, C(O)-CH₂-CH₂-CH₂ of the PCL repeating unit), 24.68 (s, C(O)-CH₂-CH₂) (Figure S8 in ESI[†]).

PCL-based norbornene macromonomers. White powder. [CL]₀/[**NB**]₀/[TBD]₀ = 20/1/0.34 (Table 1, run 4); conversion > 99%; *DP*_{n,NMR} = 24; *M*_{n,SEC} = 2 900 g.mol⁻¹; *D*_M = 1.18. ¹H NMR (400 MHz, CDCl₃), δ (ppm): 6.17 (s, 2H, CH=CH), 4.23 (m, 4H, CH-CH₂-O-C(O)), 4.06 (t, *J* = 6.4 Hz, 46H, CH₂-O-C(O) of the PCL repeating unit), 3.65 (t, *J* = 6.4 Hz, 4H, CH₂-OH), 2.72 (m, 2H, =CH-CH), 2.30 (t, *J* = 7.2 Hz, 46H, O-C(O)-CH₂ of the PCL repeating unit), 1.85 (m, 2H, =CH-CH-CH), 1.75-1.55 (m, 96H, C(O)-CH₂-CH₂-CH₂-CH₂ of the PCL repeating unit), 1.50 (m, 2H, =CH-CH-CH₂), 1.45-1.35 (m, 48H, C(O)-(CH₂)₂-CH₂ of the PCL repeating unit) (Figure 2A). ¹³C NMR (100 MHz, CDCl₃), δ (ppm): 173.20 (s, C=O), 137.01 (s, CH=CH), 65.13 (s, CH-CH₂-OC(O)), 63.96 (s, CH₂-O-C(O) of the PCL repeating unit), 62.20 (s, -CH₂OH), 44.62 (s, =CH-CH), 42.27 (s, =CH-CH-CH₂), 39.34 (s, =CH-CH-CH), 34.06 (s, O-C(O)-CH₂ of the PCL repeating unit), 32.35 (s, -CH₂-CH₂-OH), 28.20 (s, C(O)-CH₂-CH₂-CH₂-CH₂ of the PCL repeating unit), 25.27 (s, C(O)-CH₂-CH₂-CH₂ of the PCL repeating unit), 24.68 (s, C(O)-CH₂-CH₂) (Figure S2 in ESI[†]).

General procedure for the preparation of graft copolymers via ROMP

In a typical experiment, a dry Schlenk flask was charged with the macromonomer (100 mg) and a stir bar. The Schlenk flask was capped with a rubber septum, and cycled five times between vacuum and argon to remove oxygen. The desired quantity of degassed, anhydrous toluene or THF ([*M*]₀ = 0.04 mol/L) was added *via* a syringe under an argon atmosphere to dissolve the macromonomer. A stock solution of Grubbs' catalyst in degassed anhydrous toluene or THF was prepared in a separate vial. All experiments have been conducted with a catalyst concentration [*I*]₀ = 7 μ mol/L. The Schlenk flask was immersed in an oil bath preset at 25 °C or at 70 °C when **G3'** and **G2** were respectively used, and was stirred under argon for 10 min. The desired quantity of catalyst was injected into the macromonomer solution to initiate the polymerization. The reaction mixture was stirred

over 3 h. The polymerization was quenched by the addition of two drops of ethyl vinyl ether. The solvent was removed under reduced pressure for NMR and SEC measurements.

Polyoxanorborene-g-poly(ϵ -caprolactone) **POX₁₀-g-PCL₂₄**

- 5 Brown plastic. $[\text{OX-PCL}_{24}]_0/[\text{G2}]_0 = 10$ (Table 2, run 1); conversion : 92%; $M_{n,calc} = 29\,024\text{ g}\cdot\text{mol}^{-1}$; $M_{n,SEC} = 35\,900\text{ g}\cdot\text{mol}^{-1}$; $D_M = 1.17$. ^1H NMR (400 MHz, CDCl_3), δ (ppm): 5.90-5.25 (bs, 20H, $\text{CH}=\text{CH}$), 4.24 (m, 40H, O-CH-CH-CH_2), 4.07 (t, $J = 6.8\text{ Hz}$, 460H, $\text{CH}_2\text{-CH}_2\text{-O-C(O)}$ of the PCL repeating unit), 10 3.65 (t, $J = 6.4\text{ Hz}$, 40H, $\text{CH}_2\text{-OH}$), 2.30 (t, $J = 7.6\text{ Hz}$, 480H, $\text{O-C(O)-CH}_2\text{-CH}_2$ of the PCL repeating unit), 1.97 (bs, 20H, O-CH-CH), 1.60 (m, 960H, $\text{C(O)-CH}_2\text{-CH}_2\text{-CH}_2\text{-CH}_2$ of the PCL repeating unit), 1.40 (m, 480H, $\text{C(O)-CH}_2\text{-CH}_2$ of the PCL repeating unit) (Figure S5B in ESI†). ^{13}C NMR (100 MHz, CDCl_3), δ (ppm): 173.49 (s, C=O), 64.05 (s, $\text{CH}_2\text{-O-C(O)}$ of the PCL repeating unit), 62.57 (s, $-\text{CH}_2\text{OH}$), 34.04 (s, O-C(O)-CH_2 of the PCL repeating unit), 32.35 (s, $-\text{CH}_2\text{-CH}_2\text{-OH}$), 28.42 (s, $\text{C(O)-CH}_2\text{-CH}_2\text{-CH}_2\text{-CH}_2$ of the PCL repeating unit), 25.51 (s, $\text{C(O)-CH}_2\text{-CH}_2\text{-CH}_2$ of the PCL repeating unit), 24.47 (s, $\text{C(O)-CH}_2\text{-CH}_2$ of the PCL repeating unit) (Figure S10 in ESI†).

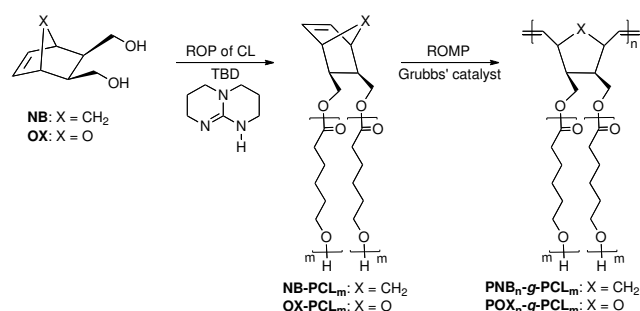
- 20 *Polynorborene-g-poly(ϵ -caprolactone)* **PNB₁₀-g-PCL₂₄**. Brown plastic. $[\text{NB-PCL}_{24}]_0/[\text{G2}]_0 = 10$ (Table 2, run 8); conversion : 95%; $M_{n,calc} = 29\,004\text{ g}\cdot\text{mol}^{-1}$; $M_{n,SEC} = 52\,200\text{ g}\cdot\text{mol}^{-1}$; $D_M = 1.29$. ^1H NMR (400 MHz, CDCl_3), δ (ppm): 5.75-5.15 (bs, 20H, $\text{CH}=\text{CH}$), 4.24 (m, 40H, O-CH-CH-CH_2), 4.07 (t, $J = 6.8\text{ Hz}$, 460H, $\text{CH}_2\text{-CH}_2\text{-O-C(O)}$ of the PCL repeating unit), 3.65 (t, $J = 6.4\text{ Hz}$, 40H, $\text{CH}_2\text{-OH}$), 2.30 (t, $J = 7.6\text{ Hz}$, 480H, $\text{O-C(O)-CH}_2\text{-CH}_2$ of the PCL repeating unit), 1.89 (bs, 20H, $=\text{CH-CH-CH}$), 1.60 (m, 960H, $\text{C(O)-CH}_2\text{-CH}_2\text{-CH}_2\text{-CH}_2$ of the PCL repeating unit), 1.52 (bs, 20H, $\text{CH}_2\text{-CH-CH=}$), 1.40 (m, 480H, $\text{C(O)-CH}_2\text{-CH}_2$ of the PCL repeating unit) (Figure 2B). ^{13}C NMR (100 MHz, CDCl_3), δ (ppm): 173.57 (s, C=O), 65.84 (s, $\text{CH-CH}_2\text{-OC(O)}$), 64.17 (s, $\text{CH}_2\text{-O-C(O)}$ of the PCL repeating unit), 62.50 (s, $-\text{CH}_2\text{OH}$), 34.08 (s, O-C(O)-CH_2 of the PCL repeating unit), 32.41 (s, $-\text{CH}_2\text{-CH}_2\text{-OH}$), 28.34 (s, $\text{C(O)-CH}_2\text{-CH}_2\text{-CH}_2\text{-CH}_2$ of the PCL repeating unit), 25.48 (s, $\text{C(O)-CH}_2\text{-CH}_2\text{-CH}_2$ of the PCL repeating unit), 24.52 (s, $\text{C(O)-CH}_2\text{-CH}_2$ of the PCL repeating unit) (Figure S11 in ESI†).

40 Results and discussion

Synthesis of poly(ϵ -caprolactone)-based (oxa)norborene macromonomers

- Poly(ϵ -caprolactone)-based (oxa)norborene macromonomers were synthesized by ring-opening polymerization (ROP) of ϵ -caprolactone (CL) in the presence of dihydroxyl derivatives of (oxa)norborene, *i.e.*, bicyclo[2.2.1]hept-5-ene-2-*exo*, 3-*exo* dimethanol (**NB**) and 7-oxabicyclo[2.2.1]hept-5-ene-2-*exo*, 3-*exo* dimethanol (**OX**), as initiators with $[\text{CL}]_0/[(\text{oxa})\text{norborene}]_0$ feed ratios ranging from 20/1 to 96/1 (Scheme 1). The

- 50 polymerization was performed at 25 °C in tetrahydrofuran (THF) or toluene, selecting 1,5,7-triazabicyclo[4.4.0]dec-5-ene (TBD) as the catalyst for its efficiency in promoting the ROP of CL.⁴⁰⁻⁴²



55 **Scheme 1** Synthesis of PCL macromonomers from dihydroxyl (oxa)norborene inimers and their subsequent ROMP

- The molecular characteristics of the macromonomers are shown in Table 1. All the samples have been characterized by ^1H NMR and size exclusion chromatography (SEC). The SEC traces of the poly(ϵ -caprolactone)-based (oxa)norborene macromonomers displayed a monomodal distribution with rather narrow dispersity values ranging from 1.16 to 1.25 as depicted in Figure 1 for poly(ϵ -caprolactone)-based norbornene macromonomers (**NB-PCL**) (Figure S1 in ESI† for PCL-based oxanorborene macromonomers, **OX-PCL**).

- The presence of the (oxa)norborene ring in the PCL chains has been confirmed by ^1H NMR spectroscopy. The chemical shift corresponding to olefinic signals on the norbornene ring at $\delta = 6.17\text{ ppm}$ ($\delta = 6.39\text{ ppm}$ for oxanorborene ring) together with the downfield shift of methylene protons of the initiating ROP group from $\delta = 3.70\text{--}3.75\text{ ppm}$ in (oxa)norborene to $\delta = 4.20\text{--}4.23\text{ ppm}$ in (oxa)norborene-functionalized PCL macromonomers, as illustrated in Figure 2 for **NB-PCL₂₄** (Figures S3-S7 in ESI† for **NB-PCL₅₁**, **NB-PCL₉₈**, **OX-PCL₂₄**, **OX-PCL₅₂**, **OX-PCL₉₂**, respectively) testifies the attachment of the (oxa)norborenyl group. Number-average degrees of polymerization (\overline{DP}_n) were determined by ^1H NMR analysis, based on the comparison of the integrations of the olefinic signals on the norbornene ring at $\delta = 6.17\text{ ppm}$ (labeled (a) in Figure 2A) or the oxanorborene ring at $\delta = 6.39\text{ ppm}$ (labeled (a) in Figure S5A) against the O-C(O)-CH_2 methylene triplet of the PCL at $\delta = 2.30\text{ ppm}$ (labeled (e) in Figures 2A and S5A) (Figures S3-S7 in ESI†). Consistently, the experimental $\overline{DP}_{n,NMR}$ values of PCL macromonomers, determined by ^1H NMR, agrees with the theoretical value and number-average molecular weight (\overline{M}_n) measured by SEC (Table 1).

Table 1 Characteristics of the **OX-PCL** and **NB-PCL** macromonomers synthesized upon ROP of CL mediated by TBD catalyst at 25 °C with inimer **OX** and **NB** initiator, respectively

Run	Sample ^a	[CL] ₀ /[inimer] ₀ /[TBD] ₀	Solvent	Reaction time ^b (h)	Conv. ^c (%)	$\overline{DP}_{n,NMR}$ ^d (g.mol ⁻¹)	$\overline{M}_{n,NMR}$ ^e (g.mol ⁻¹)	$\overline{M}_{n,SEC}$ ^f (g.mol ⁻¹)	\overline{D}_M ^f
1	OX-PCL ₂₄	20/1/0.34	THF	5	> 99	24	2 890	2 900	1.23
2	OX-PCL ₅₂	48/1/0.65	Toluene	5	> 99	52	6 080	5 000	1.23
3	OX-PCL ₉₂	96/1/0.65	Toluene	10	> 99	92	10 640	8 150	1.19
4	NB-PCL ₂₄	20/1/0.34	THF	5	> 99	24	2 890	2 900	1.18
5	NB-PCL ₅₁	48/1/0.65	THF	5	> 99	51	5 970	4 700	1.16
6	NB-PCL ₉₈	96/1/0.65	Toluene	10	> 99	98	11 330	9 000	1.25

^a In the sample name, the first two letters denote the inimer and the last number in subscript refers to the number of CL repeating units determined by ¹H NMR. ^b The reaction time was not optimized. ^c The CL monomer conversions were determined by comparing the peak areas of the methylene triplet of PCL at δ = 4.00–4.14 ppm and the methylene group of CL at δ = 4.19 ppm from ¹H NMR spectra of the crude mixture. ^d Calculated from ¹H NMR spectra by comparing the peak areas of the norbornene or oxanorbornene alkene protons at δ = 6.17 and 6.39 ppm, respectively and the O-C(O)-CH₂ methylene triplet at δ = 2.30 ppm. ^e Determined by ¹H NMR analysis from $\overline{M}_{n,NMR} = (\overline{DP}_{n,NMR} \times M_{CL}) + M_{inimer}$ with M_{CL} = 114 g.mol⁻¹, M_{inimer} NB = 154 g.mol⁻¹ and M_{inimer} OX = 156 g.mol⁻¹. ^f Determined by SEC in tetrahydrofuran (THF) with RI detector, calibrated with linear polystyrene standards (corrected values—refer to experimental section).

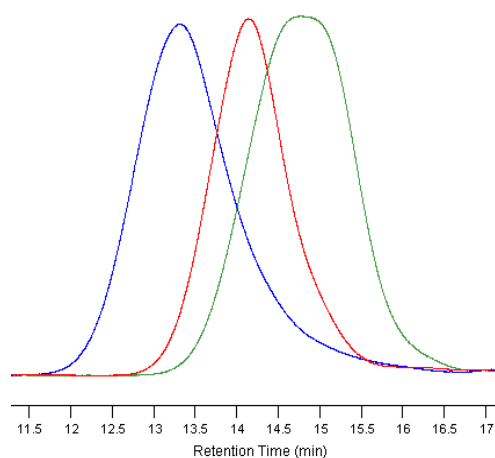


Fig. 1 SEC traces for the (A) **NB-PCL₂₄** (Table 1, run 4), (B) **NB-PCL₅₁** (Table 1, run 5) and (C) **NB-PCL₉₈** (Table 1, run 6)

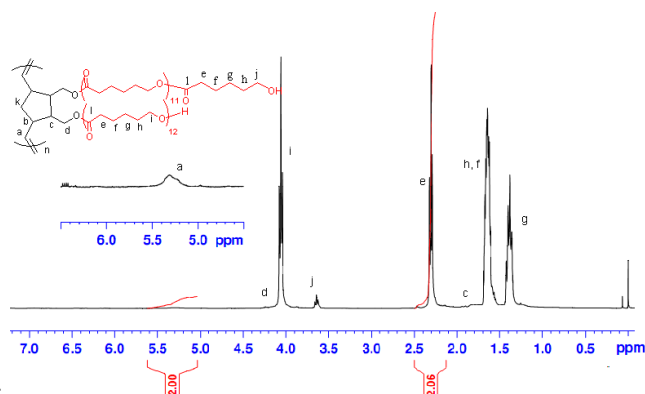
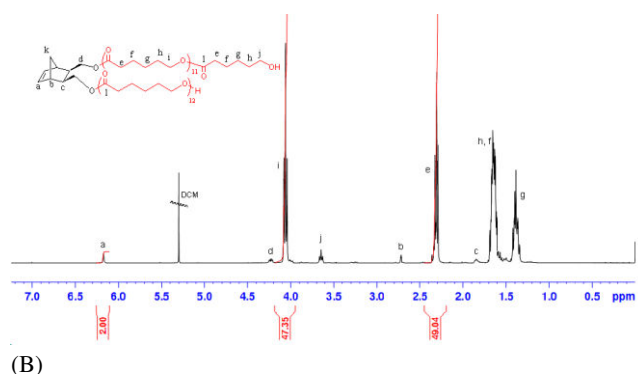


Fig. 2 ¹H NMR spectra (400 MHz, CDCl₃, 25 °C) of (A) precipitated **NB-PCL₂₄** from the ROP of CL in THF at 25°C using **NB** as the initiator and TBD as the catalyst with [CL]₀/[NB]₀ = 20 (Table 1, run 4) and (B) crude **PNB₁₀-g-PCL₂₄** obtained from the ROMP of **NB-PCL₂₄** in toluene at 70°C using **G2** as the catalyst with [NB-PCL₂₄]/[G2] = 10 for a reaction time of 3 h (Table 2, run 8)

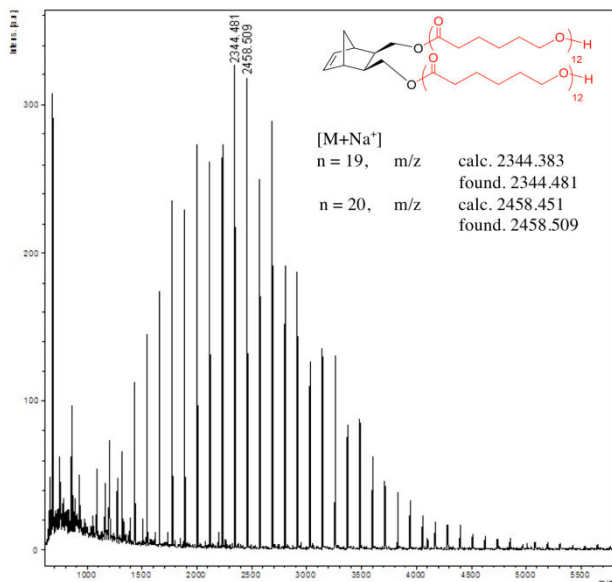


Fig. 3 MALDI-TOF mass spectrum (matrix: *trans*-2-[3-(4-*tert*-butylphenyl)-2-methyl-2-propenylidene]malononitrile (DCTB) + sodium trifluoroacetate (NaTFA)) of the PCL-based norbornene synthesized by ROP using **NB** as the initiator and TBD as the catalyst in THF at 25°C with [CL]₀/[NB]₀ = 20/1 (Table 1, run 4)

ROMP of poly(ϵ -caprolactone)-based (oxa)norborene macromonomers

Poly(oxa)norborene-g-poly(ϵ -caprolactone)s were synthesized via ROMP of PCL-based (oxa)norborene macromonomers with macromonomer-to-catalyst ratios ranging from 10 to 100 (Scheme 1).

ROMP of PCL-based oxanorborene macromonomers. ROMPs were carried out at 70°C in toluene with a macromonomer concentration of 0.04 mol.L⁻¹, selecting Grubbs' second generation catalyst, which is well-known to successfully polymerize sterically hindered substrates with bulky substituents, resulting in polymers with a narrow molecular distribution.^{43,44} After 3h, the reactions were terminated with ethyl vinyl ether.

The ROMP performance of the oxanorborene macromonomer **OX-PCL₂₄** (Table 1, run 1) was first studied. As determined by SEC analysis (Figure S12B in ESI[†]), a high conversion (> 90%) was obtained for a macromonomer-to-catalyst ratio of 10 (Table 2, run 1). This was confirmed by ¹H NMR spectroscopy which showed the appearance of the vinyl proton resonances of the grafted copolymer at 5.25 - 5.90 ppm (Figure S5B in ESI[†]) and the concomitant disappearance of the vinyl proton signal of **OX-PCL₂₄** at 6.39 ppm. Further increasing macromonomer-to-catalyst ratios to 50 and 100 (Table 2, runs 2 and 3) results in a partial conversion of the macromonomer as ascertained by SEC analyses (Figure S13 in ESI[†]). In the same way, **OX-PCL₅₂** and **OX-PCL₉₂** were only able to form polyoxanorborene-g-poly(ϵ -caprolactone) with a short targeted backbone length of 10 (Table 2, runs 4 and 6; Figures S14 and S15 in ESI[†]). Such a behavior is due to steric crowding of the growing polymacromonomer, which decreases the reactivity of the propagating center and, consequently, hinders the incorporation of the next macromonomer unit.⁴⁵

ROMP of PCL-based norbornene macromonomers. **NB-PCL₂₄** was easily polymerized to near quantitative yield with macromonomer-to-catalyst ratios up to 50 (Table 2, runs 8 and 9). As revealed by the SEC traces (Figure 4), polymacromonomers showed symmetrical peaks and narrow molecular distribution ($D_M \leq 1.35$) as well as high conversion (> 92%). The quantitative conversion of macromonomers was also proven by ¹H NMR spectroscopy, which indicated the disappearance of the vinyl proton signal of the poly(ϵ -caprolactone)-based macromonomers at 6.17 ppm for the norbornenyl ring, and the appearance of the vinyl proton resonances of the grafted copolymer at 5.15-5.75 ppm (Figure 2B). For ROMP of **NB-PCL₂₄** with a macromonomer-to-catalyst ratio of 100 (Table 2, run 10), the SEC trace displays a shoulder-peak in the high retention time region corresponding to unreacted macromonomer (Figure S16 in ESI[†]), and an incomplete conversion is reached. This result confirms that the ROMP is highly affected by steric hindrance arising from the macromonomers.^{12, 42-45}

Polymerization of PCL-based norbornene macromonomers with longer PCL chains has then been investigated. ROMP of **NB-PCL₅₁** using a macromonomer-to-catalyst ratio of 10 and 50 (Table 2, runs 11 and 12) went to near completion (conversion \geq 85%) as ascertained by the SEC traces (Figures 5B and 5C). However, attempts to polymerize PCL macromonomer with a PCL chain of around 90 (Table 2, runs 16 and 17) resulted in a copolymer contaminated with unreacted macromonomer (Figure S17 in ESI[†]). Incomplete conversion results from the limiting effect of the macromonomer steric hindrance during the propagation step.^{12, 42-45} Moreover, as already observed for the ROMP of **OX-PCL₂₄** compared to that of **NB-PCL₂₄** (Table 2, run 3 vs. run 10), **OX-PCL₅₂** showed a lower reactivity in ROMP than **NB-PCL₅₁** of similar PCL chain length (Table 2, run 5 vs. run 12). This difference in reactivity could be the consequence of the possible coordination between the oxanorborene cyclic ether and the catalyst, which may attenuate its ability to polymerize.⁴⁶

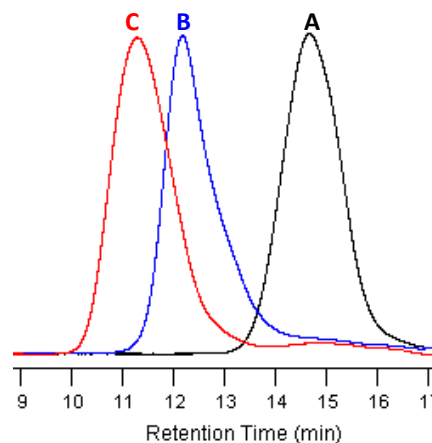


Fig. 4 SEC traces for the (A) precipitated **NB-PCL₂₄** (Table 1, run 4), (B) crude **PNB₁₀-g-PCL₂₄** (Table 2, run 8) and (C) crude **PNB₅₀-g-PCL₂₄** (Table 2, run 9) obtained by ROMP of **NB-PCL₂₄** initiated by **G2**

Table 2 ROMP of PCL macromonomers using Grubbs' catalyst with a reaction time of 3h^a

Run	Grafted copolymer	[M] ₀ /[I] ₀ ^b	Catalyst	$\overline{M}_{n, calc.}^c$ (g.mol ⁻¹)	Conv. ^d SEC (%)	$\overline{M}_{n, SEC}^e$ (g.mol ⁻¹)	D_M^e
1	POX ₁₀ -g-PCL ₂₄	10	G2	29 024	92	35 900	1.17
2	POX ₅₀ -g-PCL ₂₄	50	G2	144 704	82	47 200	1.20
3	POX ₁₀₀ -g-PCL ₂₄	100	G2	289 304	34	58 700	1.21
4	POX ₁₀ -g-PCL ₅₂	10	G2	60 944	95	64 000	1.14
5	POX ₅₀ -g-PCL ₅₂	50	G2	304 304	65	^f	^f
6	POX ₁₀ -g-PCL ₉₂	10	G2	106 544	95	74 900	1.15
7	POX ₅₀ -g-PCL ₉₂	50	G2	532 304	38	^g	^g
8	PNB ₁₀ -g-PCL ₂₄	10	G2	29 004	95	52 200	1.29
9	PNB ₅₀ -g-PCL ₂₄	50	G2	144 604	93	97 600	1.35
10	PNB ₁₀₀ -g-PCL ₂₄	100	G2	289 104	60	134 400	1.54
11	PNB ₁₀ -g-PCL ₅₁	10	G2	59 784	93	67 200	1.19
12	PNB ₅₀ -g-PCL ₅₁	50	G2	298 504	85	^g	^g
13	PNB ₅₀ -g-PCL ₅₁	50	G3'	298 504	97	178 400	1.18
14	PNB ₁₀₀ -g-PCL ₅₁	100	G3'	596 904	98	^g	^g
15	PNB ₂₀₀ -g-PCL ₅₁	200	G3'	1 193 704	60	^g	^g
16	PNB ₁₀ -g-PCL ₉₈	10	G2	113 364	85	133 000	1.17
17	PNB ₅₀ -g-PCL ₉₈	50	G2	566 404	10	^f	^f

^a Experiments using second generation Grubbs' catalyst were conducted at 70°C in toluene while those using third generation Grubbs' catalyst were conducted at 25°C in THF. ^b Macromonomer-to-catalyst molar ratio. ^c $\overline{M}_{n, calc.} = \overline{M}_{n, NMR} (PCL \text{ macromonomer}) * [M]_0/[I]_0 + M_{extr.}$ with $M_{extr.} = 104 \text{ g.mol}^{-1}$.

^d Determined by comparing the peak areas of grafted copolymer and residual macromonomer from SEC measurement of the crude product. ^e Determined by SEC in THF with RI detector, calibrated with linear polystyrene standards. ^f Not determined: bimodal distribution. ^g Not determined. Part of the chromatogram is out of the SEC calibration.

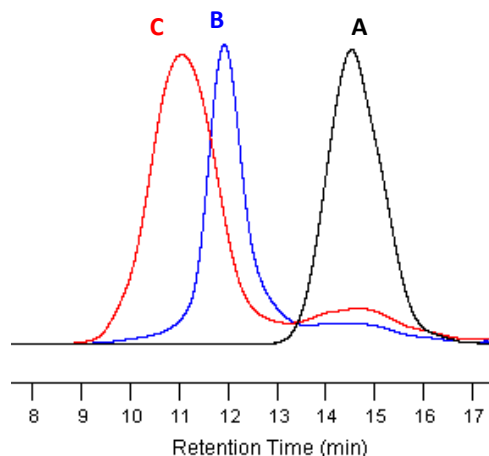


Fig. 5 SEC traces for the (A) precipitated **NB-PCL₅₁** (Table 1, run 4), (B) crude **PNB₁₀-g-PCL₅₁** (Table 2, run 8) and (C) crude **PNB₅₀-g-PCL₅₁** (Table 2, run 9) obtained by ROMP of **NB-PCL₅₁** initiated by **G2**

ROMP of poly(ϵ -caprolactone)-based norbornene macromonomers using Grubbs' third generation catalyst. Third

generation Grubbs' catalyst 1,3-bis(2,4,6-trimethylphenyl)-2-imidazolidinylidene dichloro(phenylmethylene) bis(pyridine) ruthenium (**G3'**) was used to polymerize the more reactive PCL-based norbornene macromonomer. This bis-pyridine complex **G3'** exhibits fast initiation and propagation⁴⁷ and has been proven

useful for graft-through synthesis of functional bottle-brush polymers.^{46,48-50} Reactions were carried out in THF using **NB-PCL₅₁** with macromonomer-to-catalyst ratios from 50 to 200 at room temperature with a macromonomer concentration of 0.04 mol.L⁻¹ (Table 2, runs 13-15). As evidenced by the SEC traces, **NB-PCL₅₁** reached near quantitative conversion (i.e., > 95%) for a macromonomer-to-catalyst ratio up to 100 (Figure 6 and Figure S18 in ESI†). The resulting bottle-brush polymers were monomodal and their SEC traces exhibited the expected inverse

relationship between molecular weight and retention time (Figures 6B and 6C). Additionally, dispersity values were low, around 1.18 as previously reported for graft-through ROMP polymerizations using **G3'**.^{46,48-50} The fast initiation, high reactivity, and high functional group tolerance of **G3'** make it ideal for the ROMP of sterically demanding macromonomers. The limitation in backbone length of these **PNB-g-PCL** compared to other reported graft polynorbornenes arises from the huge steric hindrance around the ROMP-able site as the norbornene ring is located at the center of the PCL chain instead of at the macromonomer chain-end.^{46,48-50}

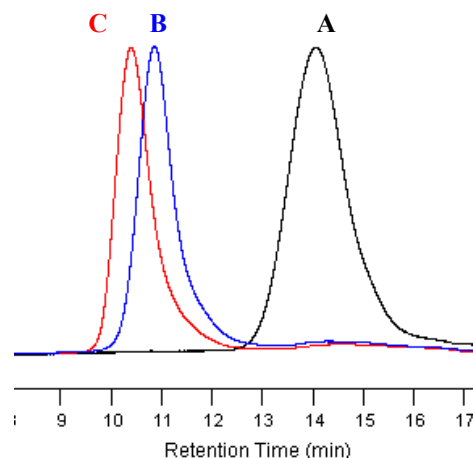


Fig. 6 SEC traces for the (A) precipitated **NB-PCL₅₁** (Table 1, run 4), (B) crude **PNB₅₀-g-PCL₅₁** (Table 2, run 13) and (C) crude **PNB₁₀₀-g-PCL₅₁** (Table 2, run 14) obtained by ROMP of **NB-PCL₅₁** initiated by **G3'**

Table 3 DSC and TGA results for the **OX-PCL₅₂** and **NB-PCL₅₁** macromonomers and corresponding **POX₅₀-g-PCL₅₂** and **PNB₅₀-g-PCL₅₁** graft copolymers

Run	Sample	Melting and crystallization properties				Degradation behavior		
		T_c^a (°C)	ΔH_c^a (J/g)	T_m^b (°C)	ΔH_m^b (J/g)	χ_c^c	$T_{\text{degradation}}^d$ (°C)	$T_{\text{max, deg}}^e$ (°C)
1	OX-PCL ₅₂	32	118	51	121	86	264	530
2	POX ₅₀ -g-PCL ₅₂	23	78	50	79	56	321	525
3	NB-PCL ₅₁	23	98	49	128	91	227	500
4	PNB ₅₀ -g-PCL ₅₁	21	53	47	53	38	270	500

^a The crystallization phase temperature (T_c) and the associated enthalpy (ΔH_c) were deduced from the second heating curve (heating rate of 10°C/min). ^b The melting phase temperature (T_m) and the associated enthalpy (ΔH_m) were deduced from the second heating curve (heating rate of 10°C/min). ^c Degree of crystallinity calculated by comparison with the reported enthalpy of fusion for the parent polymer crystal: $\chi_c = \Delta H_m / \Delta H_m^{100\%}$ 100% crystalline polymer, where $\Delta H_m^{100\%}$ crystalline PCL⁵³ = 140 J.g⁻¹. ^d Temperature at 5% mass loss determined by TGA. ^e Maximal temperature of degradation determined by TGA.

Thermal properties of poly(ϵ -caprolactone)-based (oxa)norbornene macromonomers and resulting graft copolymers

Graft copolymers and the corresponding macromonomer precursors have been analyzed by differential scanning calorimetry (DSC) and the results are shown in Table 3. Only the second heating was evaluated to exclude the influence of the thermal history of the samples. The DSC thermograms of **NB-PCL₅₁** and its resulting graft copolymer **PNB₅₀-g-PCL₅₁** are depicted in Figure 7 (Figure S19 in ESI† for **OX-PCL₅₂** and **POX₅₀-g-PCL₅₂**). The melting phase temperature for the PCL graft copolymers is in the same range as their PCL-based macromonomer precursors (Table 3, run 2 vs. run 1 and run 4 vs. run 3) and is similar to previously reported values for PCL-based structures.^{50,51} The melting peak at around 50°C prevents glass phase transition temperature (T_g) of the polynorbornene backbone from being observed.⁵²

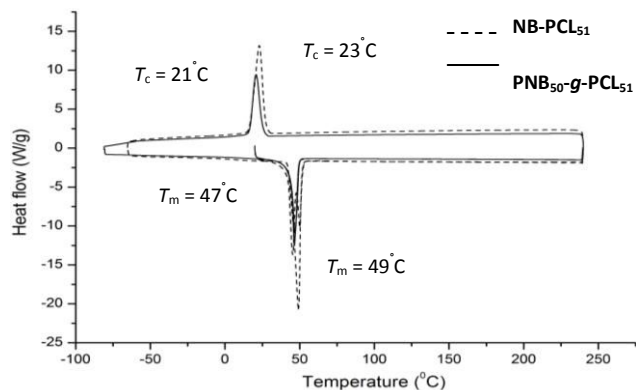


Fig. 7 DSC traces of **PNB₅₀-g-PCL₅₁** (full line) (Table 2, run 13) and **NB-PCL₅₁** (dashed line) (Table 1, run 5)

The crystallinity values have been determined by comparing the enthalpy of fusion ΔH_m with the ΔH_m value for 100% crystalline PCL⁵³ ($\Delta H_m, \text{PCL} = 140 \text{ J.g}^{-1}$). Graft copolymers demonstrated much lower crystallinities as compared with their corresponding macromonomers. For instance, **NB-PCL₅₁** had 91% crystallinity whereas the resulting **PNB₅₀-g-PCL₅₁** possessed only about 38% crystallinity. This is a direct result of the brush structure of the copolymer, which causes a restriction of conformational freedom by the grafted chains and hinders the crystallinity of the PCL grafts.

The thermal stability of macromonomers and corresponding graft copolymers was studied by thermogravimetric analysis (Table 3, Figure 8 and Figure S20 in ESI†). Graft copolymers **PNB₅₀-g-PCL₅₁** and **POX₅₀-g-PCL₅₂** show an increase in thermal stability with a higher initial decomposition temperature

compared to the PCL-based macromonomers. Such a behavior has been attributed to the strong intramolecular Van der Waals interactions among the PCL side chains of the bottle-brush polymers.^{50,54}

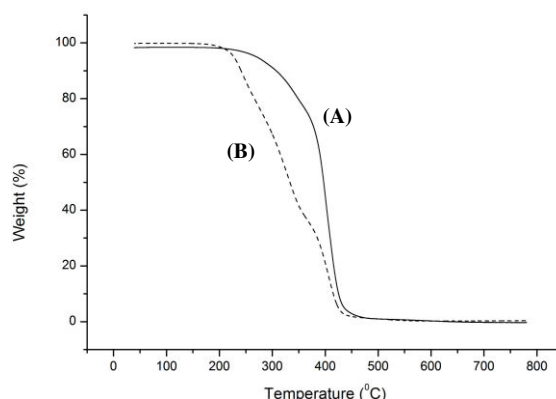


Fig. 8 Comparison of TGA curves for (A) **PNB₅₀-g-PCL₅₁** (full line) (Table 2, run 13) and (B) **NB-PCL₅₁** (dashed line) (Table 1, run 5)

Conclusions

High grafting density bottle-brush copolymers having a poly(oxa)norbornene backbone and two PCL side chains on the same unit as grafts were successfully synthesized according to a 'grafting through' strategy from PCL-based (oxa)norbornene macromonomers. First, a series of well-defined PCL-based macromonomers with two PCL chains have been obtained by organocatalyst mediated ROP of CL with a length of each PCL chain ranging from 1 400 to 5 500 g/mol. Macromonomers were subjected to ROMP using Grubbs' catalysts. The results using Grubbs' second generation catalyst showed that this initiator was effective for the polymerization of macromonomers, although the efficiency of the ROMP process was affected by the molecular weight of the macromonomers. This was particularly true for PCL-based oxanorbornene macromonomers because of the possible coordination between oxanorbornene cyclic ether and the catalyst. Grubbs' third generation catalyst with bis-pyridine ligands was successfully applied to the synthesis of graft copolymers resulting in long polynorbornene backbone chain and long PCL grafts length. Thermal properties of the resultant bottle-brush polymers show that the crystallization process of PCL chains in the poly(oxa)norbornene-g-PCL is hindered by Van der Waals interactions between the grafts. These well-defined bottle-brush polymers with (bio)degradable PCL grafts make them attractive candidates for the design of copolymers with desired degradability.

Acknowledgments

We thank Emmanuelle Mebold and Corentin Jacquemmoz for MALDI-TOF mass spectrometry and NMR analyses. D. A. N. thanks the University of Science and Technology of Hanoi (USTH) and the Vietnamese government for financial support.

Notes and references

^a Institut des Molécules et Matériaux du Mans (IMMM), UMR CNRS 6283, Université du Maine, Avenue Olivier Messiaen, 72085 Le Mans Cedex 9, France. Fax: +33 (0)2 43 83 37 54; Tel: +33 (0)2 43 83 33 30 ;

E-Mail : laurent.fontaine@univ-lemans.fr

† Electronic Supplementary Information (ESI) available: Additional ¹H and ¹³C NMR spectra, SEC traces, MALDI-TOF mass spectra of macromonomers and copolymers, DSC and TGA thermograms. See DOI: 10.1039/b000000x/

- 1 S. S. Sheiko, B. S. Sumerlin and K. Matyjaszewski, *Prog. Polym. Sci.*, 2008, **33**, 759-785.
- 2 C. Feng, Y. Li, D. Yang, J. Hu, X. Zhang and X. Huang, *Chem. Soc. Rev.*, 2011, **40**, 1282-1295.
- 3 N. Hadjichristidis, M. Pitsikalis, H. Iatrou, P. Driva, M. Chatzichristidi, G. Sakellariou and D. Lohse, *Encyclopedia of Polymer Science and Technology*, 4th Ed., H. M. Mark Ed., John Wiley and Sons, 2014, 467-526.
- 4 K. Ito, *Prog. Polym. Sci.*, 1998, **23**, 581-620.
- 5 C. Tsitsilianis, Synthesis of Block and Graft Copolymers in *Controlled/Living Polymerizations*, K. Matyjaszewski and A. H. E. Müller Ed., Wiley-VCH: Weinheim, 2009, 445-492.
- 6 D. Uhrig and J. Mays, *Polym. Chem.*, 2011, **2**, 69-76.
- 7 M. Zhang and A. H. E. Müller, *J. Polym. Sci., Part A: Polym. Chem.*, 2005, **43**, 3461-3481.
- 8 N. Hadjichristidis, M. Pitsikalis, H. Iatrou and S. Pispas, *Macromol. Rapid Commun.*, 2003, **24**, 979-1013.
- 9 N. Hadjichristidis, H. Iatrou, M. Pitsikalis and J. Mays, *Prog. Polym. Sci.*, 2006, **31**, 1068-1132.
- 10 M. Xie, J. Dang, H. Han, W. Wang, J. Liu, X. He and Y. Zhang, *Macromolecules*, 2008, **41**, 9004-9010.
- 11 Y. Xia, J. A. Kornfield and R. H. Grubbs, *Macromolecules*, 2009, **42**, 3761-3766.
- 12 Y. Xia, B. D. Olsen, J. A. Kornfield and R. H. Grubbs, *J. Am. Chem. Soc.*, 2009, **131**, 18525-18532.
- 13 C. Cheng, K. Qi, E. Khosdel and K. L. Wooley, *J. Am. Chem. Soc.*, 2006, **128**, 6808-6809.
- 14 Z. Li, K. Zhang, J. Ma, C. Cheng and K. L. Wooley, *J. Polym. Sci., Part A: Polym. Chem.*, 2009, **47**, 5557-5563.
- 15 D. Le, V. Montembault, J.-C. Soutif, M. Rutnakornpituk and L. Fontaine, *Macromolecules*, 2010, **43**, 5611-5617.
- 16 Z. Li, J. Ma, C. Cheng and K. Wooley, *Macromolecules*, 2010, **43**, 1182-1184.
- 17 Y. Li, J. Ma, G. Sun, Z. Li, S. Cho, C. Clark and K. L. Wooley, *J. Polym. Sci., Part A: Polym. Chem.*, 2012, **50**, 1681-1688.
- 18 J. Ma, N. S. Lee and K. L. Wooley, *J. Am. Chem. Soc.*, 2011, **133**, 1228-1231.
- 19 D. J. Liaw, C. C. Huang and J. Y. Ju, *J. Polym. Sci., Part A: Polym. Chem.*, 2006, **44**, 3382-3392.
- 20 G. Morandi, G. Mantovani, V. Montembault, D. M. Haddleton and L. Fontaine, *New J. Chem.*, 2007, **31**, 1826-1829.
- 21 H. Durmaz, A. Dag, N. Cerit, O. Sirkecioglu, G. Hizal and U. Tunca, *J. Polym. Sci., Part A: Polym. Chem.*, 2010, **48**, 5982-5991.
- 22 D. L. Patton and R. C. Advincula, *Macromolecules*, 2006, **39**, 8674-8683.
- 23 J. Ma, C. Cheng and K. L. Wooley, *Aust. J. Chem.*, 2009, **62**, 1507-1519.
- 24 Y. Li, E. Themistou, J. Zou, B. P. Das, M. Tsianou and C. Cheng, *ACS Macro Lett.*, 2012, **1**, 52-56.
- 25 W. J. Feast, V. C. Gibson, A. F. Johnson, E. Khosravi and M. A. Mohsin, *Polymer*, 1994, **35**, 3542-3548.
- 26 S. T. Alfred, Z. M. Al-Badri, A. E. Madkour, K. Lienkamp and G. N. Tew, *J. Polym. Sci., Part A: Polym. Chem.*, 2008, **46**, 2640-2648.
- 27 I. Czelusniak, E. Khosravi, A. M. Kenwright and C. W. G. Ansell, *Macromolecules*, 2007, **40**, 1444-1452.
- 28 A.-C. Albertsson and I. K. Varma, *Biomacromolecules*, 2003, **4**, 1466-1486.
- 29 M. A. Woodruff and D. W. Huttmacher, *Prog. Polym. Sci.*, 2010, **35**, 1217-1256.
- 30 A. L. Sisson, D. Ekinici and A. Lendlein, *Polymer*, 2013, **54**, 4333-4350.
- 31 M. Fevre, J. Pinaud, Y. Gnanou, J. Vignolle and D. Taton, *Chem. Soc. Rev.*, 2013, **42**, 2142-2172.
- 32 A. P. Dove, *ACS Macro Lett.*, 2012, **1**, 1409-1412.
- 33 M. K. Kiesewetter, E. J. Shin, J. L. Hedrick and M. R. Waymouth, *Macromolecules*, 2010, **43**, 2093-2107.
- 34 N. E. Kamber, W. Jeong, R. M. Waymouth, R. C. Pratt, B. G. G. Lohmeijer and J. L. Hedrick, *Chem. Rev.*, 2007, **107**, 5813-5840.
- 35 O. Dechy-Cabaret, B. Martin-Vaca and D. Bourissou, *Chem. Rev.*, 2004, **104**, 6147-6176.
- 36 M. Save, M.; Schappacher and A. Soum, *Macromol. Chem. Phys.*, 2002, **203**, 889-899.
- 37 S. M. Guillaume, M.; Schappacher and A. Soum, *Macromolecules*, 2003, **36**, 54-60.
- 38 J. Das, T. Vu, D. N. Harris and M. L. Ogletre, *J. Med. Chem.*, 1988, **31**, 930-935.
- 39 J. A. Love, J. P. Morgan, T. M. Trnka and R. H. Grubbs, *Angew. Chem. Int. Ed.*, 2002, **114**, 4207-4209.
- 40 B. G. G. Lohmeijer, R. C. Pratt, F. Leibfarth, J. W. Logan, D. A. Long, A. P. Dove, F. Niederberg, J. Choi, C. Wade, R. M. Waymouth and J. L. Hedrick, *Macromolecules*, 2006, **39**, 8574-8583.
- 41 R. C. Pratt, B. G. G. Lohmeijer, D. A. Long, R. M. Waymouth and J. L. Hedrick, *J. Am. Chem. Soc.*, 2006, **128**, 4556-4557.
- 42 S. Jha, S. Dutta and N. B. Bowden, *Macromolecules*, 2004, **37**, 4365-4374.
- 43 F. Leroux, V. Montembault, S. Pascual, W. Guérin, S. M. Guillaume and L. Fontaine, *Polym. Chem.*, 2014, **5**, 3476-3486.
- 44 W. J. Feast, V. C. Gibson, A. F. Johnson, E. Khosravi and M. A. Mohsin, *J. Mol. Catal. A: Chem.*, 1997, **115**, 37-42.
- 45 G. Morandi, V. Montembault, S. Pascual, S. Legoupy and L. Fontaine, *Macromolecules*, 2006, **39**, 2732-2735.
- 46 C. Bielawski and R. H. Grubbs, *Angew. Chem. Int. Ed.*, 2000, **39**, 2903-2905.
- 47 T. L. Choi and R. H. Grubbs, *Angew. Chem. Int. Ed.*, 2003, **42**, 1743-1746.
- 48 J. A. Johnson, Y. Y. Lu, A. O. Burts, Y. H. Lim, M. G. Finn, J. T. Koberstein, N. J. Turro, D. A. Tirrell and R. H. Grubbs, *J. Am. Chem. Soc.*, 2011, **133**, 559-566.
- 49 S. C. Radzinski, J. C. Foster and J. B. Matson, *Polym. Chem.*, 2015, **6**, 5643-5652.
- 50 Q. Fu, J. M. Ren and G. G. Qiao, *Polym. Chem.*, 2012, **3**, 343-351.
- 51 W. Yuan, J. Yuan, F. Zhang, X. Xie and C. Pan, *Macromolecules*, 2007, **40**, 9094-9102.
- 52 P. Lecomte, D. Mecerreyes, P. Dubois, A. Demonceau, A. Noels and R. Jérôme, *Polym. Bull.*, 1998, **40**, 631-638.
- 53 M. Avella, M. E. Errico, P. Laurienzo, E. Martuscelli, M. Raimo and R. Rimedio, *Polymer*, 2000, **41**, 3875-3881.
- 54 L. Wang, J.-L. Wang and C.-M. Dong, *J. Polym. Sci., Part A: Polym. Chem.*, 2005, **43**, 4721-4730.

Supporting Information

Synthesis and characterization of high grafting density bottle-brush poly(oxa)norbornene-g- poly(ϵ -caprolactone)

*Duc Anh N'Guyen, Flavien Leroux, Véronique Montembault, Sagrario Pascual and
Laurent Fontaine**

Institut des Molécules et Matériaux du Mans (IMMM), Equipe Méthodologie et
Synthèse des Polymères, UMR CNRS 6283, Université du Maine, Avenue Olivier
Messiaen, 72085 Le Mans Cedex 9, France

* Corresponding author: laurent.fontaine@univ-lemans.fr

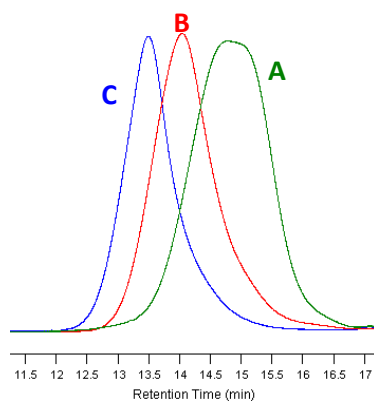


Figure S1. SEC traces for the (A) **OX-PCL₂₄** (Table 1, run 1), (B) **OX-PCL₅₂** (Table 1, run 2) and (C) **OX-PCL₉₂** (Table 1, run 3).

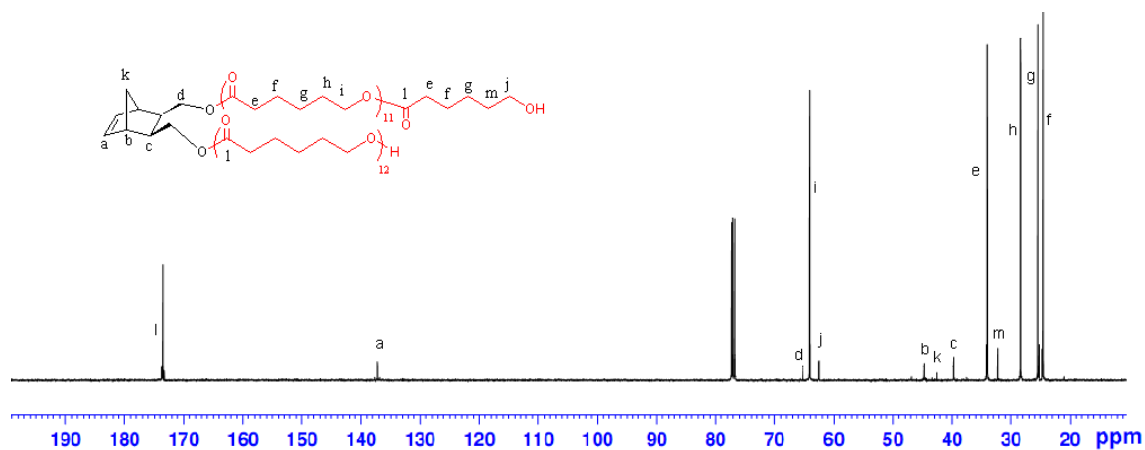


Figure S2. ^{13}C NMR spectrum (100 MHz, CDCl_3 , 25 °C) of precipitated NB-PCL₂₄ from the ROP of CL in THF at 25°C using **NB** as the initiator and TBD as the catalyst with $[\text{CL}]_0/[\text{NB}]_0 = 20$ (Table 1, run 4).

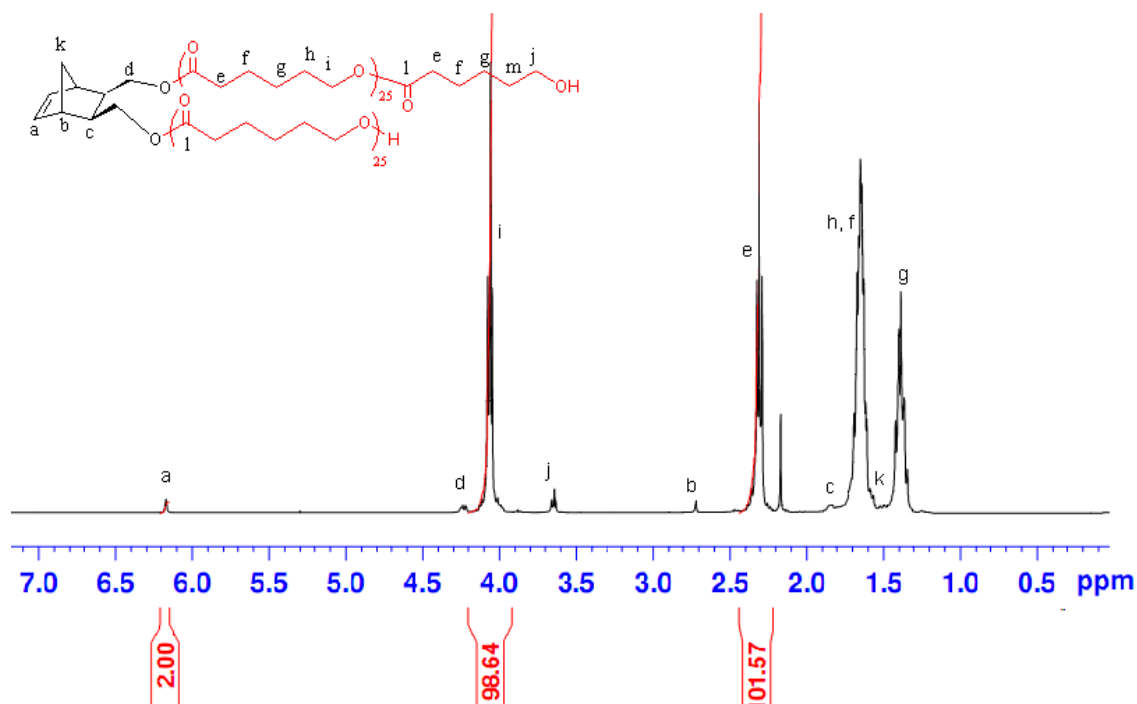


Figure S3. ^1H NMR spectrum (400 MHz, CDCl_3 , 25 °C) of precipitated NB-PCL₅₁ from the ROP of CL in THF at 25°C using **NB** as the initiator and TBD as the catalyst with $[\text{CL}]_0/[\text{NB}]_0 = 48$ (Table 1, run 5).

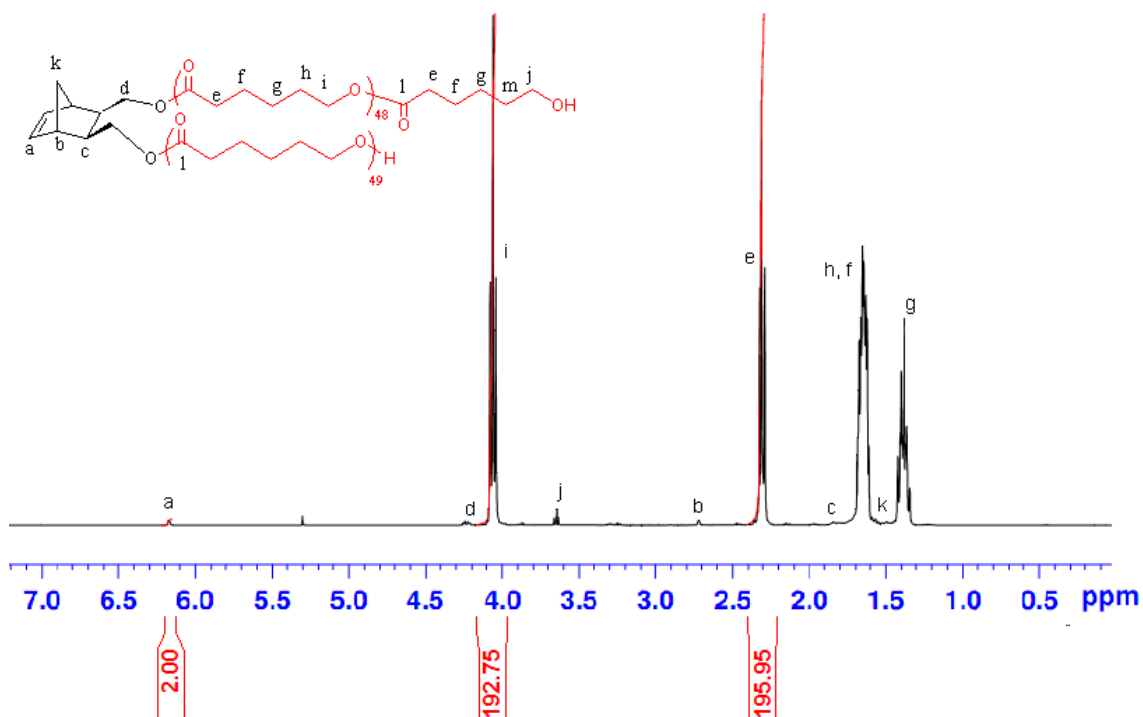


Figure S4. ^1H NMR spectrum (400 MHz, CDCl_3 , 25 °C) of precipitated **NB-PCL**₉₈ from the ROP of CL in THF at 25°C using **NB** as the initiator and TBD as the catalyst with $[\text{CL}]_0/[\text{NB}]_0 = 96$ (Table 1, run 6).

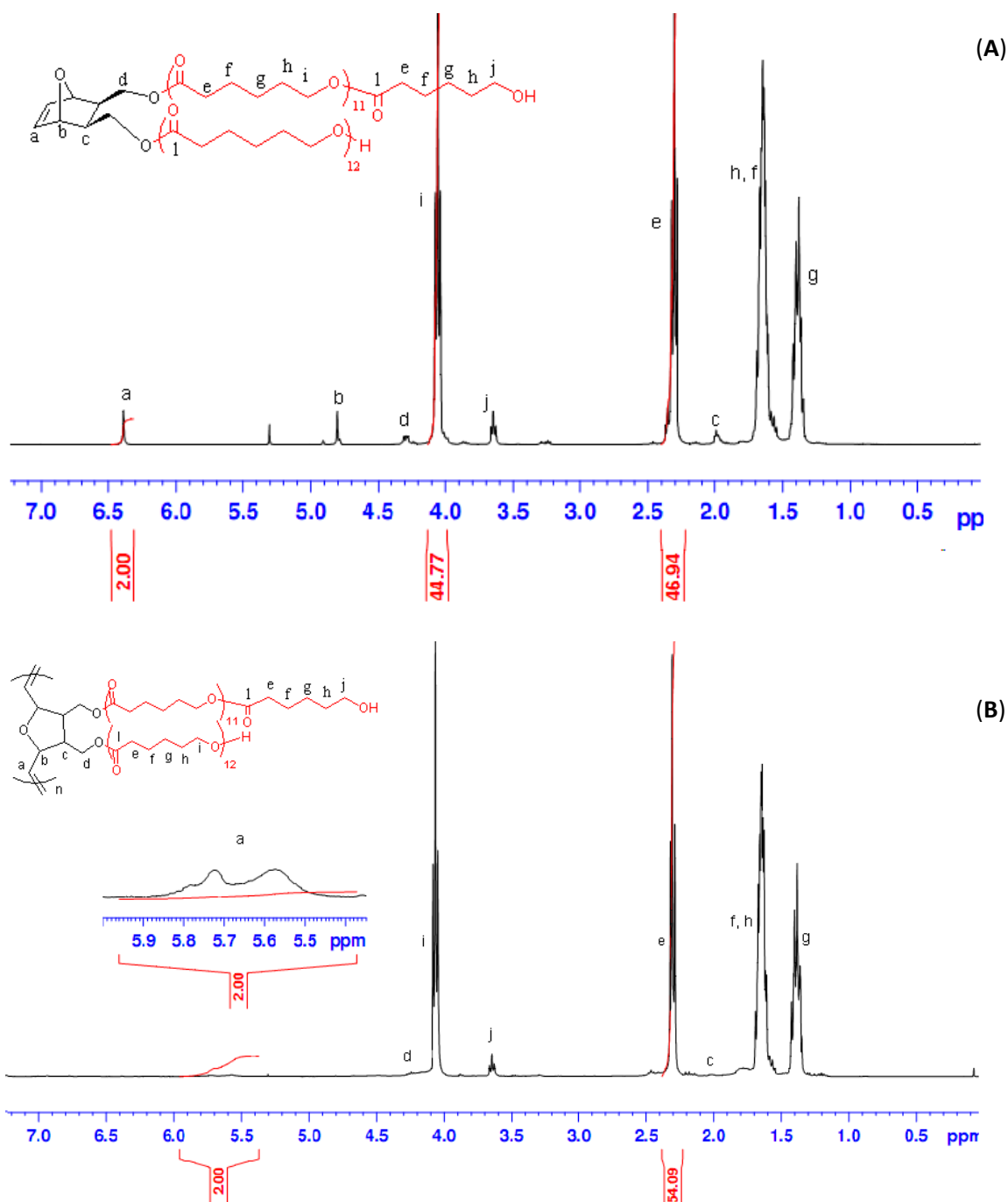


Figure S5. ^1H NMR spectra (400 MHz, CDCl_3 , 25 $^\circ\text{C}$) of (A) precipitated **OX-PCL₂₄** from the ROP of CL in THF at 25 $^\circ\text{C}$ using **OX** as the initiator and TBD as the catalyst with $[\text{CL}]_0/[\text{OX}]_0 = 20$ (Table 1, run 1) and (B) crude **POX₁₀-g-PCL₂₄** obtained from the ROMP of **OX-PCL₂₄** in toluene at 70 $^\circ\text{C}$ using **G2** as the catalyst with $[\text{OX-PCL}_{24}]/[\text{G2}] = 10$ for a reaction time of 3 h (Table 2, run 1).

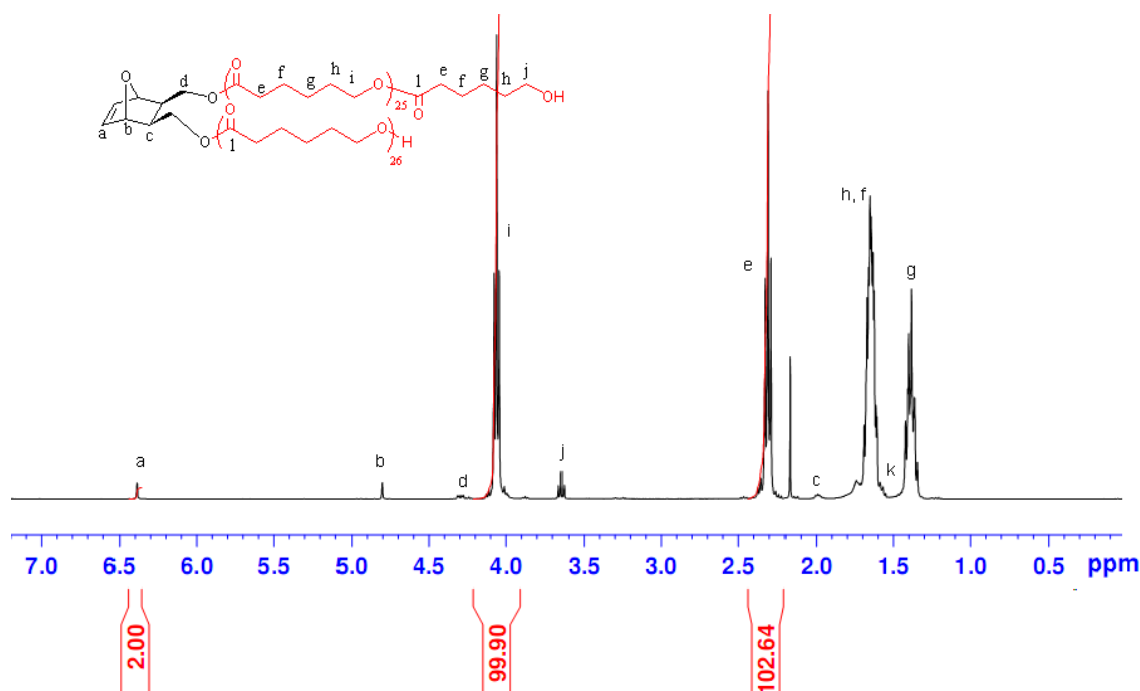


Figure S6. ^1H NMR spectrum (400 MHz, CDCl_3 , 25 $^\circ\text{C}$) of precipitated **OX-PCL₅₂** from the ROP of CL in THF at 25 $^\circ\text{C}$ using **OX** as the initiator and TBD as the catalyst with $[\text{CL}]_0/[\text{OX}]_0 = 48$ (Table 1, run 2).

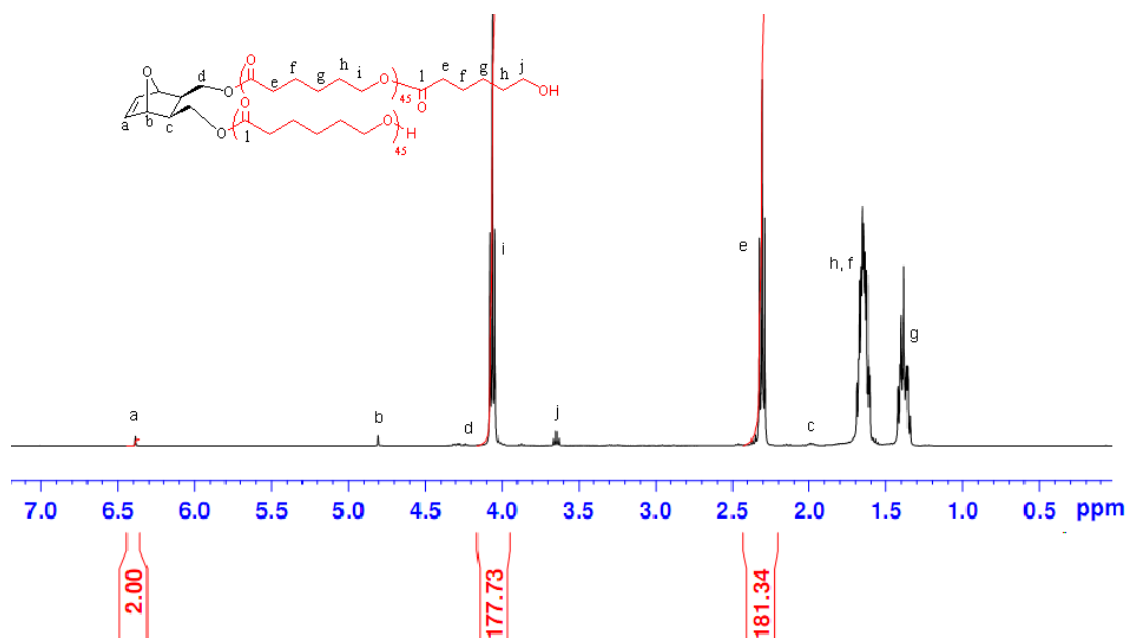


Figure S7. ^1H NMR spectrum (400 MHz, CDCl_3 , 25 $^\circ\text{C}$) of precipitated **OX-PCL₉₂** from the ROP of CL in THF at 25 $^\circ\text{C}$ using **OX** as the initiator and TBD as the catalyst with $[\text{CL}]_0/[\text{OX}]_0 = 96$ (Table 1, run 3).

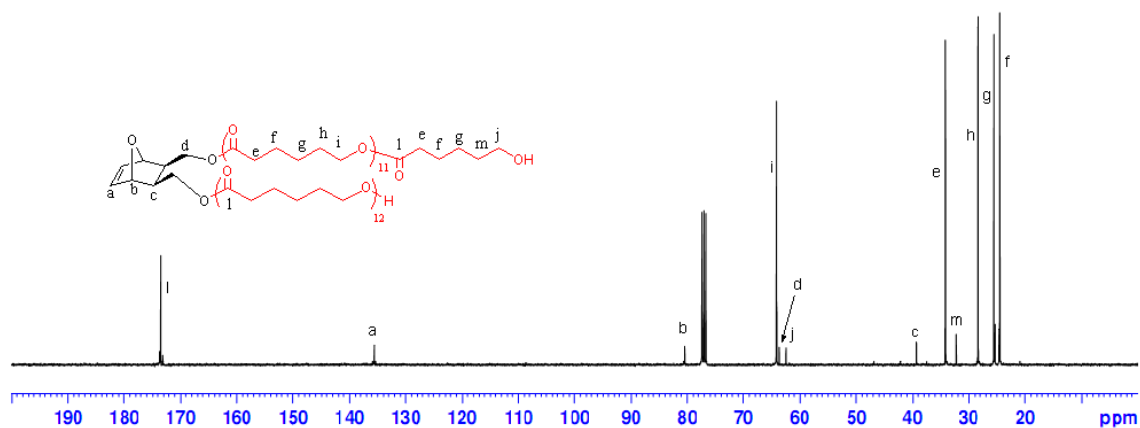


Figure S8. ^{13}C NMR spectrum (100 MHz, CDCl_3 , 25 °C) of precipitated **OX-PCL**₂₄ from the ROP of CL in THF at 25°C using **OX** as the initiator and TBD as the catalyst with $[\text{CL}]_0/[\text{OX}]_0 = 20$ (Table 1, run 1).

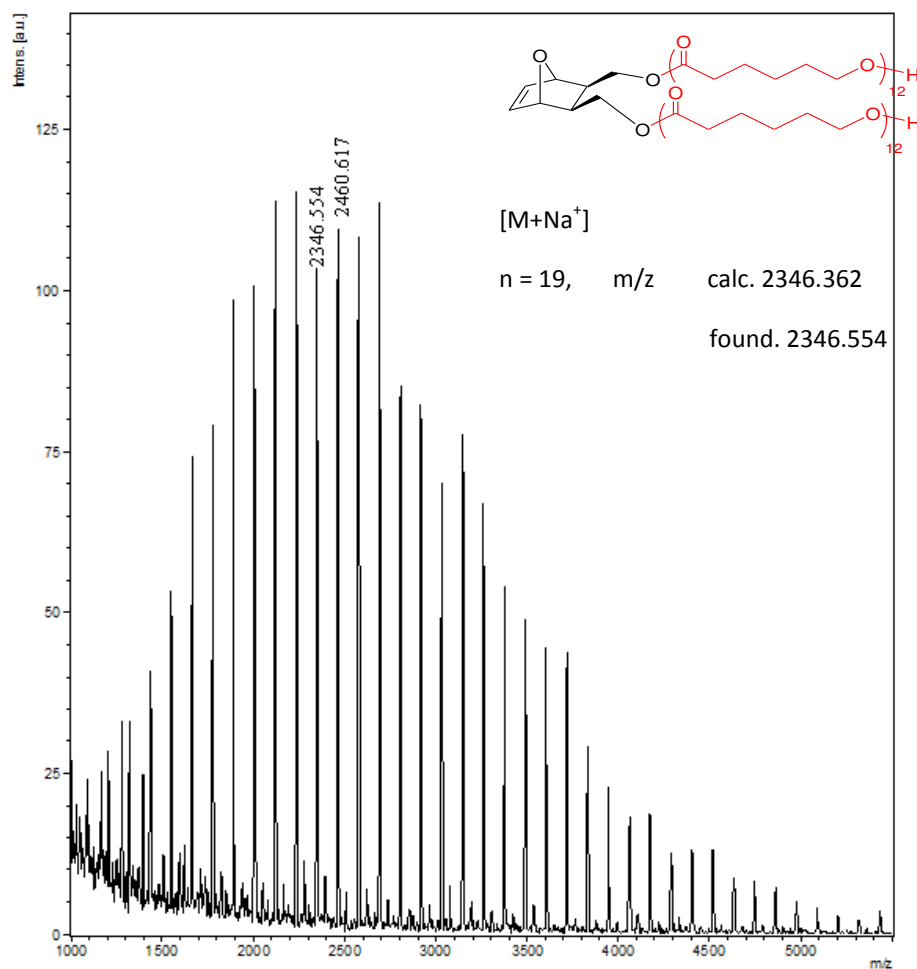


Figure S9. MALDI-TOF mass spectrum (matrix: *trans*-2-[3-(4-*tert*-butylphenyl)-2-methyl-2-propenylidene]malononitrile (DCTB) + sodium trifluoroacetate (NaTFA)) of the PCL-based norbornene synthesized by ROP using **OX** as the initiator and TBD as the catalyst in THF at 25°C with $[CL]_0/[OX]_0 = 20/1$ (Table 1, run 1).

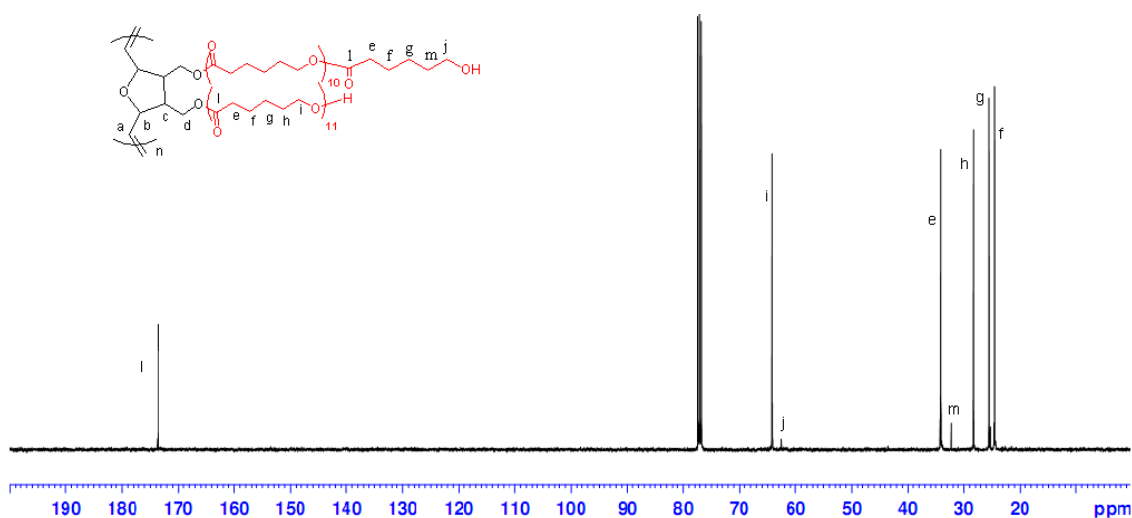


Figure S10. ^{13}C NMR spectrum (100 MHz, CDCl_3 , 25 $^\circ\text{C}$) of **POX₁₀-g-PCL₂₄** obtained from the ROMP of **OX-PCL₂₄** in toluene at 70 $^\circ\text{C}$ using **G2** as the catalyst with $[\text{OX-PCL}_{24}]/[\text{G2}] = 10$ for a reaction time of 3 h (Table 2, run 1).

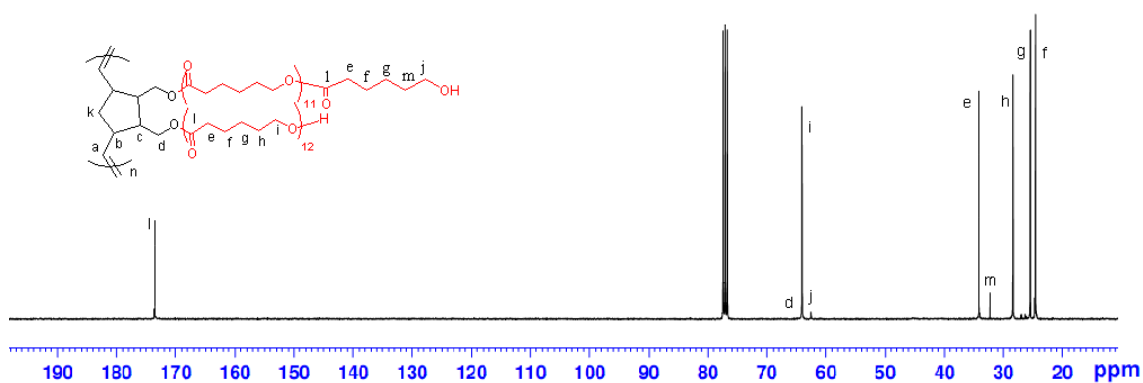


Figure S11. ^{13}C NMR spectrum (100 MHz, CDCl_3 , 25 $^\circ\text{C}$) of **PNB₁₀-g-PCL₂₄** obtained from the ROMP of **NB-PCL₂₄** in toluene at 70 $^\circ\text{C}$ using **G2** as the catalyst with $[\text{NB-PCL}_{24}]/[\text{G2}] = 10$ for a reaction time of 3 h (Table 2, run 8).

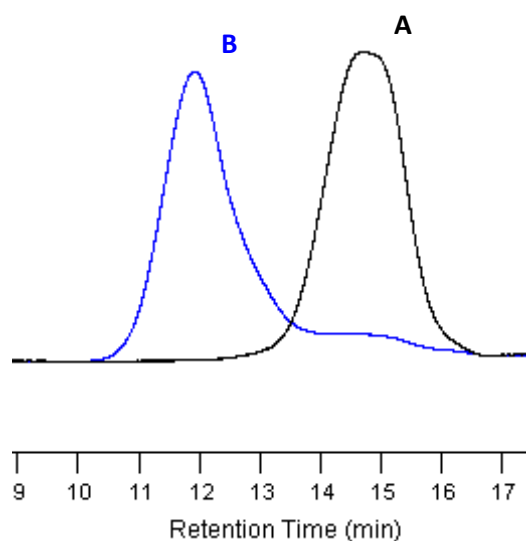


Figure S12. SEC traces for the (A) precipitated **OX-PCL₂₄** (Table 1, run 1) and (B) crude **POX₁₀-g-PCL₂₄** obtained by ROMP of **OX-PCL₂₄** initiated by **G2** (Table 2, run 1).

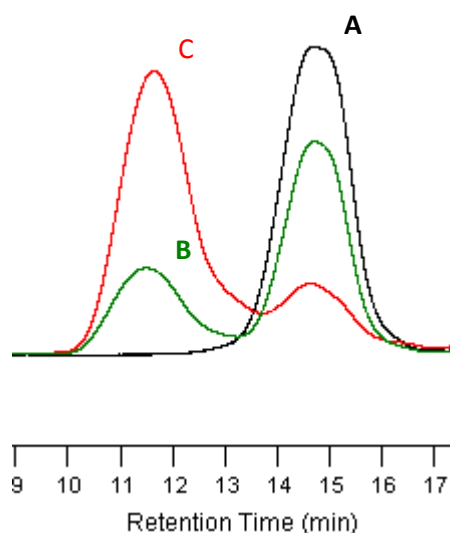


Figure S13. SEC traces for the (A) precipitated **OX-PCL₂₄** (Table 1, run 1), (B) crude **POX₅₀-g-PCL₂₄** (Table 2, run 2) and (C) crude **POX₁₀₀-g-PCL₂₄** (Table 2, run 3) obtained by ROMP of **OX-PCL₂₄** initiated by **G2**.

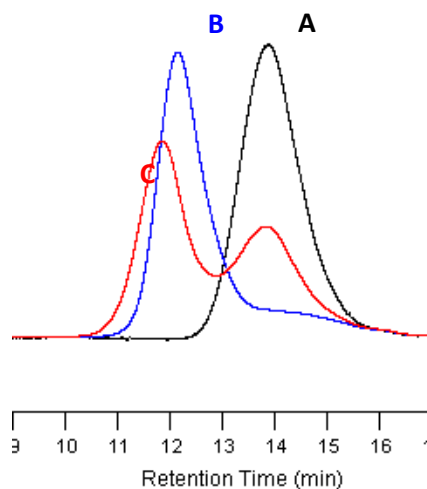


Figure S14. SEC traces for the (A) precipitated **OX-PCL₅₂** (Table 1, run 2), (B) crude **POX_{10-g}-PCL₅₂** (Table 2, run 4) and (C) crude **POX_{50-g}-PCL₅₂** (Table 2, run 5) obtained by ROMP of **OX-PCL₅₂** initiated by **G2**.

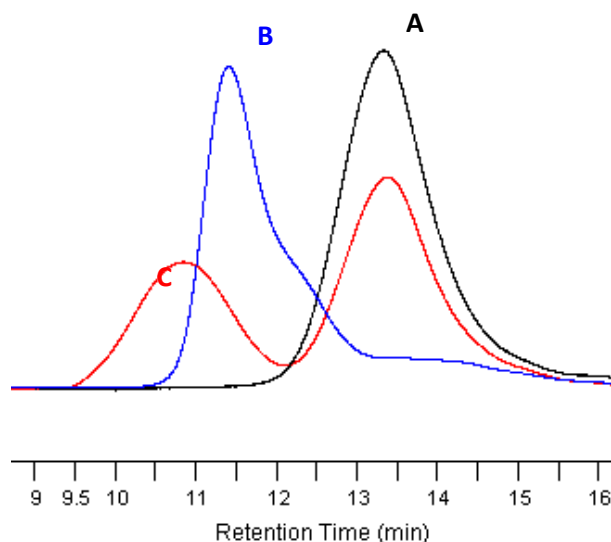


Figure S15. SEC traces for the (A) precipitated **OX-PCL₉₂** (Table 1, run 3), (B) crude **POX_{10-g}-PCL₉₂** (Table 2, run 6) and (C) crude **POX_{50-g}-PCL₉₂** (Table 2, run 7) obtained by ROMP of **OX-PCL₉₂** initiated by **G2**.

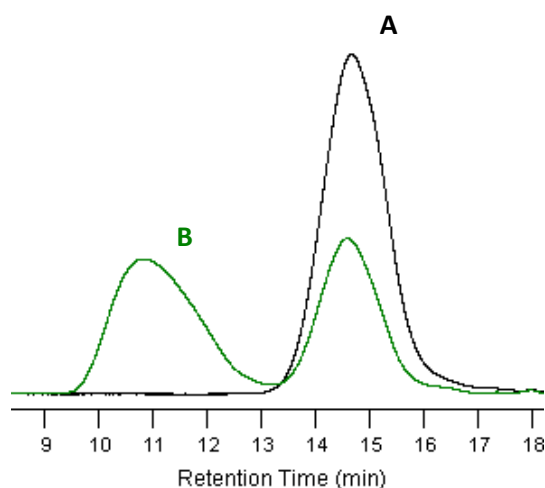


Figure S16. SEC traces for the (A) precipitated **NB-PCL₂₄** (Table 1, run 4) and (B) crude **PNB_{100-g}-PCL₂₄** obtained by ROMP of **NB-PCL₂₄** initiated by **G2** (Table 2, run 10).

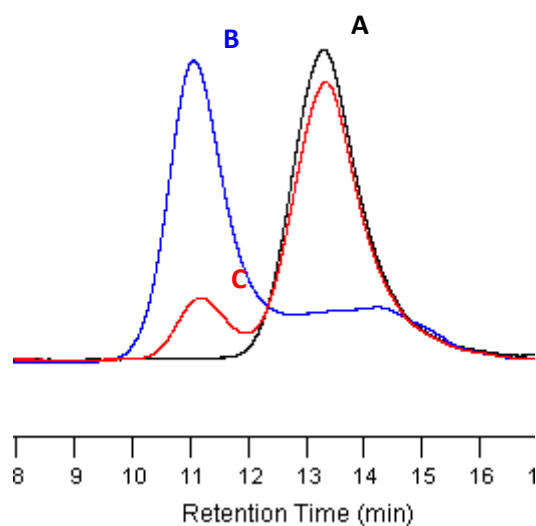


Figure S17. SEC traces for the (A) precipitated **NB-PCL₉₈** (Table 1, run 6), (B) crude **PNB_{10-g}-PCL₉₈** (Table 2, run 16) and (C) crude **PNB_{50-g}-PCL₉₈** (Table 2, run 17) obtained by ROMP of **NB-PCL₉₈** initiated by **G2**.

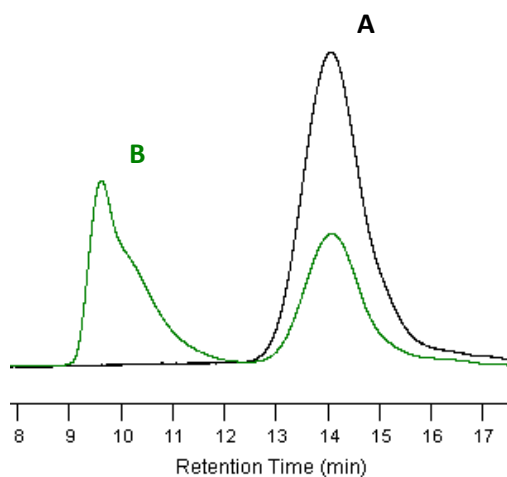


Figure S18. SEC traces for the (A) precipitated **NB-PCL₅₁** (Table 1, run 4) and (B) crude **PNB₂₀₀-*g*-PCL₅₁** (Table 2, run 15) obtained by ROMP of **NB-PCL₅₁** initiated by **G3'**.

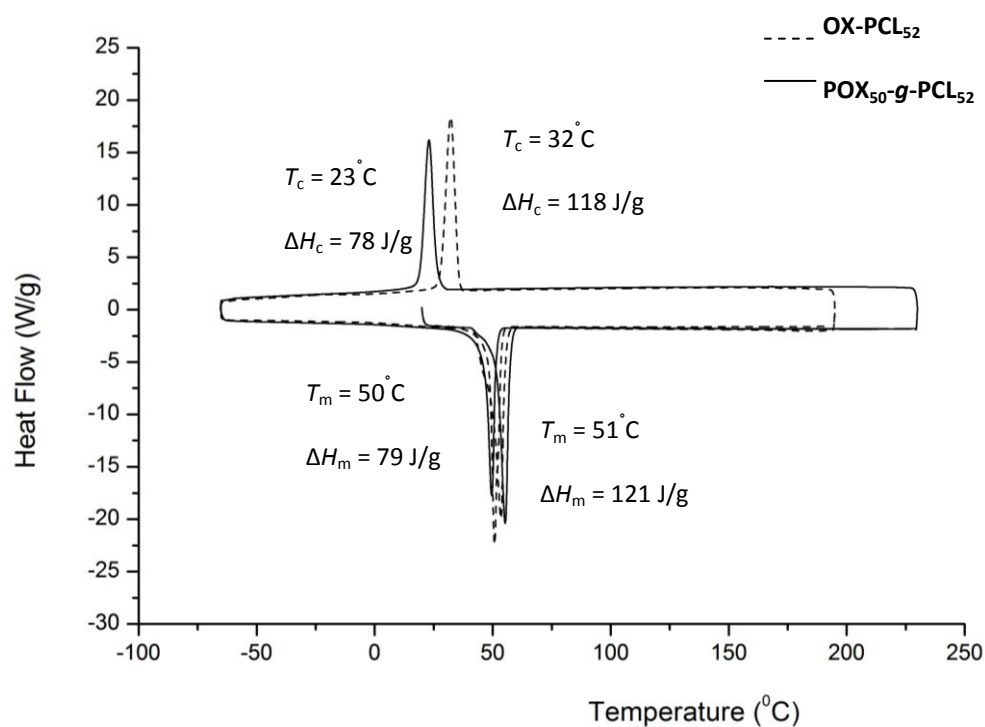


Figure S19. DSC traces of **POX₅₀-g-PCL₅₂** (full line) (Table 2, run 5) and **OX-PCL₅₂** (dashed line) (Table 1, run 2).

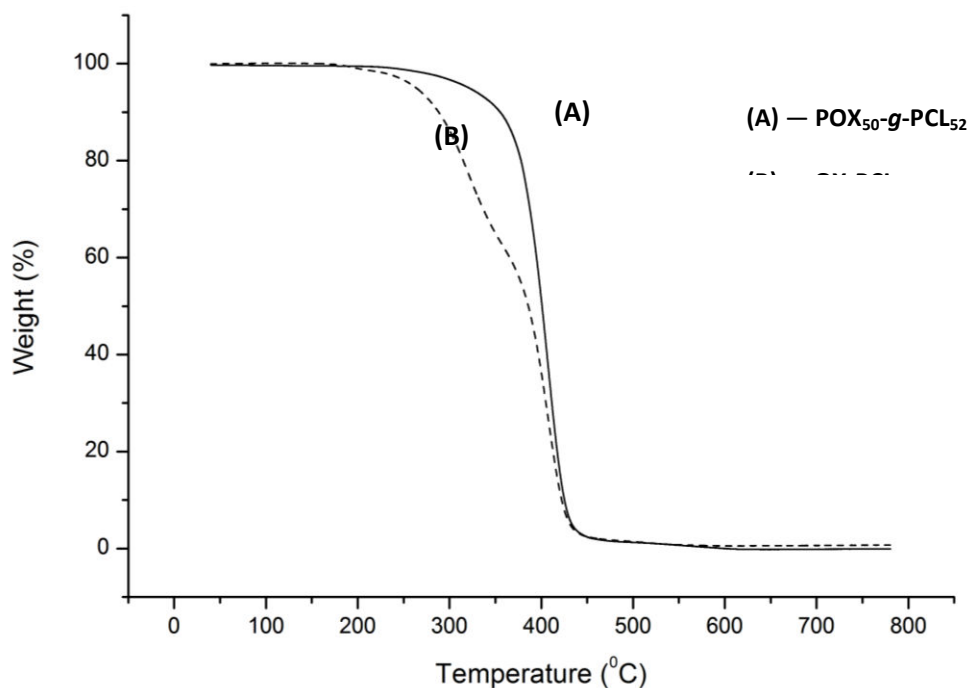


Figure S20. Comparison of TGA curves for (A) **POX₅₀-g-PCL₅₂** (full line) (Table 2, run 5) and (B) **OX-PCL₅₂** (dashed line) (Table 1, run 2).

Chapter 3

Synthesis and self-assembling properties of amphiphilic (oxa)norbornenyl-functionalized PEO-*b*-PCL copolymers

Introduction

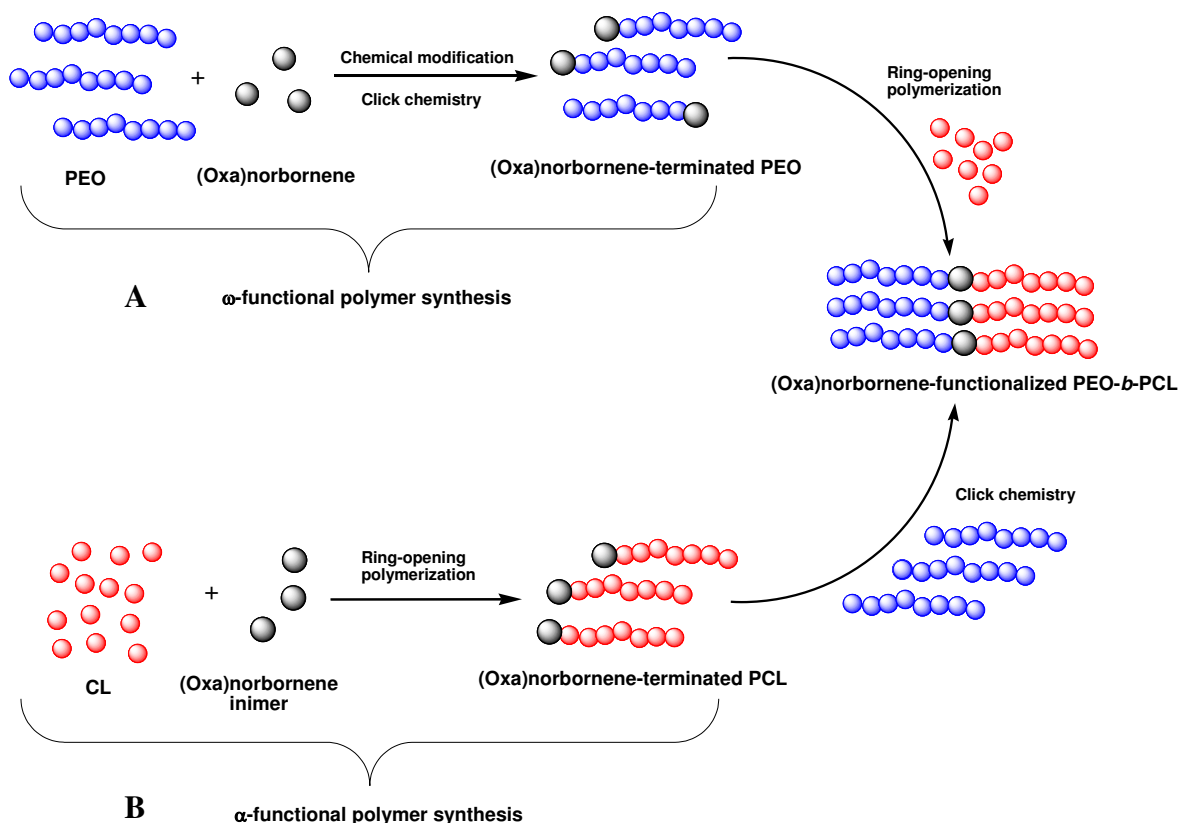
Polymers including the olefin functionality can be used as a platform to target various architectures such as graft, bottle-brush, and star copolymers. Indeed, polymers containing an olefin-derived polymerizable group (macromonomers) can be polymerized in order to generate graft copolymers.¹ Through the emergence of the ‘grafting-through’ or macromonomer technique, the synthesis of well-defined graft copolymers has become easier and more diverse thanks to the various choices of graft/backbone combination, the design of polymerization methods and functional groups.² In addition, olefin-functionalized polymers can be engaged into thiol-ene reactions to obtain block,³ star, or networks copolymers.^{4,5}

Normally, olefin functionality group referred to a vinyl group, but the polymers that contain a (cyclo)olefin functionality can also be polymerized by ring-opening metathesis polymerization (ROMP), a powerful and variously applicable polymerization method.⁶ Oxanorbornene (ONB) an norbornene (NB) are well-known as highly reactive groups toward ROMP,⁷⁻¹⁷ as well as toward thiol-ene reactions.^{6,18-22} Such a high reactivity gives rise to their use for obtaining various structures of copolymers with different applications.

The synthesis of (cyclo)olefin-functionalized (co)polymers can be accomplished by two methods (Scheme III.1):²³⁻²⁵

- The ω -functional polymer synthesis: the polymer chains are functionalized with the polymerizable group after the synthesis (Scheme III.1, A).
- The α -functional polymer synthesis: the polymerization is initiated by an initiator containing the polymerizable group or *inimer* (as defined *ini* for initiator and *mer* for monomer) (Scheme III.1, B).

Based on that methods, we have investigated the synthesis of well-defined olefin functionality block copolymers containing a poly(ethylene oxide) (PEO) block, a poly(ϵ -caprolactone) (PCL) block, and a norbornene (NB) or oxanorbornene (ONB) as the olefin functionality at the junction of the two polymer segments (Scheme III.1).



Scheme III.1. Synthesis of (oxa)norbornenyl-functionalized PEO-*b*-PCL using (A) ω -functional macromonomer synthesis and (B) α -functional macromonomer synthesis.

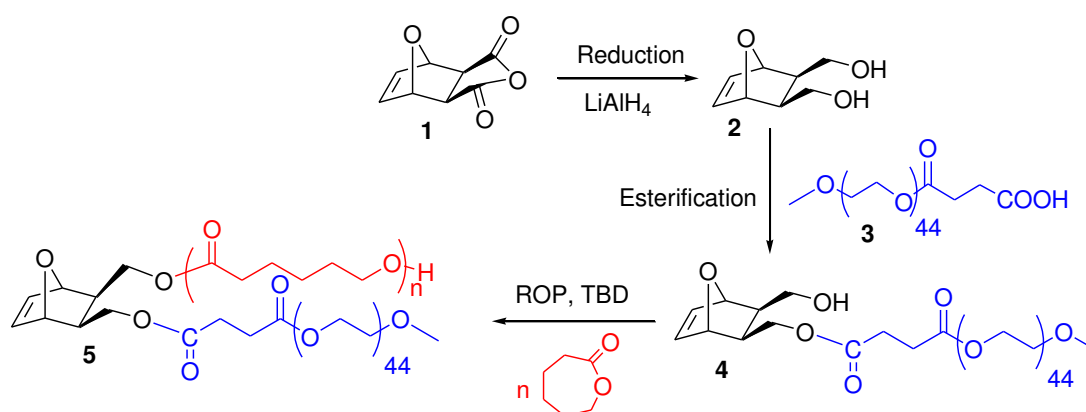
Exo norbornene anhydride is a well-known commercially available product. Pure *exo* oxanorbornene diastereoisomer is easily prepared from *exo* 7-oxabicyclo[2.2.1]hept-5-ene-2,3-dicarboxylic anhydride, available in high yield through a Diels-Alder cycloaddition reaction.²⁶⁻²⁸ PEO is a commercially available, neutral, hydrophilic, highly mobile, synthetic, and non-toxic polymer which has found numerous applications in the fields of biomaterials and biotechnologies.²⁹⁻³¹ PEO of number average molar mass (M_n) of 2000 has been chosen for its hydrophilic capability and its ability to generate nanosized particles.³² PCL is a very useful polymer with various applicability and interesting properties such as insolubility in water at room temperature³³, biocompatibility,³⁴ controlled degradation.³⁵ PCL is easily synthesized *via* ROP of ϵ -caprolactone (CL)³⁶ with well-defined structure giving the ability to

control the hydrophilic/hydrophobic balance of the final copolymer. PEO-*b*-PCL copolymers have been synthesized as they exhibit self-assembling properties in forming micelles in aqueous media with hydrophilic corona and hydrophobic core.³⁷ Micelles based on PEO-*b*-PCL copolymers are used as candidates for applications such as drug transportation and delivery systems.^{38,39}

In this chapter, we present the synthesis of (oxa)norbornenyl precursors and the synthesis of amphiphilic (oxa)norbornene-functionalized PEO-*b*-PCL copolymers. Two strategies have been investigated: (i) the combination of chemical modification and ROP and (ii) the combination of ‘click’ chemistry and ROP. The self-assembling properties in water of the resulting amphiphilic copolymers are also described.

I. Synthesis of oxanorbornenyl-functionalized PEO-PCL copolymers from *exo* oxanorbornene dimethanol

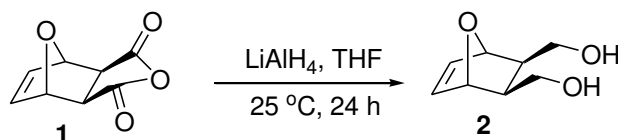
Exo oxanorbornenyl-functionalized PEO-*b*-PCL copolymers have been synthesized in a two-step procedure from *exo* oxanorbornene dimethanol **2**. The first hydroxyl functionality has been used to introduce PEO by a chemical modification and the second hydroxyl served as an initiating group for the ROP of CL. First, a ONB-terminated PEO macromonomer **4** has been obtained by esterification between *exo* oxanorbornene dimethanol **2**, issued from the reduction of *exo* oxanorbornene anhydride **1**, and a carboxylic acid-terminated PEO **3** (Scheme III.2). Thereafter, the second hydroxyl group of **4** has been used as an initiating group for the ROP of CL using organocatalyst 1,5,7-triazabicyclodec-5-ene (TBD) to reach *exo* oxanorbornenyl-functionalized PEO-*b*-PCL copolymers **5** (Scheme III.2).



Scheme III.2. Synthesis of *exo* oxanorbornenyl-functionalized PEO-*b*-PCL **5** from *exo* oxanorbornene dimethanol **2**.

1.1. Synthesis of *exo* 7-oxabicyclo[2.2.1]hept-5-ene-2,3-dimethanol

Exo 7-oxabicyclo[2.2.1]hept-5-ene-2,3-dimethanol **2** (also named *exo* oxanorbornene dimethanol) has been obtained by reduction with lithium aluminium hydride (LiAlH_4) in tetrahydrofuran (THF) of the oxanorbornene anhydride **1** (Scheme III.3) in 70% yield.⁴⁰



Scheme III.3. Synthesis of *exo* oxanorbornene dimethanol **2**.

The proton nuclear magnetic resonance (^1H NMR) spectrum (Figure III.1) of *exo* oxanorbornene dimethanol **2** shows the presence of a peak at $\square \square \square \square \square \square \square$ ppm attributed to the methylene protons of the hydroxymethyl group of **2** (labelled d, Figure III.1). Furthermore, comparison of the integrations of the protons of the hydroxymethyl groups at $\square = 3.83$ ppm (labelled d, Figure III.1) and the protons of $-\text{CH}=\text{CH}-$ at $\square = 6.41$ ppm (labelled a, Figure III.1) gave a 4.17:2.00 ratio, indicating a quantitative conversion.

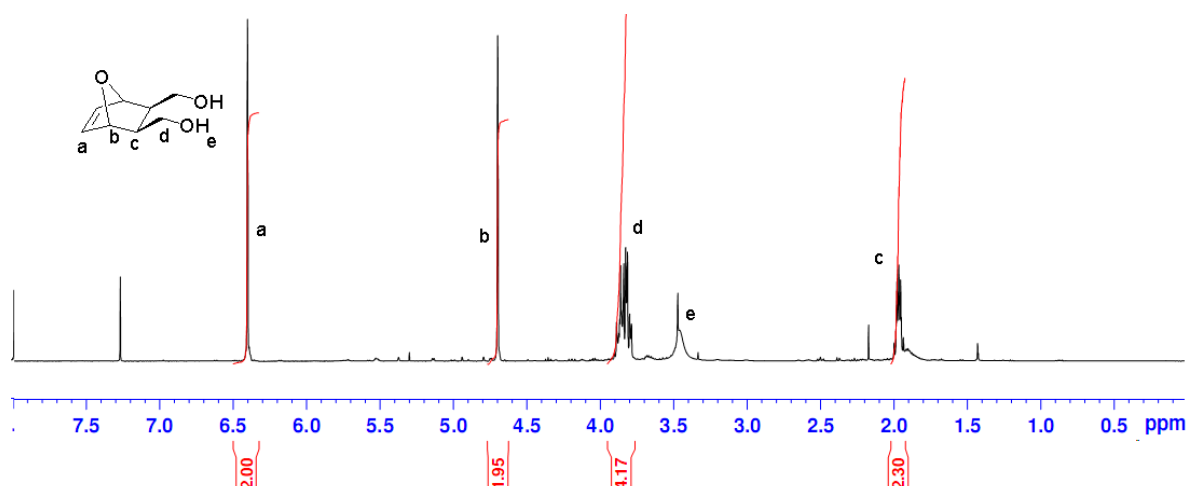
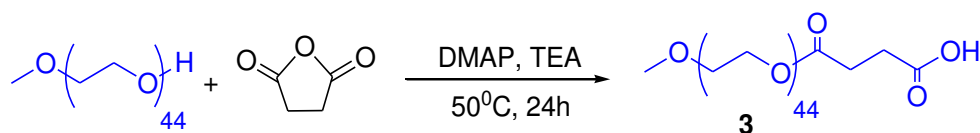


Figure III.1. ^1H NMR spectrum (400 MHz, 25 $^\circ\text{C}$) of *exo* oxanorbornene-2,3-dimethanol **2**; solvent: CDCl_3 .

The high-resolution mass spectrometry (HRMS) analysis confirmed the formation of the pure product ($[\text{M}+\text{H}^+]_{\text{found}} = 157.0859$ and $[\text{M}+\text{H}^+]_{\text{calc}} = 157.0786$).

1.2. Synthesis of *exo* oxanorbornene-terminated PEO

PEO has then been introduced by chemical modification between the *exo* oxanorbornene dimethanol **2** and a carboxylic acid-terminated PEO **3**. This carboxylic acid-terminated PEO **3** has been synthesized from the commercially available PEO monomethyl ether 2 000 g/mol and succinic acid in the presence of 4-(*N,N*-dimethylamino)pyridine (DMAP) and triethylamine (TEA) according to a literature procedure (Scheme III.4).⁴¹



Scheme III.4. Synthesis of the carboxylic acid-terminated PEO **3**.

The carboxylic acid functionality of the PEO has been calculated from ^1H NMR spectroscopy (Figure III.2) by comparing the integrations of the protons of the methoxy group of the PEO at $\delta = 3.38$ ppm (labelled a, Figure III.2) and of the protons of $-\text{CH}_2\text{CH}_2\text{OCO}-$ at $\delta = 4.24$ ppm (labelled c, Figure III.2) and has been estimated to be 100%.

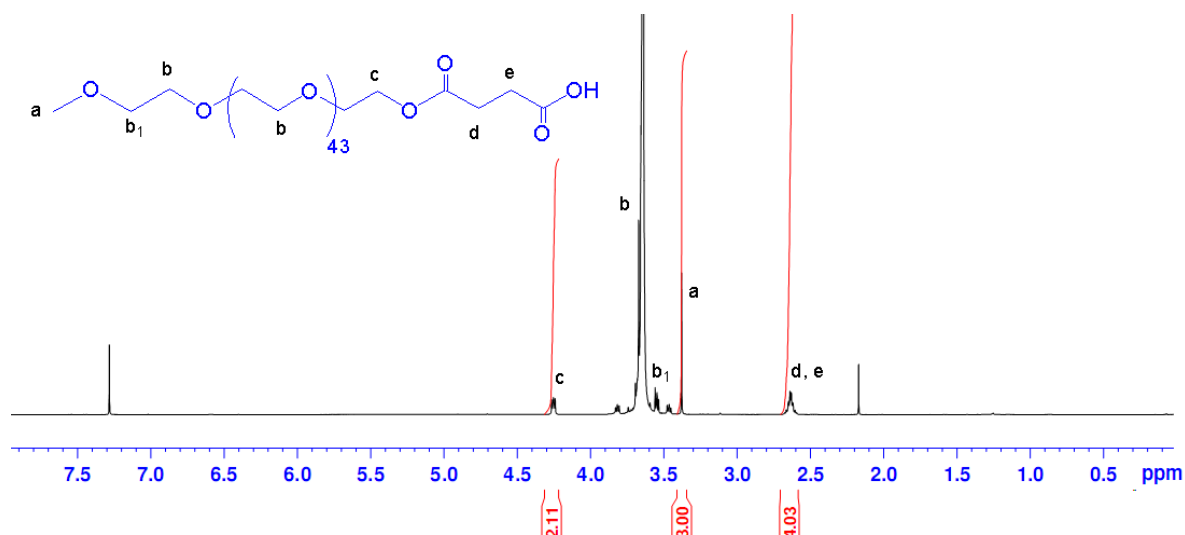


Figure III.2. ¹H NMR spectrum (400 MHz, 25 °C) of carboxylic acid-terminated PEO **3**; solvent: CDCl₃.

The matrix-assisted laser desorption-ionization time of flight (MALDI-ToF) mass spectrum of **3** is shown in Figure III.3. The spectrum shows 3 populations. The difference in mass of each signal of both series was roughly estimated as 44, indicating the signals are assignable to PEO homologues. The first series is attributed to sodium-ionized PEO with a methoxy group at one chain-end and a carboxylic acid group at the other chain-end ($m/z = 2004.34$, calculated value = 2004.13 for 42 repeating units). The second series corresponds to the proton-ionized PEO homologue ($m/z = 1982.39$, calculated value = 1982.15 for 42 repeating units). The third series corresponds to the sodium-ionized commercial PEO monomethyl ether 2000 g/mol which are unreacted in reaction ($m/z = 1992.23$, calculated value = 1992.17 for 44 repeating units).

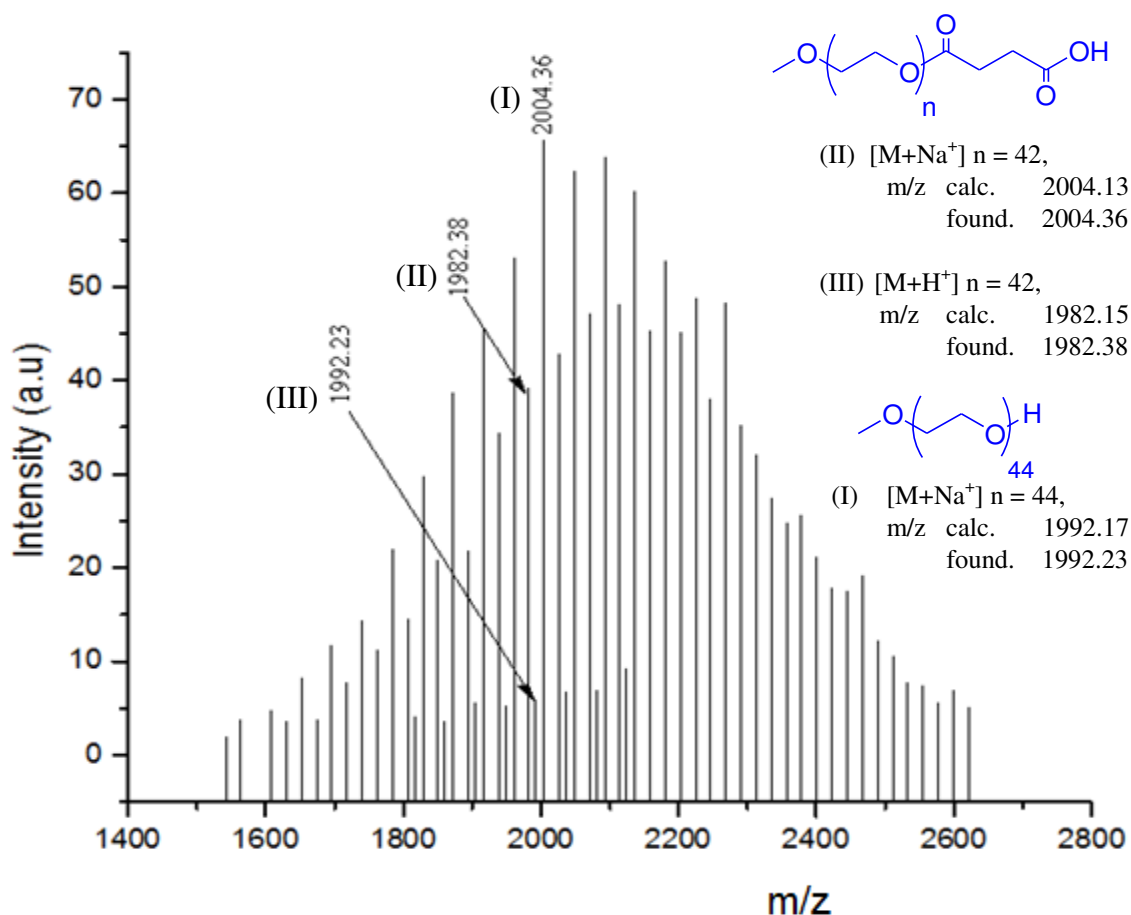
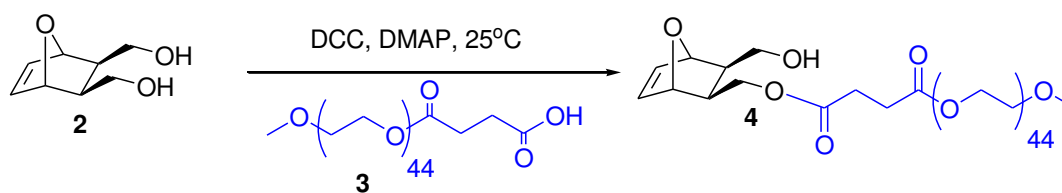


Figure III.3. MALDI-ToF mass spectrum of carboxylic acid-terminated PEO **3**; matrix: 2-[(2*E*)-3-(4-*tert*-butylphenyl)-2-methylprop-2-enylidene]malononitrile (DCTB), sodium trifluoroacetate (NaTFA)

Oxanorbornene-terminated PEO macromonomer **4** was synthesized by chemical modification between the *exo* oxanorbornene dimethanol **2** and the carboxylic acid-terminated PEO **3** with dicyclohexylcarbodiimide (DCC) and DMAP (Scheme III.5)⁴² in dichloromethane (DCM) at room temperature. All the conditions tested are reported in Table III.1.



Scheme III.5. Synthesis of oxanorbornene-terminated PEO copolymer **4**.

Table III.1. Experimental conditions used for the synthesis of the oxanorbornene-terminated PEO **4**.^a

Entry	Reactants				Add	Time	Conversion ^d	Yield
	(mmol)					(h)	(%)	(%)
	3 ^b	DCC	DMAP	2 ^c				
1	1	1	1	2	2 to 3	144	38	nd ^e
2	1	1	0.67	0.67	2 to 3	24	43	50
3	1	1.5	0.5	4	2 to 3	168	62	nd
4	1	1.1	0.1	4	3 to 2	96	54	55
5	1	1.1	0.5	4	3 to 2	96	52	55

^a All the experiments were done in DCM at 25°C.

^b **3**: Carboxylic acid-terminated PEO

^c **2**: *Exo* oxanorbornene dimethanol

^d The conversion was calculated from the integrations of the protons of the methoxy group of the PEO at δ = 3.38 ppm (labelled **l**, Figure III.4) and of the protons $-\text{CH}=\text{CH}-$ of oxanorbornene at δ = 6.41 ppm (labelled **a** & **a'**, Figure III.4).

^e not determined

Whatever the conditions used, the conversion, calculated using the integrations of the signal characteristic of the protons of the methoxy group of the PEO at δ = 3.38 ppm (labelled **l**, Figure III.4) and of the shifted signals of the protons of $\text{CH}-\text{CH}=\text{CH}-\text{CH}$ of oxanorbornene at δ = 4.90 ppm and at δ = 4.78 ppm (labelled **b** & **c**, Figure III.4), is limited to 62%.

The MALDI-ToF mass spectrum of the oxanorbornene-terminated PEO **4** (Table III.1, run 2) reveals the presence of a population corresponding to the condensation between carboxylic acid-terminated PEO **3** and the unreacted commercial PEO from the last step during the synthesis of oxanorbornene-terminated PEO copolymer **4** (Figure III.5, III) in addition to the expected structure **4** (Figure III.5, II) and residual PEO (Figure III.5, I).

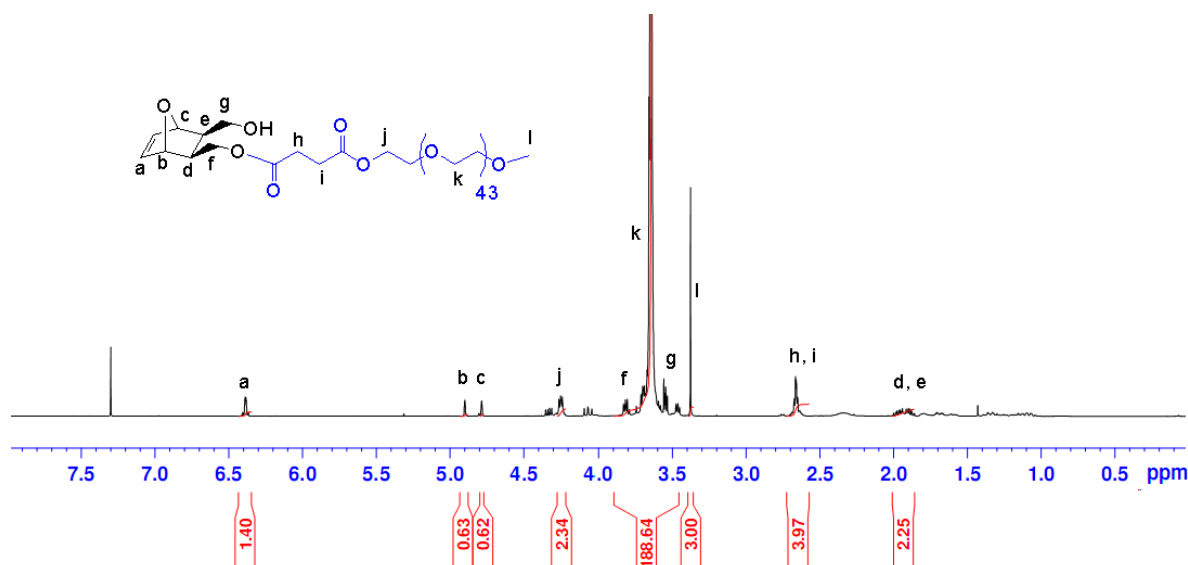


Figure III.4. ^1H NMR spectrum (400 MHz, 25 °C) of the oxanorbornene-terminated PEO **4** (Table III.1, run 2); solvent: CDCl_3 .

Nevertheless, the product that is constituted of residual PEO and oxanorbornene-terminated PEO **4** has been used to initiate the ROP of CL from the hydroxyl functionality. The purification of oxanorbornenyl-functionalized PEO-*b*-PCL copolymer **5** will be done afterwards.

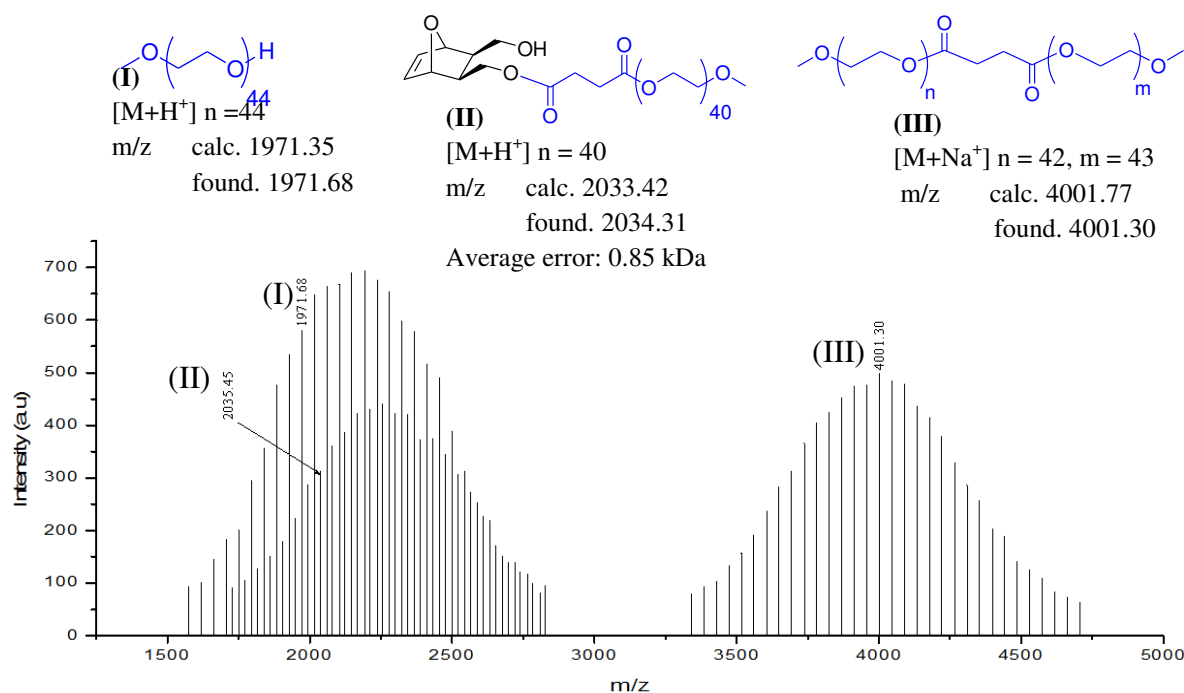
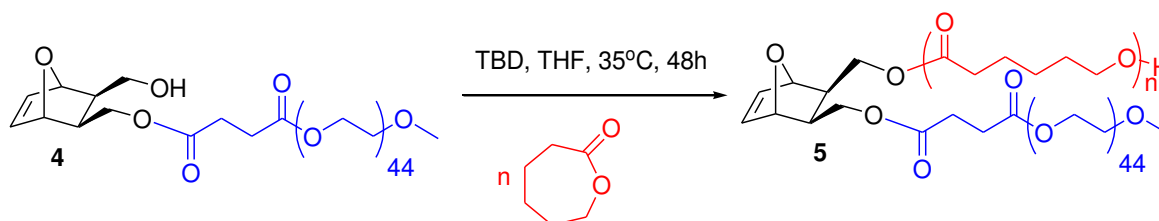


Figure III.5. MALDI-ToF mass spectrum of the oxanorbornene-terminated PEO **4**; matrix: DCTB, NaTFA

1.3. Synthesis of oxanorbornenyl-functionalized PEO-*b*-PCL copolymers

The ROP of CL from **4** has been performed at 35°C in THF selecting 1,5,7-triazabicyclo[4.4.0]dec-5-ene (TBD) as the catalyst for its efficiency in promoting the ROP of CL (Scheme III.6).⁴³ Organocatalyzed ROP has been chosen as it has the advantages over stannous octoate-catalyzed ROP to require lower temperatures that are compatible with the oxanorbornene thermal stability. The ROP reaction was carried out in the presence of **4**, CL and TBD in 1/60/0.5 molar ratio to reach the expected number-average degree of polymerization (DP_n) of 60. The resulting copolymer **5** was recovered by precipitation of the product in cold diethyl ether.



Scheme III.6. Synthesis of *exo* oxanorbornene-functionalized PEO-*b*-PCL copolymer

5.

DP_n of CL is calculated from the 1H NMR spectrum of the crude mixture (Figure III.6) by the comparison of the integrations of the signal related to the protons of $-CH_2CH_2O-$ of the PCL chain at δ = 4.00-4.10 ppm (labelled r, Figure III.6) and of the protons $-CH=CH-$ of oxanorbornene at δ = 6.41 ppm (labelled a & a', Figure III.6), is estimated to be 41. The monomer conversion, calculated from the comparison of the integrations of the signal related to the protons $-CH_2CH_2COO-$ of the PCL chain at δ = 2.25-2.35 ppm (labelled m, Figure III.6), and of the protons of CL at δ = 2.65-2.75 ppm (labelled m', Figure III.6), is 80%.

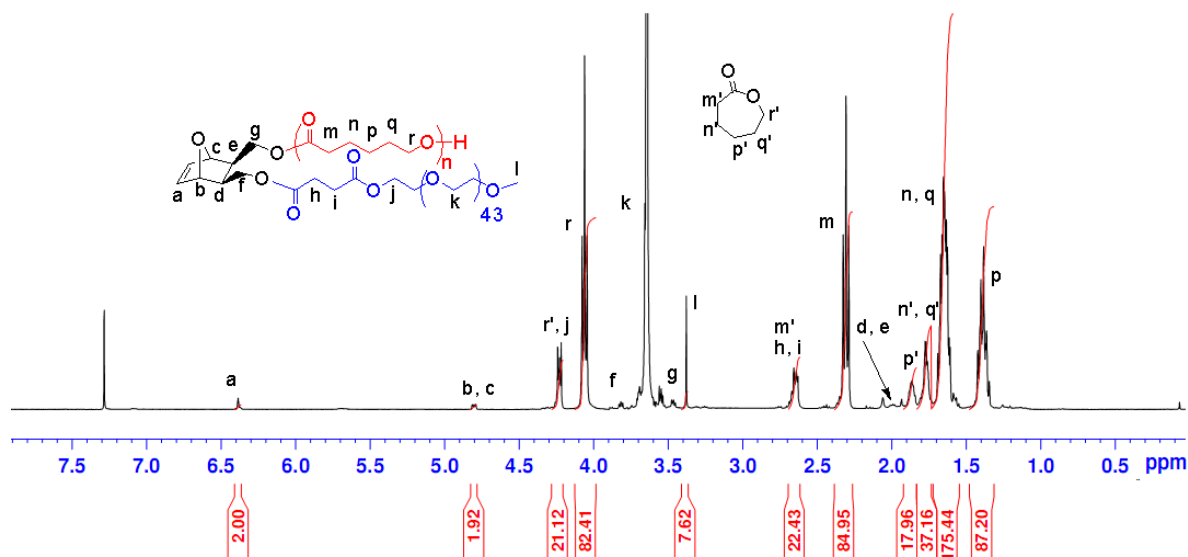


Figure III.6. ^1H NMR spectrum (400 MHz, 25 $^\circ\text{C}$) of the oxanorbornenyl-functionalized PEO-*b*-PCL copolymer **5**; solvent: CDCl_3 .

The size exclusion chromatography (SEC) trace showed two peaks (Figure III.7, B). The first one at the higher retention time is attributed to the oxanorbornene-terminated PEO **4** and the second one to lower retention time is the oxanorbornenyl-functionalized PEO-*b*-PCL copolymers **5**. The product has then been subjected to a selective precipitation in order to isolate the oxanorbornenyl-functionalized PEO-*b*-PCL copolymer **5** from the by-products. The SEC analysis after precipitation (Figure III.7, C) always shows the presence of undesired residual products.

It thus seems that this strategy is not suitable for the synthesis of pure oxanorbornene-functionalized PEO-*b*-PCL copolymer.

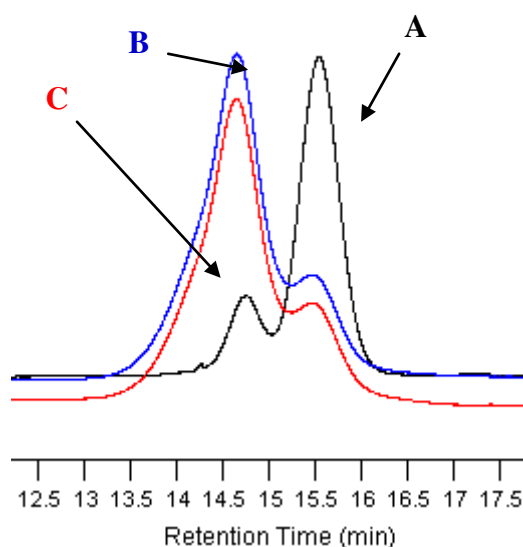
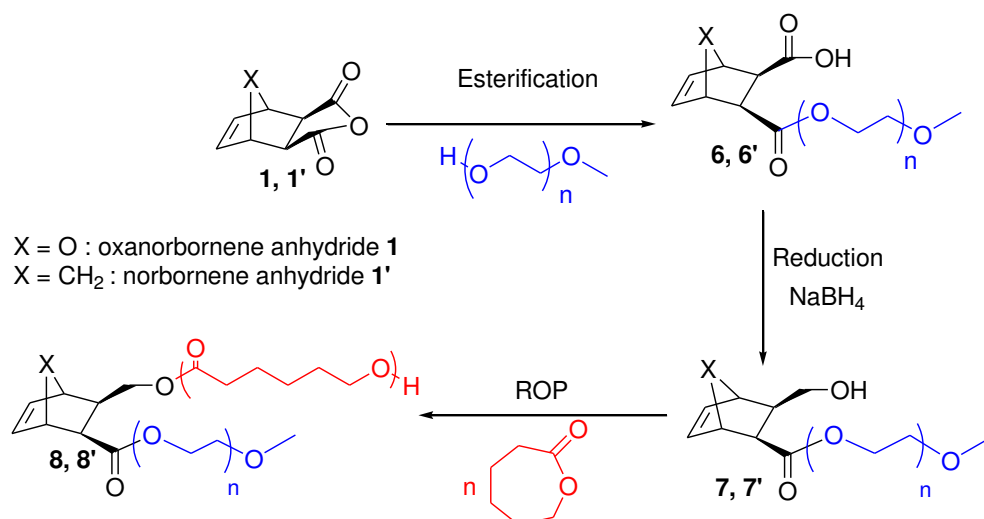


Figure III.7. SEC traces of (A) oxanorbornenyl-terminated PEO **4**, (B) oxanorbornenyl-functionalized PEO-*b*-PCL **5** before purification and (C) oxanorbornenyl-functionalized PEO-*b*-PCL **5** after purification.

II. Synthesis of (oxa)norbornenyl-functionalized PEO copolymers from (oxa)norbornene anhydrides

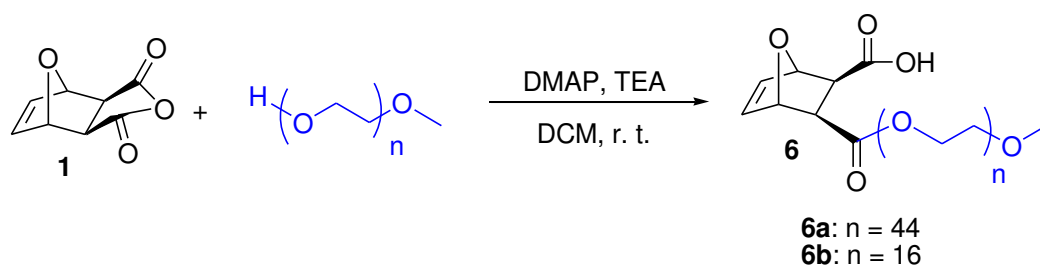
We have then moved to a new strategy (Scheme III.7), which consists in condensing directly the commercially available PEO onto the oxanorbornene anhydride **1**. This strategy has also been applied to the commercially available norbornene anhydride **1'**, in order to study the eventual influence of the ROMP-able functionality. The (oxa)norbornene-terminated PEO **6** and **6'** will thereafter be subjected to a selective reduction of the carboxylic acid group while retaining the ester group as already reported in the literature,⁴⁴ in order to introduce the hydroxyl functionality for subsequent ROP.



Scheme III.7. Synthesis of (oxa)norbornenyl-functionalized PEO-*b*-PCL **8** and **8'** from (oxa)norbornene anhydride **1** & **1'**.

II.1. Esterification between oxanorbornene anhydride and PEO

Oxanorbornene-terminated PEO **6** was synthesized by the direct esterification of commercially available PEO 2000 g/mol ($n = 44$) or PEO 750 g/mol ($n = 16$) with oxanorbornene anhydride in the presence of DMAP and triethylamine (TEA) in 1/1.5/0.5/1.2 initial molar ratio in DCM at room temperature (Scheme III.8).⁴¹



Scheme III.8. Synthesis of oxanorbornene-terminated PEO **6** from oxanorbornene anhydride **1**.

The ¹H NMR spectrum (Figure III.8) of the resulting oxanorbornene-terminated PEO 2000 g/mol **6a** showed new signals at $\delta = 4.48$ ppm and at $\delta = 4.14$ ppm (labelled g_1 & g_2 , Figure III.8) attributed to the methylene group -COO-CH₂- generated after reaction. The conversion, calculated from the integrations of the protons -COOCH₂CH₂O- at $\delta = 4.48$ ppm (labelled g_1 , Figure III.8) and at $\delta = 4.14$ ppm (labelled g_2 , Figure III.8) and of the protons -CH=CH- at $\delta = 6.41$ ppm (labelled a , Figure III.8), is estimated to be quantitative (1.58:1.62 ratio). Nevertheless, comparison between the

integration of the methoxy end-group of PEO at $\delta = 3.38$ ppm (labelled i, Figure III.8) and the protons -COOCH₂CH₂O- at $\delta = 4.48$ ppm and at $\delta = 4.14$ ppm showed a 1.62/3.00 ratio indicating that PEO 2000 g/mol is present in excess in the resulting product.

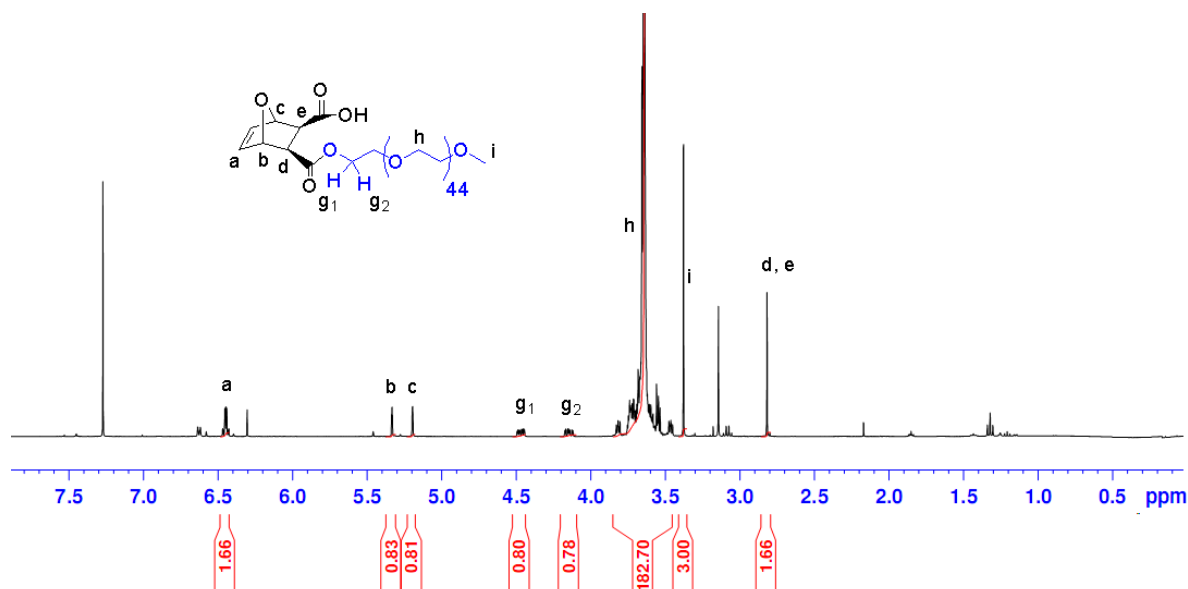


Figure III.8. ¹H NMR spectrum (400 MHz, 25 °C) of oxanorbornene-terminated PEO 2000 g/mol **6a**; solvent: CDCl₃.

The low purity of oxanorbornene-terminated PEO **6a** obtained from oxanorbornene anhydride and PEO 2000 g/mol leads us to test the esterification between the commercially available PEO 750 g/mol, which has a shorter PEO length (Scheme III.8).

Unfortunately, the ¹H NMR spectrum (Figure III.9) of the oxanorbornene-terminated PEO 750 g/mol **6b** shows a result in total agreement with the one obtained with oxanorbornene-terminated PEO 2000 g/mol **6a** as PEO 750 g/mol is still present in excess in resulting product.

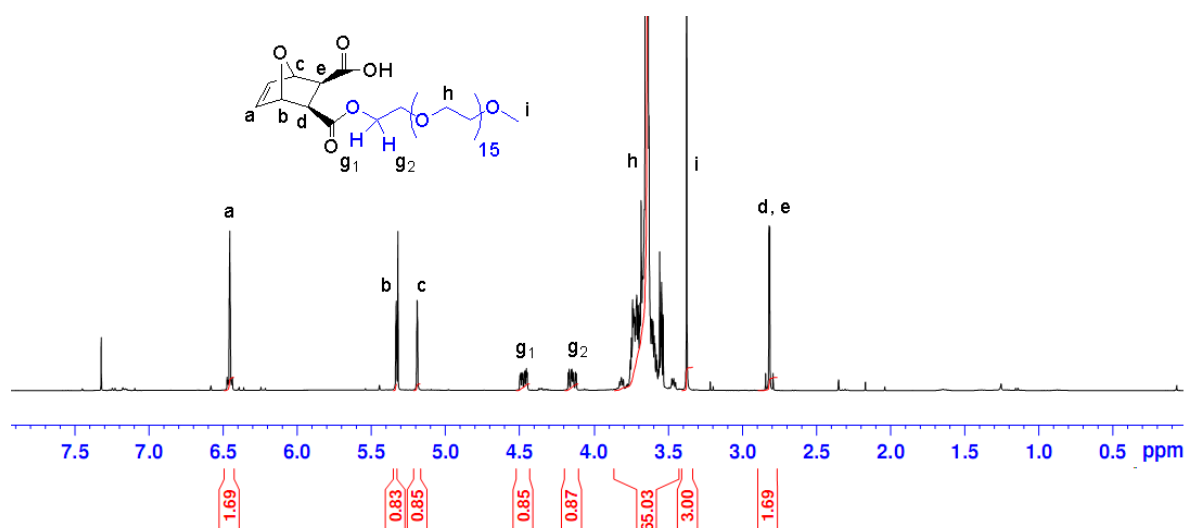
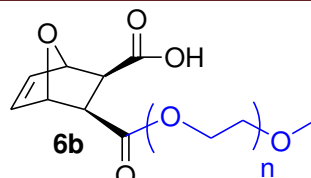


Figure III.9. ^1H NMR spectrum (400 MHz, 25 $^\circ\text{C}$) of oxanorbornene-terminated PEO 750 g/mol **6b**; solvent: CDCl_3 .

The MALDI-ToF mass spectrum of the resulting oxanorbornene-terminated PEO **6b** (Figure III.10) includes 4 series of peaks. The difference in mass of each signal of each series was estimated to 44, indicating the signals are assignable to PEO homologues. The first series is attributed to the sodium-ionized PEO monomethyl ether 750 ($m/z = 759.423$, calculated value = 758.886 for 16 repeating units). The second series corresponds to the proton-ionized PEO monomethyl ether 750 ($m/z = 869.112$, calculated value = 869.013 for 19 repeating units). The third series corresponds to the proton-ionized oxanorbornene-terminated PEO **6b** ($m/z = 903.425$, calculated value = 903.028 for 16 repeating units). The fourth series corresponds to the sodium-ionized oxanorbornene-terminated PEO **6b** ($m/z = 881.448$, calculated value = 880.975 for 15 repeating units).



Structure II

[M+H ⁺] n = 16	m/z	calc. 903.028
		found. 903.425
[M+Na ⁺] n = 15	m/z	calc. 880.975
		found. 881.448

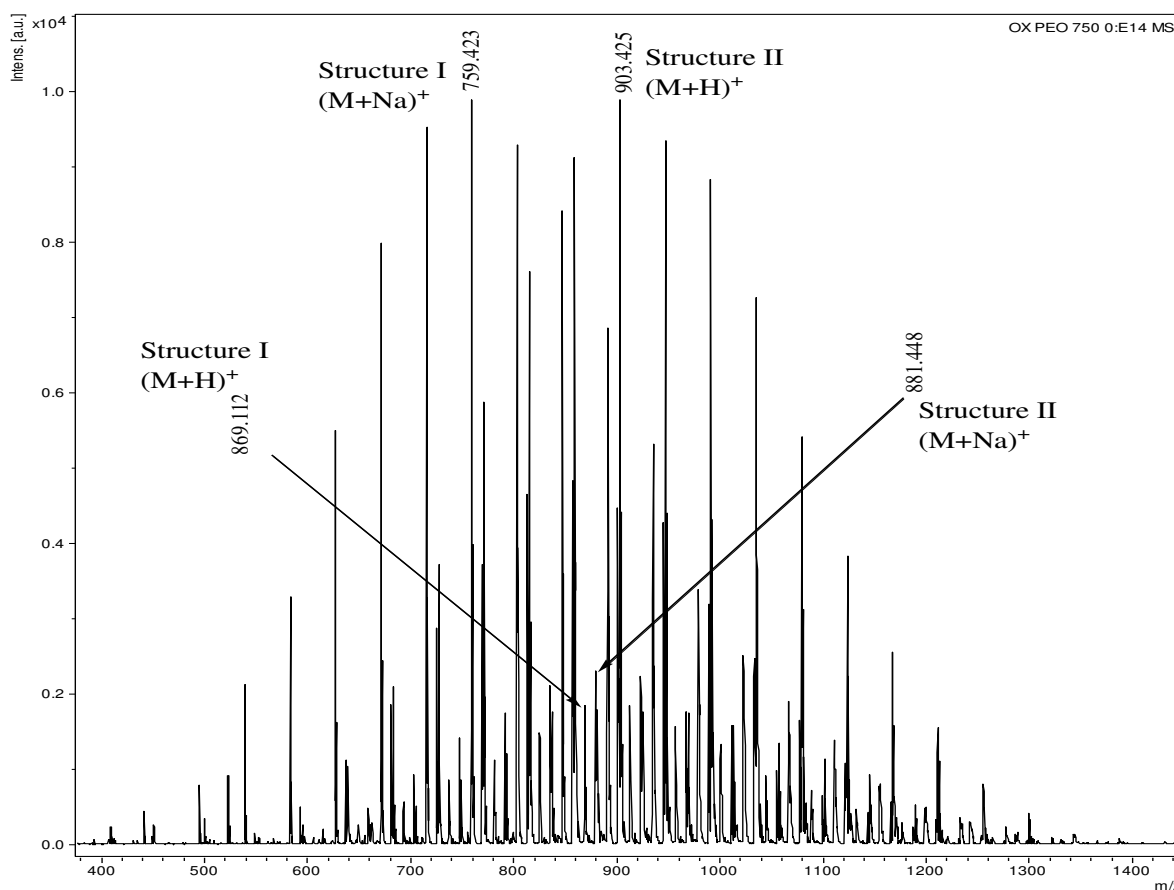
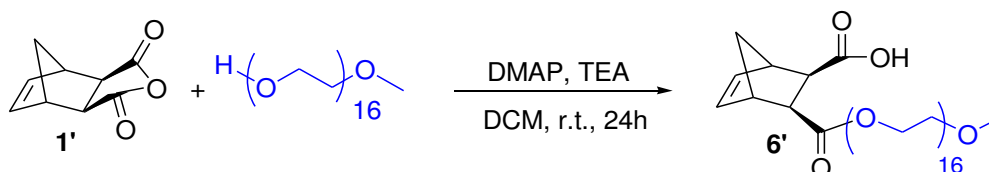


Figure III.10. MALDI-ToF mass spectrum of oxanorbornene-terminated PEO **6b**; matrix: DCTB, NaTFA.

Commercial PEOs are always present in excess in resulting products either using PEO 2000 g/mol or PEO 750 g/mol as starting compounds even with an initial excess of oxanorbornene anhydride before the esterification. We then moved to a more hydrophobic ROMP-able moiety, i.e. norbornene, to test the esterification with PEO.

II.2. Esterification between norbornene anhydride and PEO

Norbornene-terminated PEO **6'** was synthesized from norbornene anhydride **1'** according to the experimental conditions used for the esterification between oxanorbornene anhydride **1** and PEO 750 g/mol (Scheme III.9).⁴¹



Scheme III.9. Synthesis of norbornene-terminated PEO **6'** from norbornene anhydride **1'**.

The ¹H NMR spectrum (Figure III.11) of the resulting norbornene-terminated PEO **6'** showed new signals at $\delta = 4.48$ ppm and at $\delta = 4.14$ ppm (labelled g_1 & g_2 , Figure III.11) attributed to the methylene group $-\text{COO}-\text{CH}_2-$ generated after reaction. The conversion, calculated from the integrations of protons $-\text{COOCH}_2\text{CH}_2\text{O}-$ at $\delta = 4.48$ ppm (labelled g_1 , Figure III.11) and at $\delta = 4.14$ ppm (labelled g_2 , Figure III.11) and of the protons $-\text{CH}=\text{CH}-$ at $\delta = 6.19$ ppm (labelled a & b , Figure III.11), shows a quantitative conversion (2.03/2.05 ratio). Furthermore, the comparison of the integrations of methoxy end-group of PEO at $\delta = 3.38$ ppm (labelled i , Figure III.11) and of the protons $-\text{COOCH}_2\text{CH}_2\text{O}-$ at $\delta = 4.48$ ppm and at $\delta = 4.14$ ppm (labelled g_1 & g_2 , Figure III.11) confirmed the quantitative conversion (3.00/2.03).

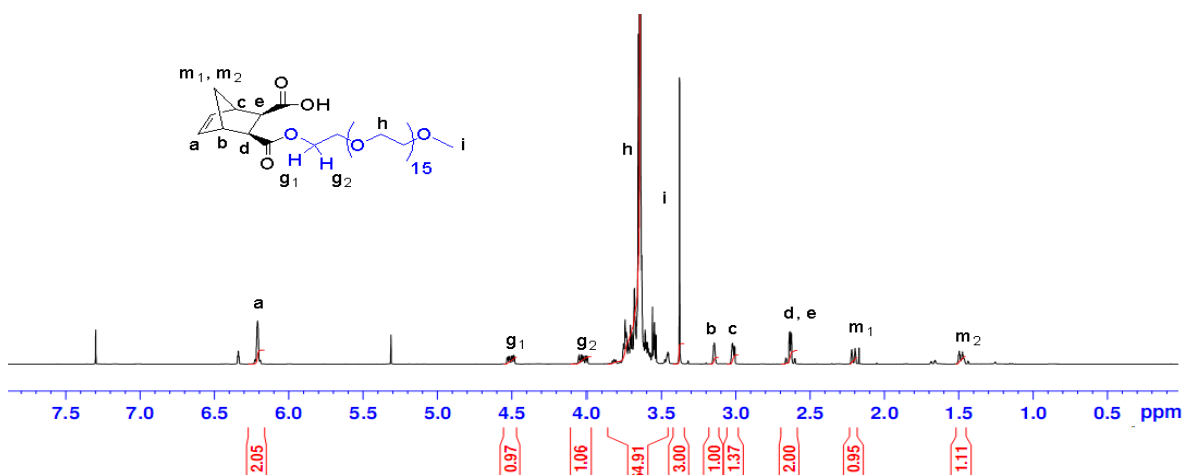


Figure III.11. ¹H NMR spectrum (400 MHz, 25 °C) of norbornene-terminated PEO **6'**; solvent: CDCl₃

The MALDI-ToF mass spectrum of norbornene-terminated PEO 750 g/mol **6'** (Figure III.12) showed that there are different populations including 3 series with a difference in mass of each series estimated to 44, indicating that signals are assignable to PEO homologues. The first and second series correspond to the proton-ionized ($m/z = 945.439$, calculated value = 945.527 for 17 repeating units) and sodium-ionized ($m/z = 923.458$, calculated value = 923.483 for 16 repeating units) norbornene-terminated PEO **6'**, respectively. The third series is attributed to sodium-ionized commercial PEO monomethyl ether 750 ($m/z = 803.433$, calculated value = 803.461 for 17 repeating units).

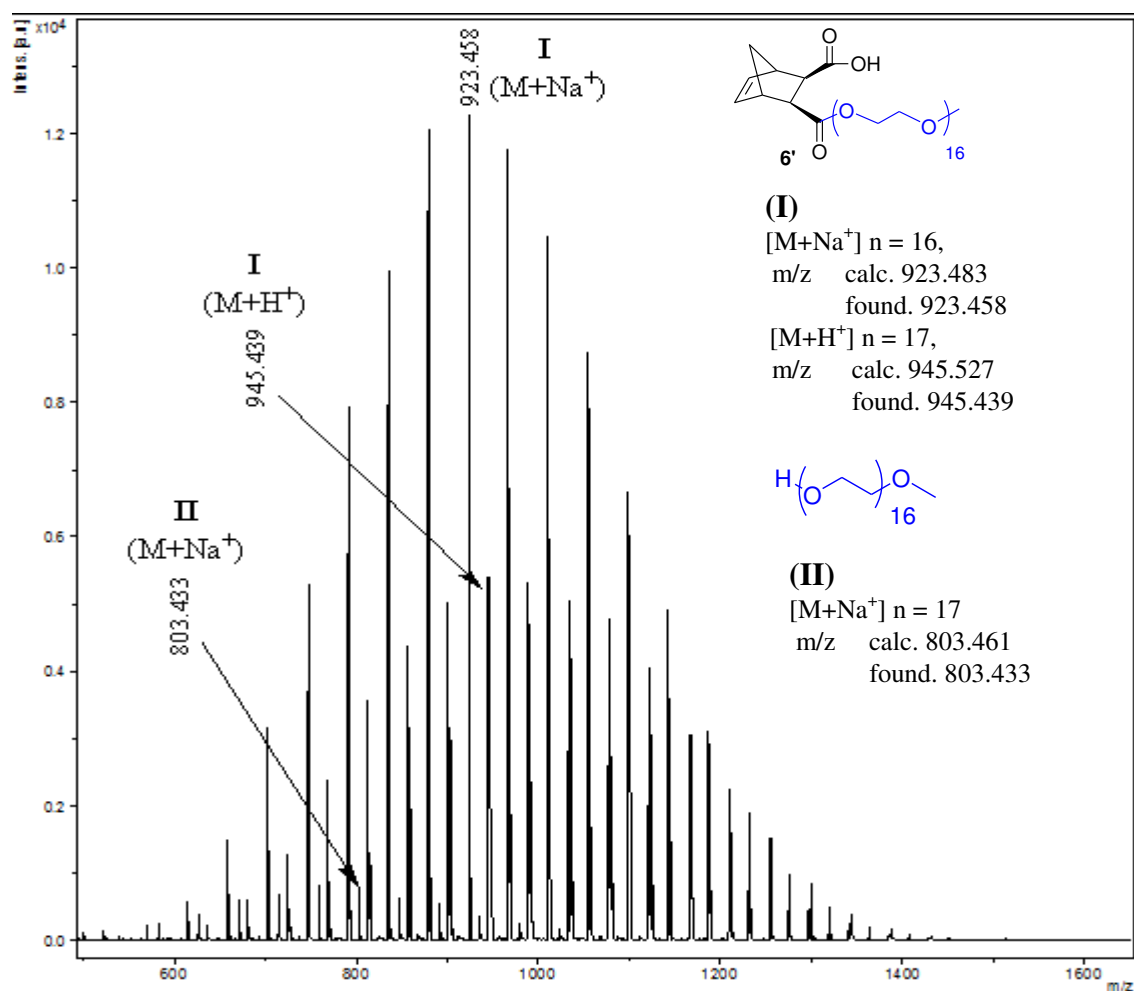
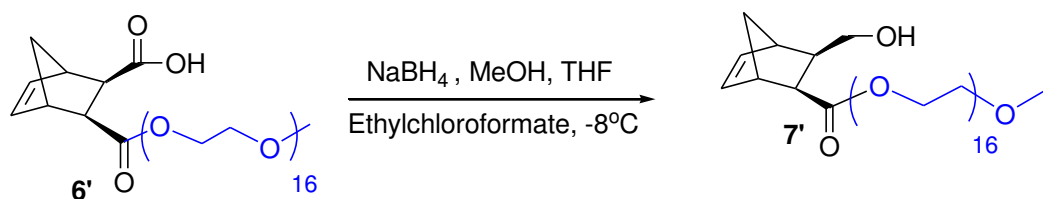


Figure III.12. MALDI-ToF mass spectrum of norbornene-terminated PEO **6'**; matrix: DCTB, NaTFA

The carboxylic acid functionality of the norbornene-terminated PEO **6'** has then been subjected to a reduction to obtain a hydroxyl group to be used as an initiating functionality for the ROP of CL.

II.3. Reduction of carboxylic acid-functionalized norbornene-terminated PEO

The carboxylic acid functionality of norbornene-terminated PEO **6'** was selectively reduced while retaining the ester functionality in the presence of ethylchloroformate as a protecting agent for the ester functionality and sodium borohydride (NaBH_4) as a reducing agent at -8°C in MeOH/THF⁴⁵ (Scheme III.10).



Scheme III.10. Synthesis of hydroxyl-functionalized norbornene-terminated PEO **7'**

The comparison of the FT-IR spectra of **6'** and the product mixture (Figure III.13) didn't show any significant modification as the peak at 1737 cm^{-1} corresponding to C=O bond is also present in both spectra.

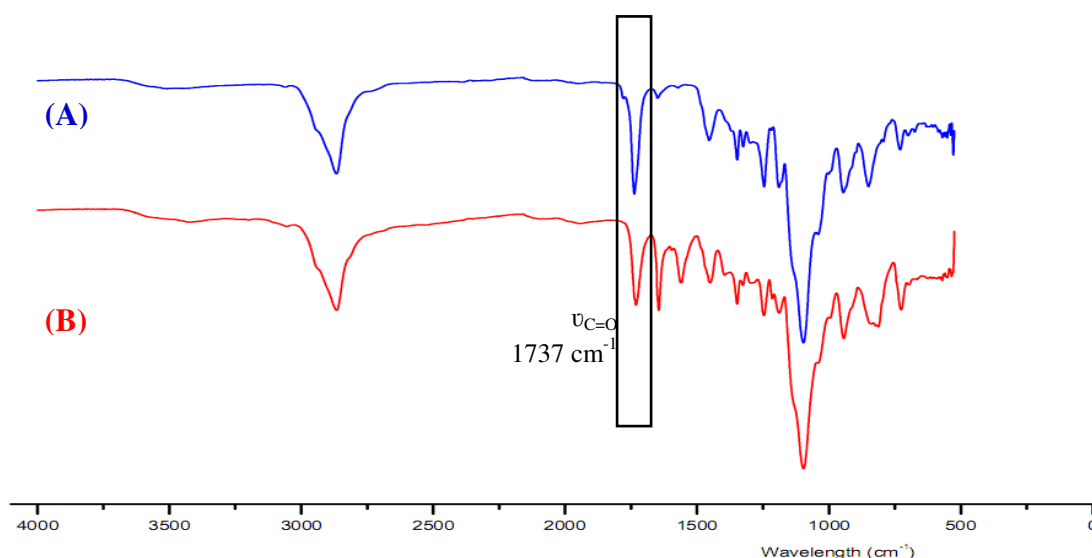


Figure III.13. FT-IR spectra of (A) the product mixture and (B) **6'**

Furthermore, the comparison of ^1H NMR spectra before and after reduction (Figure III.14) shows that the proton $-\text{CHCH}-\text{COOH}$ (labelled c, Figure III.14, A) is still present. The integration of the signal at corresponding to a proton $\text{COO}-\text{CH}_2\text{CH}_2\text{O}$ at $\delta = 4.48\text{ ppm}$ (labelled g'_1 , Figure III.14, A) reduced from 1 (labelled g_1 , Figure III.14, B)

to 0.37, suggesting a breakage of ester bond in the presence of reduction agent. A new signal appears at $\delta = 1.85$ ppm corresponding to proton $\text{HOCH}_2\text{CHCH}=\text{CH}$ (labelled c'), Figure III.14, A) showed that the reduction worked but with low conversion.

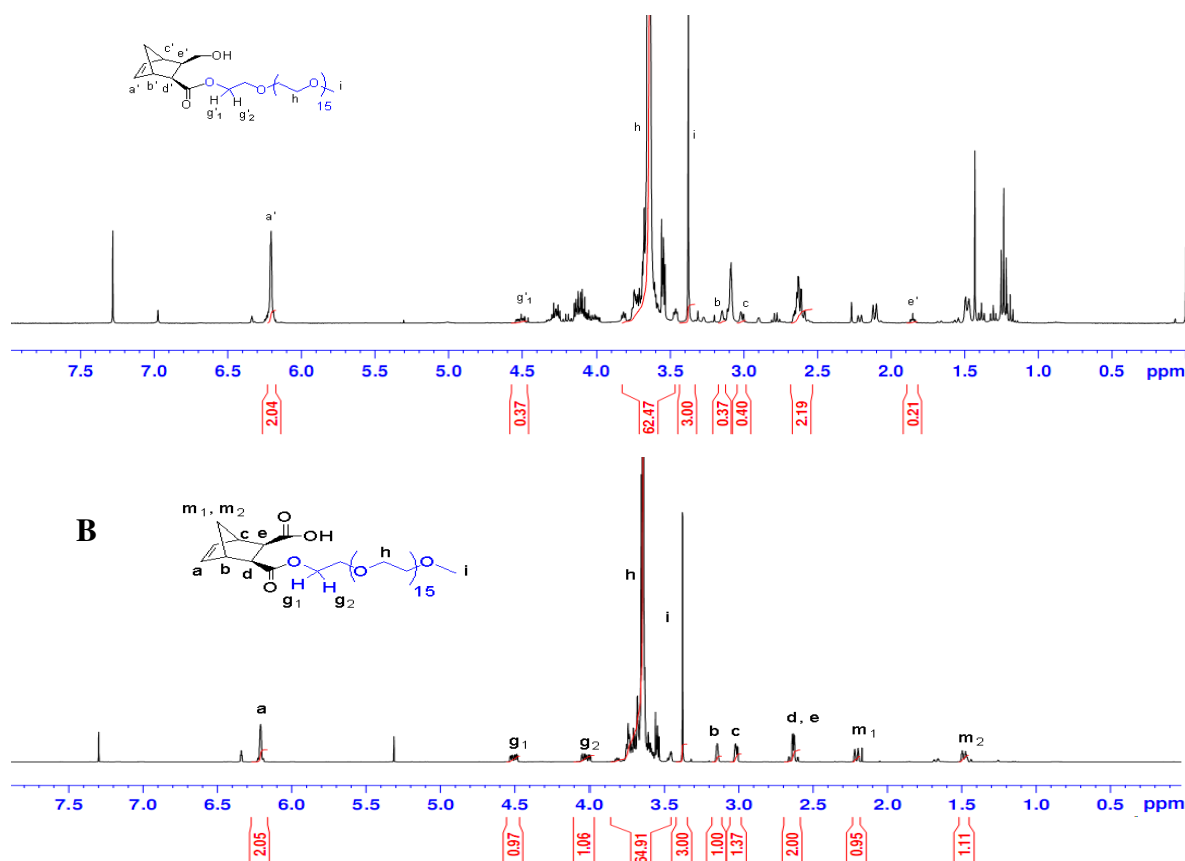


Figure III.14. ^1H NMR spectra (400 MHz, 25 $^\circ\text{C}$) of hydroxyl-functionalized norbornenyl-terminated PEO **7'** and carboxylic acid-functionalized norbornene-terminated PEO **6'**; solvent: CDCl_3

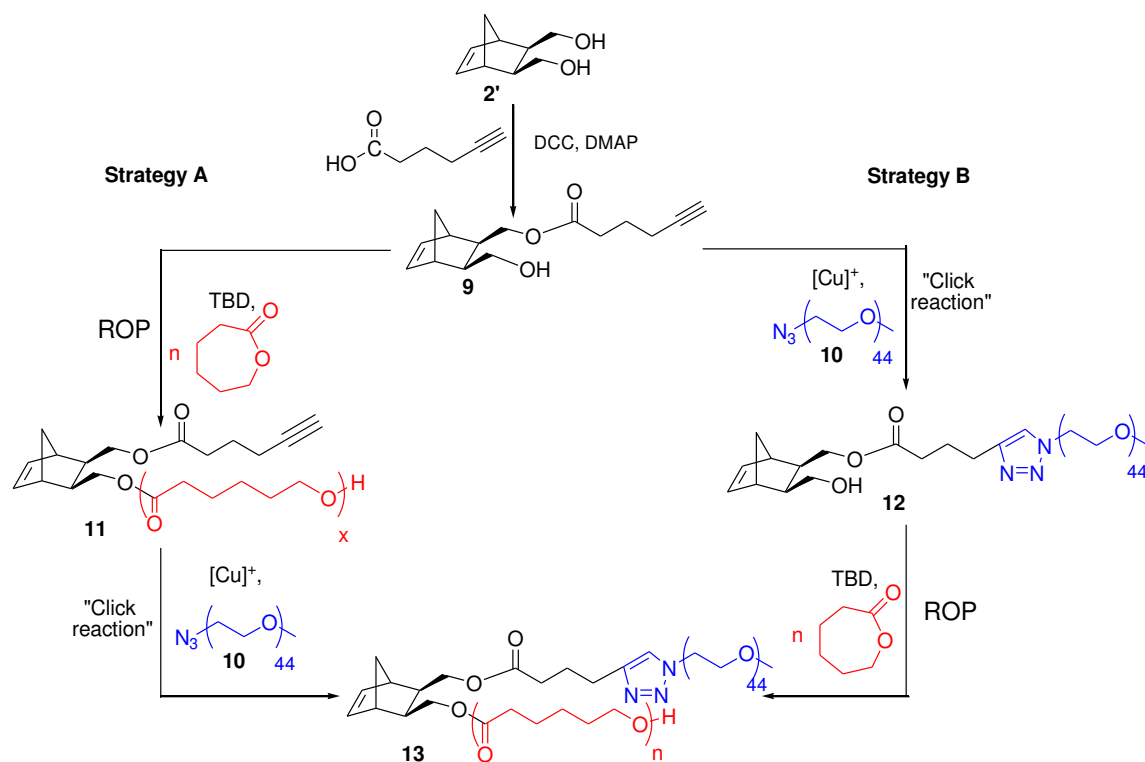
The results showed the reduction reaction has several side reactions and this strategy is thus not suitable to synthesize amphiphilic (oxa)norbornenyl-functionalized PEO-*b*-PCL copolymers. This can be ascribed to difficult exhaustive drying of PEO.

III. Synthesis of norbornenyl-functionalized PEO-*b*-PCL copolymers by combination of “click chemistry” and ROP

Because of the unsuccessful results obtained from the chemical modification for the synthesis of pure norbornenyl-functionalized PEO-*b*-PCL copolymers, we then moved to another strategy, which consists in the combination of a ‘click’ reaction and ROP to prepare amphiphilic copolymers based on norbornene. Indeed, the ‘click’ copper-catalyzed azide-alkyne cycloaddition (CuAAC) reaction is not sensitive to the traces of water that are difficult to remove from commercial PEO. Synthesis of norbornene-based PEO copolymers from an alkyne-functionalized norbornene and an azido-terminated PEO with M_n ranging from 500 to 5000 g/mol according to the copper-catalyzed azide-alkyne ‘click’ reaction has already been previously reported in the literature.⁴⁶

Norbornenyl-functionalized PEO-*b*-PCL copolymers were synthesized from norbornene dimethanol **2'**, issued from the reduction of norbornene anhydride **1'**, followed by the monofunctionalization with 5-hexynoic acid to generate an alkyne functionality, while retaining a hydroxyl functionality in the resulting hydroxyl- and alkynyl-functionalized norbornene **9** for a further ROP.

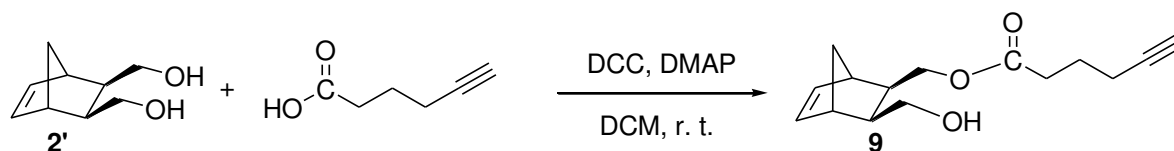
Norbornenyl-functionalized PEO-*b*-PCL copolymers **13** were synthesized according to two strategies (Scheme III.11). In the first one, the hydroxyl functionality of **9** was used as an initiator for the ROP of CL to afford the targeting norbornenyl-terminated PCL **11**. Then the ‘click’ reaction was carried out between the alkyne functionality of the norbornenyl-terminated PCL **11** and the azide-terminated PEO⁴⁰ **10** according to a 1,3-dipolar ‘click’ reaction. The reaction was realized in the presence of a catalytic amount of Cu(I)Br with *N,N,N',N',N''*-pentamethyldiethylenetriamine (PMDETA) as the ligand⁴⁷ to reach amphiphilic norbornenyl-functionalized PEO-*b*-PCL copolymers **13** (Strategy A, Scheme III.11). The second strategy consists in the ‘click’ reaction between alkyne functionality of **9** with an azide-terminated PEO **10** in the presence of CuBr and PMDETA to target norbornene-terminated PEO **12** followed by the ROP of CL which was initiated by the hydroxyl-functionality of **12** to reach amphiphilic norbornenyl-functionalized PEO-*b*-PCL copolymers **13** (Strategy B, Scheme III.11).



Scheme III.11. Synthesis of norbornenyl-functionalized PEO-*b*-PCL copolymer **13**

III.1. Synthesis of hydroxyl- and alkynyl-functionalized norbornene

Hydroxyl- and alkynyl-functionalized norbornene **9** was obtained from **2'** and 5-hexynoic acid in a 1/1 molar ratio using DMAP/DCC as the catalyst⁴¹ in DCM at room temperature (Scheme III.12). The precursor **9** was obtained in 45% yield after a silica gel column chromatography purification using cyclohexane/ethyl acetate as the eluent.



Scheme III.12. Synthesis of hydroxyl- and alkynyl-terminated norbornene **9**

¹H NMR spectrum of hydroxyl- and alkynyl-terminated norbornene **9** (Figure III.15) showed the shifts of the signals corresponding to the methylene protons -CHCH₂O- of the norbornene dimethanol at $\delta = 3.62 - 3.92$ ppm (labelled h', Figure III.15, B) before reaction, to $\delta = 4.06$ ppm and $\delta = 4.27$ ppm (labelled i, Figure III.15, A) and $\delta = 3.84$ ppm and $\delta = 3.58$ ppm (labelled h, Figure III.15, A) after esterification. The full conversion was demonstrated from the integrations of protons -CHCH₂OCO at

$\delta = 4.06$ ppm and $\delta = 4.27$ ppm (labelled i, Figure III.15, A) and protons of $-\text{CH}=\text{CH}-$ at $\delta = 6.19$ ppm (labelled a, Figure III.15, A).

The molar mass of **9** from HRMS analysis ($[\text{M}+\text{H}^+]_{\text{found}} = 249.1488$) was in good agreement with the calculated value ($[\text{M}+\text{H}^+]_{\text{cal.}} = 249.1490$).

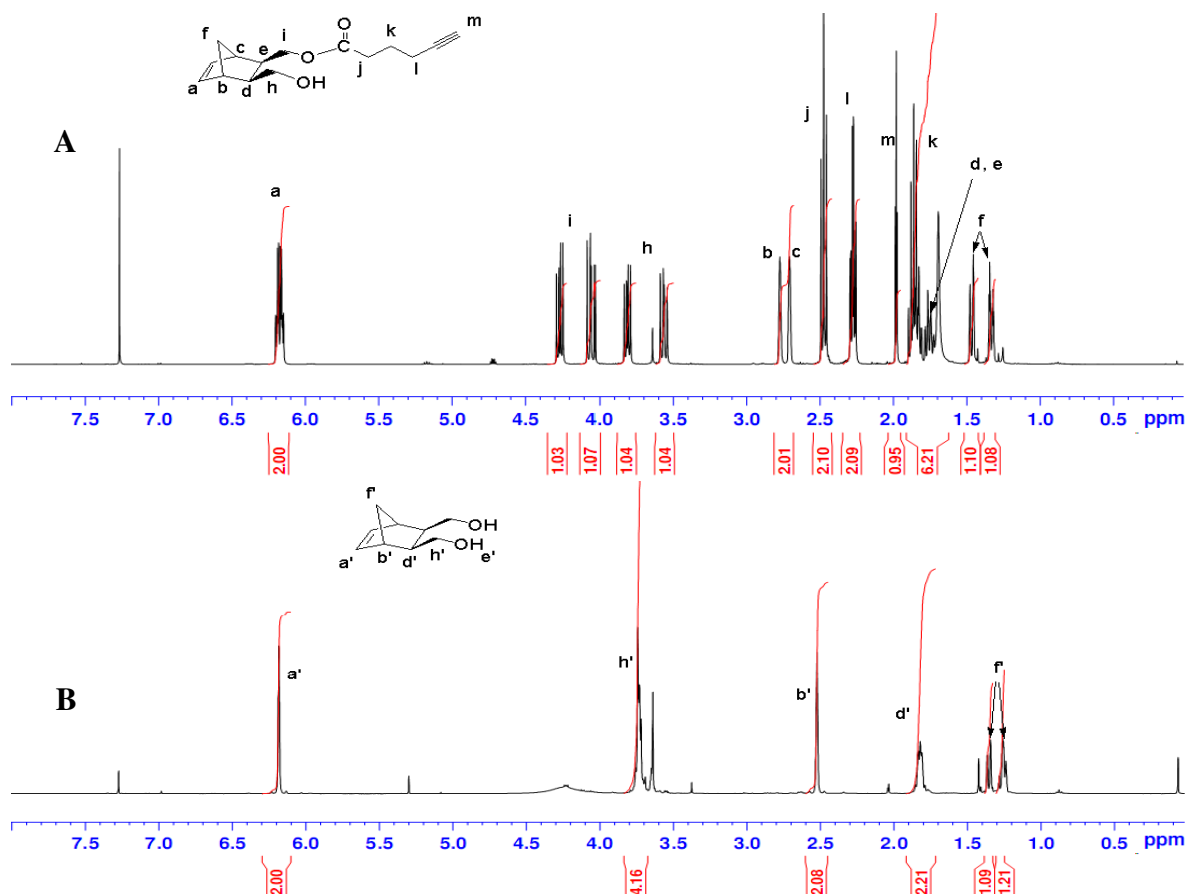
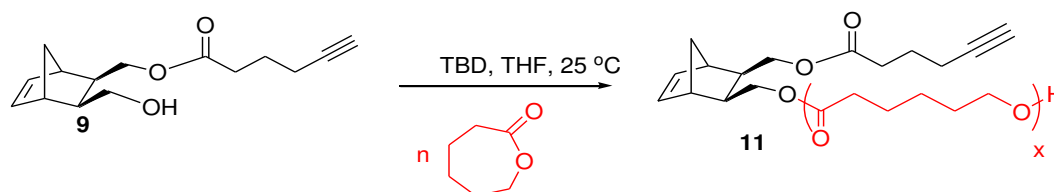


Figure III.15. ^1H NMR spectra (400 MHz, 25 °C) of (A) dihydroxyl- and alkynyl-terminated norbornene **9** and (B) norbornene dimethanol **2'**; solvent: CDCl_3

III.2. Synthesis of norbornenyl-functionalized PEO-*b*-PCL copolymers by ROP of CL followed by 'click' reaction

III.2.1. Synthesis of alkynyl-functionalized norbornenyl-terminated PCL

Hydroxyl functionality of **9** was first used to initiate the ROP of CL. The reaction has been performed at 25 °C in THF selecting TBD as the catalyst in a $[\mathbf{9}]_0/[\text{CL}]_0/[\text{TBD}]_0$ molar ratio of 1:20:0.34 (Scheme III.13). The resulting alkynyl-functionalized norbornenyl-terminated PCL **11** was recovered by precipitation in cold diethyl ether as a white powder in 75% yield.



Scheme III.13. Synthesis of alkynyl-functionalized norbornenyl-terminated PCL **11**

^1H NMR spectrum of **11** showed the appearance of new peaks related to the protons of PCL at $\delta = 4.00$ - 4.20 ppm (labelled t, Figure III.16). The $\text{DP}_{\text{n,NMR}}$ value of CL was calculated from the ^1H NMR spectrum by comparison of integration areas of the protons of $-\text{CH}_2\text{CH}_2\text{O}-$ of PCL chains at $\delta = 4.00$ - 4.20 ppm (labelled t, Figure III.16) and protons of $-\text{CH}=\text{CH}-$ of norbornene entity at $\delta = 6.19$ ppm (labelled a, Figure III.16), and is estimated to be 22.

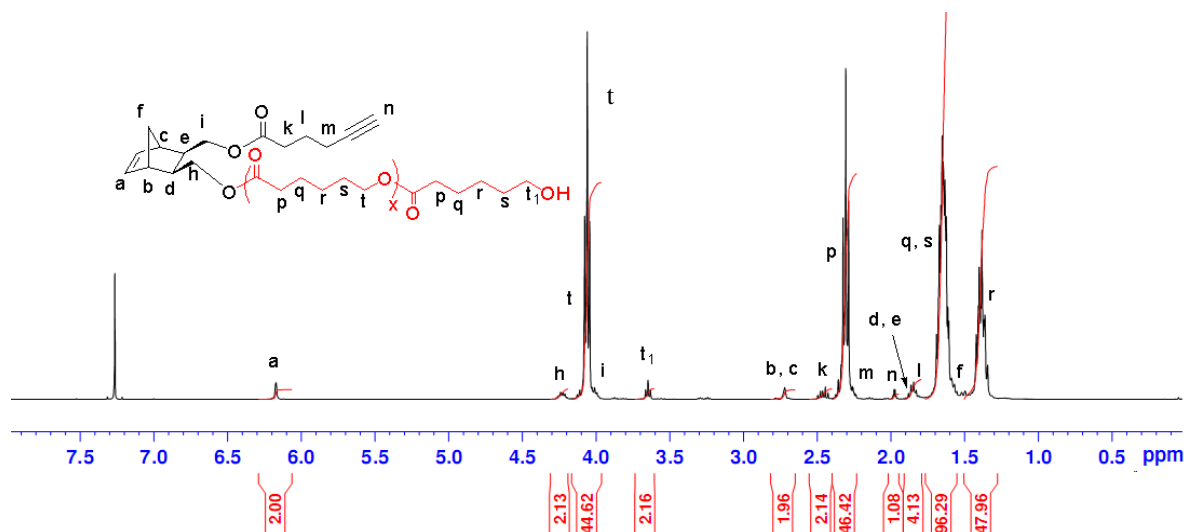


Figure III.16. ^1H NMR spectrum (400 MHz, 25 °C) of alkynyl-functionalized norbornenyl-terminated PCL **11**; solvent: CDCl_3

The SEC trace of **11** (Figure III.17) showed only one unsymmetrical peak exhibiting the back-biting of PCL chains in the presence of TBD.⁴⁸

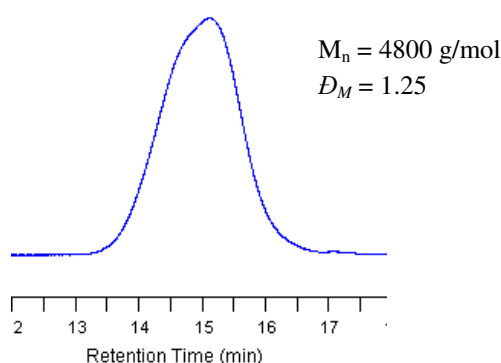
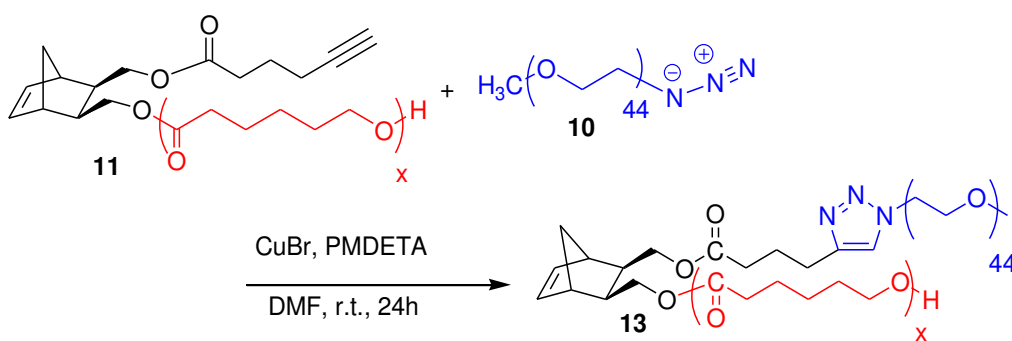


Figure III.17. SEC trace of alkynyl-functionalized norbornene-terminated PCL **11**.

11 has then been engaged in a ‘click’ reaction between the alkyne functionality of **11** and the azido-terminated PEO **10**, in order to obtain norbornenyl-functionalized PEO-*b*-PCL.

III.2.2. Synthesis of norbornenyl-functionalized PEO-*b*-PCL copolymers

Norbornenyl-functionalized PEO-*b*-PCL copolymer **13** has been synthesized by a ‘click’ reaction between **11** and **10**, according to a reported procedure^{42,49} in the presence of CuBr and PMDETA using **10/11/CuBr/PMDETA** initial molar ratio of 1/1/0.5/1.2 in *N,N*-dimethylformamide (DMF) at room temperature (Scheme III.14).



Scheme III.14. Synthesis of norbornenyl-functionalized PEO-*b*-PCL copolymer **13**.

The ¹H NMR spectrum showed the concomitant appearance of the proton on the triazole ring at $\delta = 7.51$ ppm (labelled m, Figure III.18) and the methylene group near to the triazole ring at $\delta = 4.50$ ppm (labelled n₁, Figure III.18). A nearly quantitative ‘click’ reaction (95%) was obtained as ascertained by comparing the integration areas of the new proton in triazole ring (labelled m, Figure III.18) at $\delta = 7.51$ ppm and of the two protons -CH=CH- in the norbornene ring at $\delta = 6.19$ ppm (labelled a, Figure III.18).

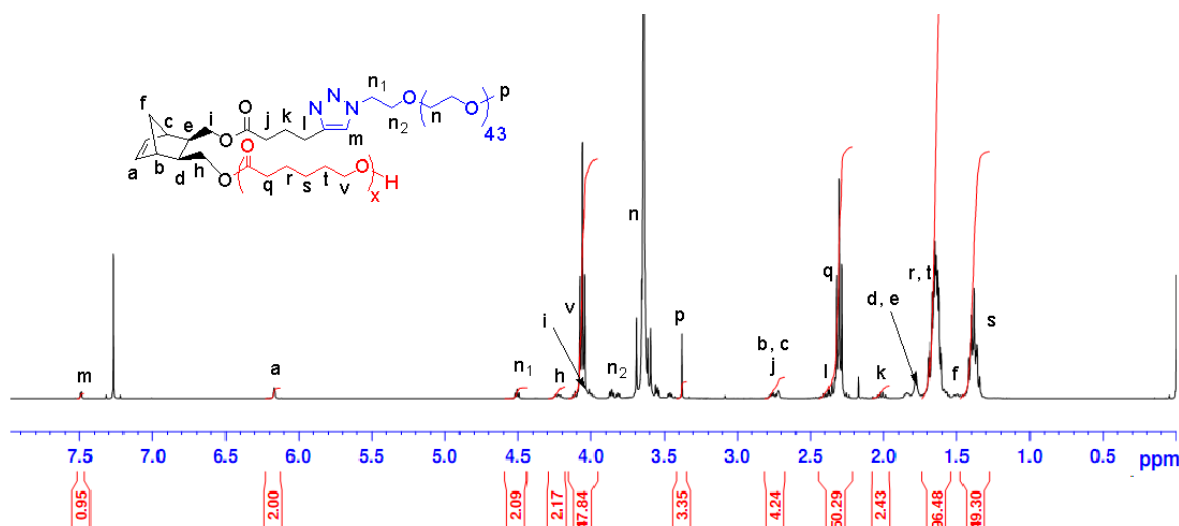


Figure III.18. ^1H NMR spectrum (400 MHz, 25 °C) of norbornenyl-functionalized PEO-*b*-PCL **13**; solvent: CDCl_3 .

Unfortunately, the SEC trace (A, Figure III.19) showed 2 peaks, the first one at the higher retention time is attributed to the azide-terminated PEO **10** and the second one at lower retention time is the norbornenyl-functionalized PEO-*b*-PCL copolymer **13**. This result is in good agreement with the ^1H NMR spectrum of **13** (Figure III.18), which shows integration areas for methoxy group of PEO at $\delta = 3.38$ ppm (labelled p, Figure III.18) and triazole proton $\delta = 7.51$ ppm (labelled m, Figure III.18) in a 3.35/0.95 ratio. The non-quantitative ‘click’ reaction observed in this case confirms previous results reported in literature⁵⁰ concerning ‘click’ reaction between polymers and lead us to test strategy B (Scheme III.11).

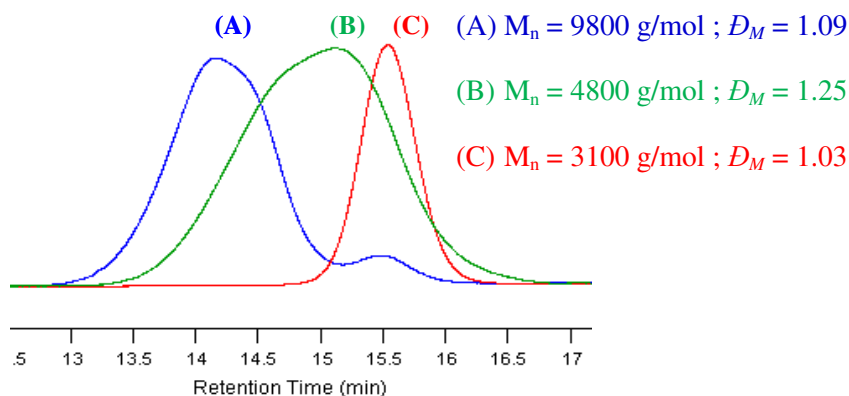
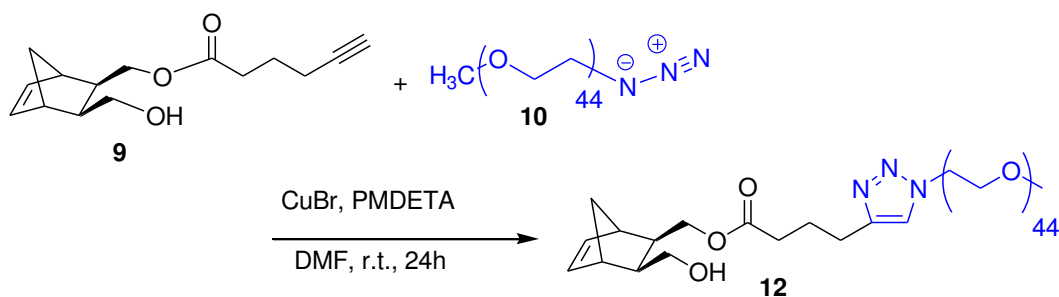


Figure III.19. SEC traces of (A) norbornenyl-functionalized PEO-*b*-PCL **13**, (B) alkynyl-functionalized norbornene-terminated PCL **11** and (C) azido-terminated PEO **10**.

III.3. Synthesis of norbornenyl-functionalized PEO-*b*-PCL copolymers by ‘click’ reaction followed by ROP of CL

III.3.1. Synthesis of hydroxyl-functionalized norbornenyl-terminated PEO.

Hydroxy-functionalized PEO-terminated norbornene **12** was prepared by a ‘click’ reaction between **9** and azido-terminated PEO **10**, synthesized according to a reported procedure^{40,46} in the presence of CuBr and PMDETA in DMF as the solvent at room temperature (Scheme III.15). **12** was obtained as a white powder in 75% yield.



Scheme III.15. Synthesis of hydroxyl-functionalized norbornenyl-terminated PEO **12** via ‘click’ reaction.

After 24 h of reaction, the purified polymer was analyzed by ¹H NMR spectroscopy and MALDI-ToF mass spectrometry. The ¹H NMR spectrum showed the appearance of the proton on the triazole ring at $\delta = 7.51$ ppm (labelled m, Figure III.20). The

methylene group near the triazole ring appears at $\delta = 4.50$ ppm (labelled n_1 , Figure III.20). Furthermore, a quantitative conversion of ‘click’ reaction was obtained as ascertained by comparing integration areas of the new proton in triazole ring (labelled m , Figure III.20) at $\delta = 7.51$ ppm and of two protons $-\text{CH}=\text{CH}-$ in the norbornene ring at $\delta = 6.18$ ppm (labelled a & b , Figure III.20).

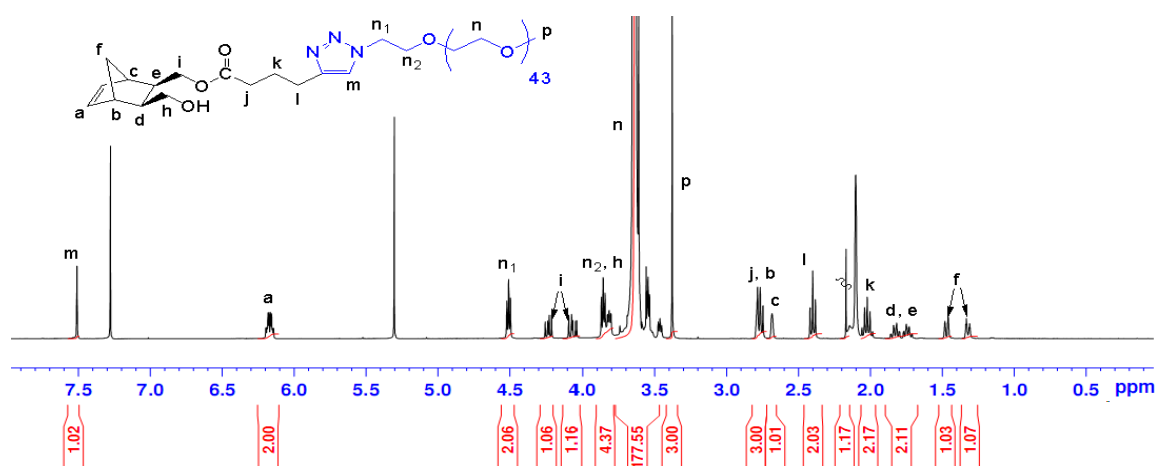


Figure III.20. ^1H NMR spectrum (400 MHz, 25 °C) of hydroxyl-functionalized norbornenyl-terminated PEO **12**; solvent: CDCl_3 .

The MALDI-ToF mass spectrum (Figure III.21) reveals only one population corresponding to sodium-ionized **12** ($m/z_{\text{found}} = 2309.363$ and $m/z_{\text{calc}} = 2309.343$ for 44 ethylene oxide units).

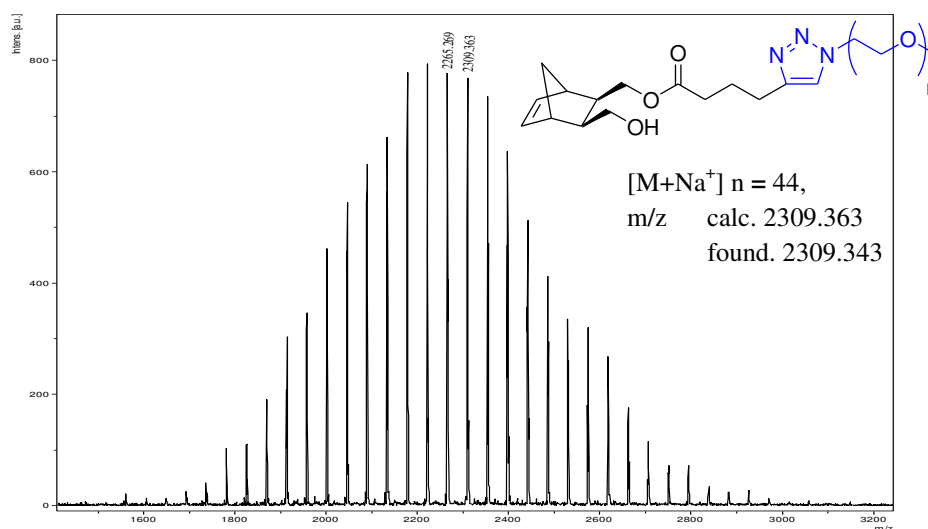
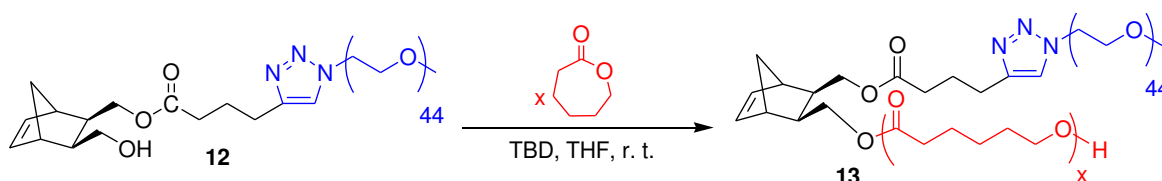


Figure III.21. MALDI-ToF mass spectrum of hydroxyl-functionalized norbornenyl-terminated PEO **12**; matrix: DCTB, NaTFA.

Well-defined NB-functionalized PEO macromonomer **12** with a hydroxyl functionality was then used as an initiator for the ROP of CL.

III.3.2. Synthesis of norbornenyl-functionalized PEO-*b*-PCL

The ROP of CL has been performed at 25 °C in THF with TBD as the catalyst (Scheme III.16) with a [**12**]₀/[CL]₀/[TBD]₀ molar ratio of 1:15:0.34. The resulting PEO-*b*-PCL copolymer **13** was precipitated in cold diethyl ether as a white powder in 80% yield.



Scheme III.16. Synthesis of norbornenyl-functionalized PEO-*b*-PCL copolymer **13** via ‘click’ reaction followed by ROP of CL.

¹H NMR spectrum of **13** showed the concomitant appearance of new peaks related to the protons of PCL at $\delta = 4.00$ - 4.20 ppm (labelled v, Figure III.22), at $\delta = 2.25$ - 2.35 ppm (labelled q, Figure III.22), at $\delta = 1.55$ - 1.75 ppm (labelled r & t, Figure III.22) and at $\delta = 1.35$ - 1.45 ppm (labelled s, Figure III.22). The DP_{n,NMR} of the PCL was calculated from the ¹H NMR spectrum by the comparison of integration areas of the signal indicating to the protons of -CH₂CH₂O- of PCL chains at $\delta = 4.00$ - 4.20 ppm (labelled v, Figure III.22) and protons of -CH=CH- of norbornene entity at $\delta = 6.19$ ppm (labelled a & b, Figure III.22). The experimental DP_{n,NMR} value of 15 is in good agreement with the initial [**11**]/[CL] molar ratio of 1:15.

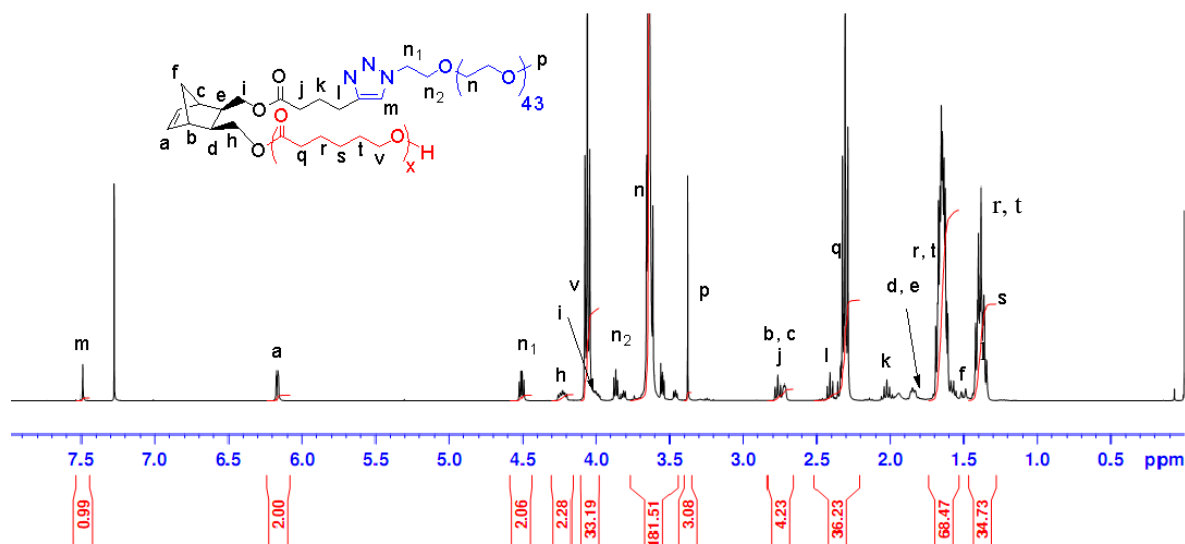


Figure III.22. ¹H NMR spectrum (400 MHz, 25 °C) of norbornenyl-functionalized PEO-*b*-PCL **13**; solvent: CDCl₃.

The SEC trace of purified norbornenyl-functionalized PEO-*b*-PCL **13** shows only one symmetrical peak of narrow distribution (dispersity $D_M = 1.08$) with a shift toward low retention time in comparison with **12** and **10** (Figure III.23). This result shows the successful synthesis of the amphiphilic norbornenyl-functionalized PEO-*b*-PCL copolymer *via* the combination of ‘click’ reaction and ROP.

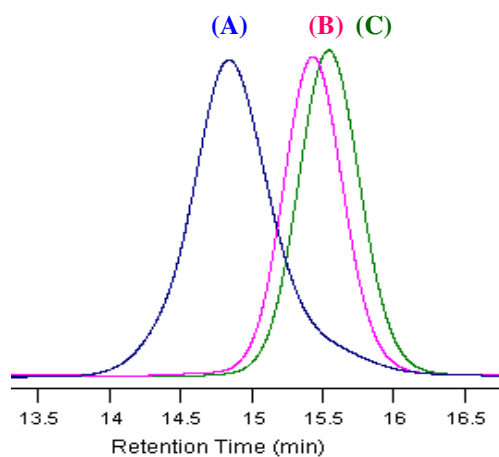


Figure III.23. SEC traces of (A) norbornenyl-functionalized PEO-*b*-PCL **13**, (B) Hydroxyl-functionalized norbornenyl-terminated PEO **12** and (C) PEO-N₃ **10**.

A series of norbornenyl-functionalized PEO-*b*-PCL copolymers with different PCL/PEO molar ratios was next obtained through the ROP of CL from the hydroxyl-functionalized norbornenyl-terminated PEO **12** with an initial $[CL]_0/[12]_0$ molar ratio ranging from 10 to 40 (Table III.2). The $DP_{n,NMR}$ values, calculated from 1H NMR analysis, are similar to $DP_{n,theo}$ and increase with the $[CL]_0/[inimer]_0$ molar ratio.

Table III.2. Norbornenyl-functionalized PEO₄₄-*b*-PCL_x copolymers **13** of different lengths in PCL obtained by ROP of CL in THF at room temperature using TBD as the initiator.

Sample	$[CL]_0/[12]_0/[TBD]_0$	Time (h)	Conv. ^a (%)	$DP_{n,theo}$ ^b	$DP_{n,NMR}$ ^c	$M_{n,NMR}$ ^d g/mol	$M_{n,SEC}$ ^e g/mol	\bar{D}_M ^e
PEO ₄₄ NBPCL ₁₀	10/1/0.65	5	99	10	10	3380	5600	1.08
PEO ₄₄ NBPCL ₁₅	20/1/0.65	5	80	16	15	3950	6300	1.09
PEO ₄₄ NBPCL ₂₅	25/1/0.65	10	99	25	25	5090	8500	1.11
PEO ₄₄ NBPCL ₃₆	40/1/0.65	10	90	36	36	6345	8900	1.20

^a The CL monomer conversions were determined by comparing the peak areas of methylene triplet of PCL at $\delta = 4.00$ -4.20 ppm and the methylene group of CL at $\delta = 4.20$ -4.30 ppm from the 1H NMR spectra of the crude mixture. ^b Calculated from initials $[CL]_0/[12]_0$ ratios and conversions of respective reactions which calculated in ^a. ^c Calculated from 1H NMR spectra by comparing the peaks areas of the norbornene alkene protons at $\delta = 6.19$ ppm and the $-CH_2CH_2O-$ methylene triplet at $\delta = 4.00$ -4.20 ppm; $M_{n,NMR} = (DP_{n,NMR} \times M_{CL}) + (44 \times M_{EO}) + M_{NB \text{ derivatives}}$ with $M_{CL} = 114$ g/mol, $M_{EO} = 44$ g/mol and $M_{NB \text{ derivatives}} = 305$ g/mol. ^d Calculated from $DP_{n,NMR}$ ^c with molar mass of CL unit of 114. ^e Determined by SEC in THF with RI detector, calibrated with linear polystyrene standards.

Furthermore, SEC traces (Figure III.24) showed symmetrical chromatograms, confirming the control of the ROP.

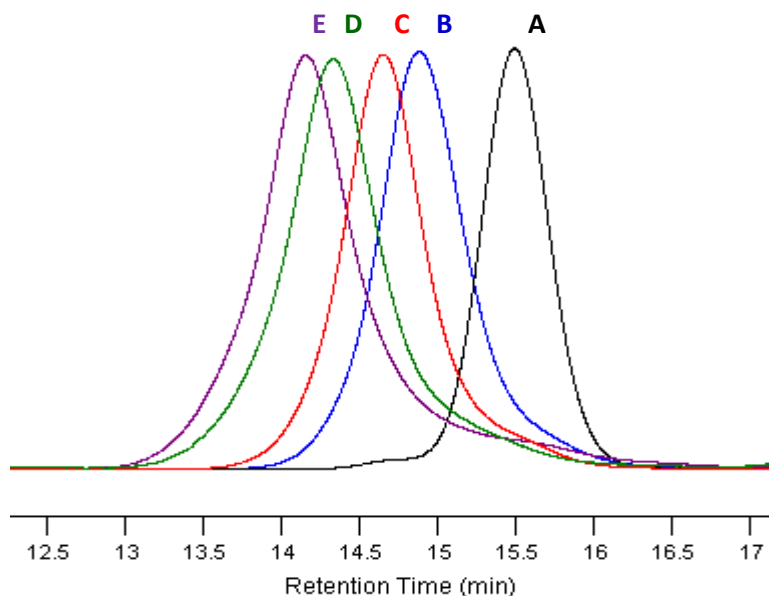


Figure III.24. SEC traces of (A) NBPEO₄₄ **12**, (B) PEO₄₄NBPCL₁₀, (C) PEO₄₄NBPCL₁₅, (D) PEO₄₄NBPCL₂₅ and (E) PEO₄₄NBPCL₃₆

The combination of the click azide-alkyne reaction with ROP was found an efficient and controlled strategy for obtaining a series of well-defined amphiphilic norbornenyl-functionalized PEO-*b*-PCL copolymers. The difficulty of removing water from PEO that hampered to esterification strategies was overcome thanks to the insensitive toward water of the click reaction.

IV. Self-assembling properties of amphiphilic norbornenyl PEO-*b*-PCL copolymers

As shown previously, well-defined amphiphilic norbornenyl PEO-*b*-PCL copolymers have been successfully synthesized by the combination of ‘click’ azide-alkyne reaction followed by ROP of CL. These copolymers containing a hydrophilic PEO block and a hydrophobic PCL block could give rise to self-organization in water. Self-organization of norbornenyl PEO-*b*-PCL copolymers was studied by steady state fluorescence spectroscopy in order to determine critical micellar concentration (CMC). The influence of PCL chain length on CMC values of copolymers has been pointed out. Size distribution and hydrodynamic diameters of micelles formed from a PCL

hydrophobic core and a PEO hydrophilic corona in water have been measured by dynamic light scattering (DLS).

IV.1. Critical micellar concentration (CMC) of copolymers in water

Amphiphilic copolymers can self-organize in water. CMC of an amphiphilic copolymer is the concentration value where the self-organization in micelles begins (Figure IV.1). Above the CMC, micelles and copolymers exist in a dynamic equilibrium.⁵¹

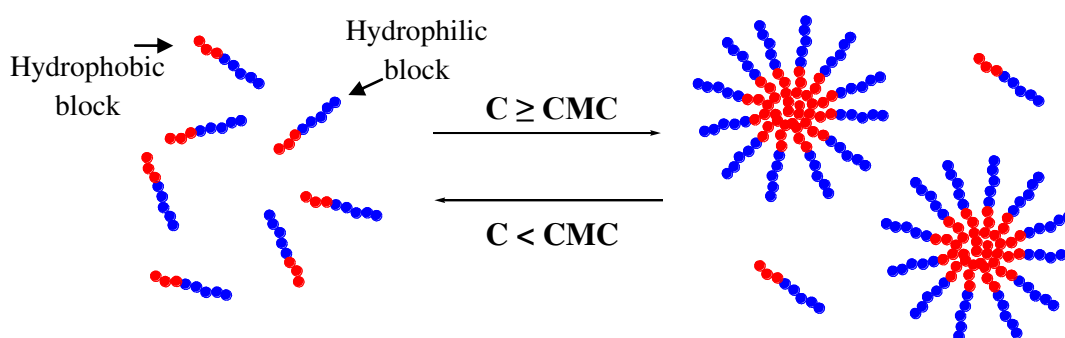


Figure III.25. The self-organization of amphiphilic copolymers in water

The most common used techniques to determine CMC value of amphiphilic copolymer are surface tension measurement, conductimetric measurement, UV-visible spectroscopy, light scattering or fluorescence spectroscopy.⁵²⁻⁵⁴

In our study, the CMC of amphiphilic norbornenyl PEO-*b*-PCL copolymers has been determined by the steady state fluorescence spectroscopy using pyrene as a probe.⁵⁵⁻⁵⁷ Pyrene exhibits different fluorescence behaviors depending on the polarity of its environment. Such changes have been used to determine the CMC.

Four norbornenyl PEO-*b*-PCL copolymers with the same hydrophilic PEO chain length of $DP_n = 44$ and different hydrophobic PCL chain length (10, 15, 25 and 36 in DP_n values of PCL, respectively) were studied by steady state fluorescence spectroscopy in order to determine their CMC. Micellization of copolymers was achieved through a co-solvent evaporation method: Millipore water was added to a solution of copolymers in THF, the mixture was magnetically stirred for 2 hours followed by the evaporation of THF.. These copolymer solutions, with concentrations ranging from 10^{-4} to 5 g/L, were prepared in flasks containing a thin film of pyrene that

generate pyrene concentration in solution of 6.10^{-7} mol/L. These solutions were kept stirring for 24 hours at room temperature to ensure full dissolution. Typical excitation spectra of aqueous solutions of pyrene and norbornenyl PEO-*b*-PCL copolymer at various concentrations are shown in Figure III.26. The change of copolymer concentration on water leads to the change of solution polarity, which was shown as the shift of the first vibronic band of pyrene excitation spectra from 334 nm (I_{334}) to 337.4 nm ($I_{337.4}$) as the lowest to highest copolymers concentration. The distinct shift provides evidence for a transfer of pyrene molecules from a polar environment (non-micellar solution) to an apolar environment (in micelles cores) (Figure III.26).

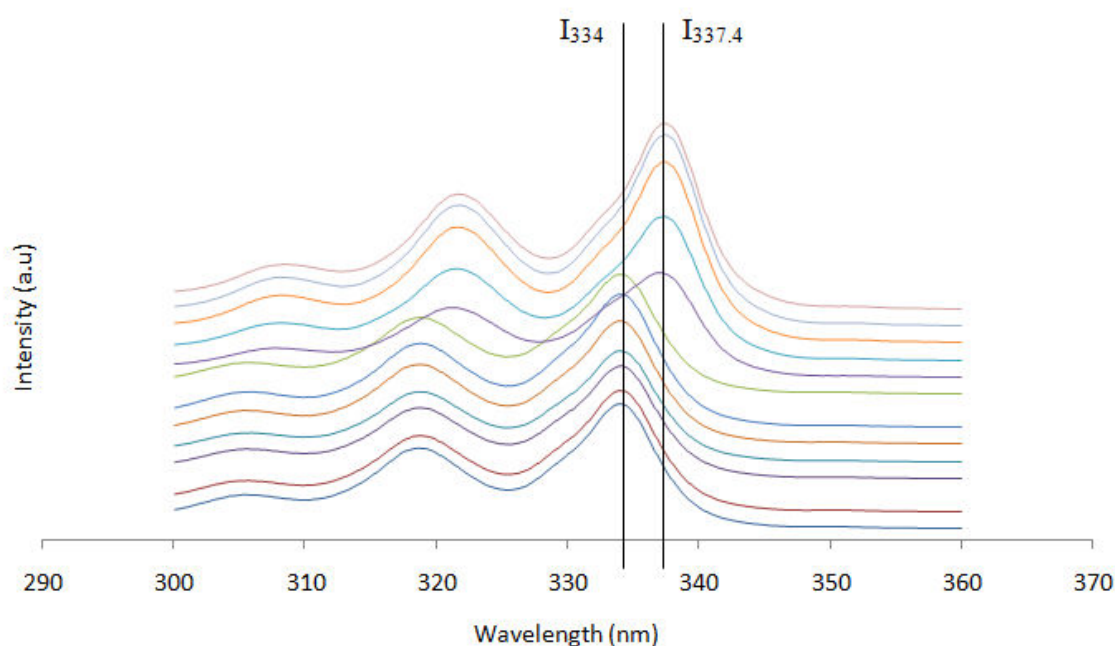


Figure III.26. Excitation spectra pyrene solutions in the presence of norbornenyl-functionalized $\text{PEO}_{44}\text{-}b\text{-PCL}_{10}$ copolymer. From bottom to top, concentration of copolymers ranged from 10^{-4} to 5 g/L

The intensity ratios of the excitation bands at 337.4 nm and 334 nm ($I_{337.4}/I_{334}$) for copolymers bearing PCL block of various lengths are shown in Figure III.27. At low concentration of copolymers in water, a negligible change of $I_{337.4}/I_{334}$ ratio was observed. However, at a certain concentration for each copolymer, the $I_{337.4}/I_{334}$ ratio showed a significant increase, suggesting that pyrene molecules transferred from aqueous medium into hydrophobic medium in core region upon micellar aggregation.

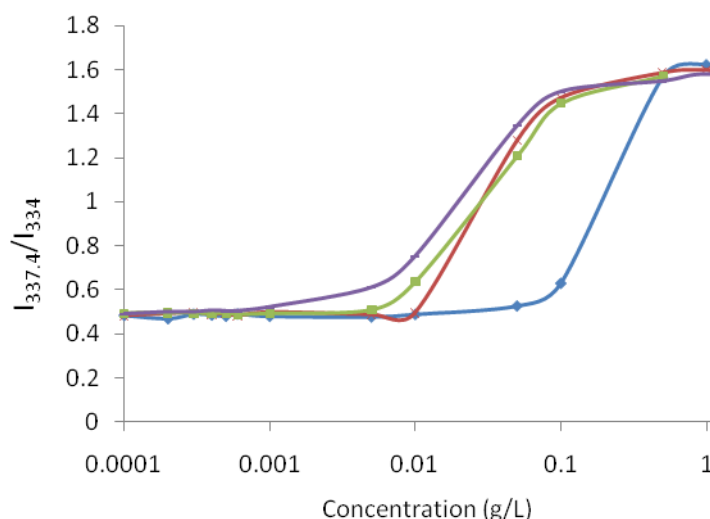


Figure III.27. Fluorescence intensity ratios $I_{337.4}/I_{334}$ (from pyrene excitation spectra) as a function of concentrations for (♦) $\text{PEO}_{44}\text{NB-PCL}_{10}$, (x) $\text{PEO}_{44}\text{NB-PCL}_{15}$, (■) $\text{PEO}_{44}\text{NB-PCL}_{25}$ and (—) $\text{PEO}_{44}\text{NB-PCL}_{36}$.

The CMC values given by the tangent method of copolymers were determined and reported in Table III.3.

Table III.3. CMC values of norbornenyl-functionalized $\text{PEO}_{44}\text{-}b\text{-PCL}_x$ and $\text{PEO}_{44}\text{-}b\text{-PCL}_x$ block copolymers

Run	NB $\text{PEO}_{44}\text{-}b\text{-PCL}_x$	CMC (mg/L)	$\text{PEO}_{44}\text{-}b\text{-PCL}_x^*$	CMC (mg/L)
1	$\text{PEO}_{44}\text{NB-PCL}_{10}$	80	$\text{PEO}_{44}\text{-}b\text{-PCL}_5$	100
2	$\text{PEO}_{44}\text{NB-PCL}_{15}$	8	$\text{PEO}_{44}\text{-}b\text{-PCL}_{19}$	10
3	$\text{PEO}_{44}\text{NB-PCL}_{25}$	6.6	-	-
4	$\text{PEO}_{44}\text{NB-PCL}_{36}$	5.6	$\text{PEO}_{44}\text{-}b\text{-PCL}_{38}$	5

CMC values were observed for all copolymers indicating their self-organization capability in water. The CMC values of norbornenyl PEO-*b*-PCL copolymers in water decrease with the increase of PCL chain length and were in agreement with results in the literature.^{58,59} The CMC values of copolymers are similar to the CMC of PEO-*b*-PCL block copolymers which have the same PEO block length and similar PCL block

* CMC values of $\text{PEO}_{44}\text{-}b\text{-PCL}_x$ diblock copolymers were from previous measurements of our group using same preparation and fluorescence spectroscopy conditions.

length. The results demonstrate that the presence of norbornene, as junction of the two blocks, do not influence the self-assembling properties of the copolymers.

IV.2. Determination of hydrodynamic diameter of micelles via dynamic light scattering (DLS)

The hydrodynamic diameter (D) of micelles obtained from norbornenyl PEO-*b*-PCL copolymers at a concentration of 1 g/L which is above CMC values, were measured by DLS.

PEO-*b*-PCL copolymers have been well known to form micelles in water, where their size is strongly dependent on their preparation method.⁶⁰ The preparation of copolymer solutions was achieved by addition of water to copolymer solution in an organic solvent (co-solvent). The influence of the co-solvent for the micellization process was studied. Organic solvents including THF and acetone were used in order to dissolve NBPEO₄₄-*b*-PCL₁₅ copolymer with concentrations of copolymer in organic solvent equal to 100, 40 and 20 g/L. Hydrodynamic diameters and size distribution (PDI) of micelles formed by this method were measured through DLS and are collected in Table III.4.

Table III.4. Hydrodynamic diameters and size distributions of PEO₄₄NBPCL₁₅ micellization using acetone and THF as co-solvent

Run	Co-solvent	Concentration (g/L)	Z-Ave. ^a (nm)	PDI ^b	D ^h _{number} ^c (nm)
1	Acetone	20	23.3*	0.222	11.49
2	Acetone	40	22.0	0.231	14.09
3	Acetone	100	17.9	0.143	11.28
4	THF	20	22.9	0.248	9.83
5	THF	40	18.4	0.151	10.99
6	THF	100	17.4	0.131	10.62

^a Z-average value

^b Polydispersity (Size distribution)

^c Number average diameter

In comparison to acetone, the use of THF as co-solvent gives rise to lower number average diameters and polydispersity values of micelles in water, indicating the higher uniformity of micelles particles (Table III.4, runs 1-3 versus runs 4-6, respectively). In both case, the increase of copolymer concentration in co-solvent leads to the lower size distribution. Thus, the preparation used in Run 6, Table III.4 is employed to compare

micelles properties prepared from the other copolymers, PEO₄₄NBPCL₁₀, PEO₄₄NBPCL₂₅ and PEO₄₄NBPCL₃₆.

The preparation of copolymer solutions was achieved by addition of THF at a concentration of 100 g/L. Millipore water was added and the remaining THF in the resulting micellar solution was removed to target final concentration of copolymer in water equals to 1 g/L. These solutions were kept stirring for 48 hours for full dissolution. The hydrodynamic diameters and size distribution of micelles were determined through DLS at 25°C (Table III.5).

Table III.5. Hydrodynamic diameters and size distribution of micelles obtained from NBPEO₄₄-*b*-PCL_x copolymers

Run	Copolymers	Z-Ave. ^a (nm)	PDI ^b	D ^h _{number} ^c (nm)
1	PEO ₄₄ NBPCL ₁₀	24.1 [*]	0.393	10.23
2	PEO ₄₄ NBPCL ₁₅	17.4	0.131	10.62
3	PEO ₄₄ NBPCL ₂₅	18.9	0.052	15.09
4	PEO ₄₄ NBPCL ₃₆	31.9	0.115	21.94

^a Z-average value

^b Polydispersity (Size distribution)

^c Number average diameter

^{*} Two populations observed, see Figure III.28

The average hydrodynamic diameters of micelles ranged from 10.23 to 21.94 nm (number average diameters), and increase with the longer hydrophobic PCL chain in copolymers. In case of short PCL chain (Table III.5, run 1), the higher polydispersity value suggested that micelles were aggregated to form bigger particles: such explanation was confirmed by the presence of 2 populations in size distribution by intensity (Figure III.28, A) and a higher Z-average value.

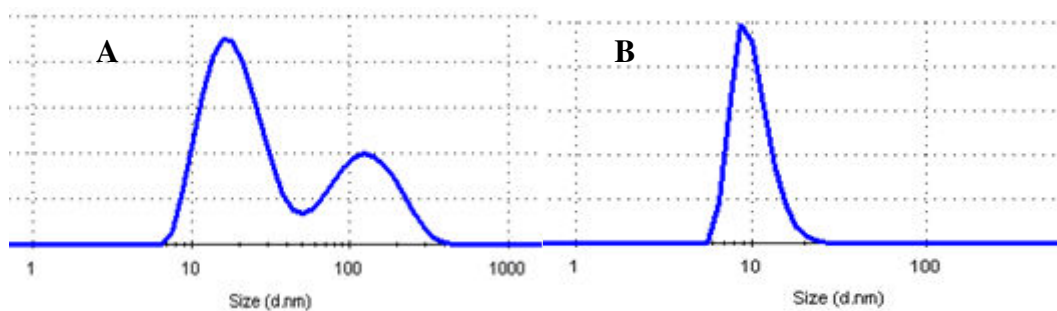
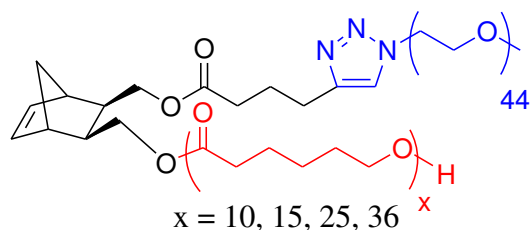


Figure III.28. (A) Intensity and (B) number-average diameters of $\text{PEO}_{44}\text{NB PCL}_{10}$ copolymer

However, for the case of longer PCL chain (Table III.5, runs 2, 3, 4), the size distribution values are low, indicating the high uniformity in size of micellar particles in water.

Conclusions

A series of original norbornenyl-functionalized PEO-*b*-PCL copolymers (Scheme III.17) have been synthesized.



Scheme III.17. Norbornenyl-functionalized PEO-*b*-PCL copolymers synthesized from norbornene anhydride by the combination of ‘click’ reaction followed by ROP of CL.

Three different pathways have been investigated :

- The first one, consisting in esterification of *exo* oxanorbornene dimethanol and carboxylic acid-terminated PEO followed by ROP of CL in the presence of TBD to obtain oxanorbornenyl-functionalized PEO-*b*-PCL copolymer, has led to oxanorbornenyl-functionalized PEO-*b*-PCL copolymer with the presence of undesired residual products with the formation of a PEO chain resulting from the condensation of commercial PEO and carboxylic acid-terminated PEO.
- The second one, consisting in direct esterification of *exo* (oxa)norbornene anhydride and commercially available PEO 2000 g/mol and PEO 750 g/mol followed by reduction of carboxylic acid group to introduce the hydroxyl functionality which will initiate ROP of CL, failed in the reduction of carboxylic acid group of (oxa)norbornenyl-terminated PEO.
- The third one was conducted according to a combination of ‘click’ reaction and ROP of CL. The ‘click’ reaction followed by ROP of CL has proven to be more efficient than the reverse one, as ‘click’ reaction between polymers is not quantitative. The combination of ‘click’ reaction and subsequent ROP of CL has led to norbornenyl-functionalized PEO-*b*-PCL copolymers with controlled PCL lengths and various PEO/PCL ratios. ¹H NMR, MALDI-ToF and SEC analysis

of the resulting copolymers indicated the ‘click’ reaction occurs in a quantitative way and a good control of ROP of CL.

The unsuccessfully first and second strategies can be read as non-quantitative esterification because of the presence of water that are difficult to remove from initial PEO. The traces water in PEO hampered the esterification between PEO and precursors, led to the presence of PEO in excess and undesired residual products. That difficulty was overcome using ‘click’ azide-alkyne reaction that are well-known as insensitive reaction toward water. The combination of ‘click’ azide-alkyne reaction and ROP was found as an efficient and versatile strategy to obtain well-defined norbornenyl-functionalized PEO-*b*-PCL copolymers.

The self-assembling properties of amphiphilic norbornenyl-functionalized PEO-*b*-PCL copolymers in water have been studied. The self-organization of norbornenyl-functionalized PEO-*b*-PCL copolymers in water was observed with CMC values ranging from 0.006 to 0.08 g/L as measured by steady state fluorescence spectroscopy. The size of the micelles measured by DLS are in the range 10.6 to 22.0 nm with narrow polydispersity ($\text{PDI} \leq 0.131$).

References

- ¹ Y. Gnanou, P. Lutz, *Makromol. Chem.* **1989**, *190*, 577-588
- ² C. Loubat, S. Soulier, B. Boutevin, *Polym. Bull.* **2001**, *45*, 487-494
- ³ L. M. Campos, K. L. Killops, R. Sakai, J. M. J. Paulusse, D. Damiron, E. Drockenmuller, B. W. Messmore, C. J. Hawker, *Macromolecules* **2008**, *41*, 7063-7070
- ⁴ K. L. Killops, L. M. Campos and C. J. Hawker, *J. Am. Chem. Soc.* **2008**, *130*, 5062-5064
- ⁵ C. C. Lin, C. S. Ki, H. Shih, *J. App. Polym. Sci.* **2015**, DOI: 10.1002/App.41563
- ⁶ C. W. Bielawski, R. H. Grubbs, *Prog. Polym. Sci.* **2007**, *32*, 1-29
- ⁷ V. Lapinte, L. Fontaine, V. Montembault, I. Campistron, D. Reyx, *J. Mol. Catal. A: Chem.* **2002**, *190*, 117-129
- ⁸ C. Cheng, K. Qi, E. Khoshdel, K. L. Wooley, *J. Am. Chem. Soc.* **2006**, *128*, 6808-6809
- ⁹ Cheng, E. Khoshdel, K. L. Wooley, *Nano. Lett.* **2006**, *6*, 1741-1746
- ¹⁰ A. Nystrom, M. Malkoch, I. Furo, D. Nystrom, K. Unal, P. Antoni, G. Vamvounis, C. Hawker, K. Wooley, E. Malmström, A. Hult, *Macromolecules* **2006**, *39*, 7241-7249
- ¹¹ J. Ma, C. Cheng, K. L. Wooley, *Aust. J. Chem.* **2009**, *62*, 1507-1519
- ¹² J. O. Zou, G. Jafr, E. Themistou, Y. Yap, Z. A. P. Wintrob, P. Alexandridis, A. C. Ceacareanu and C. Cheng, *Chem. Commun.* **2011**, *47*, 4493-4495
- ¹³ J. B. Matson, R. H. Grubbs, *J. Am. Chem. Soc.* **2008**, *130*, 6731-6733
- ¹⁴ G. Morandi, G. Mantovani, V. Montembault, D.M. Haddleton, L. Fontaine, *New J. Chem.* **2007**, *31*, 1826-1829
- ¹⁵ I. Czelusniak, E. Khosravi, A.M. Kenwright, C.W.G. Ansell, *Macromolecules* **2007**, *40*, 1444-1452
- ¹⁶ M. Xie, J. Dang, H. Han, W. Wang, J. Liu, X. He, Y. Zhang, *Macromolecules* **2008**, *41*, 9004-9010
- ¹⁷ D. Le, V. Montembault, J. C. Soutif, M. Rutnakornpituk, L. Fontaine, *Macromolecules* **2010**, *43*, 5611-5617
- ¹⁸ A. B. Lowe, *Polym. Chem.* **2014**, *5*, 4820-4870
- ¹⁹ B. H. Northrop, R. N. Coffey, *J. Am. Chem. Soc.* **2012**, *134*, 13804-13817
- ²⁰ C. N. Walker, J. M. Sarapas, V. Kung, A. L. Hall, G. N. Tew, *ACS Macro Letter* **2014**, *3*, 453-457
- ²¹ M. M. Stamenović, P. Espeel, W. V. Camp, P. E. Du Prez, *Macromolecules* **2011**, *44*, 5619-5630
- ²² Q. Fu, J. Liu, W. Shi, *Prog. Org. Coat.* **2008**, *63*, 100-109

- ²³ S. Piog  , G. Morandi, S. Legoupy, V. Montembault, S. Pascual, L. Fontaine, *Macromolecules* **2008**, *41*, 9595-9601
- ²⁴ V. H  ro  uez, Y. Gnanou, M. Fontanille, *Macromol. Rapid Commun.* **1996**, *17*, 137-142
- ²⁵ V. H  ro  uez, S. Breunig, Y. Gnanou, M. Fontanille, *Macromolecules* **1996**, *29*, 4459-4464
- ²⁶ K. F. Castner, N. Calderon, *J. Mol. Catal.* **1982**, *15*, 47-59
- ²⁷ N. Seehof, S. Grutke, W. Risse, *Macromolecules* **1993**, *26*, 695-700
- ²⁸ P. S. Wolfe, K. B. Wagener, *Macromolecules* **1999**, *32*, 7961-7967
- ²⁹ A. Iyer, K. Mody, B. Jha, *Enzyme and Microbial Technology* **2006**, *38*, 220-222
- ³⁰ G. M. T. Calazans, R. C. Lima, F. P. De Fran  a, C. E. Lopes, *Int. J. Biol. Macromol.* **2000**, *27*, 245-247
- ³¹ M. M. Amiji, *Biomaterials* **1995**, *16*, 593-599
- ³² B. N. Manjula, A. Malavalli, P. K. Smithi, N. L. Chan, A. Arnone, *J. Biol. Chem.* **2000**, *275*, 5527-5534
- ³³ M. Labet, W. Thielemans, *Chem. Soc. Rev.* **2009**, *38*, 3484-3504
- ³⁴ V. R. Sinha, K. Bansal, R. Kaushik, R. Kumria and A. Trehan, *Int. J. Pharm.* **2004**, *278*, 1-23
- ³⁵ R. Chandra and R. Rustgi, *Prog. Polym. Sci.* **1998**, *23*, 1273-1335
- ³⁶ C. X. F. Lam, S. H. Teoh, D. W. Hutmacher, *Polym. Int.* **2007**, *56*, 718-728
- ³⁷ A. Khanna, Y. Sudha, S. Pillai and S. Rath, *J. Mol. Model.* **2008**, *14*, 367-374
- ³⁸ X. Zhu, M. Fryd, B. B. Wayland, *Polymer* **2014**, *55*, 1467-1473
- ³⁹ X. Zhu, V. D. Sharma, M. Fryd, M. A. Ilies, B. B. Wayland, *Polymer* **2013**, *54*, 2879-2886
- ⁴⁰ X. Zhu, M. Fryd, B. D. Tran, M. A. Ilies, B. B. Wayland, *Macromolecules* **2012**, *45*, 660-665
- ⁴¹ J. Das, T. Vu, D. N. Harris, M. L. Ogletree, *J. Med. Chem.* **1988**, *31*, 930-935
- ⁴² S. Hou, L. K. McCauley, P. X. Ma, *Macromol. Biosci.* **2007**, *7*, 620-628
- ⁴³ D. Le, V. Montembault, S. Pascual, S. Legoupy, L. Fontaine, *Macromolecules* **2012**, *45*, 7758-7769
- ⁴⁴ B. G. G. Lohmeijer, R. C. Pratt, F. Leibfarth, J. W. Logan, D. A. Long, A. P. Dove, F. Nederberg, J. Choi, C. Wade, R. M. Waymouth, J. L. Hedrick, *Macromolecules* **2006**, *39*, 8574-8583
- ⁴⁵ K. Soai, S. Yokoyama, K. Mochida, *Synthesis* **1987**, 647 - 648

- ⁴⁶ H. J. Zhu, C. U. Pittman Jr., *Synt. Commun.* **2003**, 33, 1733-1750
- ⁴⁷ H. Gao, K. Matyjaszewski, *J. Am. Chem. Soc.* **2007**, 129, 6633-6639
- ⁴⁸ L. Balas, B. Jousseau, B. Langwest, *Tetrahedron* **1989**, 30, 4525-4527
- ⁴⁹ T. T. T. N'Guyen, H. T. T. Duong, J. Basuki, V. Montembault, S. Pascual, C. Guibert, J. Fresnais, C. Boyer, M. R. Whittaker, T. P. Davis, L. Fontaine, *Angew. Chem. Int. Ed.* **2013**, 52, 14152-14156
- ⁵⁰ H. Gao, K. Matyjaszewski, *Macromolecules* **2006**, 39, 4960-4965
- ⁵¹ P. Alexandridis, B. Lindman, *Amphiphilic block copolymers - Self-assembly and applications*, 1st Ed., Elsevier, **2000**
- ⁵² G. Riess, *Prog. Polym. Sci.* **2003**, 28, 1107-1170
- ⁵³ I. Astafieva, X. F. Zhong, A. Eisenberg, *Macromolecules* **1993**, 26, 7339-7352
- ⁵⁴ C. Zhao, M. A. Winnick, G. Riess, M. D. Croucher, *Langmuir* **1990**, 6, 514-516
- ⁵⁵ K. P. Ananthapadmanabhan, E. D. Goddard, N. J. Turroand, P. L. Kuo, *Langmuir* **1985**, 1, 352-355
- ⁵⁶ S. Piogé, L. Fontaine, C. Gaillard, E. Nicol, S. Pascual, *Macromolecules* **2009**, 42, 4262-4272
- ⁵⁷ D. Le, V. Montembault, S. Pascual, F. Collette, V. Héroguez, L. Fontaine, *Polym. Chem.* **2013**, 4, 2168-2173
- ⁵⁸ A. L. Glover, S. M. Nikles, J. A. Nikles, C. S. Brazel, D. E. Nikles, *Langmuir* **2012**, 28, 10653-10660
- ⁵⁹ W. Xie, W. Zhu, Z. Shen, *Polymer* **2007**, 48, 6791-6798
- ⁶⁰ P. Vangeyte, S. Gautier, R. Jérôme, *Coll. Surf. A* **2004**, 242, 203-211

Materials

Prior to use, poly(ethylene oxide) monomethyl ethers (mPEG) 750 ($M_{n,NMR} = 752$ g/mol, Aldrich), 2000 ($M_{n,NMR} = 2010$ g/mol, Aldrich) were azeotropic distilled at 130 °C for 3 h under nitrogen atmosphere to remove excess water. 1,5,7-triazabicyclo[4.4.0]dec-5-ene (TBD, Aldrich 98%), 4-(*N,N*-dimethylamino)pyridine (DMAP, Aldrich, 99%), 5-hexynoic acid (Aldrich, 97%), 5-Norbornene-2-exo,3-exo-dimethanol (Aldrich, 97%), acetic acid (Acros, 99.5%), copper bromide (CuBr, Aldrich, 99.999%), cyclohexane (Pro labo, 99.8%), dichloromethane (DCM, Aldrich, 99%), diethyl ether (Pro labo, 99.8%), disodium ethylenediaminetetraacetic acid (EDTA, Aldrich, 99%), ethyl chloroformate (Aldrich, 97%), ethyl acetate (Pro labo, 99.8%), furan (Acros, 99%), hydrochloric acid (HCl, Aldrich, 37%), lithium aluminiumhydride ($LiAlH_4$, Aldrich, 97.0%), magnesium sulfate ($MgSO_4$, Fisher chemical), maleic anhydride (Aldrich, 99%), methanesulfonyl chloride ($MsCl$, Fluka, 99%), methanol (MeOH, Aldrich, 99.8%) *N,N,N',N'',N'''*-pentamethyldiethylenetriamine (PMDETA, Aldrich, 99%), *N,N*-dimethylformamide (DMF, Aldrich, 99%), *N,N'*-dicyclohexylcarbodiimide (DCC, Acros, 99%), silicagel for column chromatography (Kieselgel 60, 230-400 mesh Merck), sodium azide (NaN_3 , Aldrich, 99.5%), sodium borohydride ($NaBH_4$, Acros, 99%), sodium chloride ($NaCl$, Fisher chemical), sodium sulfate (Na_2SO_4 , Sigma-Aldrich, 98%), succinic anhydride (Aldrich, 99%), anhydrous tetrahydrofuran (THF, Aldrich, 99.9%), toluene (99%), triethylamine (TEA, Aldrich, 99.9%), ϵ -caprolactone (CL, Aldrich 97%) were purchased from commercial sources and used without further purification.

Characterization

NMR spectra were recorded on a Bruker Avance 400 (200 MHz for 1H and 50 MHz for ^{13}C) or Bruker AC-400 (400 MHz for 1H and 100 MHz for ^{13}C). Chemical shifts are reported in ppm relative to the deuterated solvent resonances.

Molar masses and dispersity were measured using size exclusion chromatography (SEC) on a system equipped with a SpectraSYSTEM AS1000 autosampler, with a Guard column (Polymer Laboratories, PL gel 5 μm Guard column, 50 x 7.5 mm) followed by two columns (Polymer Laboratories, 2 PL gel 5 μm MIXED-D columns, 2 x 300 x 7.5) and with a SpectraSYSTEM RI-150 detector. The eluent used was tetrahydrofuran (THF) at a flow rate of 1 mL.min⁻¹ at 35°C. Polystyrene standards (580 - 4.83 x 10⁵ g.mol⁻¹) were used to calibrate the SEC.

High resolution mass spectra were recorded on Waters-Micromass GCT Premier spectrometers.

MALDI-ToF MS analysis were realized on a Bruker Biflex III using 2-[(2E)-3-(4-tert-butylphenyl)-2-methylprop-2-enylidene]malononitrile (DCTB) as the matrix.

Dynamic light scattering was performed with a Malvern apparatus (NanoZS ZEN3600) equipped with a 4 mW He – Ne laser (emitting vertically polarized light at $\lambda = 632.8$ nm) and a thermostat bath controller at 20 °C. The autocorrelation functions were analyzed in terms of relaxation time (τ) distribution. The method of the cumulants was generally used to analyze DLS results, while size

distribution histograms were obtained by the CONTIN method. The polydispersity index (PDI) of the micelles was estimated from the Γ_2/Γ_1^2 ratio in which represents the first and second cumulant, respectively. Measurement were made at a angle detection of 173° using a copolymer concentration of 1 g/L.

DLS samples preparation

Prior to use, sample solutions were prepared using Millipore (18.2 M Ω) water in a hood that was kept dust-free by an air circulation system. The copolymer sample was weighed into a dust-free sample vial and was dissolved in THF using a copolymer concentration of 100 g/L. Afterwards, Millipore water was added in order to obtain a concentration of macromonomers in water of 1 g/L. This solution was kept stirring for 2 hours at room temperature followed by free evaporation of THF for 24 hours. They were then filtered through 0.2 μm pore size Anotop syringe filters into a disposable PS vessel for dynamic light scattering measurements.

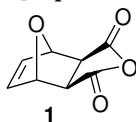
Fluorescence measurements were performed using a Horiba-Jobin Yvon fluorescence spectrophotometer in the right-angle geometry. For the fluorescence measurements, 3 mL of each sample were placed in a 1 cm^2 quartz cell. The excitation spectra were recorded using the wavelength ranging from 300 to 360 nm.

CMC samples preparation

Prior to use, sample solutions were prepared using Millipore (18.2 M Ω) water in a hood that was kept dust-free by an air circulation system. The copolymer sample was weighed into a dust-free sample vial and was dissolved in THF using a copolymer concentration of 100 g/L. Afterwards, Millipore water was added in order to obtain a concentration of macromonomers in water of 5 g/L. This solution was kept stirring for 2 hours at room temperature followed by free evaporation of THF for 24 hours. They were then diluted by addition of Millipore water to obtain final concentrations ranging from 10^{-4} to 5 g/L. The solutions were then filtered through 0.45 μm pore size Anotop syringe filters into previously prepared vials containing a thin film of pyrene in order to target the concentration of pyrene equals to 6×10^{-7} mol/L. This solution was kept stirring for 48 hours for full dissolution of pyrene before CMC measurement.

Synthesis of precursors

Synthesis of *exo* 7-Oxabicyclo[2.2.1]hept-5-ene-2,3-dicarboxylic anhydride **1**

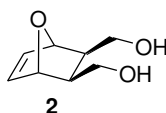


A 50-mL round-bottom flask was charged with maleic anhydride (5 g, 0.051 mol). 30 mL of toluene were added and the reaction flask was swirled until the maleic anhydride completely dissolved. Furan (5.0 mL, 0.069 mol) was added and the resulting solution was stirred for 7 days at room temperature. The product was collected by suction filtration and washed with toluene. Yield: 80%

^1H NMR (200 MHz, CDCl_3), δ (ppm): 6.56 (s, 2H, HC=), 5.43 (s, 2H, CHOCH), 3.17 (s, 2H, CHC=O).

^{13}C NMR (50 MHz, CDCl_3), δ (ppm): 170.5 (C=O), 137.3 (C=C), 82.1 (CHOCH), 48.3 (CHC=O).

Synthesis of *exo* oxanorbornene dimethanol **2**



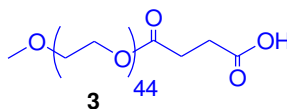
LiAlH_4 (1.096 g, 28.8 mmol) was suspended in 25 mL of anhydrous tetrahydrofuran (THF) in 250-mL round bottom flask equipped with magnetic stirrer bar and rubber septum, the solution was cooled to 0°C . **1** (3.0 g, 18 mmol) in 30 mL of anhydrous THF was added dropwise (over 30 minutes) under N_2 . The suspension solution was stirred for 24 h at 25°C . The solution was then cooled to 0°C , and 15 mL of saturated Na_2SO_4 solution was added. 40 mL diethyl ether was added into the mixture, the suspension was filtered and washed with 3x10 mL of DCM and 3x15 mL of diethyl ether. The organic solution was evaporated and the residue was dissolved in 40 mL of DCM, dried over MgSO_4 , filtered and evaporated to give a transparent oil. The residue was purified by chromatography on SiO_2 using 2/5 cyclohexane/AcOEt. Yield: 70%

^1H NMR (400 MHz, CDCl_3), δ (ppm): 6.41 (s, 2H, HC=), 4.69 (s, 2H, CHOCH), 3.83 (m, 4H, $\text{CH}_2\text{-OH}$), 1.98 (m, 2H, $\text{CH-CH}_2\text{OH}$)

^{13}C NMR (50 MHz, CDCl_3), δ (ppm): 135.48 ($=\text{CH-}$), 81.06 (CHOCH), 62.29 (CH_2OH), 42.27 ($\text{CH-CH}_2\text{OH}$).

HRMS (CI- H^+). Calc for $\text{C}_8\text{H}_{12}\text{O}_3 + \text{H}^+$: 157.0859; Found: 157.0786.

Synthesis of the carboxylic acid-terminated PEO 3

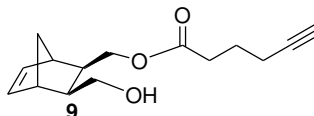


Poly(ethylene oxide) monomethyl ether 2000 g/mol (PEO-OH, 10 g, 5 mmol), succinic anhydride (1.07 g, 10 mmol) and 4-(*N,N*-dimethylamino)pyridine (DMAP, 1.44 g, 12 mmol) were dissolved in 100 mL of anhydrous THF in 250-mL round bottom flask equipped with magnetic stirrer and the mixture was cooled to 0 °C. Triethylamine (TEA 1.05 mL, 7.5 mmol) was entered and the resulting solution was kept stirring for 24 hours at 50 °C. THF was removed by rotary evaporator, the residue was dissolved in 20 mL of DCM and precipitated in 300 mL of cold diethyl ether. The product was filtered and dried under vacuum overnight. Yield: 93%.

¹H NMR (400 MHz, CDCl₃), δ (ppm): 4.24 (m, 2H, CH₂-OCO); 3.60 - 3.80 (m, 174H, CH₂); 3.38 (s, 3H, CH₃O), 2.64 (m, 4H, COCH₂CH₂COOH)

¹³C NMR (100 MHz, CDCl₃), δ (ppm): 174.3 (COOH), 173.4 (COO-), 71.9 (CH₂-O-CH₃), 70.6 (-CH₂-), 63.6 (CH₂-OCO), 59.0 (CH₃), 30.9 (CH₂-COOH), 29.4 (OCO-CH₂CH₂)

Synthesis of alkynyl-functionalized norbornene norbornene 9



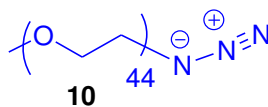
2' (0.5 g, 3.20 mmol) was dissolved in 5 mL of dried dichloromethane (DCM) in 25 mL round bottom flask charged with magnetic stirrer and rubber septum. 5-Hexynoic acid (0.358 mL, 3.25 mmol), *N,N'*-dicyclohexylcarbodiimide (DCC, 0.735 g, 3.56 mmol) and DMAP (0.0238 g, 0.195 mmol) were dissolved in 10 mL of dried DCM then added dropwise in over 10 minutes at 0 °C under N₂, the resulting mixture was kept stirring for 24 hours at room temperature. The suspension was filtered, the organic phase was washed with 2x15 mL of HCl 1N and 2x10 mL of saturated NaCl solution. The organic phase was dried over MgSO₄, DCM was removed by rotary evaporator. The product was purified by chromatography on SiO₂ using 5/1 of cyclohexane/ethyl acetate as the eluent. Yield 45%.

¹H NMR (400 MHz, CDCl₃), δ (ppm): 6.18 (m, 2H, CH=CH), 4.27, 4.06 (m, 2H, -CH₂-OCO); 3.58 - 3.84 (m, 2H, CH₂OH); 2.70, 2.80 (s, 2H, CHCH₂CH), 2.48 (m, 2H, CH₂C≡CH), 2.27 (m, 2H, OCOCH₂CH₂), 1.98 (m, 1H, C≡CH), 1.85 (m, 2H, OCOCH₂CH₂), 1.75, 1.80 (OCH₂CHCHCH₂OH), 1.32, 1.48 (m, 2H, CHCH₂CH)

¹³C NMR (100 MHz, CDCl₃), δ (ppm): 171.9 (COO-), 136.4, 135.8 (CH=CH), 82.10 (C≡CH), 68.1 (C≡CH), 64.8 (CH₂-OCO), 62.5 (-CH₂-OH), 43.6, 43.3 (CH-CH₂-CH), 42.2 (CHCH₂OCO), 41.4 (CHCH₂OH), 38.5 (CHCH₂CH), 31.8 (CH₂COO), 22.4 (CH₂CH₂COO), 16.65 (CH₂C≡CH)

HRMS (CI-H⁺). Calc for C₈H₁₂O₃ + H⁺: 249.1488; Found: 249.1490.

Synthesis of azido-terminated PEO 10



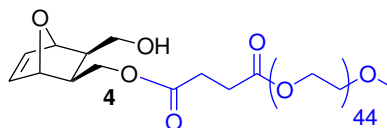
PEO-OH 2000 g/mol (10 g, 5 mmol) and TEA (4.2 mL, 31 mmol) were dissolved in 50 mL of DCM in 100-mL of round bottom flask charged with magnetic stirrer bar. The mixture was cooled to 0 °C. A solution of methanesulfonyl chloride (5.7 g, 50 mmol) in 10 mL DCM was added dropwise (over 30 min). The reaction mixture was then stirred for 24 h at room temperature. The reacting mixture was washed with 50 mL of HCl solution (1M) and 50 mL of distilled water. The organic layer was dried over MgSO₄ and precipitated into dried diethyl ether. Mesylated-PEO was obtained as a white powder. Thus, obtained mesylated-PEO was dissolved in 40 mL of *N,N*-dimethylformamide (DMF) and sodium azide (NaN₃) (3.25 g, 50 mmol) was added to this solution. After stirring overnight at room temperature, DCM was added and the organic layer was washed for another three times with water and dried over MgSO₄. The organic phase was evaporated and precipitated in diethyl ether. The obtained PEO-N₃ was dried for 24 h in a vacuum oven. Yield: 90%.

¹H NMR (200 MHz, CDCl₃), δ (ppm): 3.60-3.80 (m, 176H, CH₂); 3.38 (s, 3H, CH₃).

¹³C NMR (50 MHz, CDCl₃), δ (ppm): 71.9 (CH₂-O-CH₃) ; 70.5 (-CH₂-) ; 70.0 (CH₂-CH₂-N₃); 59.0 (CH₃) ; 50.6 (CH₂-N₃).

Synthesis of macromonomers

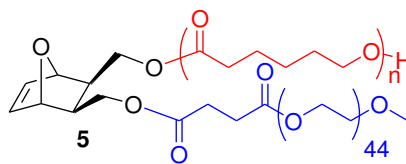
Synthesis of oxanorbornenyl-terminated PEO macromonomer 4



2 (0.156 g, 1 mmol) was dissolved in 20 mL of anhydrous DCM in a 100-mL magnetic stirrer bar charged round bottom flask. **3** (0.525 g, 0.25 mmol), DCC (0.077 g, 0.373 mmol) and DMAP (0.015 g, 0.123 mmol) were dissolved in 15 mL of anhydrous DCM and added dropwise into **2** solution. The mixture was kept stirring at room temperature for 168 hours. The mixture was filtered, the organic solution was washed with 2x30 mL of HCl 1N and 2x30 mL of saturated NaCl solution. The organic phase was dried over MgSO₄ and filtered. DCM was removed by rotary evaporation, the residue was dissolved in 3 mL of DCM and precipitated in 50 mL of cold diethyl ether. The product was filtered and dried under vacuum overnight. Conversion: 66 %.

¹H NMR (400 MHz, CDCl₃), δ (ppm): 6.41 (m, 2H, CH=CH), 4.90 (s, 1H, CH-O), 4.80 (s, 1H, CH-O), 4.25 (m, 2H, CH₂-OCO), 4.05 (t, 2H, CHCH₂OCO), 3.80 (m, 2H, CHCH₂OH), 3.45 – 3.75 (m, 174H, CH₂); 3.38 (s, 3H, CH₃O), 2.64 (m, 4H, COCH₂CH₂CO), 1.96 (m, 1H, CHCH₂OCO), 1.90 (m, 1H, CHCH₂OH).

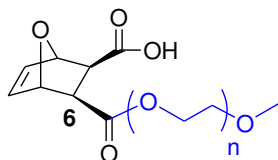
Synthesis of oxanorborneny.-functionalized PEO-b-PCL macromonomers



4 (2.1 g, 1 mmol) and 1,5,7-triazabicyclo[4,4,0]dec-5-ene (TBD, 0.0696 g, 0.5 mmol) were charged into a 25-mL dried Schlenk tube charged with magnetic stirrer and rubber septum under N₂ in glove box. 9 mL of dried THF was added to dissolve the mixture in Schlenk tube under N₂ at 35 °C. ϵ -caprolactone (CL, 3.00 mL, 30 mmol) was added, the resulting mixture was kept stirring for 3 hours. Acetic acid (1 mL) was added to quench TBD, THF was removed by rotary evaporator, the residue was dissolved in 10 mL of DCM and precipitated in 200 mL of cold diethyl ether. The mixture was filtered and resulting product was dried under vacuum overnight. Conversion: 82%

¹H NMR (400 MHz, CDCl₃), δ (ppm): 6.41 (m, 2H, CH=CH), 4.62 (m, 2H, CH-O-CH), 4.00-4.20 (m, 78H, PCL; -CH₂-OCO); 3.60–3.80 (m, 174H, PEO; CH₂); 3.38 (s, 3H, CH₃O), 2.64 (m, 4H, COCH₂CH₂CO), 2.25-2.35 (m, 78H, PCL; O-COCH₂); 1.96 (m, 2H, CHCH₂OCO), 1.55–1.75 (m, 156H, PCL; CH₂CH₂CH₂-O-CO), 1.35–1.45 (m, 78H, CH₂CH₂CH₂-O-CO).

Synthesis of oxanorbornenyl-terminated PEO 6

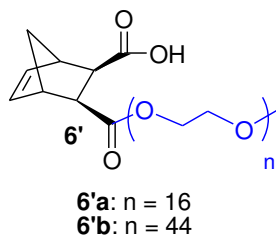


6a: n = 16
6b: n = 44

Exo oxanorbornene anhydride **1** (0.249 g, 1.5 mmol); PEO-OH 2000 g/mol (2.01 g, 1 mmol) and DMAP (0.061 g, 0.5 mmol) were dissolved in 15 mL of dried DCM in a 50 mL round bottom flask equipped with magnetic stirrer bar and rubber septum. TEA (0.121 g, 167 μ L, 1.2 mmol) was added under N₂ at 25 °C and the resulting solution was kept stirring for 24 hours at 25 °C. DCM was removed by rotary evaporator, the residue was dissolved in 5 mL of DCM and precipitated in 100 mL of cold diethyl ether. The mixture was filtered and the resulting product was dried under vacuum overnight. Yield: 85%.

¹H NMR (400 MHz, CDCl₃), δ (ppm): 6.41 (m, 2H, CH=CH), 5.20, 5.35 (s, 2H, CH-O-CH), 4.48, 4.14 (m, 2H, -CH₂-OCO); 3.60-3.80 (m, 174H (**6a**); 62H (**6b**), CH₂); 3.38 (s, 3H, CH₃O), 2.64 (m, 2H, HOOCCHCHCOO).

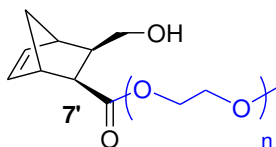
Synthesis of norbornene-terminated PEO 6'



Exo norbornene anhydride **1'** (0.246 g, 1.5 mmol); PEO 750 g/mol (0.752 g, 1 mmol) and DMAP (0.061 g, 0.5 mmol) were dissolved in 15 mL of dried DCM in a 25 mL round bottom flask equipped with magnetic stirrer bar and rubber septum. TEA (167 μ L, 1.2 mmol) was added under N₂ at 25 °C and the resulting solution was kept stirring for 24 hours at 25 °C. DCM was removed by rotary evaporator, the residue was dissolved in 5 mL of DCM and precipitated in 100 mL of cold diethyl ether. The mixture was filtered and the resulting product was dried under vacuum overnight. Yield: 90%

¹H NMR (400 MHz, CDCl₃), δ (ppm): 6.18 (m, 2H, CH=CH), 4.48, 4.14 (m, 2H, -CH₂-OCO); 3.60- 3.80 (m, 174H (**6'a**); 62H (**6'b**), CH₂); 3.38 (s, 3H, CH₃O), 3.02, 3.15 (s, 2H, CHCH₂CH), 2.64 (m, 2H, HOOCCHCHCOO), 2.20, 1.51 (m, 2H, CHCH₂CH).

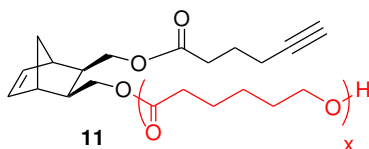
Synthesis of hydroxyl-functionalized norbornenyl-terminated PEO 7'



Norbornene-terminated PEO **6'** (0.9 g, 1 mmol) and ethyl chloroformate (77.4 μ L, 1 eq) were dissolved in 5 mL of dried THF in a 10 mL round bottom flask equipped with a magnetic stirrer and a rubber septum under N₂. The solution was cooled to -8 °C. TEA (139 μ L, 1 mmol) was added dropwise slowly into the solution. The solution was kept stirring at -8 °C for 30 minutes. The reaction mixture was then filtered and washed 3 x 5 mL of dried THF. NaBH₄ (0.038 g, 1 mmol) was added to the filtrated solution at 0 °C and 1 mL of MeOH was added dropwise to the mixture. 3 mL of HCl 1N was added dropwise into the mixture to quench NaBH₄. The solution was extracted with 3 x 30 mL of DCM and the combined organic phase was evaporated under reduced pressure to remove organic solvents.

¹H NMR (400 MHz, CDCl₃), δ (ppm): 6.18 (m, 2H, CH=CH), 4.48, 4.14 (m, 2H, -CH₂-OCO); 3.60- 3.80 (m, 62H, CH₂); 3.38 (s, 3H, CH₃O), 2.64 (m, 2H, HOOCCHCHCOO), 2.20, 1.51 (m, 2H, CHCH₂CH), 1.85 (m, 1H, CH=CHCHCHCH₂OH).

Synthesis of alkynyl-functionalized norbornenyl-terminated PCL 11

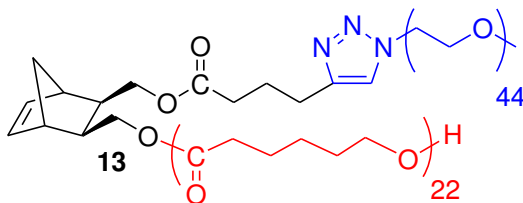


9 (0.1 g, 0.403 mmol) and TBD (0.0191 g, 0.137 mmol) were charged into a dried Schlenk tube with magnetic stirrer and rubber septum under N₂ in glove box. 2.76 mL of dried THF was added to dissolve the mixture in Schlenk tube under N₂ at 25 °C. CL (0.9 mL, 8.12 mmol) was added, the resulting mixture was kept stirring for 5 hours. Acetic acid (1 mL) was added to quench TBD, THF was removed by rotary evaporator, the residue was dissolved in 2 mL of DCM and precipitated in 30 mL of cold diethyl ether. The mixture was filtered and resulting product was dried under vacuum overnight. Yield: 75%

¹H NMR (400 MHz, CDCl₃), δ (ppm): 6.18 (m, 2H, CH=CH), 4.25 (m, 2H, CHCH₂-OPCL), 4.00 - 4.20 (m, 44H, PCL; -CH₂-OCO); 3.65 (m, 4H, PEO; CHCH₂OCO); 2.72 (s, 2H, CHCH₂CH), 2.45 (m, 2H, CH₂(CH₂)₂C≡CH), 2.25 - 2.35 (m, 46H, PCL; O-COCH₂; CH₂C≡CH); 1.98 (m, 1H, C≡CH), 1.85 (m, 4H, COOCH₂CHCH₂COO; CH₂CH₂CH₂C≡CH), 1.55 - 1.75 (m, 88H, PCL; CH₂CH₂CH₂-O-CO), 1.35 - 1.45 (m, 44H, CH₂CH₂CH₂-O-CO).

SEC: M_n = 4750 g/mol; Đ_M = 1.25

Synthesis of norbornenyl-functionalized PEO-b-PCL macromonomer 13 via 'click reaction'



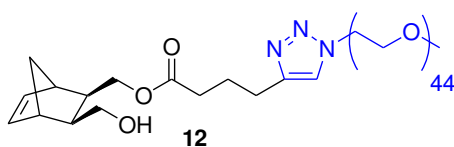
The azido-terminated PEO **10** (0.251 g, 0.125 mmol), *N,N,N',N'',N'''*-pentamethyldiethylenetriamine (PMDETA, 0.0251 g, 0.15 mmol) and **11** (0.401 g, 0.125 mmol) were charged to a dry Schlenk tube along with degassed DMF (5 mL). The tube was sealed with a rubber septum and subjected to six freeze-pump-thaw cycles. This solution was then transferred with a cannula under nitrogen into another Schlenk tube equipped with magnetic stirrer bar and rubber septum, previously evacuated and filled with nitrogen, containing CuBr (0.0096 g, 0.0625 mmol). The resulting solution was subsequently stirred at room temperature for 24 h. The reaction mixture was diluted with DCM and then washed with 3x50 mL of an aqueous disodium ethylenediaminetetraacetate EDTA solution (0.03 mol/L) to remove the catalyst. The organic layer was dried over MgSO₄ and filtered. The resulting macromonomer was isolated by precipitation into diethyl ether. The mixture was filtered and the resulting product was dried under vacuum overnight. Yield: 80%. Conversion: 97%.

¹H NMR (400 MHz, CDCl₃), δ (ppm): 7.51 (s, 1H, triazole); 6.18 (m, 2H, CH=CH), 4.50 (m, 2H, N-CH₂), 4.24 (m, 2H, CH₂OPCL), 4.00 - 4.20 (m, 44H, PCL; -CH₂-OCO); 3.85 (m, 4H, N-CH₂CH₂);

CHCH₂O-PEO), 3.60 - 3.80 (m, 172H, PEO; CH₂); 3.38 (s, 3H, CH₃O), 2.64 (m, 4H, OCOCH₂CH₂CH₂-triazole; CHCH₂CH), 2.35 (m, 2H, OCOCH₂CH₂CH₂-triazole), 2.25 - 2.35 (m, 44H, PCL; O-COCH₂); 1.98 (m, 2H, OCOCH₂CH₂CH₂-triazole), 1.85 (m, 2H, COOCH₂CHCHCH₂COO), 1.55 - 1.75 (m, 88H, PCL; CH₂CH₂CH₂-OCO; CO-CH₂CH₂), 1.50 (m, 2H, CHCH₂CH), 1.35 - 1.45 (m, 44H, CH₂CH₂CH₂-OCO).

SEC: M_n = 9800 g/mol; D_M = 1.10

Synthesis of hydroxyl-functionalized norbornenyl-terminated PEO 12



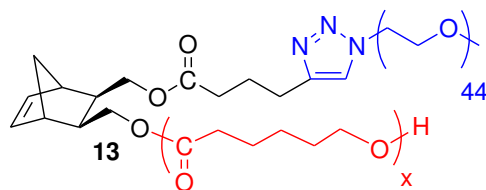
The azide-terminated PEO **10** (0.565 g, 0.282 mmol), PMDETA (0.0565 g, 0.326 mmol) and **9** (0.07 g, 0.282 mmol) were charged to a dry Schlenk tube along with degassed DMF (7.5 mL). The tube was sealed with a rubber septum and subjected to six freeze-pump-thaw cycles. This solution was then transferred with a cannula under nitrogen into another Schlenk tube, previously evacuated and filled with nitrogen, containing CuBr (0.0216 g, 0.141 mmol), and the stirrer bar. The resulting solution was subsequently stirred at room temperature for 24 h. The reaction mixture was diluted with DCM and then washed with 3x50 mL of an aqueous ethylenediaminetetraacetate EDTA solution (0.03 mol/L) to remove the catalyst. The organic layer was dried over MgSO₄ and filtered. The resulting macromonomer was isolated by precipitation into diethyl ether. The mixture was filtered and the resulting product was dried under vacuum overnight. Yield: 75%

¹H NMR (400 MHz, CDCl₃), δ (ppm): 7.51 (s, 1H, triazole); 6.18 (m, 2H, CH=CH), 4.50 (m, 2H, N-CH₂), 4.24, 4.05 (m, 2H, CH₂OPEO), 3.82 (m, 4H, CH₂OH; NCH₂CH₂), 3.60- 3.80 (m, 172H, -CH₂-), 3.38 (s, 3H, CH₃O), 2.75 (m, 3H, OCOCH₂CH₂CH₂-triazole; CHCH₂CH), 2.68 (s, 1H, CHCH₂CH), 2.38 (m, 2H, CH₂-triazole), 2.02 (m, 2H, OCOCH₂CH₂CH₂-triazole), 1.75, 1.85 (m, 2H, CH₂CHCHCH₂), 1.33, 1.45 (m, 2H, CHCH₂CH).

¹³C NMR (100 MHz, CDCl₃), δ (ppm): 173.2 (CO-O), 147.0 (triazole: CH=CHCH₂), 137.0, 137.6 (CH=CH), 122.2 (triazole: CH=CH-N), 72.0 (CH₂OCH₃), 70.6 (PEO, CH₂), 70.0 (NCH₂CH₂OCH₂), 69.6 (NCH₂CH₂), 65.9 (CH₂OCO), 63.6 (CH₂OH), 59.0 (CH₃O), 50.8 (NCH₂CH₂), 44.9, 44.6 (CH-CH₂-CH), 43.4 (CHCH₂OCO), 42.7 (CHCH₂OH), 39.7 (CHCH₂CH), 33.6 (CH₂COO), 24.8 (CH₂CH₂COO).

SEC: M_n = 3500 g/mol; D_M = 1.03

Synthesis of norbornenyl-functionalized PEO-b-PCL macromonomer 13 via ROP of CL



12 (0.4 g, 0.178 mmol) and TBD (0.0084 g, 0.061 mmol) were charged into a dried Schlenk tube equipped with magnetic stirrer and rubber septum under N₂ in glove box. 2.5 mL of dried THF was added to dissolve the mixture in Schlenk tube under N₂ at 25 °C. CL (0.201 mL, 1.78 mmol) was added, the resulting mixture was kept stirring for 5 hours. Acetic acid (1 mL) was added to quench TBD, THF was removed by rotary evaporator, the residue was dissolved in 2 mL of DCM and precipitated in 30 mL of cold diethyl ether. The mixture was filtered and resulting product was dried under vacuum overnight. Yield: 80%

¹H NMR (400 MHz, CDCl₃), δ (ppm): 7.51 (s, 1H, triazole); 6.18 (m, 2H, **CH=CH**), 4.50 (m, 2H, N-**CH**₂), 4.24 (m, 2H, **CH**₂OPCL), 4.00 - 4.20 (m, 20H, PCL; -**CH**₂-OCO); 3.85 (m, 4H, N-CH₂CH₂; CHCH₂O-PEO), 3.60 - 3.80 (m, 172H, PEO; **CH**₂); 3.38 (s, 3H, CH₃O), 2.64 (m, 4H, OCOCH₂CH₂CH₂-triazole; **CH**CH₂CH), 2.35 (m, 2H, OCOCH₂CH₂CH₂-triazole), 2.25 - 2.35 (m, 20H, PCL; O-COCH₂); 1.98 (m, 2H, OCOCH₂CH₂CH₂-triazole), 1.85 (m, 2H, COOCH₂CHCHCH₂COO), 1.55 - 1.75 (m, 40H, PCL; CH₂CH₂CH₂-OCO; CO-CH₂CH₂), 1.50 (m, 2H, CHCH₂CH) 1.35 - 1.45 (m, 20H, CH₂CH₂CH₂-OCO).

SEC: M_n = 5600 g/mol; D_M = 1.08

Chapter 4

**Norbornenyl-functionalized PEO-b-PCL block
copolymers as a platform to target comb-like,
umbrella-like graft and (mikto-arm) star copolymers**

Introduction

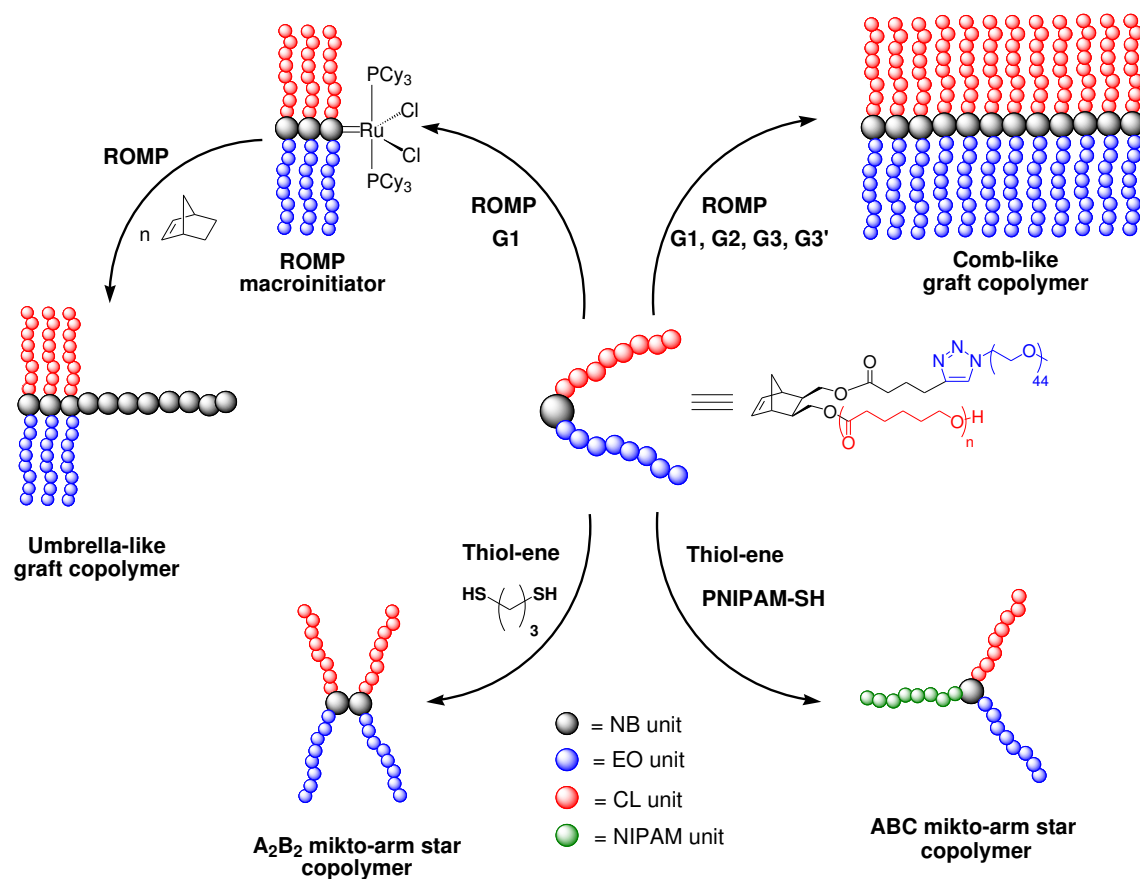
The high reactivity of the norbornene (NB) functionality in different reactions gives rise to the use of NB-terminated polymers for the synthesis of many complex architectural copolymers such as graft, block, and hyperbranched copolymers or networks. Indeed, based on their high degree of ring strain, NB and its derivatives afford rapid Ring-Opening Metathesis Polymerization (ROMP).¹⁻⁶ On the other hand, previous studies have reported the high reactivity of NB and NB derivatives toward thiol-ene reactions.⁷⁻¹⁴

Thanks to the development of well-defined catalysts, ROMP of norbornenyl macromonomers has been reported as an efficient method to prepare well-defined structural copolymers when combined with other controlled/living polymerizations.¹⁵⁻¹⁸ A wide range of studies related to the ROMP of NB-based macromonomers containing hydrophilic poly(ethylene oxide) (PEO) chain¹⁹⁻²⁵ and/or hydrophobic poly(ϵ -caprolactone) (PCL) chain²⁶⁻³⁰ have been reported. Héroguez *et al.*¹⁹ reported the first study related to ROMP of norbornenyl-terminated PEO macromonomers to synthesize graft copolymers by the ‘grafting through’ strategy. Polymacromonomers with moderate to narrow molar mass distributions have been obtained together with high NB-based macromonomer conversions (conversion = 95 - 100%). Well-defined polynorbornene-*graft*-poly(ϵ -caprolactone) (PNB-*g*-PCL) copolymers with low dispersities ($D_M = 1.10$) have been first obtained by Mecerreyes *et al.*²⁶ from ROMP of NB-functionalized PCL macromonomers with high macromonomer conversions (~90%). More recently, Hadjichristidis’ group has reported the synthesis and characterization of graft copolymers bearing different grafts including polyethylene (PE), polystyrene (PS), PEO, and PCL using ROMP copolymerization of norbornenyl-terminated macromonomers.³⁰ Those reported studies highlighted the high reactivity of the NB functionality of NB-based macromonomers toward ROMP in order to synthesize well-defined graft copolymers through the ‘macromonomer route’ method.

The thiol-ene reaction³¹ applied to NB-terminated polymers has been the object of several studies including: (i) preparation of hyperbranched polyesters,¹³ (ii) synthesis of multi-block copolymers,^{11,12} and (iii) design of hydrogels for tissue engineering applications.¹⁴ To the best of our knowledge, no previous study has been reported on the thiol-ene reaction using NB-terminated PCL or NB-terminated PEO and PCL. A few

studies have described the reactivity of NB-terminated PEO toward thiol-ene reaction. Walker *et al.*¹¹ have shown the high reactivity of NB-functionalized polymers toward thiol-ene reactions leading to random and alternated multi-block copolymers containing PEO, PS, and polydimethylsiloxane (PDMS). A recent review has been published on thiol-ene photoclick hydrogels.¹⁴ Parts of such hydrogels are crosslinked through light-mediated orthogonal reactions between multifunctional norbornene-terminated PEO and thiol-contained cross-linking agents.

Based on the previous successful synthesis and characterization of well-defined amphiphilic copolymers containing NB, hydrophilic PEO chain and hydrophobic PCL chain (Chapter 3), we herein study their reactivity toward ROMP and toward thiol-ene reaction (Scheme IV.1). Therefore, such norbornenyl-functionalized PEO-*b*-PCL copolymers could be a platform to target various architectures such as comb-like, umbrella-like graft copolymers and (mikto-arm) star copolymers.



Scheme IV.1. Various macromolecules architectures targeted from norbornenyl-functionalized PEO-*b*-PCL copolymer used as a platform

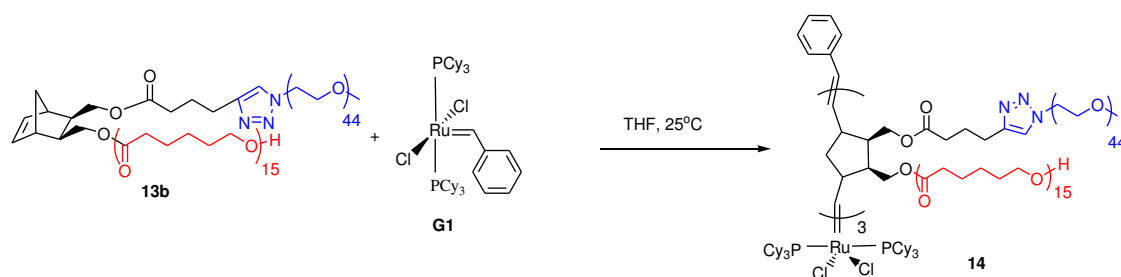
I. Synthesis of a ROMP macroinitiator and umbrella-like copolymer using ROMP macroinitiator

I.1. Synthesis of ROMP macroinitiator from norbornenyl-functionalized PEO-*b*-PCL copolymer and Grubbs 1

Grubbs 1 catalyst (G1), as described by Schwab and co-workers,³² shows a high reactivity toward ROMP of norbornene (NB), and exhibits a remarkable stability toward oxygen and moisture. However, when the ROMP of NB is realized in aqueous dispersed media using G1, practical difficulties appear. As soon as G1 is in contact with NB, a fast polymerization occurs even at room temperature. This means that G1 can not be dissolved in the monomer phase that has to be subsequently dispersed in water.³³ On the other hand, because of its hydrophobic nature, adding G1 to aqueous dispersions is problematic.² Quémener and co-workers have synthesized an original PEO-based ROMP macroinitiator using G1,³⁴ such macroinitiator was found to exhibit great catalytic activity in ROMP of NB in dispersed aqueous media.

In our study, a new ROMP macroinitiator based on norbornenyl-functionalized PEO-*b*-PCL copolymer containing 44 ethylene oxide (EO) units and 15 ϵ -caprolactone (CL) units (named PEO₄₄NBPCL₁₅ - chapter 3) and G1, was synthesized in order to study the norbornene reactivity of such a copolymer and to increase the ruthenium catalyst solubility in aqueous dispersed media.

The macroinitiator was synthesized with an initial [PEO₄₄NBPCL₁₅]₀/[G1]₀ ratio of 3/1 in tetrahydrofuran (THF) at 25 °C (Scheme IV.2).



Scheme IV.2. Synthesis of a ROMP macroinitiator **14** from PEO₄₄NBPCL₁₅ copolymer and G1

Proton nuclear magnetic resonance (^1H NMR) spectrum of the crude solution showed the appearance of a new peak at $\delta = 5.25\text{--}5.35$ ppm (labelled a', Figure IV.1, A) related to protons of double bonds in polynorbornene backbone and the absence of peak related to protons of double bond of any unreacted macromonomer (labelled a, Figure IV.1, C). Moreover, the signal at $\delta = 19.9$ ppm (labelled a', Figure IV.1, A) shows the presence of alkylidene proton.

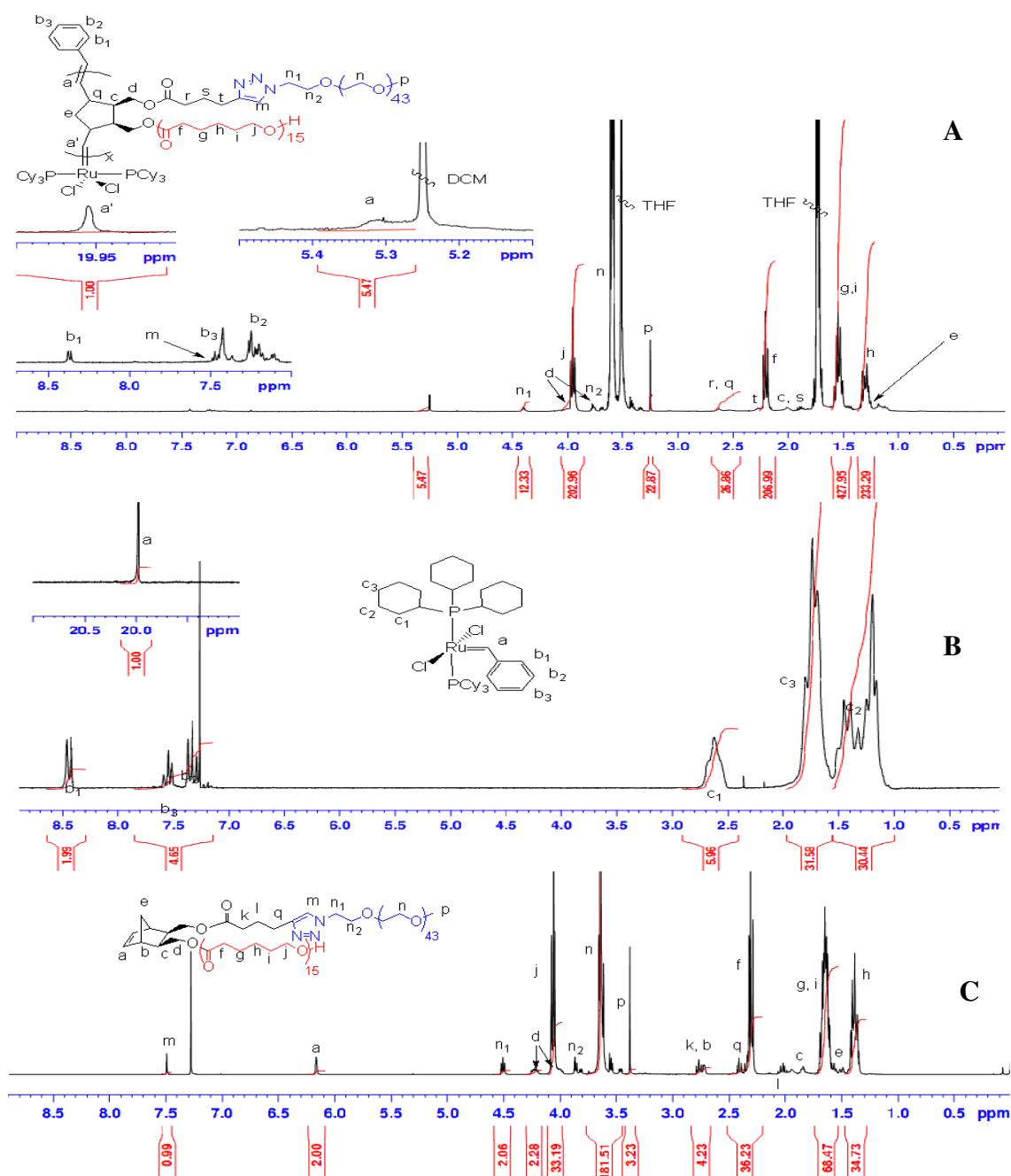


Figure IV.1. ^1H NMR spectra (400MHz, 25 °C) of (A) crude macroinitiator solution, (B) G1 and (C) $\text{PEO}_{44}\text{NBPCl}_{15}$ macromonomer; solvent: chloroform- d (CDCl_3)

Size exclusion chromatography (SEC) trace of macroinitiator **14** shows clearly only one population shifted toward lower retention times compared to the SEC trace of NBPEO₄₄PCL₁₅ macromonomer (Figure IV.2). ¹H NMR and SEC analyses show clearly the formation of the ROMP macroinitiator.

The self-assembling properties of the ROMP macroinitiator were measured by dynamic light scattering (DLS). Micellization of the macroinitiator in aqueous dispersed media was achieved through co-solvent method. Deionized water was added to a macroinitiator solution in THF targeting a final macroinitiator concentration of 1 g/L in water followed by evaporation of THF. The solution was kept stirring for 48 hours for full dissolution and filtered before measurement. Hydrodynamic diameter (*D*) and polydispersity (*PD_i*) values of micelles generated from the ROMP macroinitiator dispersed in water were 13.75 nm and 0.278, respectively.

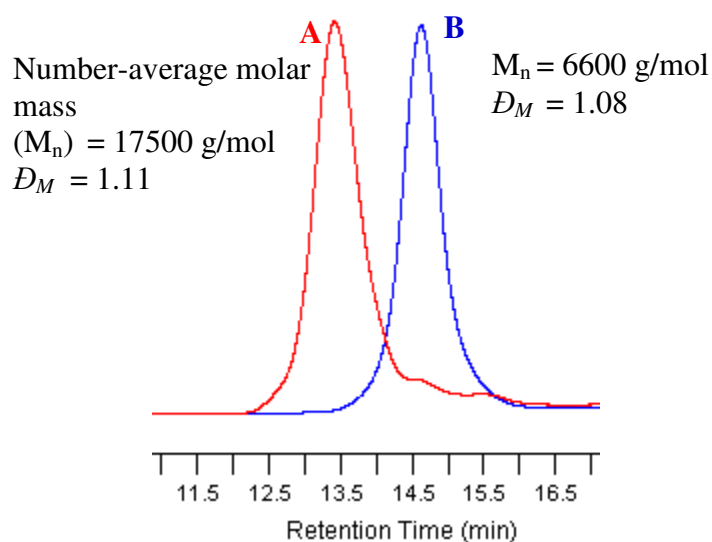
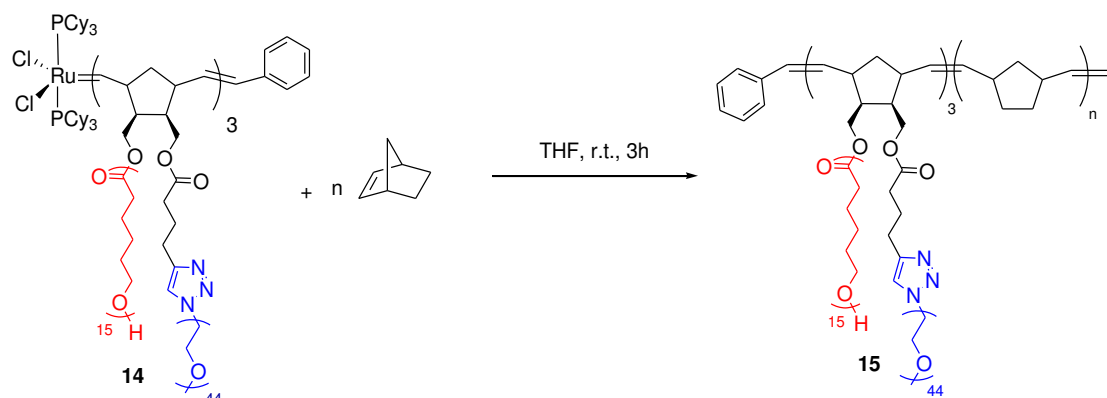


Figure IV.2. SEC traces of (A) ROMP macroinitiator, and (B) PEO₄₄NB PCL₁₅ copolymer

1.2. Synthesis of umbrella-like copolymers using ROMP macroinitiator

In order to evaluate the reactivity of the ROMP macroinitiator, a ROMP of NB was carried out in THF at 25 °C with an initial [NB]₀/[macroinitiator]₀ ratio of 1500:1 (Scheme IV.3). After 3 h of reaction, the crude polymer was characterized by SEC in THF with a refraction index (RI) detector, calibrated with linear PS standards (Figure IV.3).



Scheme IV.3. ROMP of NB initiated by macroinitiator **14**

SEC trace of crude product (Figure IV.3, A) shows two populations, the first population at lower retention times corresponds to the umbrella-like copolymer PNB-*b*-[(PNB-*g*-(PEO/PCL))] **15**, and the second one at higher retention times corresponds to the unreacted ROMP macroinitiator **14** (Figure IV.3, C). SEC result suggests that part of the ROMP macroinitiator was deactivated, probably due to a low stability despite storage in inert media. Therefore, the crude product was purified through a short column of silica using chloroform as eluent to separate PNB-*b*-[(PNB-*g*-(PEO/PCL))] from unreacted macroinitiator. As shown by SEC analysis (Figure IV.3, B), a well-defined umbrella-like copolymer was obtained.

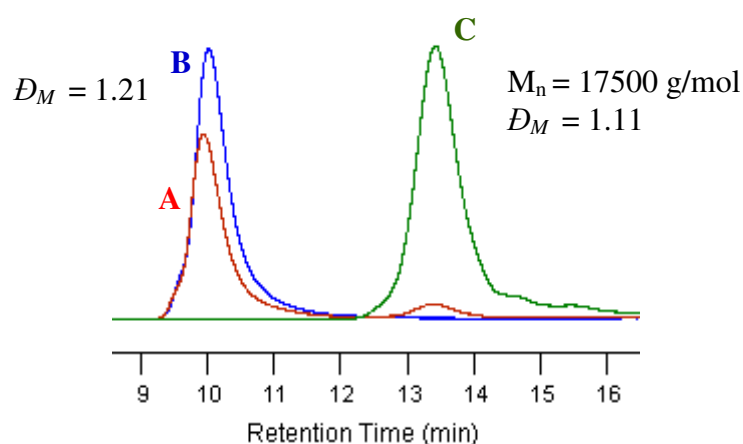


Figure IV.3. SEC traces of (A) crude [PNB-*b*-(PNB-*g*-(PEO/PCL))] copolymer **15**, (B) purified [PNB-*b*-(PNB-*g*-(PEO/PCL))] copolymer **15** and, (C) ROMP macroinitiator **14**

¹H NMR spectrum of purified PNB-*b*-[(PNB-*g*-(PEO/PCL))] **15** shows a shift of peaks corresponding to protons of the double bond of PNB backbone at $\delta = 5.28$ ppm (labelled a_{trans} , Figure IV.4, A) and $\delta = 5.13$ ppm (labelled a_{cis} , Figure IV.4, A) compared to the peak of the double bond protons of commercial NB at $\delta = 5.99$ ppm (labelled a' , Figure IV.4, B). The comparison of integrations of the signal related to protons in *cis*-position at $\delta = 5.13$ ppm (labelled a_{cis} , Figure IV.4, A) and the signal related to protons at *trans*-position at $\delta = 5.28$ ppm (labelled a_{trans} , Figure IV.4, A) showed a *cis/trans* ratio in PNB backbone equals to 12/88. DP_n calculated from the comparison of integration values of the signals related to protons of the double bonds of PNB backbone at $\delta = 5.28$ ppm (labelled a_{trans} , Figure IV.4, A) and $\delta = 5.13$ ppm (labelled a_{cis} , Figure IV.4, A) and of integration value of signal related to proton CH_3O - (PEO) at $\delta = 3.38$ ppm was approximately 5500 which was confirmed by weight-average molar mass (M_w) of 6.224×10^5 g/mol, determined in SEC-Multi Angles Laser Light Scattering (SEC-MALLS) analysis. The calculated DP_n value of PNB is much higher than expected DP_n value from initial $[NB]_0/[macroinitiator]_0$ ratio of 1500:1, in agreement with SEC results suggesting that part of the macroinitiator was deactivated. However, the ROMP macroinitiator has a high reactivity toward ROMP of NB and has led to a well-defined PNB-*b*-[(PNB-*g*-(PEO/PCL))] umbrella-like copolymer.

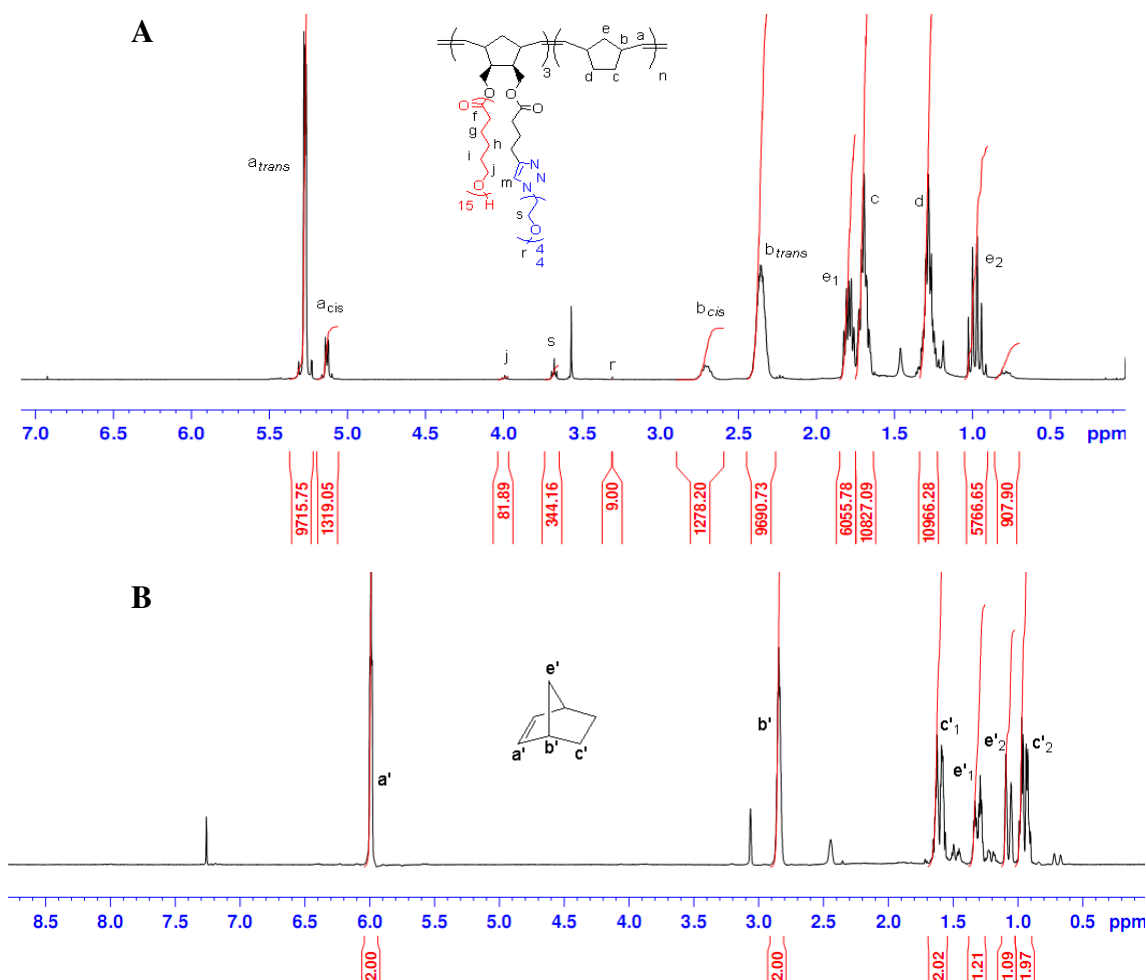
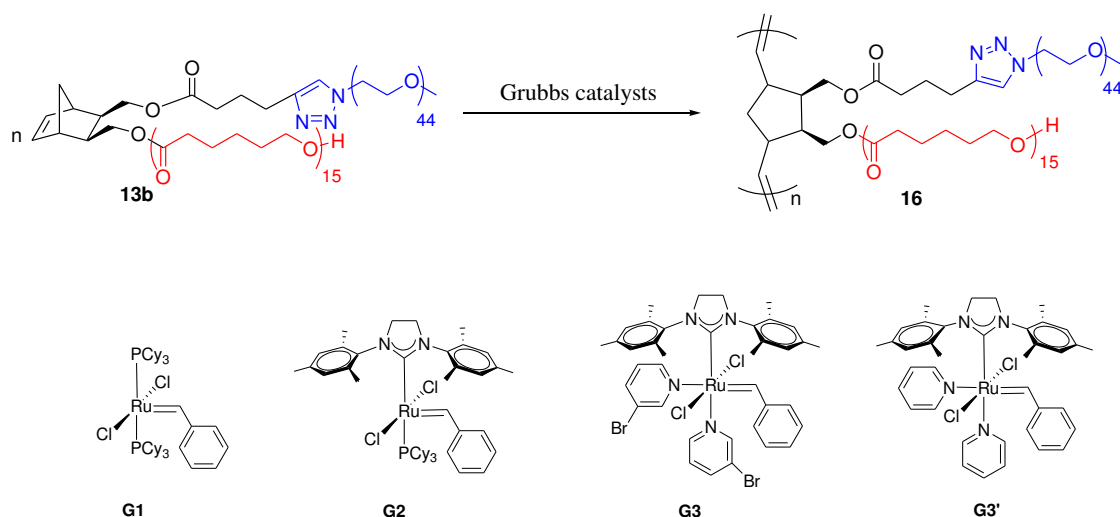


Figure IV.4. ^1H NMR spectra (400 MHz, 25 °C) of (A) purified PNB-*b*-[(PNB-*g*-(PEO/PCL))] obtained from polymerization of NB initiated by ROMP macroinitiator containing PEO and PCL and, (B) commercial NB; solvent: CDCl_3

II. Synthesis of graft copolymers from ROMP of norbornenyl-functionalized PEO-*b*-PCL macromonomer

In order to study the ROMP reactivity of norbornene functionality of norbornenyl PEO-*b*-PCL macromonomer to target graft copolymers, ROMPs of the $\text{PEO}_{44}\text{NB}\text{PCL}_{15}$ **13b** macromonomer were investigated in THF at 25 °C using Grubbs' first (G1), Grubbs' second (G2) and Grubbs' third generation (G3: bromopyridine as ligands and G3': pyridine as ligands) catalysts as initiators (Scheme IV.4).



Scheme IV.4. ROMP of norbornenyl-functionalized PEO-*b*-PCL macromonomer in THF at 25°C using G1, G2, G3 and G3' as initiators

ROMP were carried out using initial $[\text{PEO}_{44}\text{NBPCl}_{15}]_0/[\text{initiator}]_0$ ratios of 10:1 and 50:1 with an initial $[\text{PEO}_{44}\text{NBPCl}_{15}]_0$ of 0.04 mol/L for 3 hours and were terminated using ethyl vinyl ether. The macromonomer conversions were determined by SEC by comparing peak areas of populations corresponding to graft copolymer at lower retention times and to unreacted macromonomer at higher retention times. Number-average molar masses (M_n) and dispersities (D_M) were measured by SEC in THF with a RI detector and calibrated with linear PS standards (Figure IV.5). Results are summarized in Table IV.1.

Table IV.1. ROMP of $\text{PEO}_{44}\text{NBPCl}_{15}$ using Grubbs catalysts as initiators in THF at 25°C with an initial $[\text{PEO}_{44}\text{NBPCl}_{15}]_0 = 0.04$ mol/L for 3 hours

Run	Catalysts	$[\text{M}]_0/[\text{I}]_0$	$M_{n,\text{theo}}^a$ g/mol	$M_{n,\text{SEC}}^b$	Conv. ^c (%)	D_M^b
1	G1	10	39510	Bimodal distribution	-	-
2	G2	10	39510	Bimodal distribution	-	-
3	G3'	10	39510	Bimodal distribution	-	-
4	G3	10	39510	32000	97	1.10
5	G3	50	197550	45000	45	1.08

^a Calculated from $M_{n,\text{theo}} = ([\text{M}]_0/[\text{I}]_0) \times M_{n,\text{PEO}_{44}\text{NBPCl}_{15}}$ at full conversion with $M_{n,\text{PEO}_{44}\text{NBPCl}_{15}}$ determined by ^1H NMR spectroscopy equals to 3951 g/mol (as calculated in chapter 3). ^b Determined by SEC in THF with RI detector, calibrated with linear PS standards. ^c Conversion (Conv.) calculated from SEC in THF with RI detector, calibrated with linear PS standards using the comparison of peak areas corresponding to graft copolymer and to unreacted macromonomer.

The SEC traces of crude mixtures of ROMP of $\text{PEO}_{44}\text{NBPCl}_{15}$ macromonomer using G1, G2 and G3' as initiators (Figure IV.5, A, B and C) show the non-quantitative macromonomer conversions as bimodal chromatograms with a peak at higher retention time corresponding to unreacted macromonomer are observed. G3' exhibits a higher reactivity toward ROMP of $\text{PEO}_{44}\text{NBPCl}_{15}$ macromonomer in comparison to G1 and G2 as a higher peak area corresponding to graft copolymer at lower retention times is observed. However, the residual unreacted macromonomer in crude mixtures suggests that G1, G2 and G3' are not suitable initiators for ROMP of amphiphilic norbornenyl-functionalized PEO-*b*-PC⁻

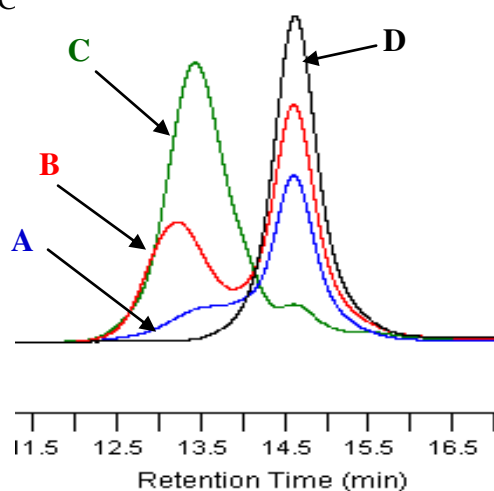


Figure IV.5. SEC traces of crude mixtures obtained from ROMP of $\text{PEO}_{44}\text{NBPCl}_{15}$ for 3h in THF at 25°C using (A) G1 (Table IV.1, run 1), (B) G2 (Table IV.1, run 2), (C) G3' (Table IV.1, run 3) initiators and (D) $\text{PEO}_{44}\text{NBPCl}_{15}$ macromonomer

On the other hand, ROMP of $\text{PEO}_{44}\text{NBPCl}_{15}$ macromonomer using G3 (Table IV.1, run 4) showed a nearly quantitative macromonomer conversion for an initial $[\text{M}]_0/[\text{I}]_0$ ratio of 10:1 (Figure IV.6, A) and a low molar mass distribution value ($\mathcal{D}_M = 1.10$). When the initial $[\text{M}]_0/[\text{I}]_0$ ratio increases to 50, ROMP using G3 (Table IV.1, run 5) was non-quantitative, as macromonomer conversion calculated by comparing chromatograms areas corresponding to graft copolymer at lower retention times and to macromonomer at higher retention times was 45% (Figure IV.6, B).

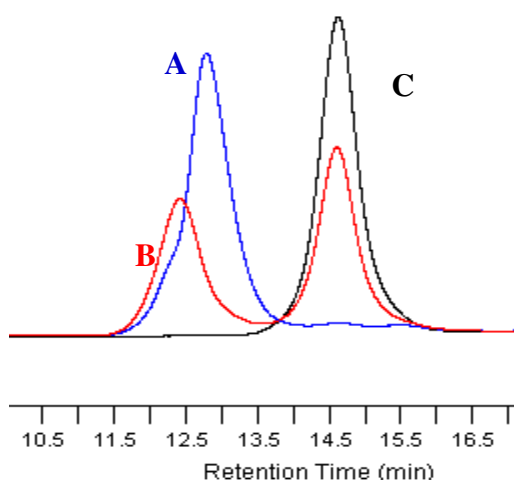


Figure IV.6. SEC traces of ROMP of $\text{PEO}_{44}\text{NBPCL}_{15}$ macromonomer using G3 with initial $[\text{M}]_0/[\text{I}]_0$ ratios of (A) 10 (Table IV.1, run 4), (B) 50 (Table IV.1, run 5) and, (C) $\text{PEO}_{44}\text{NBPCL}_{15}$ macromonomer

The crude mixture resulting from ROMP of $\text{PEO}_{44}\text{NBPCL}_{15}$ using G3 and an initial $[\text{M}]_0/[\text{I}]_0$ of 50:1 (Table IV.1, run 5) was purified through a short column of silica using CHCl_3 as eluent. The SEC trace of the copolymer after purification shows only one population, indicating an effective separation of the graft copolymer from the crude mixture containing unreacted macromonomer (Figure IV.7).

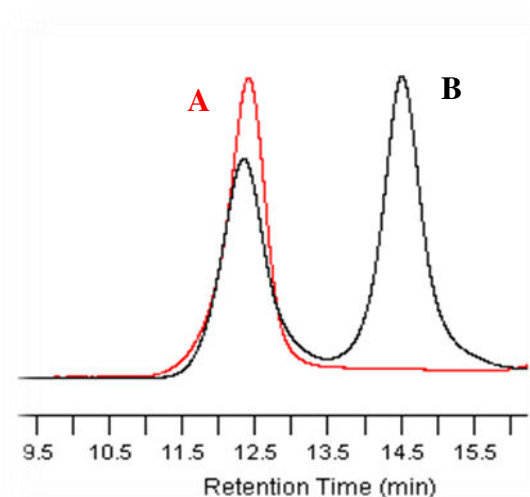


Figure IV.7. SEC traces of (A) purified PNB-*g*-(PEO;PCL) copolymer and, (B) crude product

^1H NMR spectrum of the purified copolymer shows the appearance of two new broad peaks at $\delta = 5.10\text{--}5.55$ ppm (labelled a_{cis} and a_{trans} , Figure IV.8, A) corresponding

to protons of the double bonds of the PNB backbone. The disappearance of the signal corresponding to the double bond protons of the norbornene ring at $\delta = 6.19$ ppm (labelled a, Figure IV.8, B) suggests that norbornene functionalities have been completely transformed by ROMP. The number-average degree of polymerization (DP_n) of polynorbornene backbone calculated *via* the integration values of signal corresponding to the double bonds protons of PNB backbone at $\delta = 5.10$ - 5.55 ppm (labelled a_{cis} and a_{trans} , Figure IV.8, A) and the one of the signal related to protons of vinyl-end group at $\delta = 5.05$ ppm (labelled q, Figure IV.8, A) was 11.

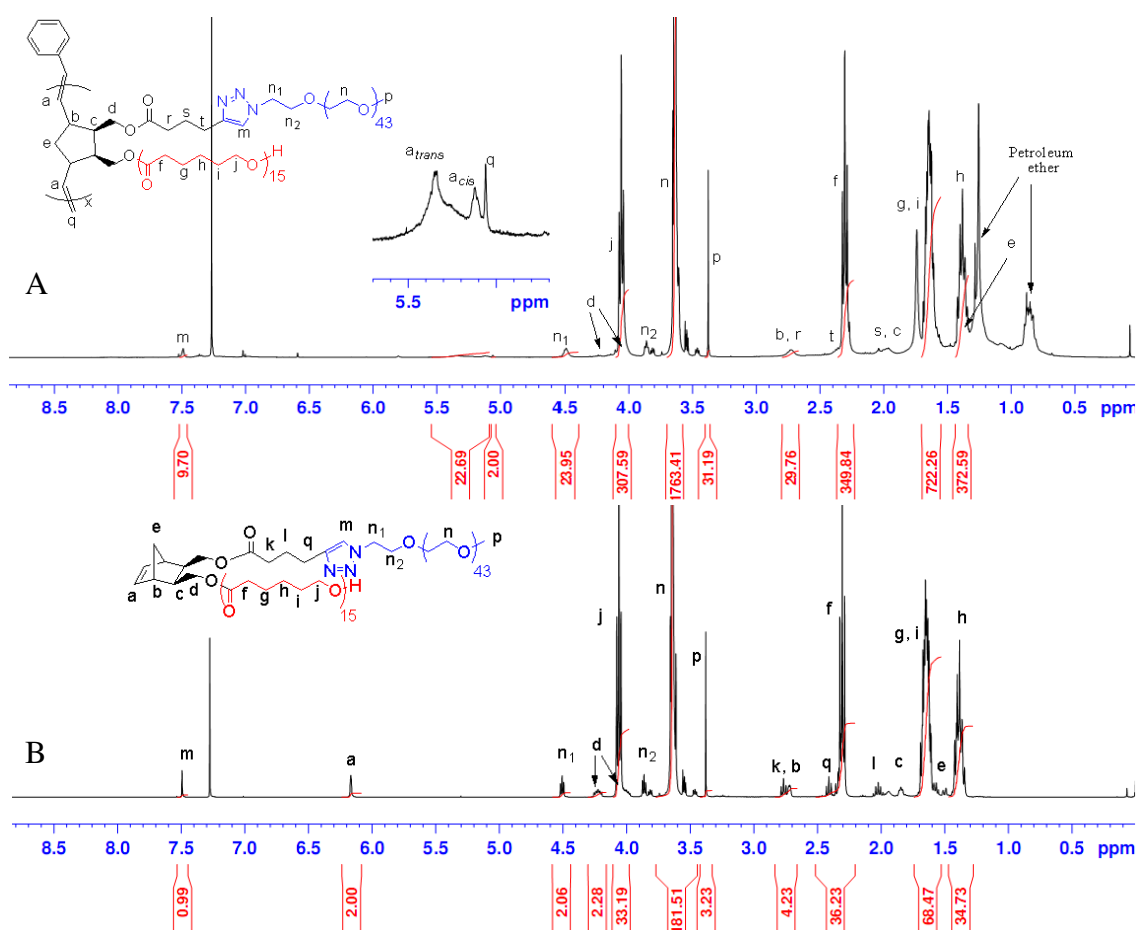


Figure IV.8. 1H NMR spectra (400 MHz, 25 °C) of (A) purified PNB-*g*-(PEO/PCL) copolymer and, (B) $PEO_{44}NB PCL_{15}$ macromonomer; solvent: $CDCl_3$

The thermal behavior of PNB_{11} -*g*-(PEO_{44}/PCL_{15}) copolymer (Table IV.1, run 5) was evaluated by thermogravimetric analysis (TGA) under N_2 in order to determine the degradation temperature of the graft copolymer compared to initial macromonomer

(Figure IV.9). Degradation temperature of the first 5% weight loss decomposition of graft copolymer was determined to be 334 °C, higher than degradation temperature of the first 5% weight loss decomposition of initial $\text{PEO}_{44}\text{NB}\text{PCL}_{15}$ macromonomer which equals to 316 °C. In both cases, a single thermal decomposition behavior was observed, which was already reported as a result of an enhanced miscibility of PEO and PCL blocks.³⁵

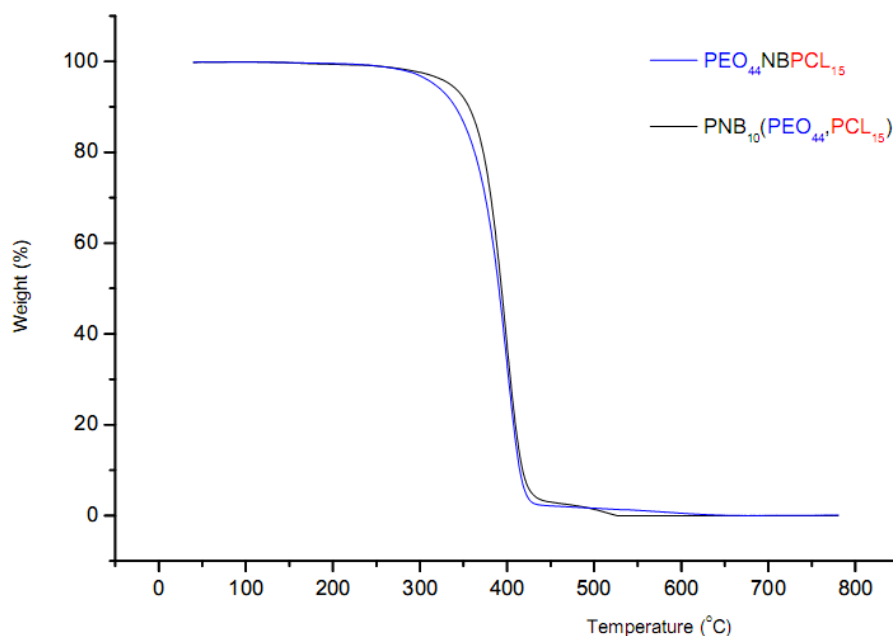


Figure IV.9. TGA thermograms of $\text{PNB}_{10}\text{-}g\text{-(PEO}_{44}\text{/PCL}_{15})$ and $\text{PEO}_{44}\text{NB}\text{PCL}_{15}$

The melting and crystallization behavior of $\text{PEO}_{44}\text{NB}\text{PCL}_{15}$ and its resulting graft copolymer were investigated by differential scanning calorimetry (DSC) as shown in Figure IV.10. The crystallization temperature T_c was obtained from the first cooling run, and the melting temperature and the degree of crystallinity were obtained from the second heating run. DSC thermogram of norbornenyl-functionalized PEO-*b*-PCL macromonomer (Figure IV.10, B) shows two peaks corresponding to two crystallization transitions, indicating the phase separation of PEO phase and PCL phase ($T_c = 16$ °C and 29 °C, respectively). Furthermore, crystallinity values (X_c) obtained by comparing crystallization enthalpy (ΔH_c) of each block with the ΔH_f values for 100% crystallized polymers ($\Delta H_{f,\text{PEO}} = 188$ J/g; $\Delta H_{f,\text{PCL}} = 140$ J/g)³⁶ are 32% for PEO phase and 25% for PCL phase. Those results are similar to DSC results of PEO-*b*-PCL in the literature,^{37,38} suggesting that the presence of the NB functionality does not affect the crystallization

behavior of PEO-*b*-PCL copolymers. In contrast, DSC thermogram of PNB₁₁-*g*-(PEO₄₄/PCL₁₅) copolymer (Figure IV.10, A) shows only one peak corresponding to a sharp crystallization transition at $T_c = 8^\circ\text{C}$, indicating the formation of only one phase from two initial separated PEO phase and PCL phase when the PNB backbone has been generated in ROMP. Melting behaviors of the graft copolymer and the macromonomer were similar with $T_m = 36^\circ\text{C}$ ($\Delta H_m = 111.2\text{ J/g}$) and $T_m = 39^\circ\text{C}$ ($\Delta H_m = 109.6\text{ J/g}$), respectively. The individual fusion enthalpies of PCL and PEO could not be calculated separately due to the partial overlapping of the melting endotherms of PCL and PEO blocks.³⁹

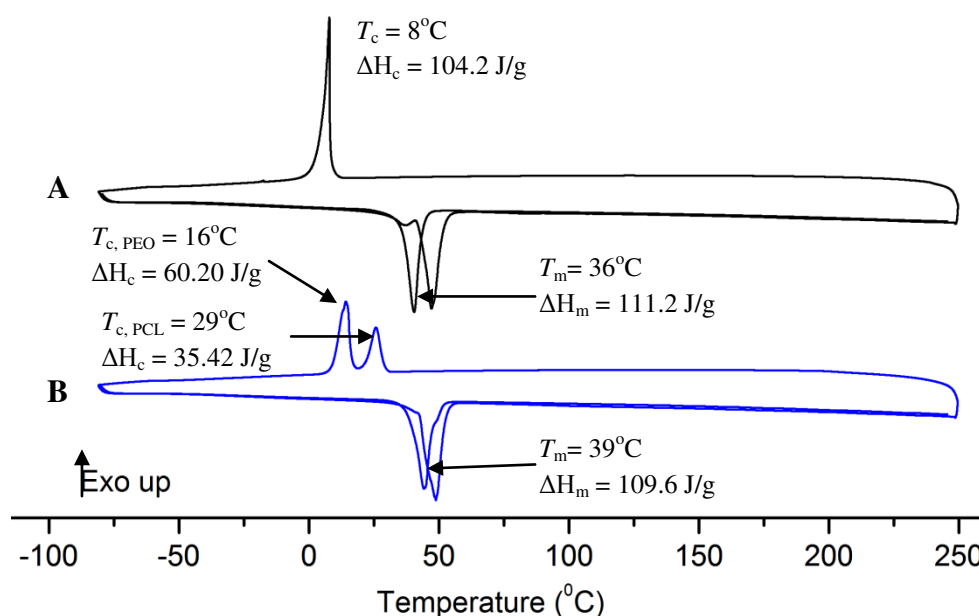


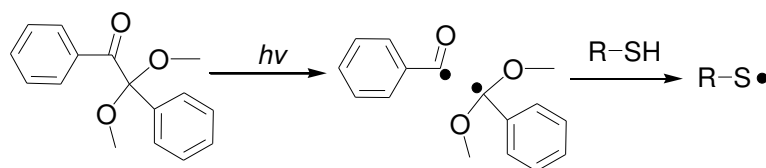
Figure IV.10. DSC thermograms of (A) PNB₁₀-*g*-(PEO₄₄;PCL₁₅) and, (B) PEO₄₄NB PCL₁₅

III. Synthesis of (mikto-arm) star copolymers by thiol-ene reactions of norbornenyl-functionalized PEO-*b*-PCL copolymer

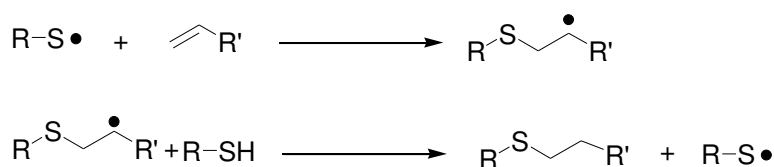
Thiol-ene reactions are generally rapid, tolerant to air and moisture, and give quantitative conversion to the thioether product.^{15,16,40} The radical thiol-ene of thiols to

unsaturated carbon–carbon bonds proceeds *via* a chain process involving initiation, propagation and chain transfer, and termination steps (Scheme IV.5).⁸

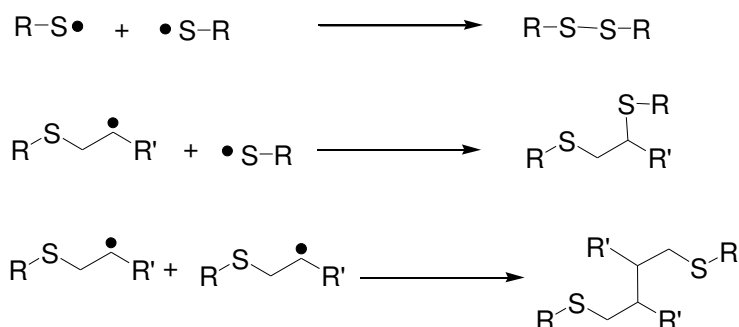
Initiation



Propagation and chain transfer



Termination

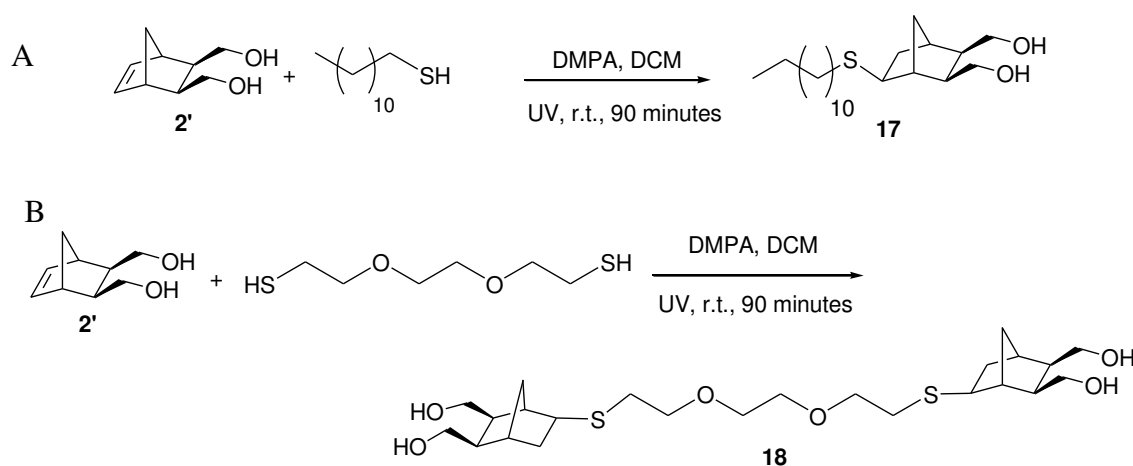


Scheme IV.5. General mechanism of thiol-ene reaction using 2,2-dimethoxy-2-phenylacetophenone (DMPA) as photoinitiator

Stamenović *et al.*¹² reported that thiol-ene reaction of norbornenyl-terminated PS obtained by reversible addition/fragmentation chain transfer (RAFT) polymerization and thiol-functionalized compounds in THF using DMPA as photoinitiator under ultraviolet (UV) light (365 nm) came rapidly to completion within 15 minutes. In our study, we will evaluate the norbornene reactivity of the norbornenyl-functionalized PEO-*b*-PCL block copolymer within thiol-ene reactions in order to target (mikto-arm) star copolymers. Thiol-ene reactions will be first carried out on norbornene dimethanol and norbornenyl-functionalized bispoly(ϵ -caprolactone) (bisPCL) as model reactions.

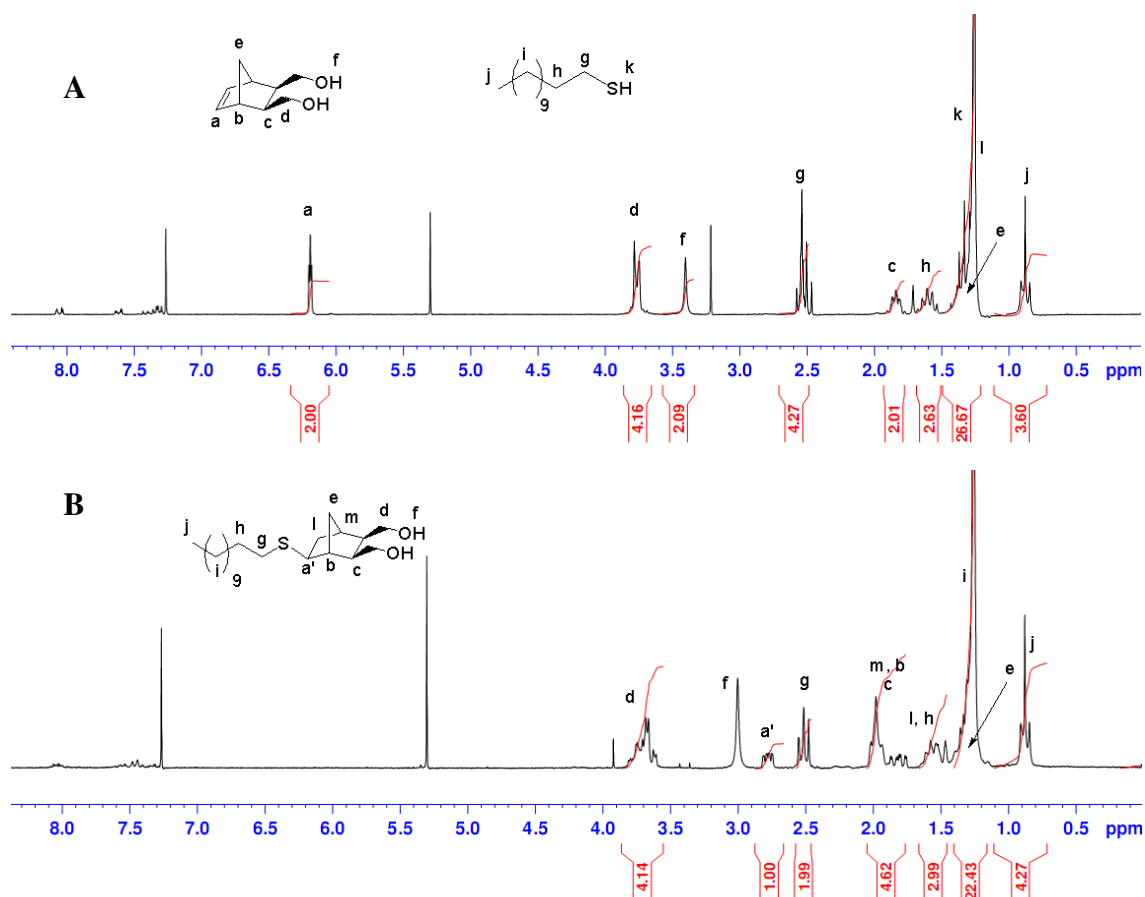
III.1. Thiol-ene reaction using norbornene dimethanol

In order to determine the norbornene reactivity in thiol-ene reaction, norbornene dimethanol **2'** was chosen as a model molecule to react with dodecanethiol (named “thiol”) using $[NB]_0/[thiol]_0$ of 1/1 and 2,2'-(ethylenedioxy)diethanethiol (named “dithiol”) using $[NB]_0/[dithiol]_0$ of 2/1 in dichloromethane (DCM) in the presence of DMPA used as photoinitiator at room temperature under 365 nm wavelength UV light (Scheme IV.6).



Scheme IV.6. Thiol-ene reactions of norbornene dimethanol **2'** with (A) dodecanethiol and (B) 2,2'-(ethylenedioxy)diethanethiol

Reaction A (Scheme IV.6, A) was analyzed by 1H NMR spectroscopy. The comparison of 1H NMR spectra of reaction solution at initial time (Figure IV.11, A) and after 90 minutes (Figure IV.11, B) shows the disappearance of the initial peak at $\delta = 6.19$ ppm (labelled a, Figure IV.11, A), related to protons of the double bond of norbornene dimethanol **2'** after 90 minutes of reaction (Figure IV.11, B) suggesting that all the norbornene functionality has reacted with dodecanethiol. A new peak related to the proton of $C_{12}H_{25}SCHCH_2-$ appears at $\delta = 2.78$ ppm (labelled a', Figure IV.11, B) and the comparison between the integration values of that peak and the one related to protons of $C_{11}H_{23}CH_2SCHCH_2-$ at $\delta = 2.52$ ppm (labelled g, Figure IV.11, B) is 1/2.05, suggesting that thiol-ene reaction of norbornene dimethanol with dodecanethiol is quantitative.



In a similar way, reaction B (Scheme IV.6, B) was analyzed by comparing ^1H NMR spectra of reaction solution at initial time (Figure IV.12, A) and after 90 minutes (Figure IV.12, B). After 90 minutes of reaction, norbornene functionality completely disappeared as shown on the ^1H NMR spectrum with the disappearance of the peak at $\delta = 6.19$ ppm (labelled a, Figure IV.12, A), related to protons of the double bond of norbornene dimethanol **2'**. A new proton of $\text{OCH}_2\text{CH}_2\text{SCHCH}_2-$ was generated after reaction as the appearance of a new peak at $\delta = 2.91$ ppm (labelled a', Figure IV.12, B). A comparison of integrations of this new peak at $\delta = 2.91$ ppm (labelled a', Figure IV.12, B) and the peak at $\delta = 2.52$ ppm (labelled g, Figure IV.12, B) related to protons $\text{OCH}_2\text{CH}_2\text{SCHCH}_2-$ is 1/1.96, suggesting that thiol-ene reaction between the norbornene dimethanol **2'** and the 2,2'-(ethylenedioxy)diethanethiol molecule is quantitative.

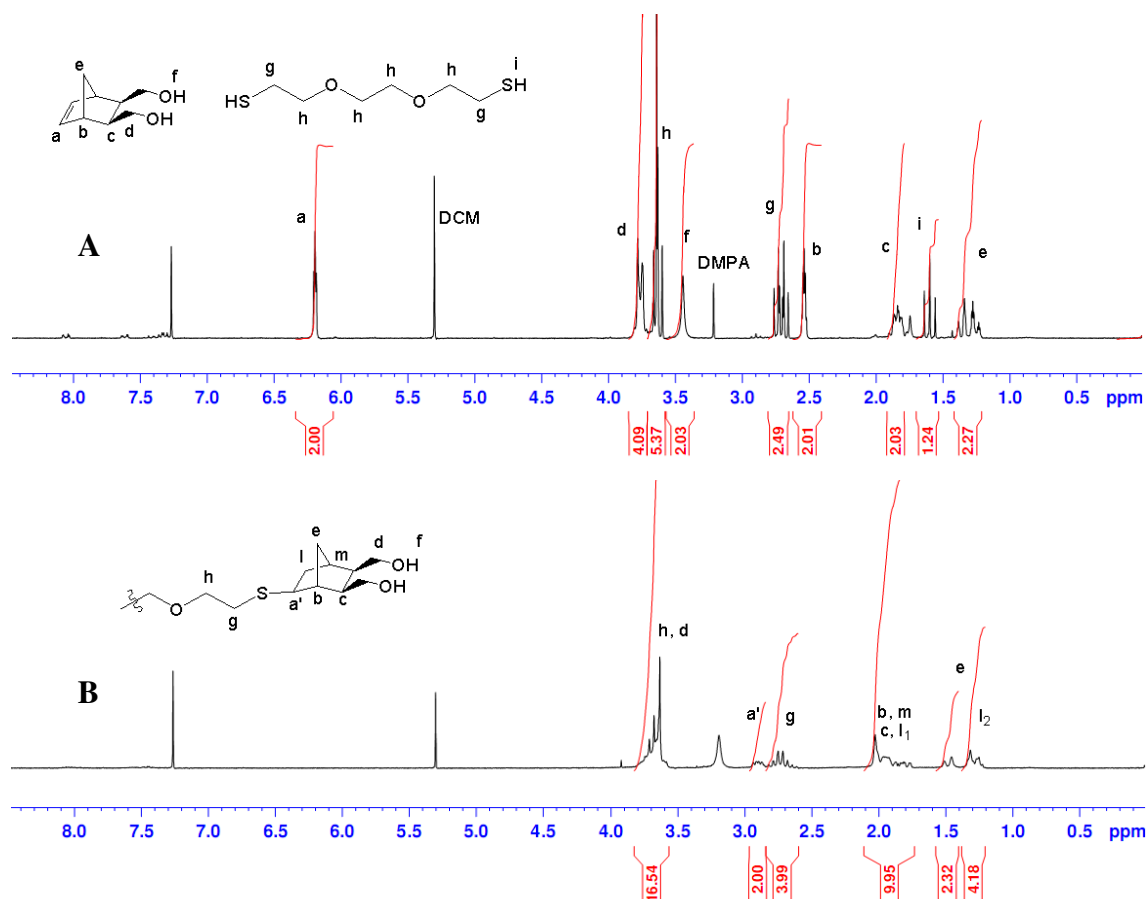
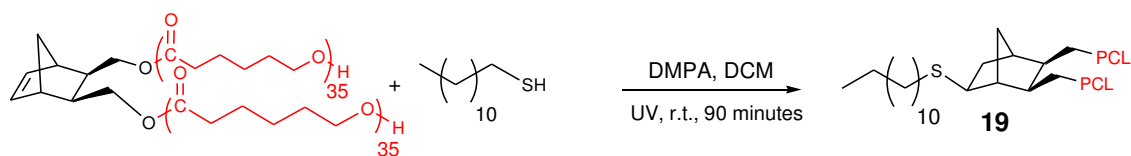


Figure IV.12. ^1H NMR spectra (200 MHz, 25 $^\circ\text{C}$) of thiol-ene reaction of norbornene dimethanol **2'** with 2,2'-(ethylenedioxy)diethanethiol at (A) initial time and (B) after 90 minutes; solvent: CDCl_3

III.2. Thiol-ene reaction using norbornenyl-functionalized bispoly(ϵ -caprolactone) copolymer

Successful thiol-ene reactions using norbornene dimethanol **2'** led us to check the reactivity of a norbornene entity contained in a polymer chain. We chose norbornenyl-functionalized bisPCL copolymer as another model compound as it is efficiently purified by precipitation; moreover, SEC and matrix-assisted laser desorption/ionization-time of flight (MALDI-ToF) mass spectrometry characterizations can be easily performed. Thiol-ene reaction between norbornenyl-functionalized bisPCL copolymer and dodecanethiol with an initial $[\text{NB}]_0/[\text{thiol}]_0$ ratio of 1:1 was realized in DCM in the presence of DMPA used as photoinitiator at room temperature under 365 nm wavelength UV light for 90 minutes (Scheme IV.7).



Scheme IV.7. Thiol-ene reaction of norbornenyl-functionalized bispoly(ϵ -caprolactone) and dodecanethiol

The reaction between norbornenyl-functionalized bisPCL copolymer and dodecanethiol (Scheme IV.7) was characterized by ^1H NMR spectroscopy and MALDI-ToF mass spectrometry. ^1H NMR spectrum of the reaction solution after 90 minutes (Figure IV.13, B) shows the complete disappearance of the signal related to protons of the double bond of norbornene at $\delta = 6.19$ ppm (labelled a, Figure IV.13, A) suggesting that the norbornene double bond completely reacts with dodecanethiol.

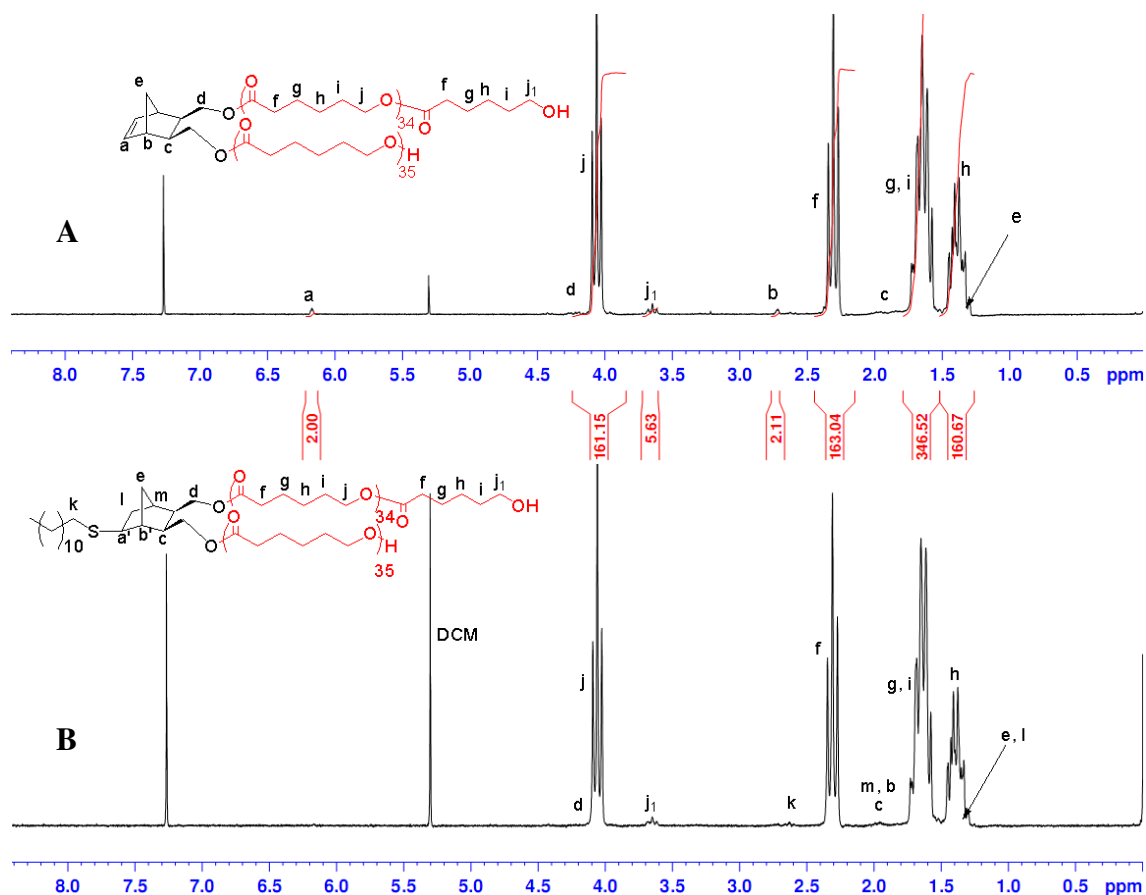


Figure IV.13. ^1H NMR spectra (200 MHz, 25 $^\circ\text{C}$) of crude mixtures from reaction between norbornenyl-functionalized bisPCL copolymer and dodecanethiol at (A) initial time and, (B) after 90 minutes; solvent: CDCl_3

The final polymer was purified by precipitation and analyzed by MALDI-ToF mass spectrometry (Figure IV.14). The MALDI-ToF mass spectrum of purified polymer showed only one population corresponding to a sodium ionized dodecylsulfonyl-functionalized bisPCL norbornene (experimental value $m/z = 7458.763$, calculated value $m/z = 7456.428$ for 62 repeating units - molar mass average error of 1.89 Dalton).

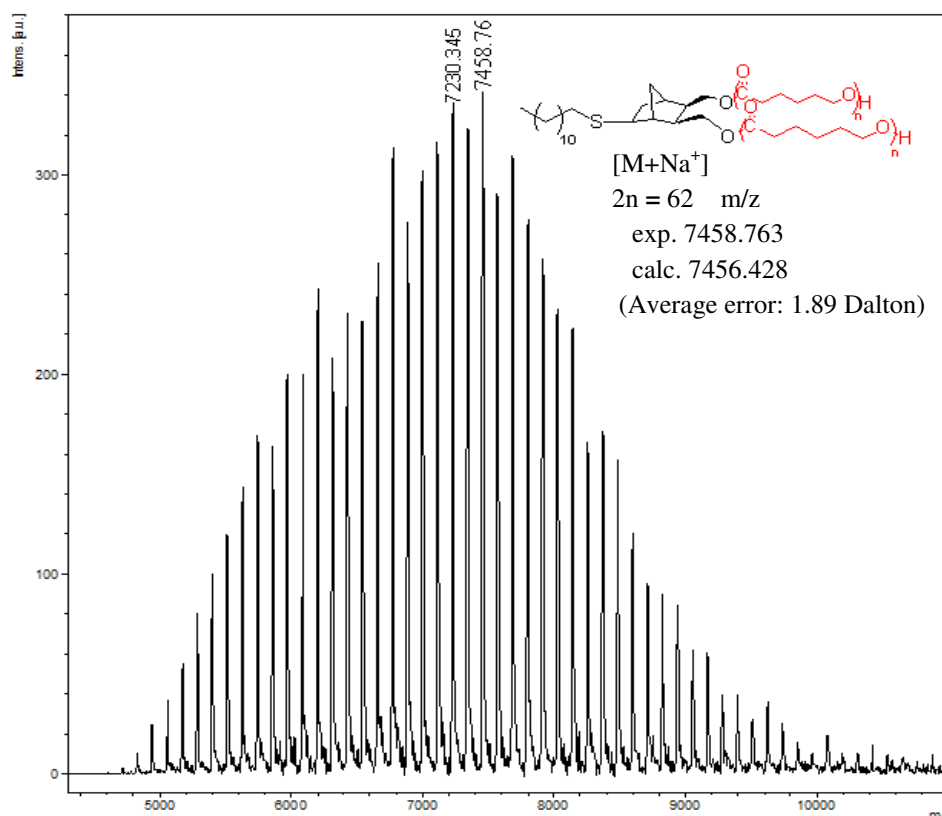
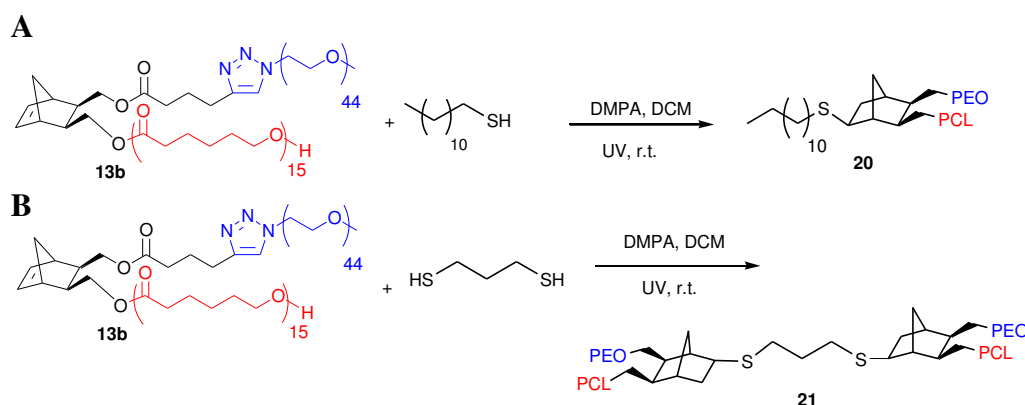


Figure IV.14. MALDI-ToF mass spectrum of dodecylsulfonyl-functionalized bisPCL norbornene, matrix: matrix: 2-[(2*E*)-3-(4-*tert*-butylphenyl)-2-methylprop-2-enylidene]malononitrile (DCTB), sodium trifluoroacetate (NaTFA)

In conclusion, a high reactivity of norbornene functionality toward thiol-ene reaction has been shown using norbornene dimethanol and norbornenyl-functionalized bisPCL copolymer with low molar mass thiol molecules.

III.3. Thiol-ene reaction using norbornenyl-functionalized PEO-*b*-PCL copolymer

The reactivity of the norbornenyl functionality within norbornenyl-functionalized PEO-*b*-PCL copolymer containing 44 units of EO and 15 units of CL (named PEO₄₄NBPCL₁₅) toward thiol-ene reaction was first evaluated with low molar mass thiol molecules to determine the influence of PEO chain and PCL chain. Thiol-ene reactions were carried out between PEO₄₄NBPCL₁₅ **13b** and PEO₄₄NBPCL₂₅ **13c** copolymers and dodecanethiol using an initial [NB]₀/[thiol]₀ ratio of 1:1 and propanedithiol using an initial [NB]₀/[dithiol]₀ ratio of 2:1. These reactions were conducted in DCM in the presence of DMPA photoinitiator under UV light (365 nm) at room temperature (Scheme IV.8).



Scheme IV.8 Thiol-ene reactions of norbornenyl-functionalized PEO-*b*-PCL copolymer with (A) dodecanethiol and, (B) propanedithiol

¹H NMR spectrum of the reaction mixture resulting from thiol-ene reaction between PEO₄₄NBPCL₁₅ and dodecanethiol after 90 minutes of reaction showed the decrease of the peak integration corresponding to protons of the double bond from norbornene ring at $\delta = 6.19$ ppm (labelled a, Figure IV.15, B) in comparison with the peak integration related to proton of the triazole ring at $\delta = 7.51$ ppm (labelled m, Figure IV.15, B). By comparing previous signals (labelled a & m, Figure IV.15), at initial time and after 90 minutes of reaction, a conversion of 80% has been reached. That conversion is lower than the one obtained during thiol-ene reaction of norbornenyl-functionalized bisPCL copolymer. Such result shows that the nature of polymer surrounding the norbornene group has an influence on the norbornene reactivity.

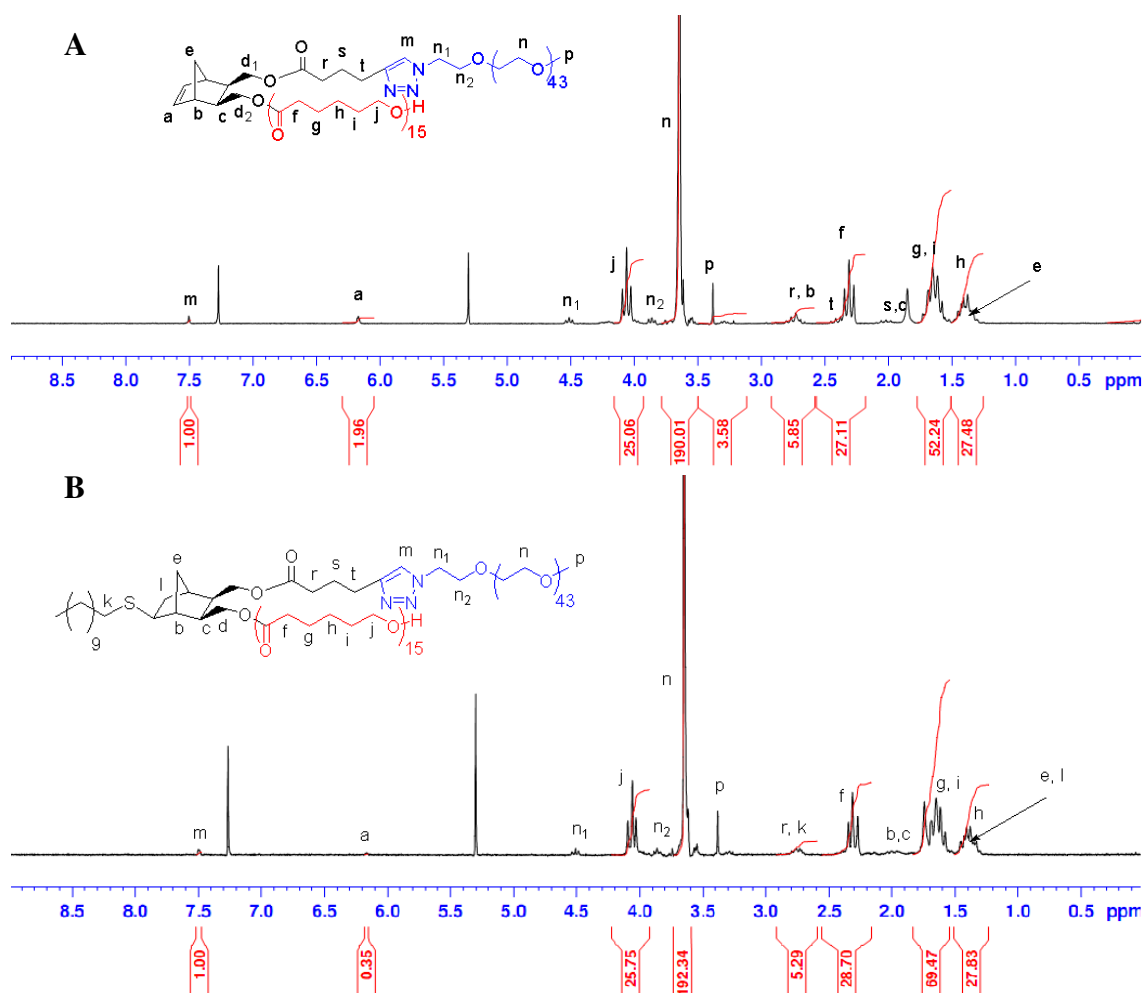


Figure IV.15. ^1H NMR spectra (200 MHz, 25 $^\circ\text{C}$) of crude mixtures resulting from thiol-ene reaction between $\text{PEO}_{44}\text{NBPCl}_{15}$ and dodecanethiol at (A) initial time and, (B) after 90 minutes; solvent: CDCl_3

Reaction of $\text{PEO}_{44}\text{NBPCl}_{15}$ and propanedithiol (Scheme IV.7, B) was carried out during 5 h to target quantitative thiol-ene conversion. Indeed, ^1H NMR spectrum after 5 h of reaction showed the complete reduction of the double bond within the norbornene functionality of initial copolymer at $\delta = 6.18$ ppm (labelled a, Figure IV.16, A), indicating that thiol-ene reaction using norbornene functionality in norbornenyl-functionalized PEO-*b*-PCL copolymer was successful with nearly quantitative conversion with a longer reaction time.

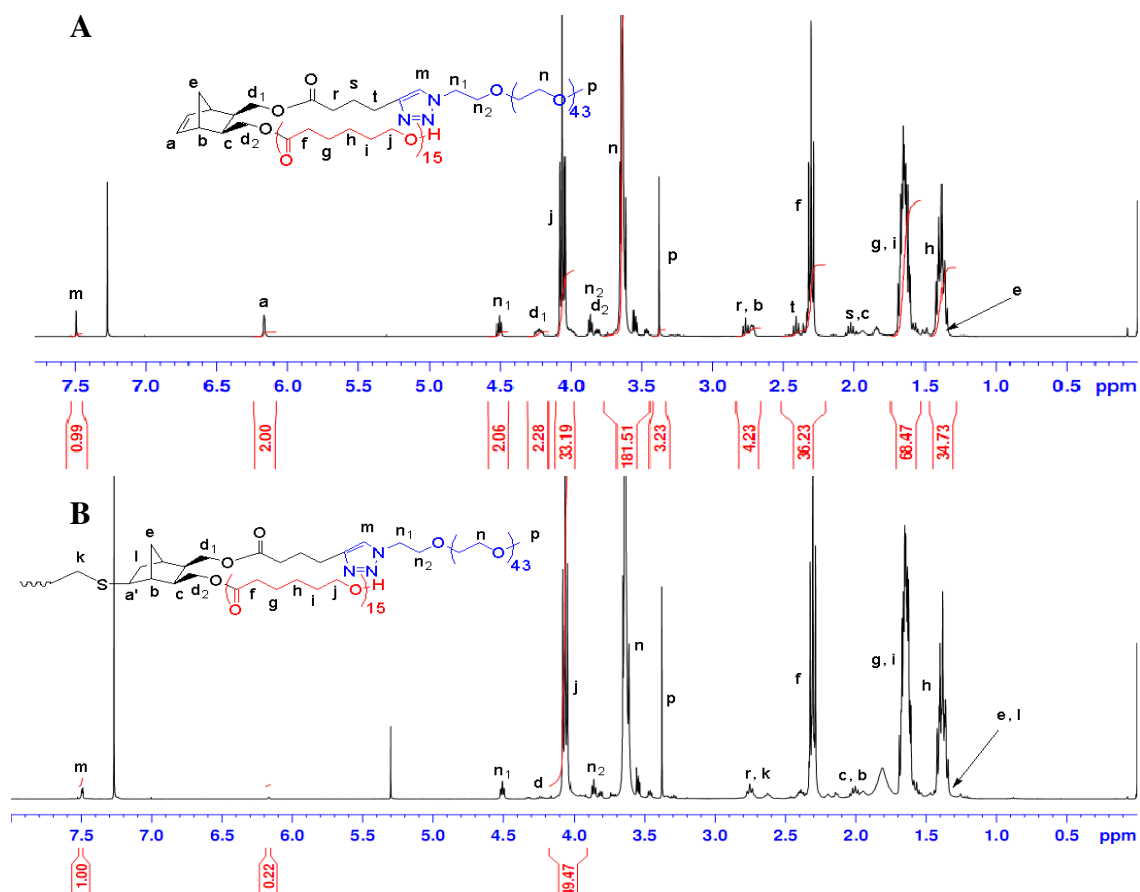


Figure IV.16. ^1H NMR spectra (400 MHz, 25 $^\circ\text{C}$) of crude mixtures resulting from thiol-ene reaction between $\text{PEO}_{44}\text{NB}\text{PCL}_{15}$ and propanedithiol at (A) initial time and, (B) after 5 hours of reaction; solvent: CDCl_3

The SEC trace of the reaction mixture after 5 h showed a shift toward lower retention times corresponding to a A_2B_2 mikto-arm star copolymer based on PCL and PEO in comparison to SEC trace of initial $\text{PEO}_{44}\text{NB}\text{PCL}_{15}$ at higher retention times (Figure IV.17) showed an agreement results with ^1H NMR analysis. Moreover, the molar mass distribution of the resulting copolymer remains low ($\mathcal{D}_M = 1.09$) showing that such synthetic strategy is effective to target well-defined (PCL_2 , PEO_2) mikto-arm star copolymer.

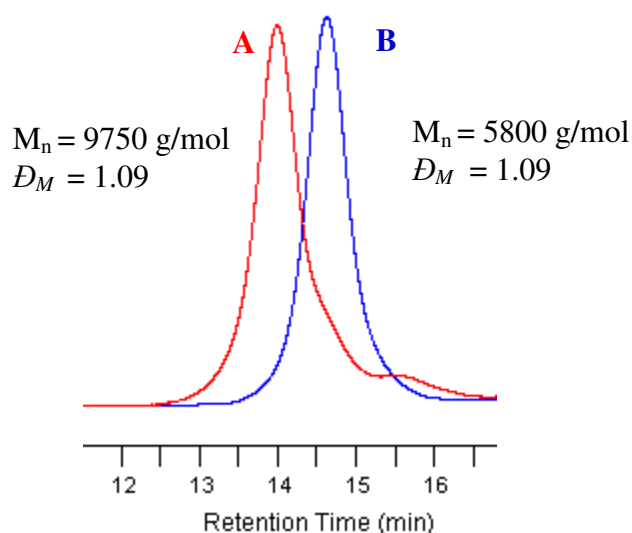


Figure IV.17. SEC traces of (A) (PCL_2 , PEO_2) mikto-arm star copolymer based on PCL and PEO and (B) $\text{PEO}_{44}\text{NBPCL}_{15}$ copolymer

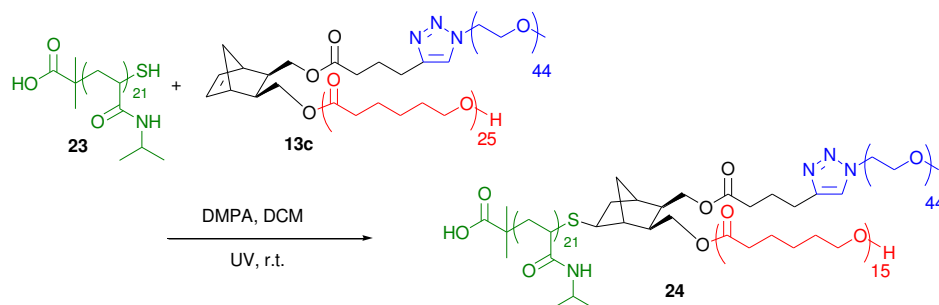
Those results highlight the high reactivity of the norbornene group in norbornenyl-functionalized PEO-*b*-PCL copolymer during thiol-ene reaction. Such reaction will now be studied in order to obtain mikto-arm star copolymer containing PEO, PCL and poly(*N*-isopropylacrylamide) (PNIPAM) chains. Such a copolymer will combine hydrophilic and biocompatible properties of PEO, biodegradable property of hydrophobic PCL and thermoresponsive property of PNIPAM.

III.4. Synthesis of (PCL , PEO , PNIPAM) mikto-arm star copolymers from norbornenyl functionalized PEO-*b*-PCL copolymer

A mikto-arm star copolymer was synthesized by thiol-ene reaction from a thiol-functionalized poly(*N*-isopropylacrylamide) PNIPAM (PNIPAM-SH) and a norbornenyl-functionalized PEO-*b*-PCL copolymer (Scheme IV.9).

The PNIPAM-SH was synthesized from RAFT polymerization of *N*-isopropylacrylamide (NIPAM) using S-dodecyl-S'-(α,α' -dimethyl- α'' -acetic acid)trithiocarbonate (DDMAT) as chain transfer agent in the presence of azobisisobutyronitrile (AIBN) in *N,N*-dimethylformamide (DMF) at 70 °C⁴¹ followed by the aminolysis of the trithiocarbonate group to generate thiol functionality⁴² as reported by our group. Resulting PNIPAM-SH has $M_n = 4250$ g/mol and $D_M = 1.16$.

Thiol-ene reaction between the PNIPAM-SH and the $\text{PEO}_{44}\text{NB}\text{PCL}_{25}$ **13c** copolymer was performed in DCM at room temperature with an initial $[\text{PEO}_{44}\text{NB}\text{PCL}_{25}]_0/[\text{PNIPAM-SH}]_0$ ratio of 1/1 in the presence of DMPA used as photoinitiator under UV light (365 nm). The reaction was carried out for 5 h and analyzed by ^1H NMR spectroscopy.



Scheme IV.9. Thiol-ene reaction between PNIPAM-SH and $\text{PEO}_{44}\text{NB}\text{PCL}_{25}$ copolymer

The ^1H NMR spectrum of the reaction mixture after 5 h shows the presence of the signal corresponding to the double bond protons of the norbornene ring at $\delta = 6.19$ ppm (labelled a, Figure IV.18, B). Such result shows that thiol-ene reaction between PNIPAM-SH and $\text{PEO}_{44}\text{NB}\text{PCL}_{25}$ was not quantitative. The integration value corresponding to the signal of double bond protons of norbornene ring at $\delta = 6.19$ ppm decreases from 2.02 (Figure IV.18, A) to 1.25 (Figure IV.18, B) after 5h of reaction using integration value of the signal corresponding to one proton in triazole ring at $\delta = 7.51$ ppm (labelled m, Figure IV.18) as internal standard. Therefore, the reaction conversion reaches 39%.

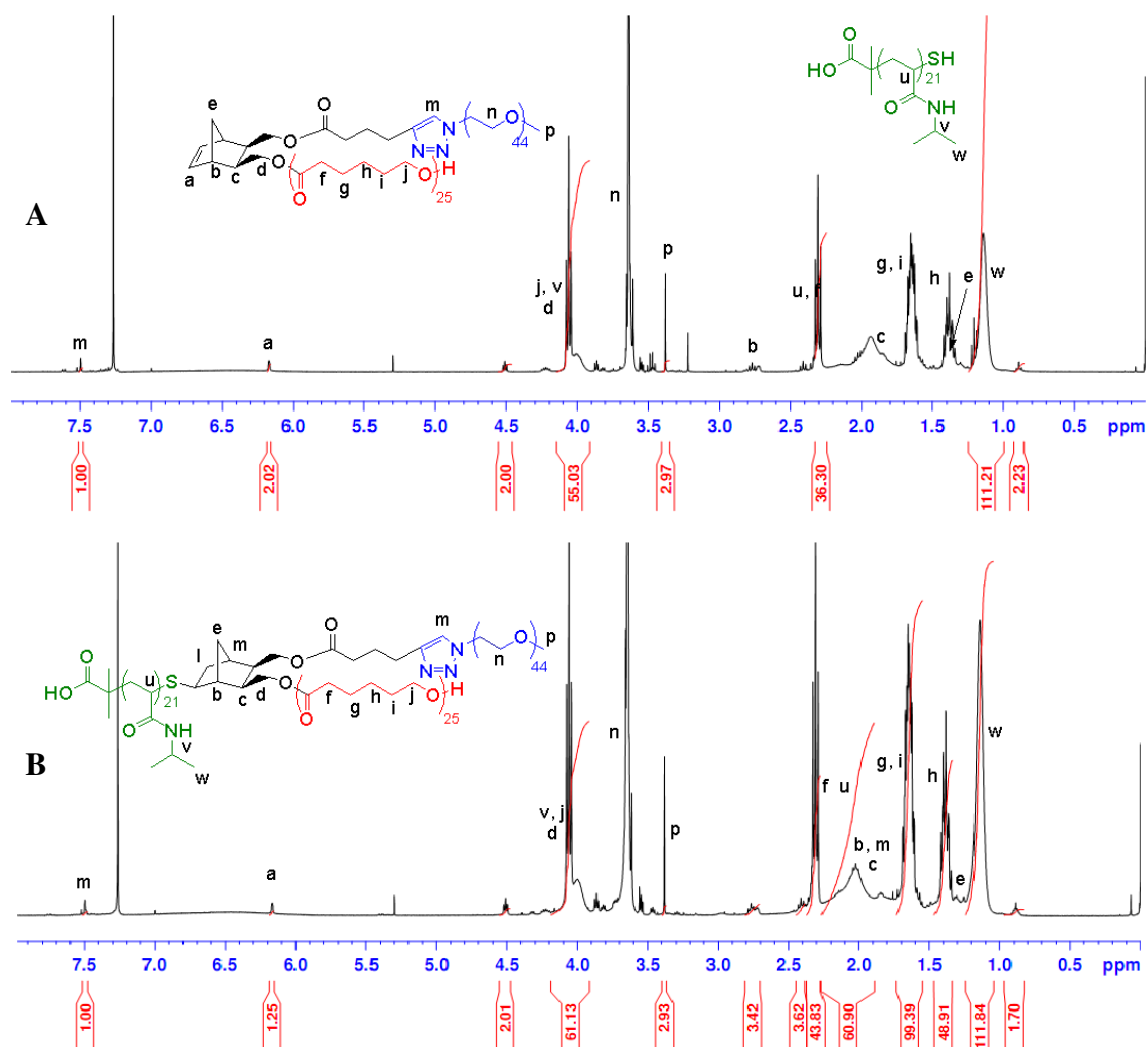


Figure IV.18. ^1H NMR spectra (400 MHz, 25 °C) of the crude mixtures resulting from thiol-ene reaction between PNIPAM-SH and $\text{PEO}_{44}\text{NBPCL}_{25}$ at (A) initial time and (B) after 5 hours of reaction; solvent: CDCl_3

The (PCL, PEO, PNIPAM) mikto-arm star copolymer was characterized by SEC in DMF with a RI detector, calibrated with linear polystyrene standards (Figure IV.19). The slight shift of SEC trace of mikto-arm star copolymer toward lower retention times in comparison with $\text{PEO}_{44}\text{NBPCL}_{25}$ and PNIPAM-SH traces confirms that the reaction between $\text{PEO}_{44}\text{NBPCL}_{25}$ and PNIPAM-SH is successful but in limited conversion. Such result is in good agreement with several studies showing that radical thiol-ene reactions between polymer - polymer are non-quantitative.⁴³

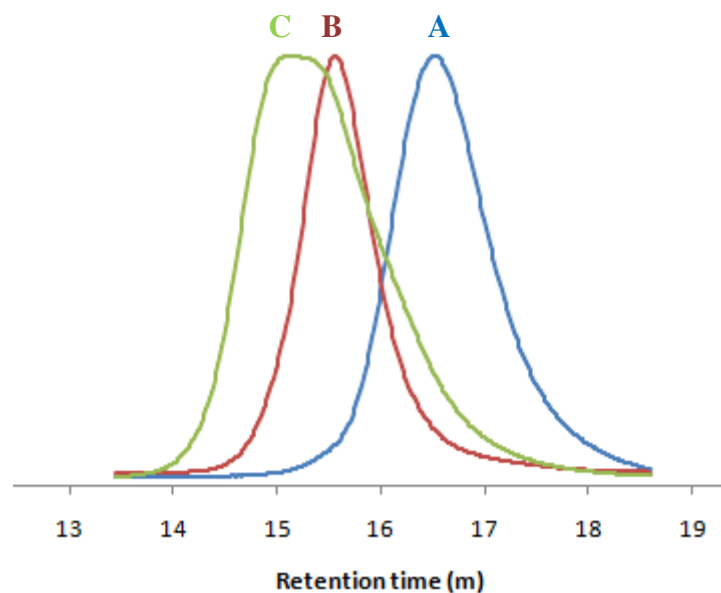


Figure IV.18. SEC traces of (A) PNIPAM-SH, (B) PEO₄₄NB-PCL₂₅ and (C) mikto-arm star copolymer based on PEO, PCL and PNIPAM

Conclusion

The reactivity of the norbornene ring within norbornenyl-functionalized PEO-*b*-PCL copolymers has been investigated in ROMP and thiol-ene reactions.

A new ROMP macroinitiator has been successfully synthesized from a norbornenyl-functionalized PEO-*b*-PCL copolymer and G1 catalyst in order to increase water-solubility of G1 catalyst. Hydrodynamic diameter and polydispersity values of micelles generated from such a macroinitiator dispersed in water are 13.75 nm and 0.278, respectively. This macroinitiator exhibits a high reactivity to initiate ROMP of NB in solution resulting in a well-defined umbrella-like PNB-*b*-[(PNB-*g*-(PEO/PCL))] umbrella-like copolymer ($D_M = 1.21$).

ROMP of norbornenyl-functionalized PEO-*b*-PCL macromonomers in solution has been studied. The results showed that the use of G1, G2 or G3' as initiators is unsuitable as the presence of unreacted macromonomers with an initial $[M]_0/[I]_0$ ratio of 10 has been observed. ROMP of norbornenyl-functionalized PEO-*b*-PCL macromonomer using G3 as an initiator reached quantitative conversion with an initial $[M]_0/[I]_0$ ratio of 10. When the initial $[M]_0/[I]_0$ ratio was increased up to 50, macromonomer conversion reached 42%. However, the resulting well-defined PNB-*g*-(PEO/PCL) graft copolymer ($D_M = 1.08$) has been successfully purified and characterized by DSC and TGA measurements. Interestingly, thermal analysis results showed the separation of crystallization processes corresponding to PEO and PCL blocks of macromonomers, but the graft copolymer shows a lower crystallization temperature compared to the crystallization temperature of either PEO or PCL blocks of its macromonomers.

Norbornene reactivity toward thiol-ene reactions was investigated using norbornene dimethanol and norbornenyl-functionalized bisPCL copolymer as model compounds. The results showed a high thiol-ene reactivity of the norbornene functionality in either small molecules or macromolecules.

Based on the high reactivity toward thiol-ene reactions of norbornene functionality in macromolecules, ABC mikto-arm star and A_2B_2 mikto-arm star copolymers were synthesized from norbornenyl-functionalized PEO-*b*-PCL copolymer with a thiol-functionalized PNIPAM and propanedithiol, respectively. ^1H NMR and SEC results demonstrated that the PEO, PCL and PNIPAM mikto-arm star (PEO; PCL; PNIPAM)

copolymer was successfully obtained *via* thiol-ene reaction. However, limited conversion of the reaction between norbornenyl-functionalized PEO-*b*-PCL copolymer and thiol-functionalized PNIPAM equals to 42% is in good agreement with non-quantitative conversions “click” reactions between two polymers as reported in the literature.^{43,44} On the other hand, norbornenyl-functionalized PEO-*b*-PCL copolymer exhibits a high reactivity toward propanedithiol resulting in a A₂B₂ mikto-arm star copolymer containing 2 PCL chain arms and 2 PEO chain arms.

Our results demonstrate that norbornenyl-functionalized PEO-*b*-PCL constitutes a versatile platform to target well-defined comb-like, umbrella-like graft copolymers, and (mikto-arm) star copolymers.

References

- ¹ R. H. Grubbs, E. Khosravi, *Handbook of Metathesis*, 2nd Ed., vol.3. Wiley-VCH, Weinheim, **2015**
- ² R. Madan, A. Srivastava, R. C. Anand, I. K. Varma, *Prog. Polym. Sci.* **1998**, 23, 621-663
- ³ C. W. Bielawski, R. H. Grubbs, *Prog. Polym. Sci.* **2007**, 32, 1-29
- ⁴ V. Lapinte, L. Fontaine, V. Montembault, I. Campistron, D. Reyx, *J. Mol. Catal. A: Chem.* **2002**, 190, 117-129
- ⁵ C. Cheng, K. Qi, E. Khoshdel, K. L. Wooley, *J. Am. Chem. Soc.* **2006**, 128, 6808-6809
- ⁶ G. Morandi, G. Mantovani, V. Montembault, D.M. Haddleton, L. Fontaine, *New J. Chem.* **2007**, 31, 1826-1829
- ⁷ C. E. Hoyle, T. Y. Lee, T. Roper, *J. Polym. Sci. Part A: Polym. Chem.* **2004**, 42, 5301-5338
- ⁸ P. Theato, H.-A. Klok, *Functional Polymers by Post-Polymerization Modification*, Wiley-VCH, Weinheim, **2012**
- ⁹ C. R. Morgan, F. Magnotta, A. D. Ketley, *J. Polym. Sci. Polym. Chem. Ed.* **1977**, 15, 627-645
- ¹⁰ B. H. Northrop, R. N. Coffey, *J. Am. Chem. Soc.* **2012**, 134, 13804-13817
- ¹¹ C. N. Walker, J. M. Sarapas, V. Kung, A. L. Hall, G. N. Tew, *ACS Macrolett.* **2014**, 3, 453-457
- ¹² M. M. Stamenović, P. Espeel, W. V. Camp, P. E. Du Prez, *Macromolecules* **2011**, 44, 5619-5630
- ¹³ Q. Fu, J. Liu, W. Shi, *Prog. Org. Coat.* **2008**, 63, 100-109
- ¹⁴ C. C. Lin, C. S. Ki, H. Shih, *J. Appl. Polym. Sci.* **2015**, DOI: 10.1002/App.41563
- ¹⁵ W. J. Feast, V. C. Gibson, A. F. Johnson, E. Khosravi, M. A. Mohsin, *J. Mol. Catal. A: Chem.* **1997**, 115, 37-42
- ¹⁶ Y. Tsukahara, S. Namba, J. Iwasa, Y. Nakano, K. Kaeriyama, M. Takahashi, *Macromolecules* **2001**, 34, 2624-2629
- ¹⁷ J. B. Matson, G. H. Grubbs, *J. Am. Chem. Soc.* **2008**, 130, 6731-6733
- ¹⁸ G. Morandi, V. Montembault, S. Pascual, S. Legoupy, L. Fontaine, *Macromolecules* **2006**, 39, 2732-2735

- ¹⁹ V. Héroguez, S. Breunig, Y. Gnanou, M. Fontanille, *Macromolecules* **1996**, *29*, 4459-4464
- ²⁰ L. Pichavant, C. Bourget, M. C. Durrieu, V. Héroguez, *Macromolecules* **2011**, *44*, 7879-7887
- ²¹ J. Zou, G. Jafr, E. Themistou, Y. Yap, Z. A. P. Wintrob, P. Alexandridis, A. C. Ceacareanu, C. Cheng, *Chem. Commun.* **2011**, *47*, 4493-4495
- ²² K. Breitenkamp, J. Simeone, E. Jin, T. Emrick, *Macromolecules* **2002**, *35*, 9249-9252
- ²³ S. F. Alfred, Z. M. Al-Bardi, A. E. Madkour, K. Lienkamp, G. N. Tew, *J. Polym. Sci., Part A: Polym. Chem.* **2008**, *46*, 2640-2648
- ²⁴ N. B. Sankaran, A. Z. Rys, R. Nassif, M. K. Nayak, K. Metera, B. Chen, H. S. Bazzi, H. F. Sleiman, *Macromolecules* **2010**, *43*, 5530-5537
- ²⁵ J. A. Johnson, Y. Y. Lu, , A. O. Burts, Y. Xia, A. C. Durrell, D. A. Tirrell, R. H. Grubbs, *Macromolecules* **2010**, *43*, 10326-10335
- ²⁶ D. Mecerreyes, D. Dahan, P. Lecomte, A. Demonceau, A. F. Noels, J. Jerome, *J. Polym. Sci., Part A: Polym. Chem.* **1999**, *37*, 2447-2455
- ²⁷ M. Xie, J. Dang, H. Han, W. Wang, J. Liu, X. He, Y. Zhang, *Macromolecules* **2008**, *41*, 9004-9010
- ²⁸ Q. Fu, J. M. Ren, G. G. Qiao, *Polym. Chem.* **2012**, *3*, 343-351
- ²⁹ D. Yang, W. Huang, J. Yu, J. Jiang, L. Zhang, M. Xie, *Polymer* **2010**, *51*, 5100-5106
- ³⁰ H. Zhang, Z. Zhang, Y. Gnanou, N. Hadjichristidis, *Macromolecules* **2015**, *48*, 3556-3562
- ³¹ A. B. Lowe, *Polym. Chem.* **2014**, *5*, 4820-4870
- ³² P. Schwab, R. H. Grubbs, J. W. Ziller, *J. Am. Chem. Soc.* **1996**, *118*, 100-110
- ³³ C. Airaud, E. Ibarboure, C. Gaillard, V. Héroguez, *Macromol. Symp.* **2009**, *281*, 31-38
- ³⁴ D. Quémener, V. Héroguez, Y. Gnanou, *J. Polym. Sci. Part A: Polym. Chem.* **2006**, *44*, 2784-2793
- ³⁵ X. Shuai, T. Merdan, F. Unger, M. Wittmar, T. Kissel, *Macromolecules* **2003**, *36*, 5751-5759
- ³⁶ J. Brandrup, E. H. Immergut, E. A. Grulke, *Polymer Handbook*, Wiley, New York, **1999**
- ³⁷ C. He, J. Sun, J. Ma, X. Chen, X. Jing, *Biomacromolecules* **2006**, *7*, 3482-3489

- ³⁸ M. Deng, X. Chen, L. Piao, X. Zhang, Z. Dai, X. Jing, *J. Polym. Sci. Part A: Polym. Chem.* **2004**, 42, 950-959
- ³⁹ W. Yuan, J. Yuan, F. Zhang, X. Xie, C. Pan, *Macromolecules* **2007**, 40, 9094-9102
- ⁴⁰ C. B. Kowollik, F. E. Du Prez, P. Espeel, C. J. Hawker, T. Junkers, H. Schlaad, W. Van Camp, *Angew. Chem.* **2011**, 50, 60-62
- ⁴¹ M. E. Levere, H. T. Ho, S. Pascual, L. Fontaine, *Polym. Chem.* **2011**, 2, 2878-2887
- ⁴² H. T. Ho, M. Levere, J. C. Soutif, V. Montembault, S. Pascual, L. Fontaine, *Polym. Chem.*, **2011**, 2, 1258-1260
- ⁴³ S. P. S. Koo, M. M. Stamenović, R. A. Prasath, A. J. Inglis, F. E. Du Prez, C. B. Kowollik, W. Van Camp, T. Junkers, *J. Polym. Sci. Part A: Polym. Chem.* **2010**, 48, 1699-1713
- ⁴⁴ H. Gao, K. Matyjaszewski, *Macromolecules* **2006**, 39, 4960-4965

Materials

Grubbs' third generation catalysts (G3 and G3') syntheses were performed as reported in the literature.² Bicyclo[2,2,1]hept-2-ene (norbornene; NB, Aldrich, 99%) was distilled over CaH₂. Azobisisobutyronitrile (AIBN, Aldrich, 99%), chloroform (CHCl₃, Aldrich, 99%), dichloromethane (DCM, Aldrich, 99.8%), diethyl ether (Pro labo, 99.8%), S-dodecyl-S'-(α,α' -dimethyl- α'' -acetic acid)trithiocarbonate (DDMAT, Aldrich, 98%), 2,2'-dimethoxy-2-phenylacetophenone (DMPA, Aldrich, 99%), dimethylphenylphosphine (DMPP, Aldrich, 99%), dodecanethiol (Aldrich, 99%), ethyl vinyl ether (Aldrich, 99%), 2,2'-(ethylenedioxy)diethanethiol (Aldrich, 95%), Grubbs' first generation (G1, Aldrich, 97%), Grubbs' second generation (G2, Aldrich, 99%), magnesium sulfate (MgSO₄, Fisher chemical), *N,N*-dimethylformamide (DMF, Aldrich, 99.8%), *n*-hexylamine, *N*-isopropylacrylamide (NIPAM, Aldrich, 97%) (propanedithiol (Janssen Chimica, 98%), silicagel for column chromatography (Kieselgel 60, 230-400 mesh Merck), anhydrous tetrahydrofuran (THF, Aldrich, 99.9%), were purchased from commercial sources and used without further purification.

Characterization

NMR spectra were recorded on a Bruker Avance 400 (200 MHz for ¹H and 50 MHz for ¹³C) or Bruker AC-400 (400 MHz for ¹H and 100 MHz for ¹³C). Chemical shifts are reported in ppm relative to the deuterated solvent resonances.

Molar masses and dispersities were measured using size exclusion chromatography (SEC) on a system equipped with a SpectraSYSTEM AS1000 autosampler, with a Guard column (Polymer Laboratories, PL gel 5 μ m Guard column, 50 x 7.5 mm) followed by two columns (Polymer Laboratories, 2 PL gel 5 μ m MIXED-D columns, 2 x 300 x 7.5) and with a SpectraSYSTEM RI-150 detector. The eluent used was tetrahydrofuran (THF) at a flow rate of 1 mL.min⁻¹ at 35 °C. Polystyrene standards (580 - 4.83 x 10⁵ g.mol⁻¹) were used to calibrate the SEC.

SEC system operating in DMF as eluent at 60 °C fitted with a guard column (PL Gel 5 mm) and two Polymer Laboratory PolarGel columns, a Waters 410 differential refractometer (DRI) and a Waters 481UV detector operating at 309 nm. The instrument was used at a flow rate of 1.0 mL/min. Polystyrene standards (580 - 4.6 x 10⁵ g/mol) were used to calibrate the SEC.

MALDI-TOF MS analyses were realized on a Bruker Biflex III using 2-[(2E)-3-(4-tert-butylphenyl)-2-methylprop-2-enylidene]malononitrile (DCTB) as the matrix.

Dynamic light scattering was performed with a Malvern apparatus (NanoZS ZEN3600) equipped with a 4 mW He - Ne laser (emitting vertically polarized light at λ = 632.8 nm) and a thermostat bath controller at 20 °C. The autocorrelation functions were analyzed in terms of relaxation time (τ)

² M. S. Sanford, J. A. Love, R. H. Grubbs, *Organometallics* **2001**, 20, 5314-5318

distribution. The method of the cumulants was generally used to analyze DLS results, while size distribution histograms were obtained by the CONTIN method. The polydispersity (PDI) of the micelles was estimated from the Γ_2/Γ_1^2 ratio in which represents the first and second cumulant, respectively. Measurements were made at a angle detection of 173° using a copolymer concentration of 1 g/L.

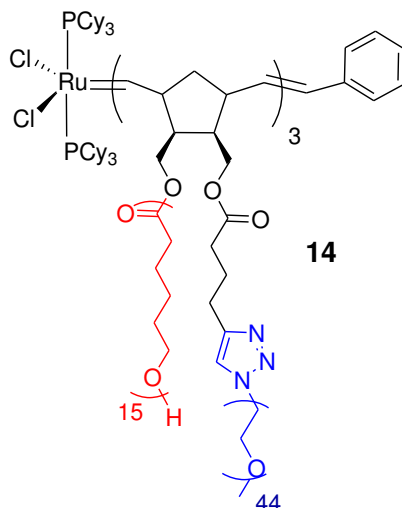
DLS samples preparation

Prior to use, sample solutions were prepared using Millipore (18.2 MΩ) water in a hood that was kept dust-free by an air circulation system. The copolymer sample was weighed into a dust-free sample vial and was dissolved in THF using a copolymer concentration of 100 g/L. Afterwards, Millipore water was added in order to obtain a concentration of macromonomers in water of 1 g/L. This solution was kept stirring for 2 hours at room temperature followed by free evaporation of THF for 24 hours. They were then filtered through 0.2 μm pore size Anotop syringe filters into a disposable PS vessel for dynamic light scattering measurements.

DSC analysis was performed on a Q100-TA Instruments under N₂ in a range of -80 °C – 250 °C using heating rate and cooling rate of 10 °C/min. The samples were quenched from 25 °C to -80 °C with a cooling rate of 10 °C/min. After holding at -80 °C for 5 minutes, the samples were heated to 250 °C with a heating rate of 10 °C/min, followed by quenched to -80 °C with a cooling rate of 10 °C/min. The operation was conducted for two cycles.

TGA analysis was performed on a Q500-TA Instruments under N₂ in a range of 40 °C – 800 °C using heating rate of 10 °C/min.

*Synthesis of ROMP macroinitiator 14 from norbornenyl-functionalized PEO-*b*-PCL copolymer and Grubbs 1*

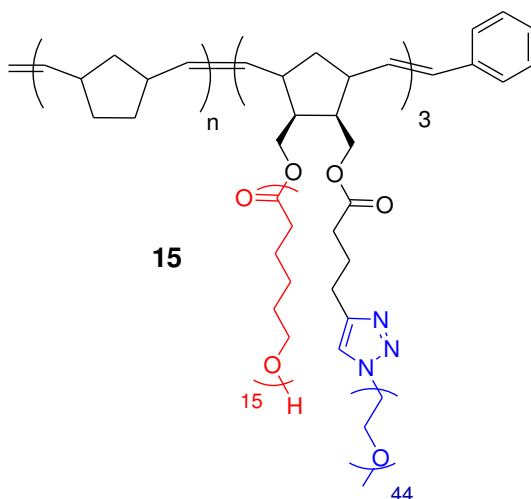


13b (Norbornenyl-functionalized PEO₄₄-*b*-PCL₁₅) (0.4 g, 1 mmol) was charged into a dried Schlenk flask equipped with a rubber septum and a magnetic stirrer under N₂ in a glove box. 4.2 mL of degassed anhydrous THF was added to dissolve **13b**. In a separated vial, G1 (0.026 g, 0.33 mmol) was charged under N₂ in a glove box followed by its dissolution in 2.1 mL of degassed anhydrous THF. 1.4 mL of **13b** solution was slowly added into G1 solution under N₂ in the glove box at room temperature and kept stirring for 1 hour. The rest of **13b** solution was then added to the previous reaction mixture. The evolution of the reaction was measured by ¹H NMR spectroscopy. A red solution was obtained (with concentration of ROMP macroinitiator of 0.0524 mmol/mL).

¹H NMR (400 MHz, CDCl₃), δ (ppm): 19.8 (s, 1H, Ru=CH-CH), 7.51 (s, 3H, triazole), 5.05-5.35 (broad, 5H, -CH=CH-), 4.45 (t, J = 5.6 Hz, 6H, triazole-CH₂-CH₂), 4.00-4.20 (t, J = 7.2 Hz, 90H, CH₂OCO, PCL), 3.60 - 3.80 (m, 516H, CH₂, PEO), 3.38 (s, 9H, -CH₃), 2.64 (m, 6H, OCOCH₂CH₂CH₂-triazole; 6H, CHCH₂CH), 2.25 - 2.35 (m, 90H, O-COCH₂, PCL), 1.98 (m, 6H, OCOCH₂CH₂CH₂-triazole), 1.85 (m, 6H, COOCH₂CHCHCH₂COO), 1.55 - 1.75 (m, 180H, CH₂CH₂CH₂-OCO; CO-CH₂CH₂, PCL), 1.35 - 1.45 (m, 90H, CH₂CH₂CH₂-OCO, PCL).

SEC: M_n = 17500 g/mol; D_M = 1.11

Synthesis of umbrella-like graft copolymer PNB-b-[(PNB-g-(PEO/PCL)] 15



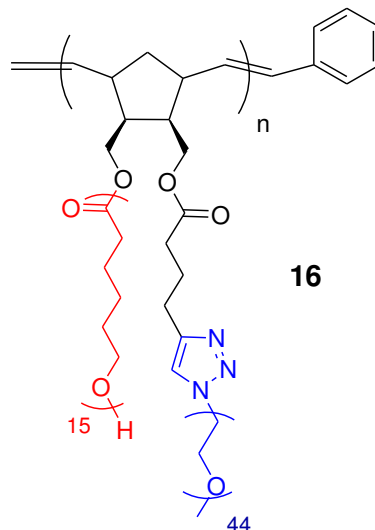
Distillated NB (0.26 g, 2.77 mmol) was dissolved in 5.2 mL of anhydrous THF in a dried Schlenk flask equipped with a rubber septum and a magnetic stirrer bar. The solution was degassed by 5 free-thaw cycles. 0.035 mL of ROMP macroinitiator solution ($\sim 1.83 \times 10^{-3}$ mmol; calculated from concentration of ROMP macroinitiator solution of 0.0524 mmol/mL in anhydrous THF) was injected into the Schlenk under N_2 in a glove box at room temperature to start the ROMP. The mixture was kept stirring for 3 hours and reaction was stopped by adding 3 drops of ethyl vinyl ether. Solvent was removed using a rotary evaporator and the reaction mixture was purified by filtration through a short column of silica using $CHCl_3$ as eluent. Yield: 60%.

1H NMR (400 MHz, $CDCl_3$), δ (ppm): 5.28 ($-CH=CH_{trans}$) and 5.13 ($-CH=CH_{cis}$) (m, 2nH); 4.00-4.20 (t, $J = 6.4$ Hz) 90H, CH_2OCO (PCL)), 3.60 - 3.80 (m, 516H, PEO; CH_2), 3.38 (s, 9H, $-CH_3$), 2.69 ($CHCH_2CH_{cis}$) and 2.37 ($CHCH_2CH_{trans}$) (m, 2nH), 1.79 and 0.97 (m, 2nH, $CHCH_2CH$), 1.70 and 1.28 (m, 4nH, $CHCH_2CH_2CH$).

^{13}C NMR (100 MHz, $CDCl_3$), δ (ppm): 134.0113 ($-CH=CH_{cis}$), 133.04 ($-CH=CH_{trans}$), 43.10 ($CHCH_2CH_{trans}$), 41.40 ($CHCH_2CH$), 38.40 ($CHCH_2CH_{cis}$), 32.30 ($CHCH_2CH_2CH$).

SEC MALLS: $M_w = 6.224 \times 10^5$ g/mol

Synthesis of comb-like graft copolymer 16 by ROMP of norbornenyl PEO-b-PCL macromonomer



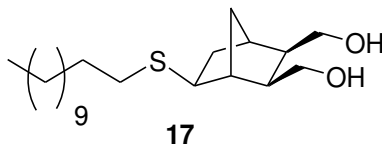
In a typical experiment, a dried Schlenk flask equipped with a rubber septum and magnetic stirrer bar was charged with the macromonomer **13b** (0.1 g, 2.5×10^{-2} mmol) and degassed using 3 vacuum/argon cycles. The anhydrous THF previously degassed by 5 freeze-thaw cycles was added ($[\mathbf{13b}]_0 = 0.04$ mol/L) *via* a syringe under argon to dissolve the macromonomer. A stock solution of Grubbs' catalyst (G1, G2, G3 or G3') in anhydrous THF was prepared in a separated vial. The Schlenk flask was immersed in an oil bath preset at 25 °C. The desired quantity of Grubbs' catalyst solution was injected into the Schlenk to initiate the reaction. The reaction mixture was stirred for 3 hours and the polymerization was quenched by the addition of 3 drops of ethyl vinyl ether. The solvent was removed using a rotary evaporator, the residue was purified by filtration through a short silica column using CHCl_3 as eluent. Yield: 50%.

^1H NMR (400 MHz, CDCl_3), δ (ppm): 7.51 (s, nH, triazole), 5.05 - 5.35 (broad, 2nH, $-\text{CH}=\text{CH}-$ *trans/cis*), 4.45 (t, $J = 6.0$ Hz, 2nH, triazole- CH_2 - CH_2), 4.00 - 4.20 (t, $J = 7.2$ Hz) 30nH, CH_2OCO (PCL)), 3.60 - 3.80 (m, 176nH, PEO; CH_2), 3.38 (s, 3nH, $-\text{CH}_3$), 2.64 (m, 4nH, $\text{OCOCH}_2\text{CH}_2\text{CH}_2$ -triazole; CHCH_2CH), 2.25 - 2.35 (m, 32nH, PCL; O-COCH_2 ; $\text{OCOCH}_2\text{CH}_2\text{CH}_2$ -triazole), 1.98 - 2.04 (m, 4nH, $\text{OCOCH}_2\text{CH}_2\text{CH}_2$ -triazole; $\text{COOCH}_2\text{CHCHCH}_2\text{COO}$), 1.55 - 1.75 (m, 30nH, PCL; $\text{CH}_2\text{CH}_2\text{CH}_2$ -OCO; $\text{CO-CH}_2\text{CH}_2$), 1.35 - 1.45 (m, 30nH, $\text{CH}_2\text{CH}_2\text{CH}_2$ -OCO).

^{13}C NMR (100 MHz, CDCl_3), δ (ppm): 173.5 ($\text{C}=\text{O}$), 70.6 (CH_2 ; PEO). 64.1 (CH_2OCO ; PCL), 59.0 (CH_3 , PEO); 34.13 (OCO-CH_2 , PCL); 28.4 ($\text{CH}_2\text{CH}_2\text{OCO}$, PCL), 25.5 ($\text{CH}_2\text{CH}_2\text{CH}_2\text{OCO}$, PCL), 24.6 ($\text{OCOCH}_2\text{CH}_2$, PCL).

SEC: $M_n = 32000$ g/mol; $D_M = 1.10$

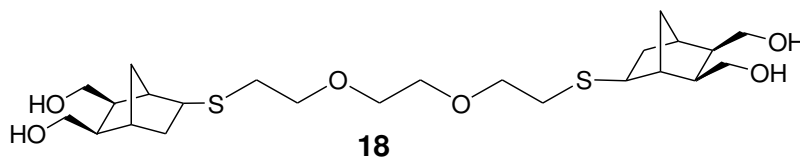
Thiol-ene reaction of norbornene dimethanol and dodecanethiol



Norbornene dimethanol **2'** (0.05 g, 0.325 mmol, 1 eq) was charged into a dried Schlenk tube equipped with a rubber septum and a magnetic stirrer bar and degassed using 3 vacuum/argon cycles. 3 mL of dried DCM was added to dissolve **2'**. Dodecanethiol (0.1052 g, 0.52 mmol) was dissolved in 1.6 mL of dried DCM in a separated vial under argon to target a dodecanethiol concentration of 0.325 mol/L. DMPA (0.0153 g, 0.069 mmol) was dissolved in 1 mL of dried DCM in another vial under argon to target a DMPA concentration of 0.06 mol/L. 1 mL of dodecanethiol solution (0.325 mmol, 1eq) was added into the Schlenk tube followed by the addition of 0.542 mL of DMPA solution (0.0325 mmol, 0.1 eq). Thiol-ene reaction started by immersing the Schlenk tube under a UV light (365 nm) at room temperature for 90 minutes. The completion of the reaction was measured by ^1H NMR analysis of the crude reaction mixture. Conversion: 100%

^1H NMR (200 MHz, CDCl_3), δ (ppm): 3.65 (m, 4H, CH_2OH), 2.95 (broad, 2H, OH), 2.75 (m, 1H, SCHCH), 2.50 (t, $J = 7.4$ Hz, 2H, $\text{CH}_2\text{CH}_2\text{S}$), 1.95 (m, 4H, $\text{CHCHCH}_2\text{CHCH}$), 1.45 and 1.80 (m, 4H, SCHCH_2), 1.45 and 1.30 (m, 2H, $\text{CH}_2\text{CH}_2\text{S}$), 1.25-1.35 (s, 20H, $\text{CH}_3(\text{CH}_2)_9\text{CH}_2$; CHCH_2CH), 0.85 (m, 3H, CH_3CH_2)

Thiol-ene reaction of norbornene dimethanol and 2,2'-(ethylenedioxy)diethanethiol

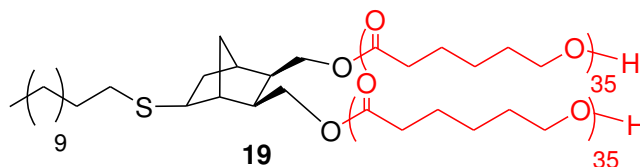


Norbornene dimethanol **2'** (0.05 g, 0.325 mmol, 2 eq) was charged into a dried Schlenk tube equipped with a rubber septum and a magnetic stirrer bar and degassed using 3 vacuum/argon cycles. 3 mL of dried DCM was added to dissolve **2'**. 2,2'-(ethylenedioxy)diethanethiol (0.0445 g, 0.244 mmol) was dissolved in 1.5 mL of dried DCM in a separated vial under argon to target a 2,2'-(ethylenedioxy)diethanethiol concentration of 0.325 mol/L. DMPA (0.0153 g, 0.069 mmol) was dissolved in 1 mL of dried DCM in another vial under argon to target a DMPA concentration of 0.06 mol/L. 1 mL of 2,2'-(ethylenedioxy)diethanethiol solution (0.1625 mmol, 1eq) was added into the Schlenk tube followed by the addition of 0.271 mL of DMPA solution (0.0163 mmol, 0.1 eq). Thiol-ene reaction started by immersing the Schlenk tube under UV light (365 nm) at room temperature for 90 minutes. The

evolution of the reaction was measured by ^1H NMR analysis of the crude reaction mixture. Conversion: 100%

^1H NMR (400 MHz, CDCl_3), δ (ppm): 3.65 (m, 16H, CH_2OH ; CH_2OCH_2), 3.20 (broad, 4H, OH), 2.85 (m, 2H, SCHCH), 2.70 (m, 4H, $\text{CH}_2\text{CH}_2\text{S}$), 1.95 (m, 4H, $\text{CHCHCH}_2\text{CHCH}$), 1.35 and 1.80 (m, 4H, SCHCH_2), 1.35 and 1.45 (m, 4H, CHCH_2CH).

Thiol-ene reaction of norbornenyl-functionalized diPCL copolymer and dodecanethiol

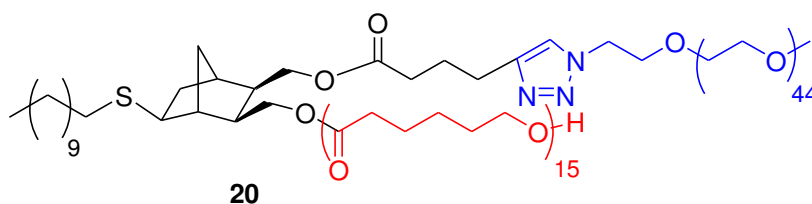


Norbornenyl-functionalized diPCL macromonomer (0.05 g, 6.10×10^{-3} mmol, 1eq) was charged into a dried Schlenk tube equipped with a rubber septum and a magnetic stirrer bar and degassed using 3 vacuum/argon cycles. 0.5 mL of dried DCM was added to dissolve the macromonomer. Dodecanethiol (28.1 mg, 0.139 mmol) was dissolved in 1.14 mL of dried DCM in a separated vial under argon to target a dodecanethiol concentration of 0.122 mol/L. DMPA (6.7 mg, 0.026 mmol) was dissolved in 3.43 mL of dried DCM in another vial under argon to target a DMPA concentration of 0.76×10^{-3} mol/L. 0.05 mL of dodecanethiol solution (6.10×10^{-3} mmol, 1eq) was added into the Schlenk tube followed by the addition of 0.08 mL of DMPA solution (0.610×10^{-3} mmol, 0.1 eq). Thiol-ene reaction started by setting the Schlenk under UV light (365 nm) at room temperature for 90 minutes. The evolution of the reaction was analyzed by ^1H NMR spectroscopy of the crude reaction mixture. Conversion: 100%

^1H NMR (200 MHz, CDCl_3), δ (ppm): 4.00-4.20 (t, $J = 6.4$ Hz, 140H, CH_2OCO (PCL)), 2.25 - 2.35 (m, 140H, PCL; O-COCH_2), 1.55 - 1.75 (m, 280H, PCL; $\text{CH}_2\text{CH}_2\text{CH}_2\text{-OCO}$; $\text{CO-CH}_2\text{CH}_2$), 1.35 - 1.45 (m, 140H, $\text{CH}_2\text{CH}_2\text{CH}_2\text{-OCO}$).

MALDI-TOF: $m/z_{\text{exp.}} = 7458.763$, $m/z_{\text{cal.}} = 7456.428$ for 62 repeating units (Average error of 1.89 Da).

Thiol-ene reaction of norbornenyl-functionalized PEO-b-PCL copolymer and dodecanethiol

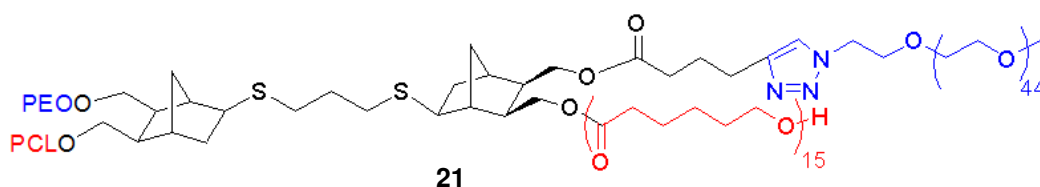


Norbornenyl-functionalized PEO-*b*-PCL macromonomer **13b** (0.05 g, 12.5×10^{-3} mmol, 1eq) was charged into a dried Schlenk tube equipped with a rubber septum and a magnetic stirrer bar and degassed

using 3 vacuum/argon cycles. 0.5 mL of dried DCM was added to dissolve macromonomer. Dodecanethiol (62.5 mg, 0.309 mmol) was dissolved in 1.24 mL of dried DCM in a separated vial under argon to target a dodecanethiol concentration of 0.25 mol/L. DMPA (3.5 mg, 0.0137 mmol) was dissolved in 1.1 mL of dried DCM in another vial under argon to target a DMPA concentration of 0.125 mol/L. 0.05 mL of dodecanethiol solution (12.5×10^{-3} mmol, 1eq) was added into the Schlenk tube followed by the addition of 0.1 mL of DMPA solution (1.25×10^{-3} mmol, 0.1 eq). Thiol-ene reaction started by setting the Schlenk under UV light (365 nm) at room temperature for 90 minutes. The evolution of the reaction was measured by ^1H NMR analysis of the crude reaction mixture. Conversion: 82%

^1H NMR (400 MHz, CDCl_3), δ (ppm): 7.51 (s, H, triazole), 6.19 (m, $\text{CH}=\text{CH}$, norbornene), 4.45 (t, $J = 5.6$ Hz, 2H, triazole- $\text{CH}_2\text{-CH}_2$), 4.00-4.20 (t, $J = 6.8$ Hz, 30H, CH_2OCO (PCL)), 3.60 - 3.80 (m, 176H, PEO; CH_2), 3.38 (s, 3H, $-\text{CH}_3$), 2.64 (m, 2H, $\text{OCOCH}_2\text{CH}_2\text{CH}_2\text{-triazole}$), 2.25 - 2.35 (m, 30H, O-COCH_2 (PCL); 2H, $\text{OCOCH}_2\text{CH}_2\text{CH}_2\text{-triazole}$), 1.95 (m, 2H, $\text{OCOCH}_2\text{CH}_2\text{CH}_2\text{-triazole}$), 1.75 (m, 4H, $\text{CHCHCH}_2\text{CHCH}$), 1.55 - 1.75 (m, 60H, $\text{CH}_2\text{CH}_2\text{CH}_2\text{-OCO}$; $\text{CO-CH}_2\text{CH}_2$ (PCL)), 1.35 - 1.45 (m, 30H, $\text{CH}_2\text{CH}_2\text{CH}_2\text{-OCO}$ (PCL); 2H, CHCH_2CH).

Thiol-ene reaction of norbornenyl-functionalized PEO-*b*-PCL copolymer and 1,3- propanedithiol



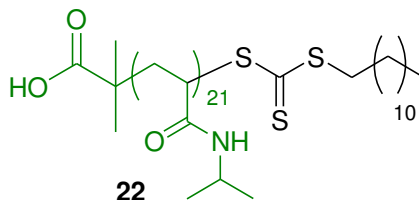
Norbornenyl-functionalized PEO-*b*-PCL macromonomer **13b** (0.1 g, 25×10^{-3} mmol, 1eq) was charged into a dried Schlenk tube equipped with a rubber septum and a magnetic stirrer bar and degassed using 3 vacuum/argon cycles. 1.2 mL of dried DCM was added to dissolve the macromonomer. 1,3-propanedithiol (46.3 mg, 0.428 mmol) was dissolved in 1.71 mL of dried DCM in a separated vial under argon to target a 1,3-propanedithiol concentration of 0.25 mol/L. DMPA (6.4 mg, 0.025 mmol) was dissolved in 1 mL of dried DCM in another vial under argon to target a DMPA concentration of 0.025 mol/L of concentration. 0.05 mL of 1,3-propanedithiol solution (12.5×10^{-3} mmol, 1eq) was added into the Schlenk tube followed by the addition of 0.05 mL of DMPA solution (1.25×10^{-3} mmol, 0.1 eq). Thiol-ene reaction started by setting the Schlenk under UV light (365 nm) at room temperature for 5 hours. The evolution of the reaction was measured by ^1H NMR analysis of the crude reaction mixture. Conversion: ~90%

^1H NMR (200 MHz, CDCl_3), δ (ppm): 7.51 (s, 2H, triazole), 4.45 (t, $J = 5.6$ Hz, 4H, triazole- $\text{CH}_2\text{-CH}_2$), 3.95-4.20 (t, $J = 7.2$ Hz, 60H, CH_2OCO (PCL)), 3.60 - 3.80 (m, 352H, PEO; CH_2), 3.38 (s, 6H, $-\text{CH}_3$), 2.64 (m, 4H, $\text{OCOCH}_2\text{CH}_2\text{CH}_2\text{-triazole}$), 2.25 - 2.35 (m, 60H, O-COCH_2 (PCL); 4H, $\text{OCOCH}_2\text{CH}_2\text{CH}_2\text{-triazole}$), 1.95 (m, 4H, $\text{OCOCH}_2\text{CH}_2\text{CH}_2\text{-triazole}$), 1.75 (m, 8H, $\text{CHCHCH}_2\text{CHCH}$),

1.55 - 1.75 (m, 60H, CH₂CH₂CH₂-OCO; CO-CH₂CH₂ (PCL)), 1.35 - 1.45 (m, 60H, CH₂CH₂CH₂-OCO (PCL); 4H, CHCH₂CH).

SEC: $M_n = 9750$ g/mol, $D_M = 1.09$

*Synthesis of poly(*N*-isopropylacrylamide) 22*



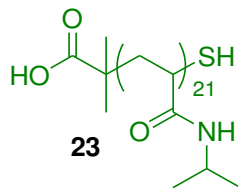
NIPAM (1.122 g, 9.915 mmol, 37 eq), DDMAT (0.0977 g, 0.268 mmol, 1 eq) and AIBN (4.4 mg, 0.0268 mmol, 0.1 eq) were charged into a dried Schlenk tube equipped with a rubber septum and a magnetic stirrer bar. DMF was added to dissolve the mixture. The solution was degassed by bubbling argon for 30 minutes. The Schlenk tube was then immersed into an oil bath preset at 70 °C and kept stirring for 1 hour to obtain a targeting conversion of 54%. DMF was completely removed under reduced pressure. The residue was dissolved in 3 mL of DCM and precipitated in cold diethyl ether. A yellow powder was obtained.

The theoretical conversion which was calculated using a ratio of targeting DP_n of 20 in comparison to initial [NIPAM]₀/[DDMAT]₀ equals to 37 was 54%. Experimental conversion which was calculated using kinetic ¹H NMR analysis of the crude mixture *versus* time of reaction equals to 53% after 1 hour of reaction. Experimental DP_n equals to 21 was calculated from ¹H NMR of purified PNIPAM by comparison of the integration values between the signal at δ = 3.75-3.95 ppm corresponding to protons of NHCH(CH₃)₂ of PNIPAM and the one of the signal at δ = 0.85 ppm corresponding to protons of methyl-end group.

. ¹H NMR (400 MHz, CDCl₃), δ (ppm): 6.70-7.70 (s, 21H, NH), 3.75-3.95 (s, 21H, NHCH(CH₃)₂), 1.80-2.20 (s, 21H, CH₂CHCO), 1.20-1.70 (m, 42H, CH₂CHCO; 6H (CH₃)₂CCOOH), 0.90-1.15 (s, 126H, NHCH(CH₃)₂; 20H, CH₃(CH₂)₁₀CH₂S), 0.85 (t, J = 7.2 Hz, 3H, CH₃CH₂).

SEC DMF (RI detection): $M_n = 4500$ g/mol, $D_M = 1.14$

Synthesis of thiol-functionalized PNIPAM 23

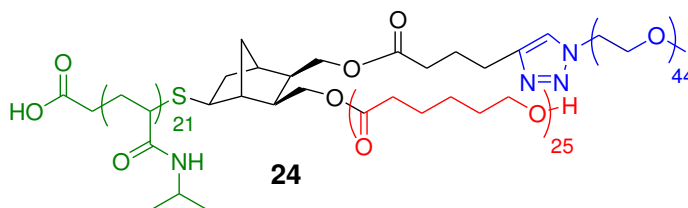


PNIPAM (0.3 g, 0.12 mmol) was charged into a dried Schlenk tube equipped with a magnetic stirrer bar and a rubber septum. Dried THF (12 mL) was added to dissolve PNIPAM and the solution was degassed by argon for 20 minutes. DMPP (0.33 g, 2.39 mmol) followed by *n*-hexylamine (0.29 g, 2.88 mmol) were added into a Schlenk tube and the solution was kept stirring for 4 hours. THF was removed using rotary evaporator, the residue was dissolved in 2 mL of DCM, precipitated in cold diethyl ether and dried under reduced pressure. Yield = 90%.

^1H NMR (400 MHz, CDCl_3), δ (ppm): 6.70-7.70 (s, 21H, NH), 3.75-3.95 (s, 21H, $\text{NHCH}(\text{CH}_3)_2$), 1.80-2.20 (s, 21H, CH_2CHCO), 1.20-1.70 (m, 42H, CH_2CHCO ; 6H $(\text{CH}_3)_2\text{CCOOH}$), 0.90-1.10 (s, 126H, $\text{NHCH}(\text{CH}_3)_2$), 0.85 (t, $J = 6.8$ Hz, 6H, $(\text{CH}_3)_2\text{P}$ (DMPP)).

SEC DMF (RI detection): $M_n = 4250$ g/mol; $D_M = 1.18$

Thiol-ene reaction of norbornenyl PEO-*b*-PCL macromonomer and thiol-functionalized PNIPAM (3-arms star copolymer)



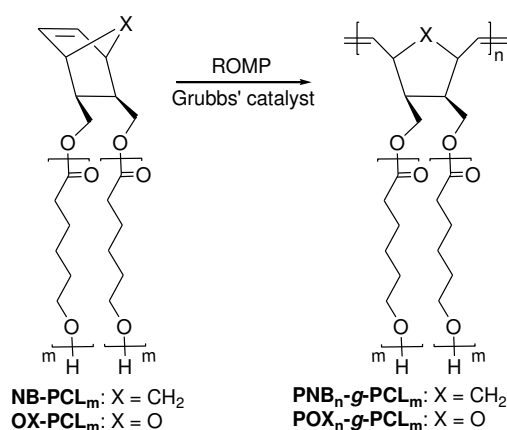
Norbornenyl-functionalized PEO-*b*-PCL macromonomer **13c** (0.125g, 0.025 mmol, 1 eq) and thiol-functionalized PNIPAM (0.05 g, 0.025 mmol, 1 eq) were charged into a dried Schlenk tube equipped with a rubber septum and a magnetic stirrer bar. 1.2 mL of dried DCM was added and the mixture was kept stirring for 10 minutes under bubbling argon. DMPA (6.5 mg, 0.025×10^{-3} mmol) was dissolved in 1 mL of dried DCM to target DMPA concentration of 0.025 mol/L in another dried vial under argon. 0.1 mL of DMPA solution (0.0025 mmol, 0.1 eq) was injected into the Schlenk tube. The Schlenk tube was set under UV light (365 nm) to start the reaction. The solution was kept stirring for 5 hours. Reaction conversion was measured by ^1H NMR spectroscopy of crude mixture. Conversion: 39%.

^1H NMR (400 MHz, CDCl_3), δ (ppm): 7.51 (s, 1H, triazole), 4.45 (t, $J = 6.0$ Hz, 2H, triazole- CH_2 - CH_2), 3.75-4.20 (m, 21H, $\text{NHCH}(\text{CH}_3)_2$, PNIPAM; 50H, CH_2OCO , PCL), 3.60 - 3.80 (m, 172H, CH_2 , PEO), 3.38 (s, 3H, $-\text{CH}_3$, PEO), 2.64 (m, 2H, $\text{OCOCH}_2\text{CH}_2\text{CH}_2$ -triazole),), 2.25 - 2.45 (m, 50H, O-COCH_2 , PCL; 2H, $\text{OCOCH}_2\text{CH}_2\text{CH}_2$ -triazole; 21H, CH_2CHCO , PNIPAM), 1.55-1.75 (m, 100H, $\text{CH}_2\text{CH}_2\text{CH}_2$ -OCO; $\text{CO-CH}_2\text{CH}_2$, PCL; m, 4H, $\text{CHCHCH}_2\text{CHCH}$), 1.35 - 1.45 (m, 50H, $\text{CH}_2\text{CH}_2\text{CH}_2$ -OCO), 0.90-1.10 (s, 126H, $\text{NHCH}(\text{CH}_3)_2$, PNIPAM).

General conclusion

The objective of the present work was the synthesis of well-defined (co)polymers containing a cycloolefin (norbornene (NB) or oxanorbornene (ONB)) functionality bearing two polymer chains including poly(ϵ -caprolactone) (PCL) and/or poly(ethylene oxide) PEO *via* ring-opening polymerization (ROP), chemical modification, and click chemistry. The as-obtained macromonomers were then used to access various copolymers structures such as comb-like and umbrella-like graft copolymers using ring-opening metathesis polymerization (ROMP) and (mikto-arm) star copolymers using the thiol-ene reaction.

We first successfully synthesized a series of well-defined NB- and ONB-functionalized macromonomers containing two PCL chains using the organocatalyzed-mediated ROP of ϵ -caprolactone (CL) with PCL chains ranging from 1400 to 5500 g/mol and with and low dispersities ($D_M < 1.25$) (Scheme 1).



Scheme I. Well-defined (oxa)norbornenyl-functionalized PCL macromonomers and their ROMP for synthesis of high grafting density bottle-brush copolymers

The PCL-based macromonomers were then subjected to ROMP using Grubbs' catalysts. We thus successfully obtained high grafting density bottle-brush copolymers having a poly(oxa)norbornene backbone and bearing two PCL chains per monomer unit according to the 'grafting through' strategy. Grubbs' second generation catalyst was found an efficient initiator for the polymerization of these macromonomers, although the ROMP was affected by the molecular weight of macromonomers, especially for oxanorbornene-functionalized macromonomers. Graft copolymers with a poly(oxa)norbornene backbone length of 10 units were obtained whatever the length of

the PCL grafts. Increasing both the PCL grafts length and the poly(oxa)norbornene backbone (50 and 100) led to non-quantitative macromonomers conversion. Grubbs's third generation catalysts containing bis-pyridine ligands enabled the synthesis of graft copolymers having both longer polynorbornene backbone and PCL grafts. Thermal properties of the resulting bottle-brush copolymers showed a lower crystallinity in comparison to PCL-based macromonomers: 38% crystallinity for PNB-*g*-PCL₅₁ copolymer compared to 91% crystallinity for NB-PCL₅₁ macromonomer. The results show that the crystallization process of PCL chains in such bottle-brush copolymers is hindered by Van der Waals interactions between the grafts.

A series of amphiphilic norbornenyl-functionalized PEO-*b*-PCL copolymers with the same PEO chain length ($DP_n = 44$) and PCL chain length ranging from 1150 to 4100 g/mol with narrow molecular weights distributions ($D_M < 1.20$) were successfully synthesized. Three different pathways were investigated in order to obtain the targeted copolymers. Strategies involving an esterification reaction between (oxa)norbornene dimethanol or (oxa)norbornene anhydride and mPEG 2000 g/mol (or mPEG 750 g/mol) are hampered by the traces water that are difficult to remove from the PEO precursors. In contrast, the combination of the click azide-alkyne reaction with ROP was found an efficient and versatile strategy for obtaining a series of well-defined amphiphilic norbornenyl-functionalized PEO-*b*-PCL copolymers (Figure 1).

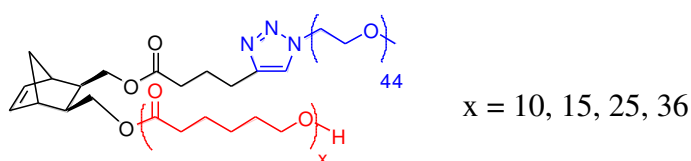


Figure 1. Amphiphilic norbornenyl-functionalized PEO-*b*-PCL copolymers with different PCL chain length obtained *via* the combination of click chemistry and ROP.

The resulting copolymers having a hydrophobic PCL chain and a hydrophilic PEO chain self-assemble in water. Critical micellar concentrations (CMC) determined by fluorescence measurements are in the range 0.08 – 0.006 g/L for copolymers with PCL chain length ranging from 10 to 36 CL units, respectively. The corresponding micelles show hydrodynamic diameters in range of 10 – 23 nm with low polydispersities. The

comparison with PEO-*b*-PCL copolymers indicates that the presence of the norbornenyl moiety does not influence the self-assembling properties of the resulting copolymers.

The successful synthesis of well-defined (co)polymers containing (bio)degradable PCL chains and/or biocompatible PEO chains opens the way to the synthesis of designed copolymers with desired degradability and biocompatibility.

Based on the successful synthesis of amphiphilic norbornenyl-functionalized PEO-*b*-PCL copolymers and ROMP processes using Grubbs' catalysts to polymerize (oxa)norbornenyl-functionalized PCL macromonomers in order to obtain high grafting density bottle-brush copolymers. We thus engaged the norbornenyl-functionalized PEO-*b*-PCL as macromonomers in ROMP to assess the reactivity of such a norbornenyl moiety bearing hydrophilic (PEO) and hydrophobic (PCL) chains.

A new ROMP macroinitiator has been successfully synthesized from a norbornenyl-functionalized PEO-*b*-PCL copolymer and Grubbs' first generation catalyst (G1) in order to increase the water-solubility of the initiator. The ROMP macroinitiator showed a good self-assembly ability in water giving rise to highly uniform micelles ($PD_i = 0.278$, hydrodynamic diameter = 13.75 nm). This ROMP macroinitiator exhibits a high reactivity toward NB in solution, giving access to a well-defined bottle-brush copolymer ($D_M = 1.21$).

Amphiphilic graft copolymers were obtained from norbornenyl-functionalized PEO-*b*-PCL copolymer by ROMP using Grubbs' catalysts. The presence of both PEO and PCL chains in the macromonomer lowered the ROMP-ability of the norbornene ring in comparison with norbornene-functionalized PCL macromonomers, whatever the initiator used (Grubbs' first, second, and third generation with pyridine ligands). The best initiator for the ROMP of norbornenyl-functionalized PEO-*b*-PCL macromonomer is Grubbs' third generation catalyst containing bromo-pyridine as ligands, although the backbone was limited at 50 units of length.

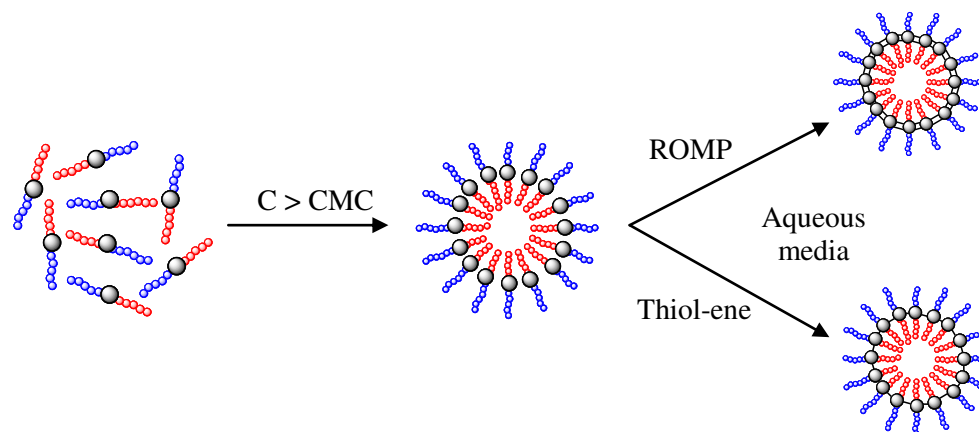
The reactivity of norbornenyl-functionalized copolymers toward thiol-ene reactions was then assessed. The norbornenyl moiety showed a high reactivity toward the thiol-ene reaction, as quantitative conversions were observed using norbornene dimethanol as a model compound. We thus investigated thiol-ene reactions with norbornenyl-

functionalized PCL polymer and norbornenyl-functionalized PEO-*b*-PCL copolymer to obtain (mikto-arm) star copolymers. Using a thiol-functionalized poly(N-isopropylacrylamide) (PNIPAM) and a norbornenyl-functionalized PEO-*b*-PCL copolymer, a mikto-arm (PEO, PCL, PNIPAM) star copolymer was successfully obtained, although the thiol-ene conversion was hampered by the steric hindrance associated with the coupling reaction between two polymers. In contrast, a well-defined star copolymer containing 4 PCL arms and a star copolymer containing 2 PCL arms and 2 PEO arms were quantitatively obtained as demonstrated by ¹H NMR and MALDI-TOF MS analysis when the thiol-ene reaction was conducted between norbornenyl-functionalized (co)polymers and a low molecular weight dithiol.

In conclusion, we have established efficient methodologies to synthesize new well-defined (co)polymers containing PCL and/or PEO with (oxa)norbornene-functionality as a junction group by the combination of click chemistry and ROP. (Oxa)norbornene-functionality brings reactivity of these (co)polymers toward either ROMP or thiol-ene reaction. Various copolymer topologies including bottle-brush, graft, and (mikto-arm) star copolymers have thus been obtained. The high reactivity of these norbornene-functionalized copolymers toward ROMP and thiol-ene reactions makes them interesting candidates as platforms in order to prepare new well-defined copolymers with controlled structures and properties through highly efficient synthetic strategies.

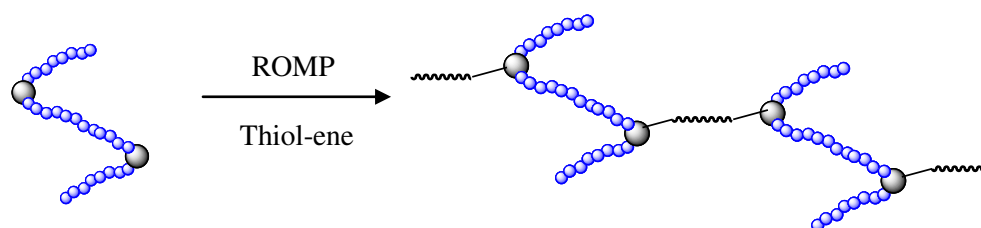
Based on the successful synthesis of well-defined amphiphilic norbornenyl-functionalized PEO-*b*-PCL macromonomers, and their self-organization as micelles in water, it is expected that such aggregates containing the hydrophobic norbornene functionalities in the micelle core (Scheme II) will lead to higher reactivity toward:

- ROMP resulting in higher molar mass of graft copolymers,
- Thiol-ene reactions.



Scheme II. Micellar reactions of amphiphilic copolymers containing cycloolefin functionality

On the other hand, our established versatile and efficient methodology of the synthesis of orthogonal multifunctional inimers followed by the synthesis of well-defined (co)polymers suggested us the synthesis of well-defined (co)polymers containing multi cycloolefin functionalities. These (co)polymers can be continuously used as a platform to obtain new structural (network) copolymers by ROMP copolymerization or thiol-ene reactions using ROMP-able monomers or multithiol functionalities compound as curing agents, respectively.



Scheme III. Network copolymers obtained from (co)polymers containing multi-cycloolefin functionalities

Thèse de Doctorat

Duc Anh NGUYEN

Cycloalkenyl macromonomers from new multifunctional inimers: A platform for graft, bottle-brush and mikto-arm star copolymers

Résumé

Le sujet de cette thèse concerne l'élaboration de macromonomères, de copolymères greffés et de polymères étoilés de type 'mikto-arm'. De telles architectures macromoléculaires ont été synthétisées par la combinaison de techniques de polymérisation contrôlées/vivantes telles que la polymérisation par ouverture de cycle (par métathèse) (RO(M)P) et de chimie 'click' orthogonales : cycloaddition 1,3-dipolaire azoture-alcyne catalysée au cuivre (CuAAC) et thiol-ène.

Dans un premier temps, des macromonomères originaux à fonctionnalité polymérisable (oxa)norbornène portant deux chaînes macromoléculaires poly(ϵ -caprolactone) (PCL) et/ou poly(oxyde d'éthylène) (POE) ont été synthétisés par combinaison ROP/CuAAC. Les macromonomères à fonctionnalité (oxa)norbornène avec deux chaînes PCL de masse molaire moyenne en nombre (M_n) compris entre 1400 et 5000 g/mol ont été obtenus par ROP organocatalysée. La synthèse des macromonomères POE₄₄-*b*-PCL_n à fonctionnalité norbornène avec un bloc PCL de longueur variable (1100 g/mol < M_n < 4100 g/mol) a été réalisée par combinaison CuAAC/ROP à partir d'un POE 2000 g/mol commercial. Ces macromonomères présentent des propriétés d'auto-assemblage dans l'eau avec une concentration micellaire critique et un rayon hydrodynamique dont les valeurs augmentent avec la longueur du bloc hydrophobe PCL.

Dans un second temps, la réactivité de la fonctionnalité (oxa)norbornène des macromonomères a été étudiée par spectroscopie RMN ¹H, chromatographie SEC et spectrométrie MALDI-ToF. Des copolymères greffés à squelette poly(oxa)norbornène à haute densité de greffons PCL et POE ont été obtenus par ROMP en présence d'amorceurs de Grubbs selon la stratégie "grafting through". La thiol-ène a également été utilisée avec succès pour accéder à des copolymères étoilés de type 'mikto-arm' à base de PCL, POE poly(*N*-isopropylacrylamide).

Mots-clés

ROMP, Chimie 'click', thiol-ène, Macromonomères à fonctionnalité (oxa)norbornène, Copolymères greffés, Copolymères étoilés de type 'mikto-arm'

Abstract

The objective of the present thesis was the preparation of complex macromolecules by the combination of controlled/living polymerization methods such as ring-opening (metathesis) polymerization (RO(M)P) and highly efficient orthogonal chemistries: copper-catalyzed azide-alkyne coupling (CuAAC) and thiol-ene reactions.

In the first part of this work, a series of well-defined structural (co)polymers containing a cycloolefin (norbornene (NB) or oxanorbornene (ONB)) functionality bearing two polymer chains including poly(ϵ -caprolactone) (PCL) and/or poly(ethylene oxide) (PEO) have been successfully prepared using the combination of ring-opening polymerization (ROP) and CuAAC 'click' chemistry. Well-defined (oxa)norbornenyl-functionalized bis-PCL polymers with PCL chain ranging from 1400 to 5000 g/mol were obtained by organocatalyst-mediated ROP. Norbornenyl-functionalized PEO-*b*-PCL block copolymers with PCL block in the range 1100 to 4100 g/mol were synthesized from commercially available PEO 2000 g/mol by CuAAC followed by ROP of CL. The presence of a hydrophilic PEO chain and a hydrophobic PCL chain in norbornenyl-functionalized PEO-*b*-PCL copolymers gives rise to self-assembling properties in water solution. Critical micellar concentrations (CMC) are in the range of 0.08 – 0.006 g/L for copolymers with PCL chain length ranging from 10 to 36 CL units, respectively. The corresponding micelles show hydrodynamic diameters in range of 10 – 23 nm with low polydispersities.

In the second part of this work, well-defined copolymers were used to prepare bottle-brush and (mikto-arm) star copolymers through reactions involving the cycloolefin functionality. On the one hand, high density grafting bottle-brush copolymers poly(oxa)norbornene-*g*-bisPCL, polynorbornene-*g*-PEO/PCL (PNB-*g*-(PEO/PCL)) and PNB-*b*-(PNB-*g*-(PEO/PCL)) were achieved by ROMP according to the 'grafting through' strategy using Grubbs' catalysts. On the other hand, PCL, PEO, PNIPAM-based 3-arms star, 4-arms star copolymers were obtained *via* radical thiol-ene reactions as demonstrated by ¹H NMR, SEC and MALDI-ToF MS analysis.

The high reactivity of these copolymers toward ROMP and thiol-ene reactions makes them interesting candidates in order to prepare new well-defined copolymers with controlled structures and properties through highly efficient synthetic strategies.

Key Words

ROMP, click chemistry, thiol-ene, (oxa)norbornene, macromonomers, well-defined copolymers, graft, bottle-brush, mikto-arm star copolymers